A NEW GLOBAL UNCONVENTIONAL NATURAL GAS RESOURCE ASSESSMENT

A Dissertation

by

ZHENZHEN DONG

Submitted to the Office of Graduate Studies of
Texas A&M University
in partial fulfillment of the requirements for the degree of

DOCTOR OF PHILOSOPHY

August 2012

Major Subject: Petroleum Engineering

A NEW GLOBAL UNCONVENTIONAL NATURAL GAS RESOURCE ASSESSMENT

A Dissertation

by

ZHENZHEN DONG

Submitted to the Office of Graduate Studies of
Texas A&M University
in partial fulfillment of the requirements for the degree of

DOCTOR OF PHILOSOPHY

Approved by:

Chair of Committee,	Stephen A. Holditch
Committee Members,	Duane A. McVay
	Walter B. Ayers
	W. John Lee
	Yuefeng Sun
Head of Department,	A. Daniel Hill

August 2012

Major Subject: Petroleum Engineering

ABSTRACT

A New Global Unconventional Natural Gas Resource Assessment. (August 2012)

Zhenzhen Dong, B.S., Northeast Petroleum University; M.S., Research Institute of Petroleum Exploration & Development

Chair of Advisory Committee: Dr. Stephen Holditch

In 1997, Rogner published a paper containing an estimate of the natural gas in place in unconventional reservoirs for 11 world regions. Rogner's work was assessing the unconventional gas resource base, and is now considered to be very conservative. Very little is known publicly about technically recoverable unconventional gas resource potential on a global scale. Driven by a new understanding of the size of gas shale resources in the United States, we estimated original gas in place (OGIP) and technically recoverable resource (TRR) in highly uncertain unconventional gas reservoirs, worldwide.

We evaluated global unconventional OGIP by (1) developing theoretical statistic relationships between conventional hydrocarbon and unconventional gas; (2) fitting these relationships to North America publically available data; and (3) applying North American theoretical statistical relationships to evaluate the volume of unconventional gas resource of the world. Estimated global unconventional OGIP ranges from 83,300 (P10) to 184,200 (P90) Tcf.

To assess global TRR from unconventional gas reservoirs, we developed a computer program that we call Unconventional Gas Resource Assessment System (UGRAS). In the program, we integrated a Monte Carlo technique with an analytical reservoir simulator to estimate the original volume of gas in place and to predict production performance. We used UGRAS to evaluate the probabilistic distribution of OGIP, TRR and recovery factor (RF) for the most productive unconventional gas formations in the North America. The P50 of recovery factor for shale gas, tight sands gas and coalbed methane is 25%, 79% and 41%, respectively.

Finally, we applied our global OGIP assessment and these distributions of recovery factor gained from our analyses of plays/formations in the United States to estimate global technically recoverable unconventional gas resource. Global technically recoverable unconventional gas resource is estimated from 43,000 (P10) to 112,000 (P90) Tcf.

DEDICATION

I dedicate this dissertation to my lovely husband for his support

To my parents, for their immense support and prayers.

To the rest of my family for always supporting me

ACKNOWLEDGEMENTS

I would never have been able to finish my dissertation without the guidance of my committee members, help from friends, and support from my family and husband.

I would like to express my deepest gratitude to my advisor, Dr. Stephen Holditch, for his advice, encouragement, and support during the course of this research and for his confidence in my ability which played an important role in the completion of this work.

I would like to thank my committee member, Dr. Duane McVay, who gave me excellent guidance and patiently corrected my writing. I would like to thank Dr. Walter Ayers was always willing to help and give his best suggestions. I appreciate Dr. John Lee, for their influence on my academic career and serving on my advisory committee. Special thanks goes to Dr. Yuefeng Sun, who was willing to participate in my final defense committee at the last moment.

I would like to thank Mr. William D. VonGonten with W.D. Von Gonten & Company for providing relevant datasets and valuable feedback to calibrate our research findings and analysis. Thanks to Dr. J.P. Spivey with Phoenix Reservoir Engineering for providing PMTx 2.0 for this research.

I would like to thank my husband, Weirong Li. He was always there cheering me up and stood by me through the good times and bad.

Finally, thanks to my friends and the department faculty and staff for making my time at Texas A&M University a great experience.

NOMENCLATURE

ERR	Economically recoverable resource
Gtoe	Gigatons of oil equivalent
MICP	Mercury Injection Capillary Pressure
NMR	Nuclear Magnetic Resonance
OGIP	Original Gas-in-place
P10	Value for which the probability is 10% that the value will not be exceeded, indicated by the 10th percentile on a cumulative probability plot. Similarly for P0, P1, P25, P50, P75 and P90, P99.
PID	Perforation Inflow Diagnostic
PIF	Productivity improvement factor
PITA	Perforation Inflow Test Analysis
TRR	Technically recoverable resource
G	Original Gas-in-place, Mscf
A	Area, acres
H	Net Pay, ft
ρ_c	Bulk Density, lb/cf
Gc	Initial Gas Content, scf/lb
Φ	Formation Porosity
S_w	Water Saturation
B_{gi}	Gas Formation Volumetric Factor, cf/scf
μ	Mean
σ	Standard deviation

Betageneral(α1, α2, min, max)	Beta distribution with defined minimum, maximum and shale parameters α1and α2.
Gamma(α, β)	Gamma distribution with shape parameter α and scale parameter β.
GEV(μ, σ, ξ)	Generalized extreme value distribution with mean μ, standard deviation σ and shape parameter ξ.
Invgauss(μ, λ)	Inverse Gaussian distribution with mean μ and shape parameter λ.
Logistic(α, β)	Logistic distribution with location parameter α and scale parameter β.
Loglogistic(γ, β, α)	Log-logistic distribution with location parameter γ, scale parameter β and shape parameter α.
Lognorm(μ, σ)	Lognormal distribution with specified mean and standard deviation.
Pearson5(α, β)	Pearson type V (or inverse gamma) distribution with shape parameter α and scale parameter β.
Normal(μ, σ)	Normal distribution with given mean μ and standard deviation σ.
Triang(min, most likely, max)	Triangular distribution with defined minimum, most likely and maximum value.
Uniform(min, max)	Uniform distribution between minimum and maximum.
Weibull(α, β)	Weibull distribution with shape parameter α and scale parameter β.

TABLE OF CONTENTS

Page

LIST OF FIGURES

LIST OF TABLES

1. INTRODUCTION

As the world reserves of liquid hydrocarbons from conventional reservoirs peaks and begins to decline, natural gas will play an increasingly important energy supply role. However, as the use of natural gas increases, additional supplies will be needed. To obtain additional natural gas supplies, the industry can develop unconventional gas resources that are often overlooked in the search for conventional hydrocarbons. Higher natural gas prices and significant technological advances have led to a dramatic increase in production of unconventional gas resources in the United States in recent years, and that trend is expected to continue unabated and to expand worldwide.

1.1 What is Unconventional Gas

Three natural gas sources—coalbed methane (CBM), tight sand gas, and shale gas—comprise today's unconventional gas. Methane hydrate reservoirs, a future candidate, are still decades away from being a potential energy source, mainly due to their location and market conditions. Gas hydrates are found in the Arctic and in deep water, neither of which have any pipeline capacity available for taking the gas to market.

1.1.1 Coalbed Methane

Coalbed methane is a natural hydrocarbon gas that is adsorbed to the surface of the coal. Coalbed methane is considered an unconventional natural gas resource, because it does not rely on "conventional"' trapping mechanisms, such as a fault or anticline, or

---

This dissertation follows the style of *SPE Journal*.

stratigraphic traps. Instead, coalbed methane is “adsorbed” or attached to the molecular structure of the coals-an efficient storage mechanism as coals can contain as much as seven times the amount of gas typically stored in a conventional natural gas reservoir such as sandstone or shale.

1.1.2 Tight Gas

Tight gas is found trapped in low permeability rock (permeability less than 0.1 md) and low porosity sandstone or limestone formations, typically at depths from a few thousand feet to well over 15,000 ft. The viability of sandstone reservoirs is determined by their porosity (the open space between grains that is capable of sorting gas and liquid) and permeability (how easily fluid or gas moves through the rock). Tight gas sandstones act purely as reservoirs, whereas coalbeds and shales can be both a source rock as well as a reservoir for the gas. Gas migrates into tight sandstones pores from the source rock; whereas, in coal and shale gas formations, gas is in part, adsorbed into the matrix of organic matter.

1.1.3 Shale Gas

Shale gas refers to natural gas (mainly methane) in fine-grained, organic-rich rocks (gas shales). When talking about shale gas, the word shale does not refer to a specific type of rock. Instead, it describes rocks with more fine-grained particles (smaller than sand) than coarse-grained particles, such as shale (fissile) and mudstone (non-

fissile), siltstone, fine-grained sandstone interlaminated with shale or mudstone, and carbonate rocks.

Gas is stored in shales in three ways: (1) adsorbed gas is gas attached to organic matter or to clays; (2) free gas is gas held within the tiny spaces in the rock (pores, porosity or micro-porosity) or in spaces created by the rock cracking (fractures or microfractures); and (3) solution gas is gas held within other liquids, such as bitumen and oil.

Gas shales are source rocks that have not released all of their generated hydrocarbons. In fact, source rocks that are "tight" or "inefficient" at expelling hydrocarbons may be the best prospects for shale gas potential.

1.1.4 Production Profile Comparison

There are differences in the typical production curves for unconventional gases (**Figure 1.1**). Many coalbed methane wells initially produce high volumes of water, often for significant periods of time. However, once the target reservoir has been depressurized by removing the water, the average production curve is relatively steady. In shale gas wells, the production curve is slightly different. The natural gas occurs both as free-gas around the rock structure and within the rocks. Once the wellbore reaches the target zone and has been successfully fracture treated, the free gas flows quickly, causing an initial high production. Production then plateaus as the natural gas absorbed in the rock is removed. Thus for a typical shale gas well, production declines between 70-90 percent in the first year, with an overall average well life of 20-30 years.

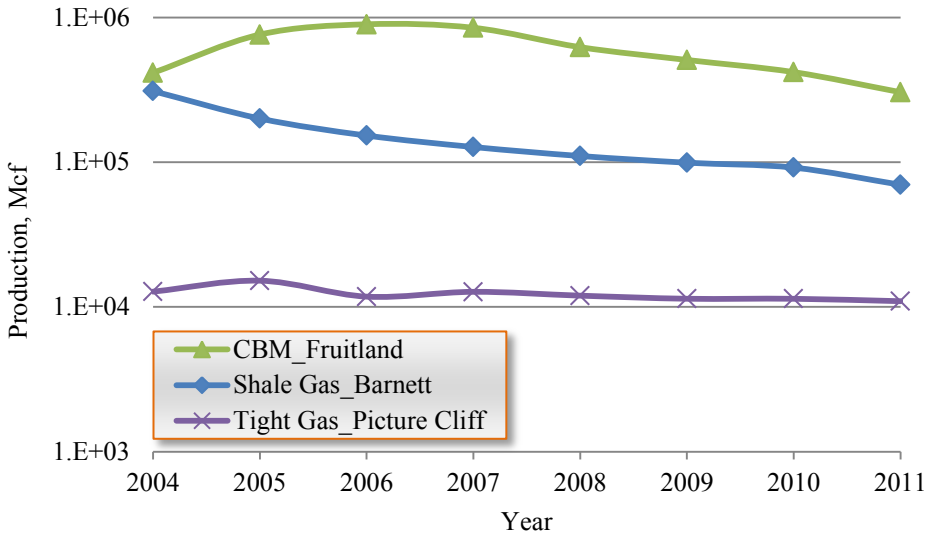

Figure 1.1—Typical production decline curves for different type of unconventional gas reservoirs

In summary, a number of features distinguish unconventional gas reservoirs from conventional gas reservoirs: (1) the unconventional gas formations are "continuous", deposited over large areas rather than in discrete traps; (2) the geologic setting of unconventional gas is several orders more complex and challenging than of conventional gas; and (3) for two of the unconventional gas types—coalbed methane and shale gas—the gas source, trap and reservoir are the same, not three distinct elements as for conventional gas.

1.1.5 The Gas Supply

Since 2000, strong oil and gas demand is causing the industry to look at unconventional gas as a source of supply. There have been dramatic increases in coalbed methane exploration and production outside of North America. In countries such as

Australia and China, coalbed methane will become an important energy source in the future. In many other countries in Asia, Eastern Europe and Latin America, coalbed methane commercial potential is not yet understood (Chakhmakhchev 2007).

Tight sands gas represents a significant portion of natural gas resources worldwide. Large reserves of tight sands gas have been identified outside of North America, such as in India, China, and several European countries. Currently, there is an emerging focus on tight sands gas reservoirs in the Middle East and North Africa to supply the growing energy needs in this region and to save the conventional oil resources for export and generation of hard currencies.

The use of horizontal drilling in conjunction with hydraulic fracturing has greatly expanded the ability of producers to profitably produce natural gas from low permeability geologic formations, particularly shale formations. A number of major and independent oil and gas companies are circling the globe looking for high-quality shale-gas plays. Currently, shale-gas exploration is underway in many parts of the world, including in the Alum shale of Sweden, the Amadeus shale in Australia, and the carbonaceous shales of Botswana. Since the delineation of shale gas is still in its infancy, global shale-gas resources have not been appraised in any systematic way.

Between 2000 and 2010, unconventional gas production from the lower 48 increased from 6.3 Tcf to 13.0 Tcf per year, and now accounts for 54% of United States consumption of natural gas (**Figure 1.2**). Without question, the United States and soon the world, is entering into the golden age of nature gas. Unconventional gas resources will play a more a more important role in supplying the world with affordable energy.

Many people in the energy industry want to know how much unconventional gas exists in place, globally. Are there sufficient supplies from unconventional gas resources?

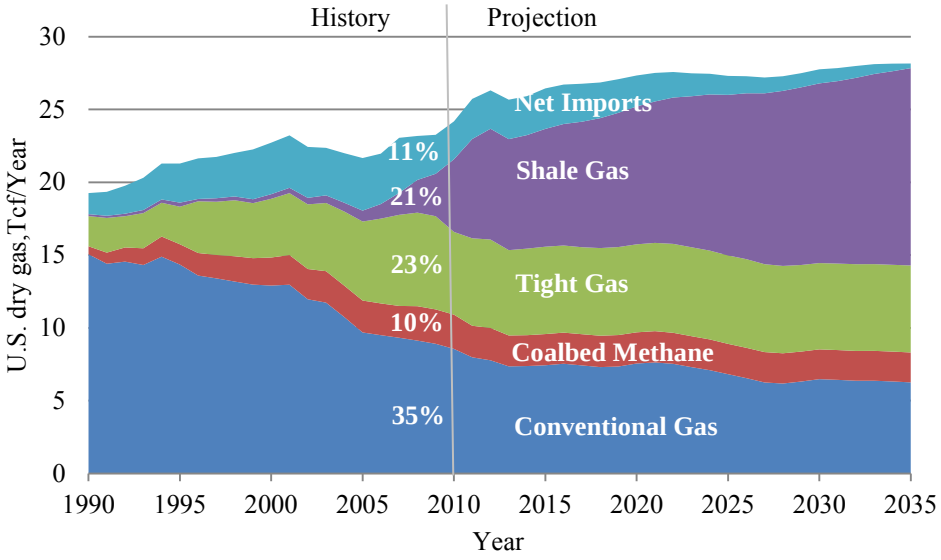

Figure 1.2—Annual consumption of natural gas in United States (EIA 2012a)

1.2 Global Unconventional Gas Base

Virtually all currently published resource endowment estimates for world unconventional gas start with Rogner's (1997) region-level study of world hydrocarbon resources. In the study, Rogner estimated unconventional gas in place for 11 groupings of the countries of the world. The main criteria for the regionalization were geography, demography, resource endowment, and level of economic development.

According to Rogner's estimates, worldwide original in place resources were 9,000 Tcf of coalbed methane, 16,000 Tcf of shale gas, and 7,400 Tcf of tight sands gas (**Table 1.1**). Rogner's 1997 global estimate is most likely quite conservative now, given the recent discovery of significant shale gas around the world. Rogner did not try to

quantify uncertainty in his estimates. There are many publications one can find on technically recoverable resource of unconventional gas in small geographic areas. However, little is known publicly about values of TRR for unconventional gas resources on a global scale. In the dissertation, we grouped some regions that Rogner estimated in his study together. For example, Central & Eastern Europe (EEU) and Western Europe (WEU) in Rogner's study were combined to be Europe (EUP) in this dissertation. And Centrally Planned Asia & China (CPA), Pacific OECD (PAO), South Asia (SAS), and Other Pacific Asia (PAS) in Rogner's study were combined together to be Austral-Asia region (AAO). Thus, 7 regions we estimated in this research are shown in Table 1.1.

Table 1.1—Geographic distribution of unconventional OGIP worldwide, in Tcf (Rogner 1997)

Region	Coalbed Methane	Shale Gas	Tight Sands Gas	Total
Austral-Asia (AAO)	1,724	6,151	1,802	9,677
North America (NAM)	3,017	3,840	1,371	8,228
Commonwealth of Independent States (CIS)	3,957	627	901	5,485
Latin America (LAM)	39	2,116	1,293	3,448
Middle East (MET)	0	2,547	823	3,369
Europe (EUP)	274	549	431	1,254
Africa (AFR)	39	274	784	1,097
World	9,051	16,103	7,405	32,559

1.3 Resource Classification

1.3.1 Petroleum Resources Management System (PRMS)

The terms 'resources' and 'reserves' have been in the past and continue to be used to represent various categories of mineral and/or hydrocarbon deposits. In March 2007, the Society of Petroleum Engineers (SPE), the American Association of Petroleum

Geologists (AAPG), the World Petroleum Council (WPC), and the Society of Petroleum Evaluation Engineers (SPEE) jointly published the Petroleum Resource Management System (PRMS) to provide an international standard for classification of oil and gas reserves and resources (**Figure 1.3a**). The broadest categories are also the least precise. For the categories at the bottom of the chart, the associated estimates of the amount of natural gas are more and more uncertain. Estimated ultimate recovery (EUR) is not a resources category in PRMS, but a term that refers to the quantities of petroleum which are estimated to be potentially recoverable from an accumulation, including those quantities that have already been produced. However, technically and economically recoverable resources are not formally classified in the system.

1.3.2 Energy Information Administration's (EIA) Classification System

According to the EIA, technically recoverable resources are the subset of the total resource base that is recoverable with existing technology. The term 'resources' represents the total quantity of hydrocarbons that are estimated, at a particular time, to be contained in: (1) known accumulations, and (2) accumulations that have yet to be discovered (prospective resources).

Economically recoverable resources are those resources for which there are economic incentives for production. Economically unrecoverable resources may, at some time in the future, become economic, if the technology to produce them becomes less expensive, or the characteristics of the market are such that companies can ensure a fair return on their investment by extracting the resources.

We rearranged categories of PRMS and presented an overview of how the estimates of technically and economically recoverable resources are broken down (**Figure 1.3b**). Those commercial resources, including cumulative production and reserves, are economically recoverable resources. Technically recoverable resources include commercial resources, contingent resources and prospective resources. Based on the classification in PRMS and definition given by EIA, we defined that 25-year cumulative production as TRR in this study. For the remainder of this dissertation, we consider only natural gas resources.

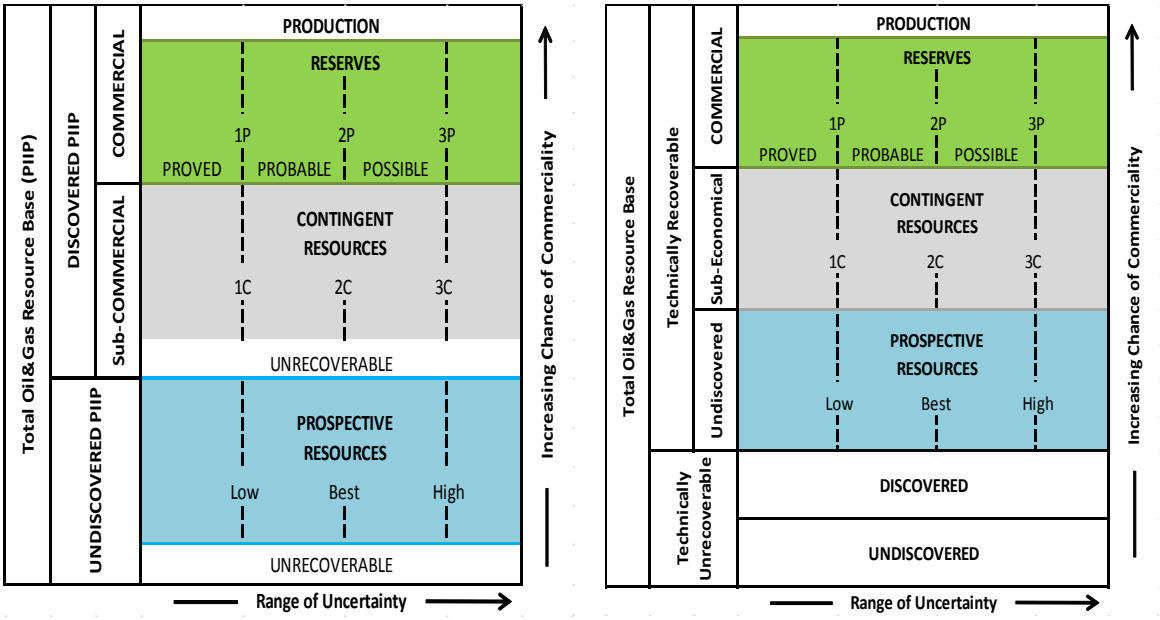

a) Resource Classification of PRMS b) EIA definitions mapped to PRMS categories

Figure 1.3—Flow chart and generalized division of resource and reserve categories

1.4 Resource Triangle

Masters (1979) suggested that hydrocarbon resource types can be assigned to various resource classes in a triangular distribution, and their positions in the triangle reflect their abundance, their reservoir quality, and the technology required for recovery (**Figure 1.4**). With depth in the gas-resource triangle, the reservoirs are lower grade, which usually means the reservoir permeability is decreasing. These low-permeability reservoirs are much larger in size than the higher-quality reservoirs (Holditch 2006).

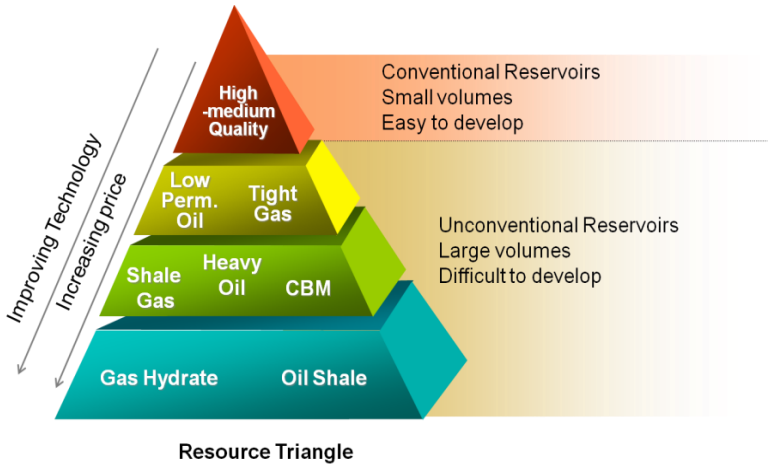

Figure 1.4—Volumes of unconventional resources are larger than conventional resources

1.5 Assessment Methodology of TRR from Unconventional Gas Reservoirs

Based on the definition of TRR, the methods which predict well performance can be used to estimate the range of TRR. The principal techniques used for production determination from early stage to mature fields are analogy, volumetric analysis, material balance analysis, decline curve analysis (DCA), and numerical simulation (**Table 1.2**). The biggest challenge is that methods that we use for conventional

reservoirs usually don't work well, without modification, for unconventional reservoirs. Rate-time production-decline curves, have real problems including a lack of long-term historical production. Volumetric analysis coupled with an assumed recovery factor, and reservoir simulation with analytical or numerical models, have its own challenges. The problems include difficulties in measuring formation properties needed for input into the computational methods.

Rogner's 1997 global estimate is most likely quite conservative now, given the recent discovery of significant shale gas around the world. And Rogner did not try to quantify uncertainty in his estimates. There are many publications one can find on technically recoverable resource of unconventional gas in small geographic areas. However, little is known publicly about the TRR assessment of unconventional gas resources on a global scale. The objective of our work was to develop the data sets, methodology and tools to determine probabilistic distribution of original gas in place (OGIP) and technically recoverable resources (TRR) in highly uncertain and risky unconventional gas reservoirs worldwide, and conduct a global unconventional gas-in-place and TRR assessment.

Table 1.2—Tools used to determine TRR

Methodology	Advantage	Disadvantage	Conventional Reservoir	Unconventional Reservoir
Analogy	• Best in blanket sands • Best prior to production	The large number of variables and parameters causes high degree of uncertainty	Can be applied in both conventional and unconventional assets	
Volumetric Method	• Any stage of depletion •Best prior to production	Has uncertainties of • recovery factor • actual drainage area	Accurate in blanket reservoir	Used only when no wells have been drilled
Material Balance	Best between 10% and 70% depletion	Requires: • accurate average pressure • reservoir fluid properties	Accurate in depletion drive reservoir	• Should never be used • Average pressure cannot be measured accurately
Decline Curve Analysis	• Best with long production history • Quick	• Boundary dominated flow • Unchanging drainage area • Fixed skin factor • ‘b’ value is constant and should lie between 0 and 1 • Underestimate reserves	Exponential decline usually accurate	Must use hyperbolic decline: • CBM: b=0~0.5 • Shale gas and tight gas: b may be larger than 1 • Use best-fit 'b' until predeterminate minimum decline rate reached, then impose exponential decline • Set 'b' to proper 'terminal value'
Reservoir Simulation	• Best with data rich wells • In conjunction with other methods any time	• Needs good history match • Cost time	Used to simulate the field	Used to simulate individual wells

Section 2 of this dissertation reviews the methodology that Rogner used to estimate global unconventional gas in place, other world unconventional gas resource assessments, and probabilistic approaches to estimate gas resources. Section 3 explains the methodologies we developed to estimate in-place and technically recoverable resources of global unconventional gas. Section 4 presents a global unconventional gas-in-place assessment. Section 5 estimates resource potential for five main shale gas plays

in the United States. Section 6 estimates resource potential for three key tight gas formations in the United States. Section 7 is resource assessments of the top two productive coalbed methane formations in the United States. Section 8 concludes the probability distribution of technically recovery factor from unconventional gas plays/formations estimated in Section 5 through 7, and estimates technically recoverable resources from unconventional gas reservoir globally. Section 9 summarizes results and conclusions.

2. LITERATURE REVIEW

2.1 Review of Rogner's Assessment Methods

Rogner (1997) estimated global coalbed methane resources by using the distribution of coal resources and estimated values for coalbed gas content. Based on Kuuskraa's study (1992), Rogner reported that the worldwide coalbed gas resources range from 85 to 262 trillion cubic meters (2,980-9,260 Tcf). However, only the top 12 coal resource countries were included in the assessment. While Rogner's initial work focused on these 12 major coal-bearing areas, many other countries, such as Spain, Hungary, and France, have smaller but significant coal reserves and by extension, coalbed gas resources. Thus, more countries should be included to improve global coalbed methane resource estimates.

Rogner's methodology for estimating world shale-gas resources, which he states is quite speculative, assumed that shale-oil occurrence outside the United States contains the gas-in-place value of 17.7 Tcf/Gt in the United States. However, it is difficult to estimate shale-oil resources, and it is not certain that the shale gas and shale gas resource occurrence even correlate. As such, we believe an improved region-level shale-gas OGIP assessment methodology is required.

Tight sands gas reservoirs are present in every petroleum province. In Rogner's (1997) work, the regional allocation (Table 1.1) was obtained by weighting Kuuskraa and Meyer's (1980) estimated global tight-sands-gas volume of almost 190 Gtoe with the regional distribution of conventional gas. However, in Rogner's work the regional

distributions of tight sands and conventional gas in place were not consistent. For example, North America has more tight-sands OGIP (1,802 Tcf) than CIS (901 Tcf), but CIS has more conventional gas in place (7,599 Tcf) than North America (2,193 Tcf). As such, we need to update the regional distribution of conventional gas in place as a guide to the amount of unconventional gas that may exist.

2.2 Region-Level World Unconventional Resource Assessments

There are no region-level estimates for global resource of tight sands gas and coalbed methane available, except Rogner's 1997 study. However, a notable basin-by-basin assessments of shale gas resources in 5 regions containing 32 countries, conducted by EIA (2011a), indicates that the shale-gas OGIP (25,300 Tcf) is larger than estimated by Rogner in 1997 (16,112 Tcf), even accounting for the fact that Russia and the Middle East were not included in EIA study (but are include in Rogner's shale gas resource numbers) (**Table 2.1**). The largest and most notable areas of difference in the shale-gas OGIP assessments are for Europe, Africa and North America.

Table 2.1—Comparison of Rogner's and EIA estimates of shale-gas OGIP, in Tcf

Region	Rogner, 1997	EIA, 2011a
AAO	6,151	7,042
NAM	3,840	7,140
LAM	2,116	4,569
EUP	549	2,587
AFR	274	3,962
MET&CIS	3,174	N/A
World	16,103	25,300

The technically recoverable resource can be estimated by multiplying the OGIP by a gas recovery factor. For instance, three basic gas recovery factors, incorporating shale mineralogy, reservoir properties and geologic complexity, are used in the EIA (2011a) basin-level assessment (**Table 2.2**). It should be noted that North America (NAM) includes United States and Canada in the EIA study. The regional level tabulations of risked gas in-place and technically recoverable shale gas resource are provided in **Table 2.3**. The average recovery factor of shale gas for the basins in the 32 countries is 25%.

Table 2.2—Recovery factors used in EIA/ARI study (EIA 2011a)

Clay Content	Geologic Complexity	Reservoir properties	Recovery Factor
Low	Low to moderate	Favorable	30%
Medium	Moderate	Average	25%
Medium to high	Moderate to high	Below average	20%

Table 2.3—Risked gas in-place and technically recoverable shale gas resources: five regions (EIA 2011a)

Region	Risked Gas In-Place, Tcf	Risked Technically Recoverable, Tcf	Average Recovery Factor
NAM	5,314	1,208	23%
AAO	7,042	1,800	26%
LAM	6,935	1,906	27%
AFR	3,962	1,024	26%
EUP	2,587	624	24%
World	25,840	6,562	25%

2.3 Monte Carlo Probabilistic Approach

Unconventional gas plays are generally characterized by low geologic risk and high commercial risk. Uncertainty exists in geologic and engineering data and, consequently, in the results of calculations made with these data. Probabilistic approaches are required to provide an assessment of uncertainty in resource estimates.

Reservoir simulation coupled with stochastic methods (e.g., Monte Carlo) provides an excellent means to predict production profiles for a wide variety of reservoir characteristics and producing conditions. The uncertainty is assessed by generating a large number of simulations, sampling from distributions of uncertain geologic, engineering and other important parameters. This topic has been an object of study for some time in conventional reservoirs (MacMillan et al. 1999; Nakayama 2000; Sawyer et al. 1999). However, few applications to unconventional reservoirs can be found in the literature. Oudinot et al. (2005) coupled Monte Carlo simulation with a fractured reservoir simulator, COMET3, to assess the EUR in coalbed methane reservoirs. Schepers et al. (2009) successfully applied this Monte Carlo-COMET3 procedure to forecast EUR for the Utica shale.

3. METHODOLOGY

The objective of this study is to update the assessment of world unconventional gas resource and assessed the TRR of unconventional gas on the global scale. In this section we introduced the new methodology that we used to estimate probabilistic distribution of unconventional OGIP and TRR on a region/county level.

3.1 Global OGIP Assessments

Using what we found from published global resource data on conventional oil and gas, we have assessed global conventional oil and gas in place. Then, we collected published data about unconventional gas-in-place assessments of North American basins. Using the concept of the resource triangle, we propose that one can estimate unconventional gas in place by knowing the volumes of oil and gas that exist in the conventional reservoirs. Thus, we evaluated global unconventional OGIP by developing theoretical statistic relationships between conventional hydrocarbon and unconventional gas.

Following are the theoretical statistic relationships we assumed to assess the distribution of unconventional gas in place.

1. We assumed the distribution of hydrocarbon resource types is similar in different basins and regions throughout the world. Since more information about conventional and, particularly, unconventional resources is available in North America than other regions of the world, we assumed that we can use knowledge of the

distributions of resource types in North America to estimate unconventional gas resources in other regions in the world.

2. The regional distribution of original coalbed methane in place is intimately linked to the geographical and geological distribution of coal deposits. We assumed that coalbed methane OGIP is proportional to original coal in place,

$$\text{CBM OGIP} = A * \text{Original Coal in place} \tag{3.1}$$

The values of 'A' represent the distribution of the average gas content in coal seams. We determined the distribution function A from the average gas content values of producing coalbed methane basins in North America.

3. Using the concept of the resource triangle, we assumed that the value of tight-sands OGIP is proportional to the value of conventional OGIP,

$$\text{Tight-Sands OGIP} = B * \text{Conventional OGIP} \tag{3.2}$$

The values of 'B' make up the distribution of the ratio of tight-sands OGIP to conventional OGIP. The distribution B was estimated from the distribution of tight sands and conventional original gas in place in North America.

4. Coal and shale are self-sourcing reservoirs that retain some hydrocarbons but also supply hydrocarbons that charge nearby tight sands and conventional reservoir rocks. We assumed the sum of coalbed OGIP and shale-gas OGIP is proportional to the sum of tight-sands OGIP and conventional hydrocarbons in place,

$$\text{CBM OGIP} + \text{Shale-gas OGIP} = C*(\text{Tight-sands OGIP} + \text{Conventional OOIP} + \text{Conventional OGIP}) \tag{3.3}$$

The values of 'C' make up the distribution of the ratio, which was estimated from the distribution of original conventional hydrocarbon and unconventional gas resources in North America. A possible limitation of that this approach is that it omits potential contributions of carbonate source rocks.

We fitted these relationships (**Eq. 3.1** through **3.3**) to North America publically available data we collected and derived the probability distribution of A, B and C. Then we applied these distributions to evaluate the volume of unconventional gas resources in the world.

3.2 Target Formation Selection

We selected the most productive formations from the top two or three unconventional gas basins in the United States and collected the publicly available data, including production data, reservoir parameters, well completion data, etc. for these formations.

3.3 Basin-Level Resource Assessments

We developed a computer program, Unconventional Gas Resource Assessment System (UGRAS), to generate probabilistic distributions of OGIP, TRR and recovery Factor (RF) for these target formations.

The workflow of our probabilistic reservoir model UGRAS is outlined in **Figure 3.1**. First, an input file is created and uncertain parameters are assigned initial density functions. There is no limitation to the number of parameters that can be varied. But we

didn't consider possible correlations among these parameters. These density functions, as well as other parameters defined in input file, were refined until a reasonable match between simulated and actual probability distribution of cumulative gas production was obtained. Next, thousands of combinations of unknown reservoir and well parameters were simulated to generate frequency and cumulative density plots for OGIP, TRR and RF. Finally, economic analysis was run to calculate the production from wells that meet economic criteria (IRR>20% before tax, payout<5 years) over production from all wells according to different F&DC costs, if necessary.

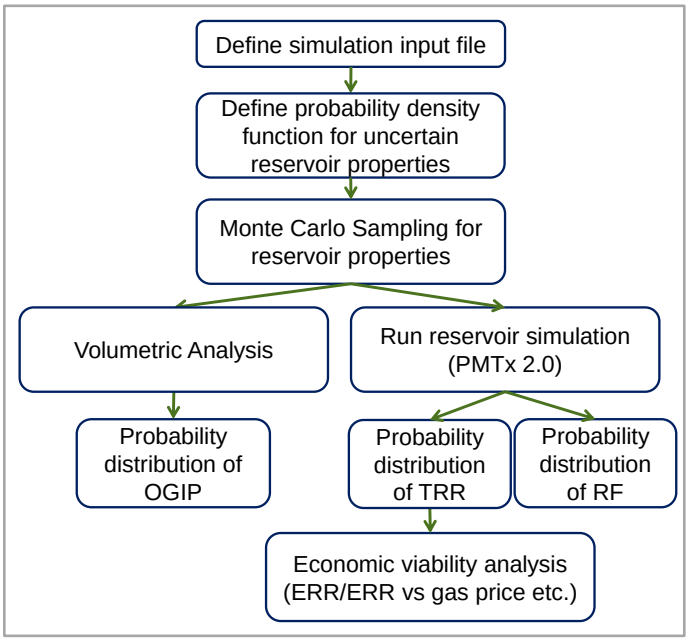

Figure 3.1—Flow chart of UGRAS

In UGRAS, OGIP is calculated using volumetric methods. Generally, in a conventional and tight sand gas reservoir, we only need to consider free gas in place. **Eq. 3.4** is used to calculate the free gas in place,

$$\text{Free GIP} = \frac{43560\text{Ah}\emptyset(1-S_w)}{B_{gi}} \quad (3.4)$$

where $B_{gi} = \frac{0.02829\,ZT}{p}$

However, some coalbed methane and shale gas in place is a combination of free gas in the matrix and adsorbed gas on the surface of the organics.

Adsorbed gas-in-place is a function of organic matter type, maturity, organic content, and gas composition. It is usually measured in the laboratory using isotherm experiments. A Langmuir isotherm is established for the prospective area of the basin using available data on TOC and thermal maturity to establish the Langmuir volume (VL) and pressure (PL).

Adsorbed gas in place is then calculated using the formula

$$\text{Adsorbed GIP} = 43560\text{Ah}\rho_c G_c(1-\emptyset) \quad (3.5)$$

where $G_c = \frac{V_L \times p}{p_L + p}$.

3.4 Global TRR Assessments

After we estimated the probabilistic distributions of unconventional gas in place at a region level and the estimate of the probability distribution of recovery factor from the target formations of United States, we generated probabilistic distributions of technically recoverable resource of unconventional gas for each region by assuming that the distribution of RF we derived from the United States is applicable to the rest of world.

4. GLOBAL UNCONVENTIONAL GAS-IN-PLACE ASSESSMENT

We first estimated global conventional hydrocarbon resource endowments from the geographic distribution of technically recoverable resources of conventional oil and gas and the probabilistic distribution of recovery factors in conventional reservoirs. Then, we collected published data about unconventional gas-in-place assessment from North American basins and determined the distributions of unconventional gas in place in North America. Next, we determined the distributions of the ratios A, B and C in North America. Finally, we used these data and distributions to assess worldwide unconventional gas in place.

4.1 Basin Types and Global Distribution of Basins

To determine whether the distribution of North American basin types are representative of the distribution of basin types in the rest of the world, we compared the 26 North American basins evaluated in this study with 151 global basins in which giant oil and gas fields are located (Mann et al. 2001) (**Table 4.1** and **Figure 4.1**). We found that there is a similar distribution of basin types between the North American and global basins that have giant fields. For example, foreland basins account for 53% of global basins and 44% of North American basins (Figure 4.1). We acknowledge that this approach is not as robust as an integrated basin-by-basin assessment of basin type, reservoirs, source rocks and resources, but such a detailed evaluation was impractical for this global study.

Table 4.1—North American basins assessed in this study

No.	Nomenclature	Full Name	No.	Nomenclature	Full Name
1	APPB	Appalachian basin	14	MICB	Michigan basin
2	ANAB	Anadarko basin	15	PARB	Paradox basin
3	ARKB	Arkoma basin	16	PERB	Permian basin
4	BHB	Big Horn basin	17	PICB	Piceance basin
5	BWB	Black Warrior basin	18	PRB	Powder River basin
6	CHKB	Cherokee basin	19	RTOB	Raton basin
7	DENB	Denver basin	20	SHB	San Juan basin
8	ETB	East Texas basin	21	WGC	Western Gulf Coast
9	FCB	Forest City basin	22	UINB	Unita basin
10	FWB	Fort Worth basin	23	WRB	Wind River basin
11	GGRB	Greater Green River basin	24	WILLB	Williston basin
12	ILLB	Illinois basin	25	WCSB	Western Canadian Sedimentary basin
13	LMS	Louisianan Mississippi Salt	26	WTB	Wyoming Thrust Belt

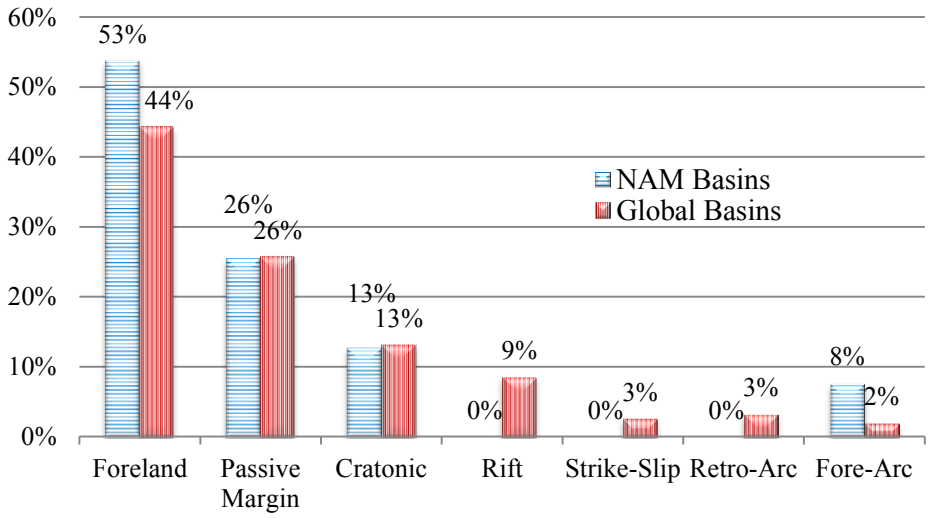

Figure 4.1—Comparison of basin types between North American and global basins

4.2 Global Conventional Oil and Gas Resource Assessments

To estimate the probability distributions of conventional gas and oil in place worldwide, we examined the geographic distribution of technically recoverable resources from conventional reservoirs for seven regions, and the probability distributions of conventional oil and gas recovery factors. We then divided technically recoverable resources by recovery factors to obtain original-in-place values of conventional oil and gas.

4.2.1 Technically Recoverable Resources of Conventional Hydrocarbons

Technically recoverable conventional hydrocarbon resources have been estimated globally by a number of organizations. Without quantifying the uncertainty, Bundesanstalt fur Geowissenschaften und Rohstoffe (BGR) updates technically recoverable resources of conventional oil and gas, as well as original coal in place, every two years. According to its latest assessments (BGR 2009), global technically recoverable resources of conventional oil and gas are 16,417 Tcfe (2,992 Bboe) and 18,972 Tcf, respectively.

On a global scale, the majority of technically recoverable conventional hydrocarbons resources are located in the Middle East (MET) region, where large quantities of crude oil (6,625 Tcfe) and natural gas (4,071 Tcf) occur (**Figure 4.2**). The next largest endowment occurs in the Commonwealth of Independent States (CIS), where substantial natural gas resources (7,529 Tcf) as well as petroleum resources (2,648 Tcfe) exist (Figure 4.2).

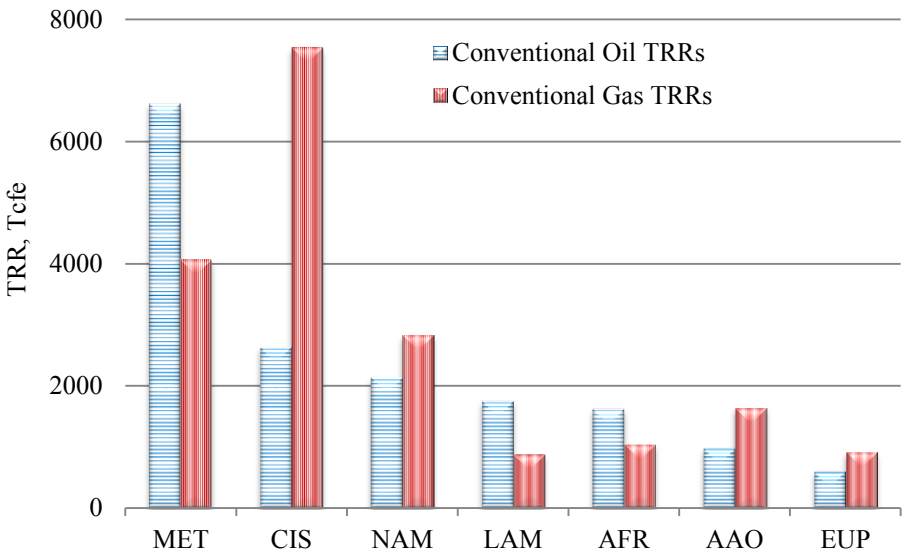

Figure 4.2—Regional distribution of technically recoverable conventional oil and gas resources (BGR 2009)

4.2.2 Recovery Factor

Recovery factor (RF) is the ratio of the volumes of technically producible oil (or gas) from a reservoir to the oil (or gas) originally in place. Laherrère (2006) reported the distribution of recovery factors from 11,500 oil fields and 8,560 gas fields outside the onshore United States (**Figure 4.3**). The values for oil recovery factor have a wide range but the average is about 25%. For gas fields, 10% of the 8,560 fields have a RF of less than 30%, 50% have a RF of less than 66% and 90% have a RF less than 80%. We fitted these data to determine that the best fitting distribution functions for gas and oil recovery are Weibull and normal distribution functions, respectively (Figure 4.3).

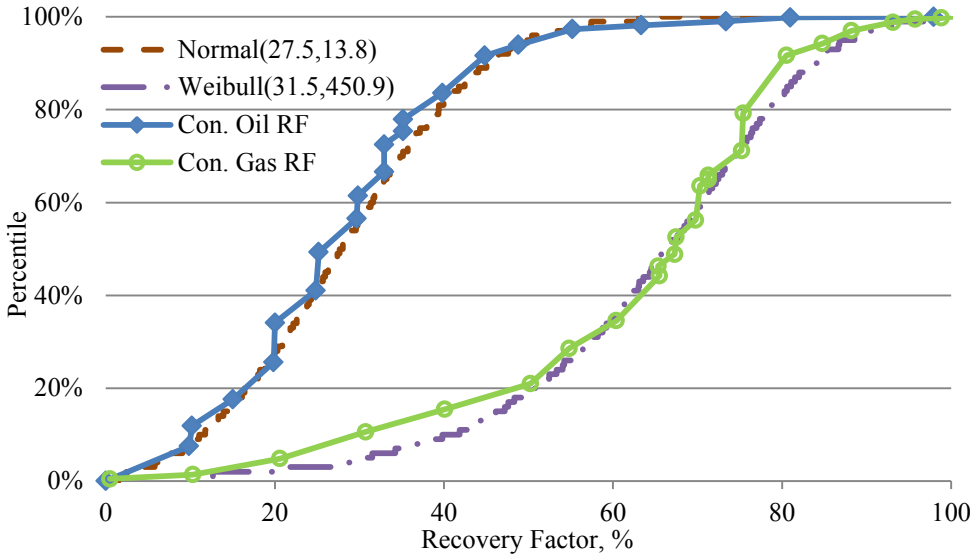

Figure 4.3—Probability distributions of conventional oil and recovery factors (Laherrere 2006)

4.2.3 Conventional Oil and Gas In-Place

Using Monte Carlo simulation, we have estimated the distributions of conventional OOIP and OGIP (**Figures 4.4 and 4.5**, respectively) by dividing technically recoverable resources of conventional oil and gas for each region (Figure 4.2) by the probability distribution functions of recovery factor (Figure 4.3). Note that P0 values in Figures 4.4 and 4.5 represent technically recoverable resources, and not cumulative production to date. **Table 4.2** lists P10, P50 and P90 values of conventional OOIP and OGIP for the seven global regions. Our estimated global resource endowments for conventional oil and gas are 36,000 (P10) - 137,200 (P90) Tcfe (6,561 (P10) - 25,005 (P90) Bboe) and 22,300 (P10) - 44,400 (P90) Tcf, respectively.

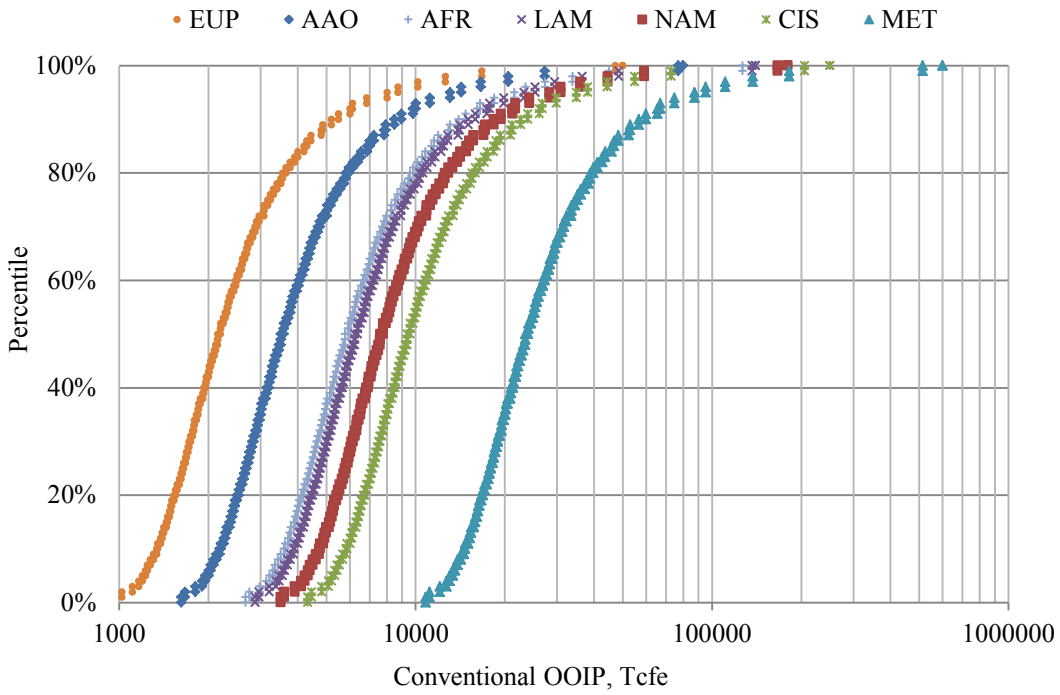

Figure 4.4—Probability distributions of conventional OOIP for 7 world regions

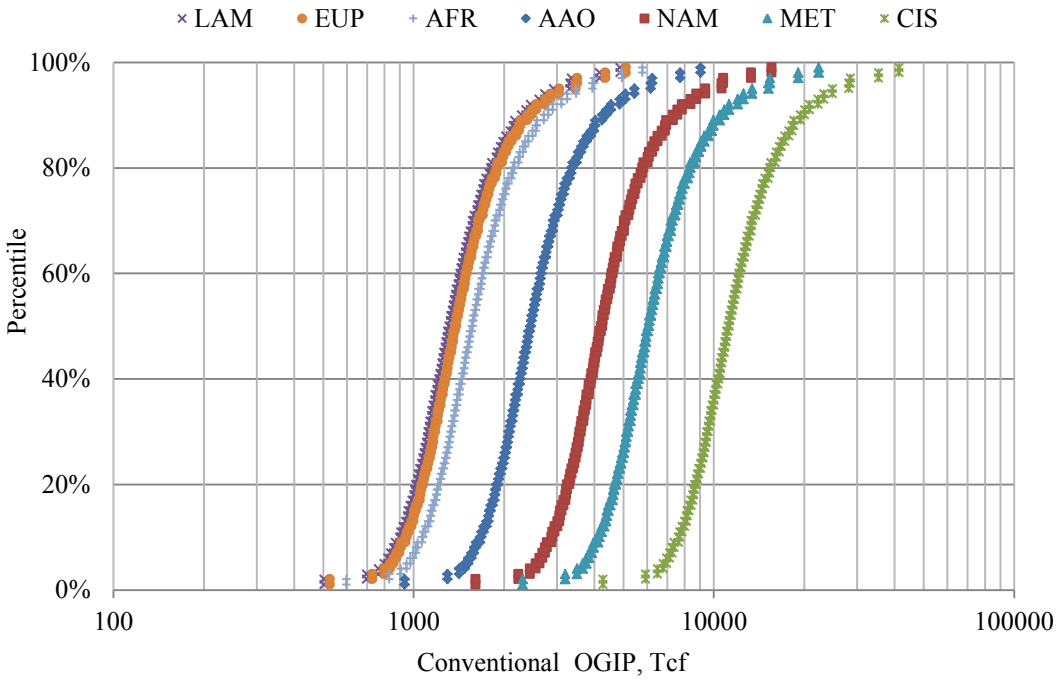

Figure 4.5—Probability distributions of conventional OGIP for 7 world regions

Table 4.2—Assessment result for conventional oil and gas worldwide

Region	TRR of Conventional Oil, Tcfe	Conventional OOIP, Tcfe			TRR of Conventional Gas, Tcf	Conventional OGIP, Tcf		
	(BGR, 2009)	P10	P50	P90	(BGR, 2009)	P10	P50	P90
CIS	2,648	5,802	9,439	22,133	7,539	8,859	11,254	17,655
MET	6,625	14,519	23,621	55,387	4,071	4,784	6,077	9,534
NAM	2,148	4,707	7,658	17,955	2,842	3,340	4,243	6,656
AAO	992	2,174	3,537	8,294	1,648	1,937	2,460	3,860
AFR	1,635	3,583	5,830	13,670	1,054	1,239	1,574	2,469
EUP	607	1,331	2,165	5,076	929	1,092	1,387	2,176
LAM	1,762	3,860	6,281	14,727	887	1,043	1,324	2,078
Total	16,417	35,976	58,531	137,243	18,972	22,294	28,319	44,428

4.3 Unconventional OGIP in North America

To date, most exploration and development of unconventional reservoirs has been in North American basins. We have decades of data and publications on unconventional gas reservoirs, as well as conventional oil and gas reservoirs, for the 26 North American basins in Table 4.1. To determine the distribution of coalbed methane, tight sands gas and shale gas originally in place in North America, we reviewed resource assessments available in the published literature for these 26 North American basins.

4.3.1 Coalbed Methane OGIP

The most notable initial work on coalbed methane gas in place was performed by Rightmire et al. (1984). We have found no more recent systematic assessments of coalbed methane in place for the United States. Rather, there have been a series of individual basin assessments performed by a variety of investigators (**Table 4.3**). Alaska was included in this study, since it has significant coal in place. The results of these

assessments for North American basins, including Alaska, targeted in this study are presented in Table 4.3. If only one assessment was available for a particular basin, we used that assessment in our study. If multiple estimates for a given basin were available, we used the minimum and maximum value among these assessments to generate a gas-in-place range. **Figures 4.6** and **4.7** shows the geographic distribution of CBM OGIP in United States and Canada, respectively. The Rocky Mountain region contains massive volumes of coalbed methane. The total estimated coalbed methane in place for the North American basins is 1,763-2,343 Tcf (Table 4.3). This range not used directly in our study, but instead as a check of our assessments based on coal in place shown later in the paper. Of these basins, Alaska (1,045 Tcf), the Greater Green River basin (30-314 Tcf) and the Western Canadian Sedimentary basin (517 Tcf) have the greatest estimated North American coalbed methane in place.

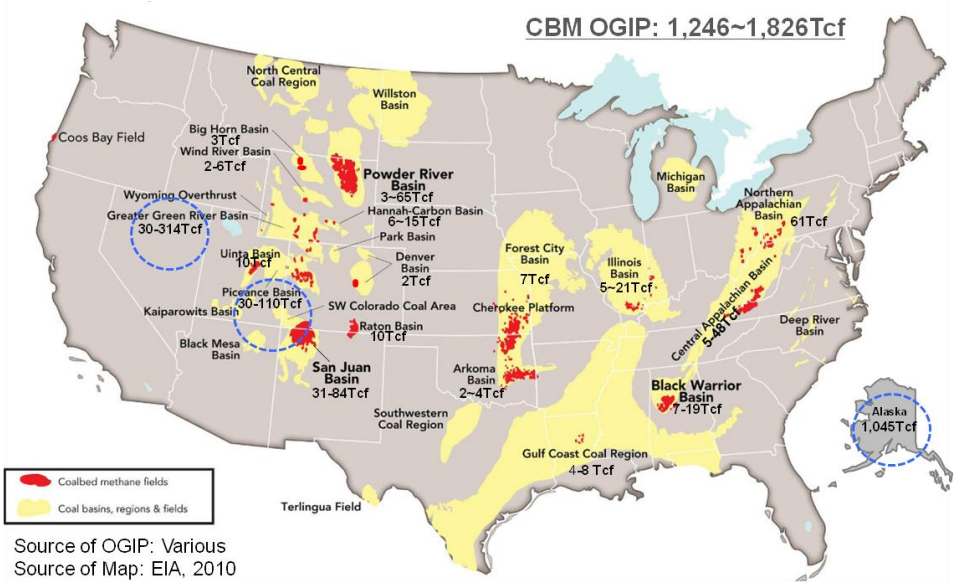

Figure 4.6—Graphic distribution of CBM OGIP in United States

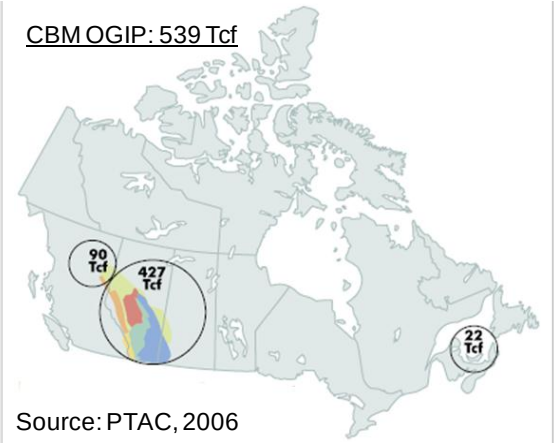

Figure 4.7—Graphic distribution of CBM OGIP in Canada

Table 4.3—Comparison of CBM OGIP assessments for North American basins, in Tcf

Basin	Rightmire et al. (1984)	Others		Used in this study
Northern APPB	61	61	(Kelafant et al. 1988)	61
Central APPB	10-48	5	(Kelafant and Boyer 1988)	5-48
ARKB	2-4			2-4
BHB		3	(Nelson 2000)	3
BWB	7-10	19	(McFall et al. 1986)	7-19
CHEB-FCB		7	(GRI 2001)	7
DENB	2			2
GGRB	30	314	(Tyler 1994)	30-314
ILLB	5-21			5-21
PRB	3-65	61	(ARI, 2002)	3-65
PICB	30-110			30-110
RATB	8-18			8-18
SJB	31	72-84	(Kelso et al. 1988; Crist et al. 1990)	31-84
WGC		4-8	(Reeves 2003)	4-8
UINB	1-5	10	(Tabet et al. 1995)	1-10
WRB	2	6	(GRI 2001)	2-6
WCSB		517	(PATC 2006)	517
Alaska		1,045	(Montgomery and Barker 2003; Barker 2002)	1,045
Total				1,763-2,343

4.3.2 Tight-Sands OGIP

The Federal Power Commission (FPC) estimated original gas in place of 600 Tcf in tight sands of the Greater Green River, Piceance, and Unita basins (Law 1993). The Federal Energy Regulatory Commission (FERC) accepted these tight sands gas estimates for the three basins appraised by the FPC and added 63 Tcf of original gas in place in the San Juan basin. This yielded a total OGIP estimate of 663 Tcf for the four basins (**Table 4.4**) (Law 1993).

Kuuskraa et al. (1978) conducted more detailed resource assessments of 9 basins in the western United States, for which they estimated a tight sands gas originally in place of 325 Tcf. The National Petroleum Council Committee (NPC) appraised 8 basins, also in the western US, and estimated a total of 227 Tcf of in-place gas (Law 1993) (Table 4.4).

Between 1987 and 1996, the Department of Energy (DOE) worked closely with the U.S. Geological Survey (USGS) to produce a series of detailed OGIP assessments for tight sands gas resources in key producing basins. These studies estimated 30 Tcf for the East Texas-Louisiana Mississippi Salt basins (Law 1993), 163 Tcf for the Appalachian basin (Law 1993), 335 Tcf for the Big Horn basin (Johnson et al. 1987), 422 Tcf for the Piceance basin (Johnson et al. 1987), 944 Tcf for the Wind River basin (Johnson et al. 1996), and 5,063 Tcf for the Greater Green River basin (Law et al. 1989). Later, the DOE confirmed prior estimates of vast volumes of OGIP in the Greater Green River and Wind River basins by analyzing more than 500 well logs. Thus, these two

assessments were given preferences. Besides, DOE added 2,530 Tcf of in-place gas in the Anadarko basin and 1,719 Tcf in the Unita basin (Table 4.4) (Boswell 2005).

Table 4.4 presents the tight sands gas resource estimates compiled for the 14 basins used in this study. If only one assessment was available for a particular basin, we used that assessment in our study. If multiple assessments were available for a basin, we used them to generate a gas-in-place range for the basin, in some cases giving preference to more recent (and typically larger) assessments, such as Greater Green River basin (GGRB). Simply summing the minimum and maximum values for each basin yields an overall range of 8,748-13,105 Tcf in place for North American basins. Approximately 90% of the resources occur in the "big five" basins (Greater Green River, Anadarko, Unita, Western Canadian Sedimentary, and Wind River basins). **Figures 4.8** and **4.9** shows the geographic distribution of tight-sands OGIP in United States and Canada, respectively.

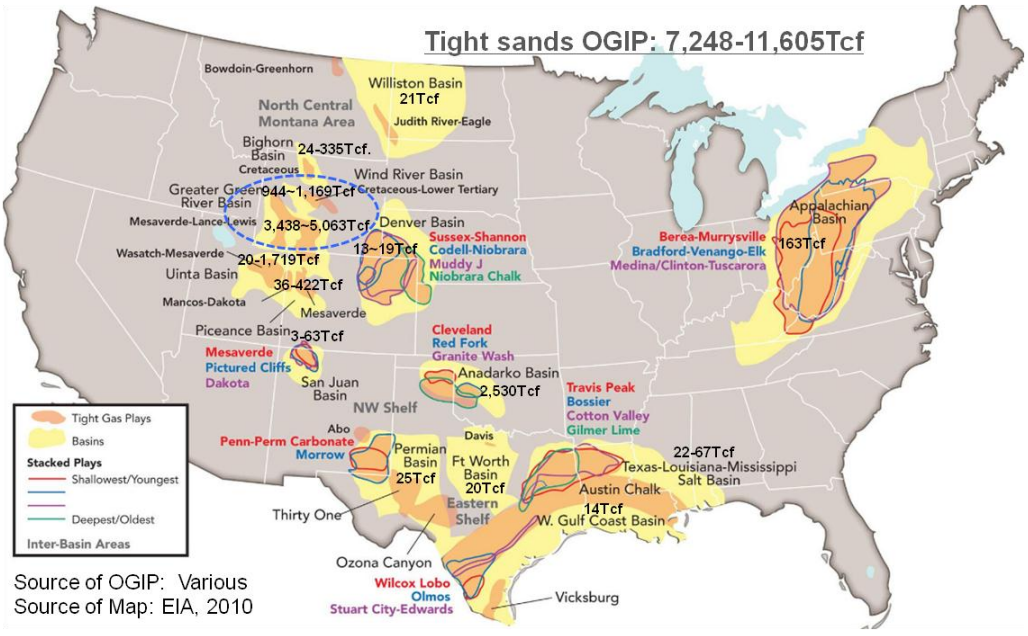

Figure 4.8—Graphic distribution of tight-sands OGIP in United States

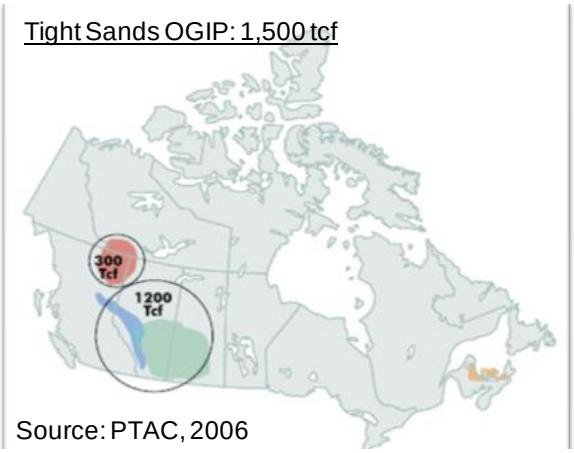

Figure 4.9—Graphic distribution of tight-sands OGIP in Canada

The resource endowment assessments reported for these 14 basins have increased significantly over the past decade, and greatly exceed Rogner's 1997 estimate of 1,371 Tcf for the total North American tight sands gas resource endowment. If the increase in North America holds for other plays around the world, Rogner's global resource endowment estimate for tight sands gas will prove to be very conservative.

The range reported in Table 4.4 (8,748-13,105 Tcf) is not a proper statistical aggregation. Indeed, we do not believe it is possible to do a proper statistical aggregation. The range was generated from multiple assessments by different organizations at different times with different data using different (and mostly deterministic) methodologies. While we believe this range provides a general indication of the uncertainty in North American tight gas sands resources, we do not believe it represents the true distribution. We believe that the range underestimates the uncertainty, so we arbitrarily decided that it represents a 50% confidence interval. In other words, we believe there is a 25% probability that the volume of OGIP in tight sands is less than or equal to 8,748 Tcf (P25), and a 75% probability that the volume is less than or equal to

13,105 Tcf (P75) in North America. Because we believe there is more uncertainty on the upside and because natural resources are usually lognormally distributed, we fit the two endpoints of the range with a lognormal distribution. The lognormal distribution fit to these two points has a mean of 11,300 Tcf and standard deviation of 3,400 Tcf (**Figure 4.10**). This distribution was used in the rest of our global tight sand OGIP analysis.

Table 4.4—Comparison of tight-sands OGIP assessments for North American basins, in Tcf

Basin	FERC (Law 1993)	Kuuskraa et al. (1978)	NPC (Law 1993)	DOE (Boswell 2005)	Others		Used in this study
ANAB				2,530			2,530
APPB					163	(Law 1993)	163
BHB		24			335	(Johnson et al. 1987)	24-335
DENB		19	13				13-19
ETB-LMS		67	22		30	(Law 1993)	22-67
FWB					20	(Thomas 2003)	20
GGRB	240	90	136	3,438	5,063	(Law et al. 1989)	3,438-5,063
SJB	63	15	3				3-63
UNIB	210	50	20	1,719			20-1,719
PICB	150	36	49		422	(Johnson et al. 1987)	36-422
WRB		3	34	1,169	944	(Johnson et al. 1996)	944-1,169
WILB		21					21
WCSB					1,500	(PACT 2006)	1,500
WGC			14				14
Total	663	325	227	8,856	6,957		8,748-13,105

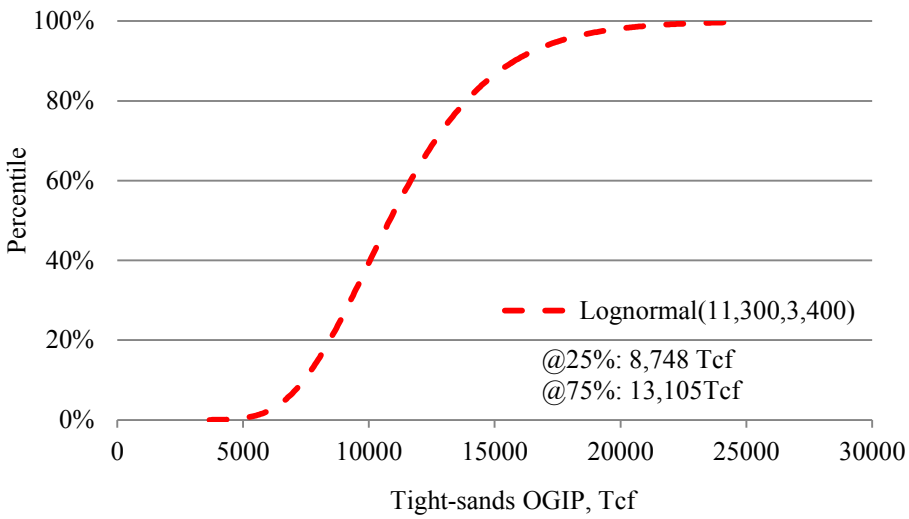

Figure 4.10—Probability distribution of tight-sands OGIP in North America

4.3.3 Shale-Gas OGIP

Shale gas is the most rapidly expanding source of gas production in North America today. Smead and Pickering (2008) estimated shale gas in place of 833 Tcf for 8 US basins (**Table 4.5**). Kuuskraa (2009) completed in-depth, basin-level assessments for seven gas shales in six North American basins. He estimated the resource endowment in these six basins is 4,789 Tcf. In the same year, DOE (2009) estimated the OGIP in Antrim and New Albany shales at 76 and 160 Tcf, respectively. Formations prospective for shale in the Western Canadian Sedimentary Basin potentially contain 1,380-1,490 Tcf of shale gas (EIA 2011a; Kuuskraa 2009).

Table 4.5 presents the shale gas resource estimates compiled for the 15 basins used in this study. **Figures 4.11** and **4.12** shows the geographic distribution of shale-gas OGIP in United States and Canada, respectively. If only one assessment was available for a particular basin, we used that assessment in our study. If multiple assessments were

available for a basin, we used the minimum and maximum value among these assessments to generate a gas-in-place range. The OGIP of in the Marcellus shale in Appalachian basin has been estimated to be 1,500 Tcf by DOE (2009) and 2,100 Tcf by Kuuskraa (2009). Williams (2006) reported the shale-gas OGIP in the Ohio shale in the Appalachian basin at 225-248 Tcf. Combining these two estimates result in a range of OGIP of 1,725 to 2,348 Tcf in the Appalachian basin for this study. Besides, the OGIP in the Fayetteville shale in the Arkoma basin has been estimated to be 52 Tcf by DOE (2009) and 320 Tcf by Kuuskraa (2009). The OGIP in the Woodford shale of the Arkoma basin was reported to be 23 Tcf (Smead and Pickering 2008). Thus, shale-gas OGIP in the Arkoma basin was added to be 75 to 343 Tcf for this study.

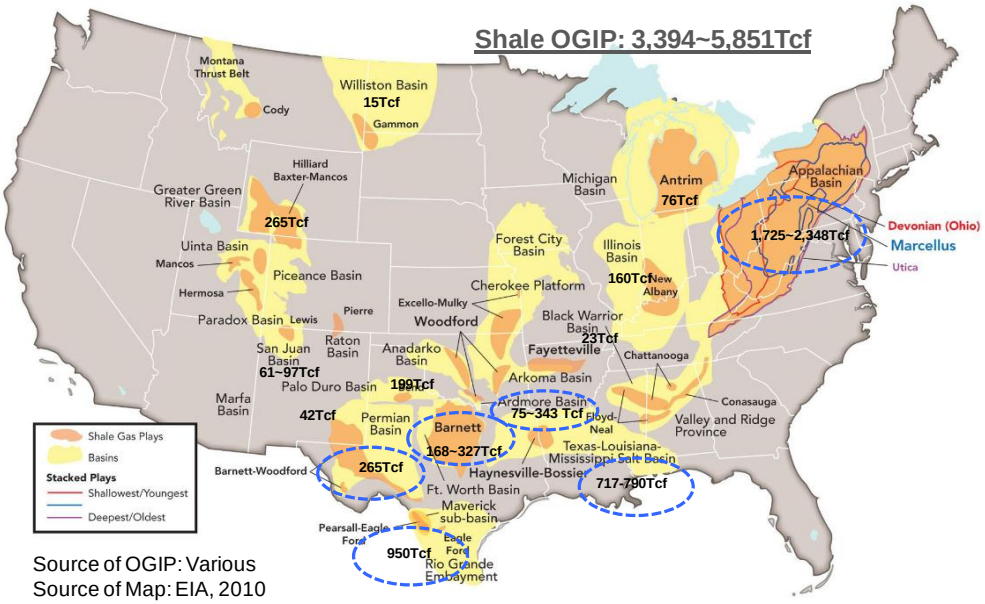

Source of OGIP: Various
Source of Map: EIA, 2010

Figure 4.11—Graphic distribution of shale-gas OGIP in United States

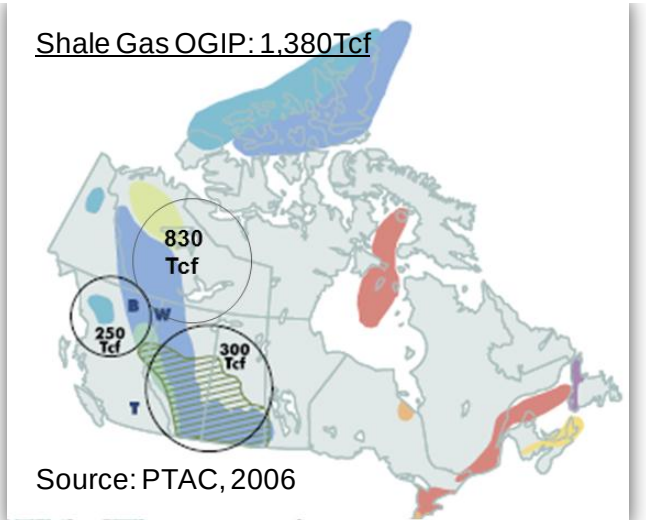

Figure 4.12—Graphic distribution of shale-gas OGIP in Canada

Table 4.5—Comparison of shale-gas OGIP assessments in North American basins, in Tcf

Basins	Smead and Pickering (2008)	Kuuskraa (2009)	DOE (2009)	Others		Used in this study
ANAB		199				199
APPB		2,100	1,500	225-248	(Williams 2006a)	1,725-2,348
ARKB	23	320	52			75-343
BWB	23					23
DENB	13					13
ETB-LMS		790	717			717-790
FWB	168	250	327			168-327
GGRB	265					265
ILLB			160			160
MICB			76			76
PERB	265					265
SJB	61			97	(Petzet 2007)	61-97
WGC				950	(Hill and Nelson 2000)	950
WIL	15					15
WCSB		1380		1,490	(EIA 2011a)	1,380-1,490
TOTAL	833	4,789	2,832	4,774	(EIA 2011a)	4,774-7,341

The total volume of original shale gas in place for the 15 North American basins was estimated to be 4,774-7,341Tcf (Table 4.5). This range obtained from more recently published assessments exceeds Rogner's (1997) estimate for total North America shale gas resources of 3,840 Tcf. The growth in estimated shale gas resource endowment will likely continue, driven by more intense development of existing shale-gas plays as well as the discovery of new plays in North America. We believe that the range underestimates the uncertainty as well, so we arbitrarily decided that it represents a 50% confidence interval. A lognormal distribution was fitted to these two points, which yielded a mean of 6,260 Tcf and standard deviation of 2,040 Tcf (**Figure 4.13**).

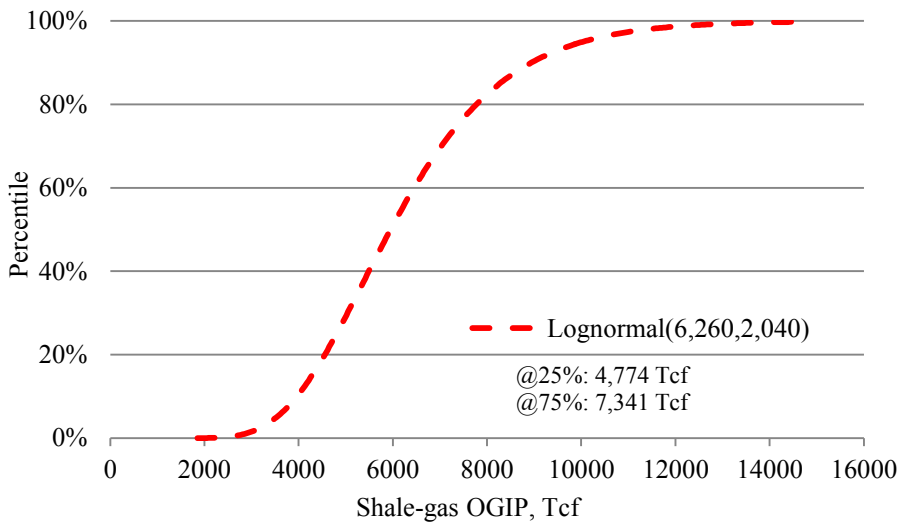

Figure 4.13—Probability distribution of original shale gas in place in North America

4.4 Global Unconventional Gas Resource Assessments

The next step in our study was to use the information from unconventional resources in the North America to estimate the volume of unconventional resources in

the rest of the world. To do so, we established the quantitative relationships between unconventional gas (coalbed methane, tight sands gas and shale gas) and conventional hydrocarbon (coal, conventional gas and oil) resource endowments in the North America in the form of distributions. These distributions calculated for North America are used in the next section to estimate how much unconventional gas is likely to be in place in different regions of the world.

4.4.1 Global Coalbed Methane OGIP

Figure 4.14 shows the regional distribution of original coal in place for 7 regions around the world. North America, including Alaska, has the largest coal in place (8.35 trillion metric ton) (BGR 2009).

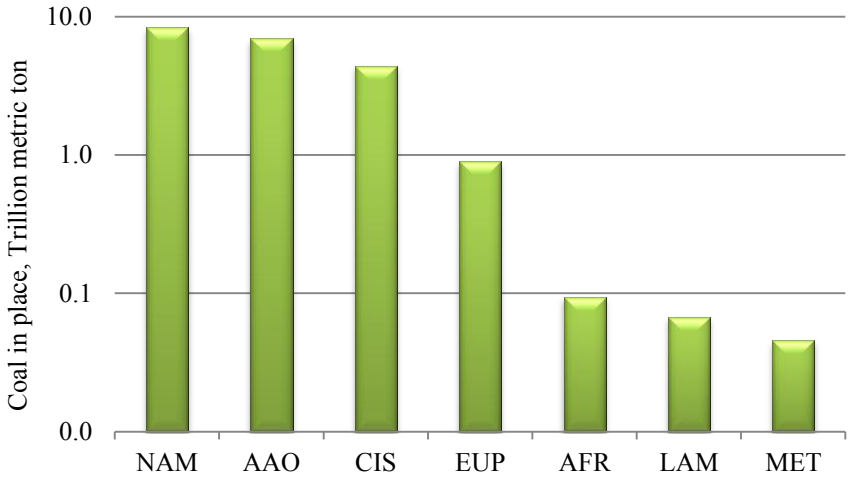

Figure 4.14—Regional distribution of global original coal in place (BGR 2009)

A in Eq. 3.1 is the gas content of coal, which is usually expressed in scf gas/ton of coal. The in-situ gas content value was obtained from published reports. The gas content ranges from 30 to 700 scf/ton for most coal seams in North America (**Table 4.6**).

We fit the average values of gas content listed in Table 4.6 with a Weibull distribution function (**Figure 4.15**). Ten percent of the coals have gas content less than 62 scf/ton, 50% have less than 192 scf/ton, and 90% have less than 392 scf/ton.

Table 4.6—Gas content of producing coalbed methane basins in North America, in scf/ton

Basins	Data Source	Minimum	Maximum	Average
Powder River	Byrer et al. 1982	13	35	24
Illinois	Byrer et al. 1982	40	150	95
Arkoma	Byrer et al. 1982	73	672	372.5
Greater Green River	Byrer et al. 1982	2	524	263
Warrior	Byrer et al. 1982	19	102	60.5
Piceance	Byrer et al. 1982	1	290	145.5
Northern Appalachian	Byrer et al. 1982	33	426	229.5
Central Appalachian	Byrer et al. 1982	250	700	475
San Juan	DOE 2004	350	450	400
Uinta	DOE 2004	250	400	325
Raton	DOE 2004	50	400	225
Alberta Plains Shallow	Allan 2004	25	120	72.5
Alberta Plains Deep	Allan 2004	150	350	250
WCSB mountains and foothills	Allan 2004	50	350	200
Restricted basins-B.C.	Allan 2004	25	250	137.5

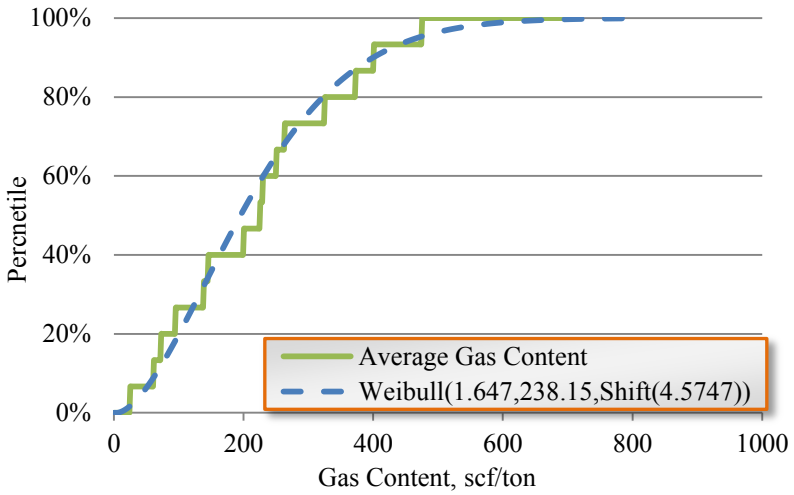

Figure 4.15—Probability distribution of the average gas content in coal in North America

Based on the assumption that gas content values in coal occurrences outside North America are distributed the same as in North America, we calculated the coalbed methane in place by multiplying coal in place values (Figure 4.14) with the distribution function of gas content (Figure 4.15). Thus, the distributions of coalbed methane resource endowments were determined for each region (**Figure 4.16)**.

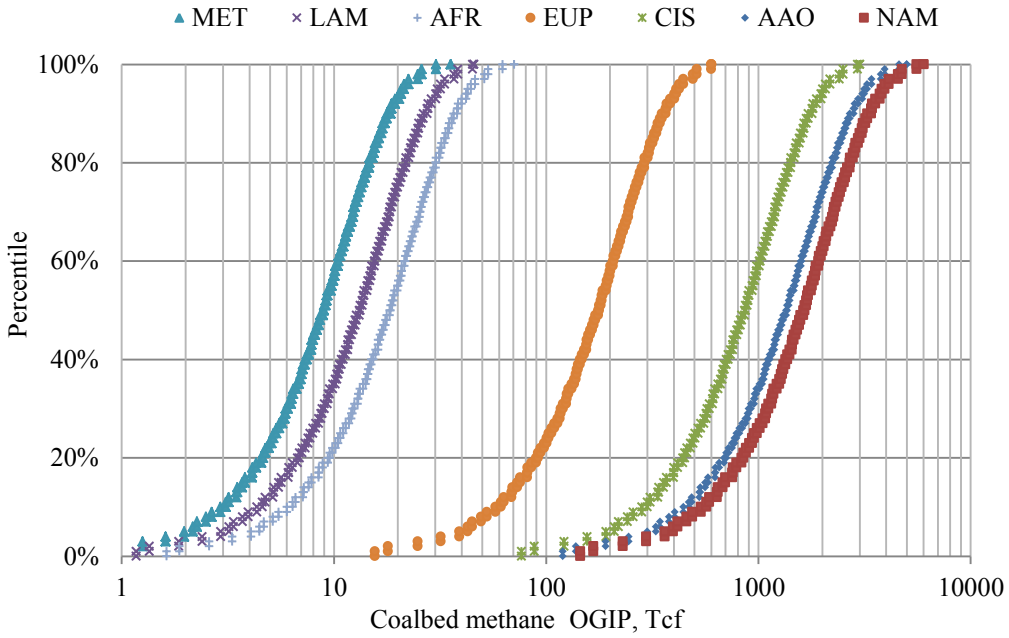

Figure 4.16—Probability distributions of CBM OGIP for 7 world regions

According to our region-by-region assessment, the coalbed methane resource endowment is 1,000 (P10)-8,000 (P90) Tcf worldwide (**Table 4.7**). North America has the largest coalbed methane in place, followed by AAO and CIS. Note that the coalbed methane resource assessment for North America includes Alaska. As a point of comparison, another country-level study by Kuuskraa (2009) estimated that coalbed methane OGIP in the world is 2,540 to 7,630 Tcf. The North American CBM OGIP (1,763-2,343 Tcf) listed in Table 4.3 falls between the 535 (P10) and 3,259 (P90) Tcf estimated by this regional study in Table 4.7.

Table 4.7—Assessment results of CBM OGIP worldwide

Region	Original coal in place, Trillion metric ton	Coalbed methane OGIP by this study, Tcf		
	BGR (2009)	P10	P50	P90
NAM	8.35	535	1,629	3,259
AAO	6.91	443	1,348	2,696
CIS	4.40	282	859	1,717
EUP	0.9	58	176	351
AFR	0.09	6	18	37
LAM	0.07	4	13	26
MET	0.05	3	9	18
World	20.76	1,331	4,052	8,105

4.4.2 Global Tight-Sands OGIP

Since the distribution of conventional gas in place (Figure 4.5) and tight sands gas in place (Figure 4.10) of North America have been determined, we used Monte Carlo simulation to calculate the distribution of the ratio 'B' using Eq. 3.2. The best fitting probability distribution function is a logistic distribution (**Figure 4.17**). The P90, P50 and P10 of this ratio are 3.7, 2.5 and 1.2, respectively.

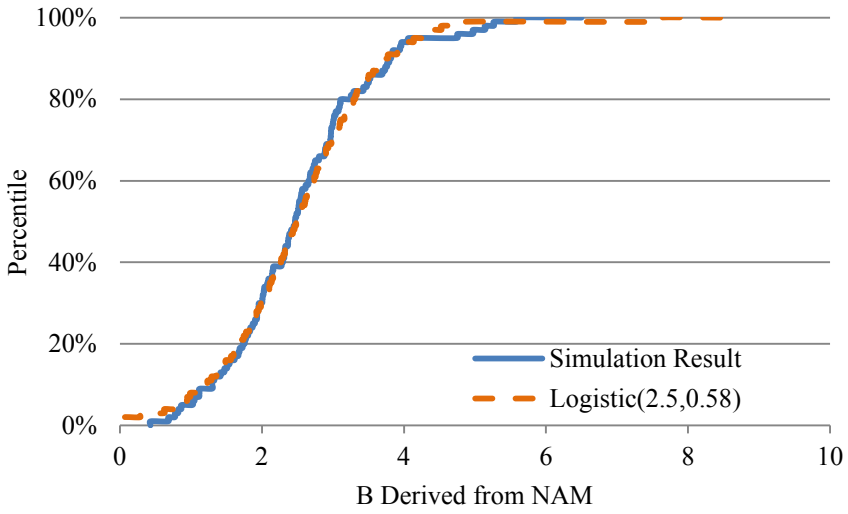

Figure 4.17—Probability distribution of the ratio B in North America

Multiplying the distribution function of the ratio B (Figure 4.17) with conventional OGIP assessments (Figure 4.5) for the other 6 global regions, the distributions of tight sands gas in place were estimated for each region (**Figure 4.18)**. Our total global tight sands gas resource assessment ranges from 49,000 Tcf (P10) to 104,000 Tcf (P90) (**Table 4.8**). Significant tight sands gas resources exist in the CIS countries and Middle East (Figure 4.18 and Table 4.8).

Table 4.8—Assessment results of tight-sands OGIP worldwide, in Tcf

Region	P10	P50	P90
CIS	19,489	28,604	41,508
MET	10,524	15,447	22,415
NAM	7,348	10,784	15,649
AAO	4,260	6,253	9,074
AFR	2,726	4,000	5,805
EUP	2,402	3,525	5,116
LAM	2,293	3,366	4,885
World	49,042	71,981	104,451

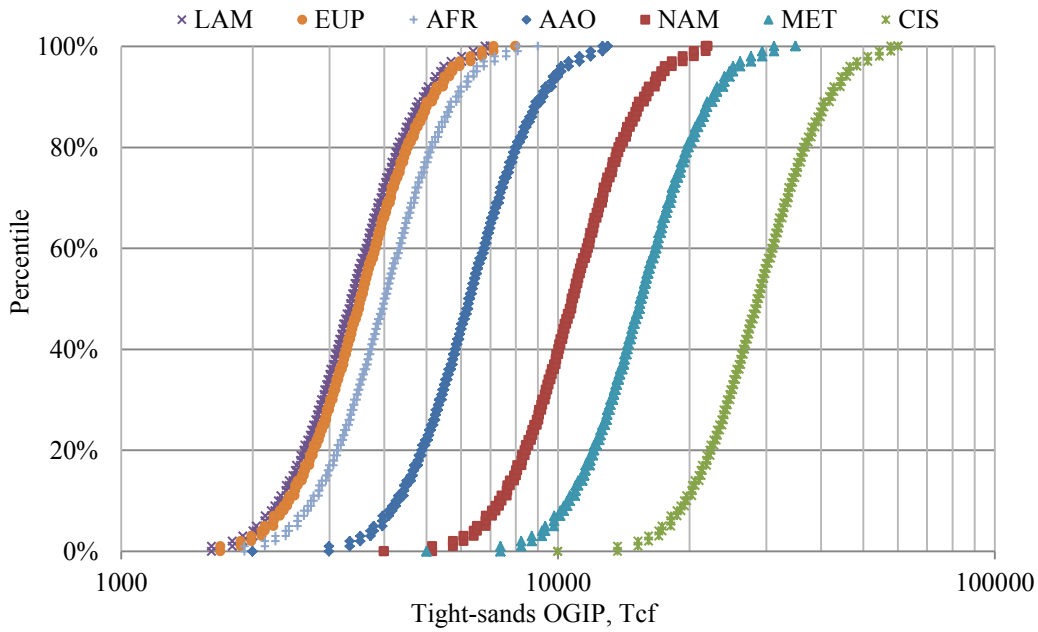

Figure 4.18—Probability distributions of tight-sands OGIP for 7 world regions

4.4.3 Global Shale-Gas OGIP

C in Eq. 3.3 is the ratio of the sum of coalbed and shale-gas OGIP to the sum of tight-sands OGIP, conventional OOIP, and conventional OGIP. Since the distributions for conventional oil (Figure 4.4), conventional gas (Figure 4.5), tight sands gas (Figure 4.10), shale gas (Figure 4.13), and coalbed methane (Figure 4.16) in place in North America have been determined, the distribution of the ratio C was calculated by Monte Carlo simulation using Eq. 3.3 (**Figure 4.19)**. The best fitting distribution function for the simulation result was a lognormal distribution, with a range from 0.01 to 0.83. The range implies that these source rocks would dispel hydrocarbons into the reservoir rocks rather than retain them.

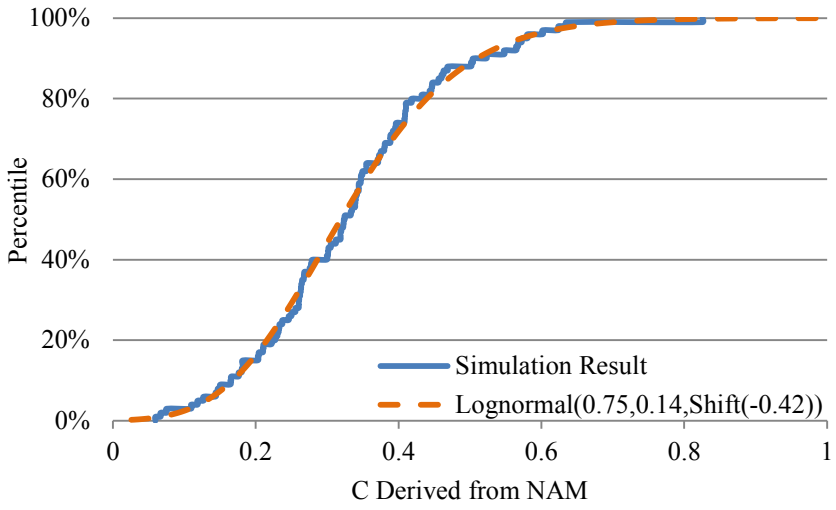

Figure 4.19—Probability distribution of the ratio C in North America

Applying the distribution function of the ratio C to the remaining six regions, Monte Carlo simulation was used to determine the distributions of shale gas in place for each region using Eq. 3.3 (**Figure 4.20)**.

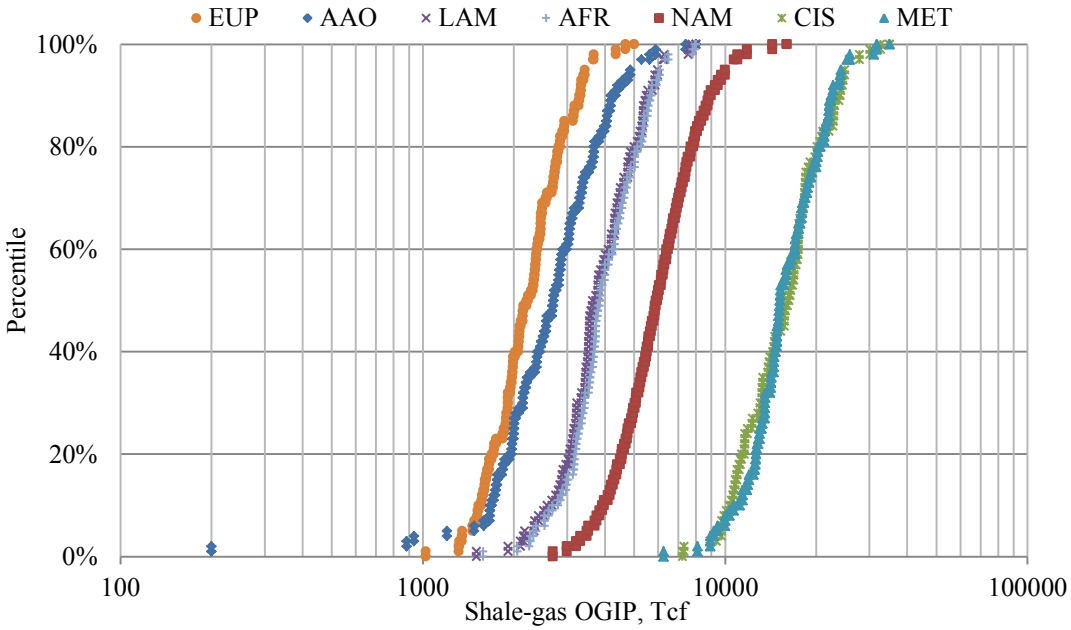

Figure 4.20—Probability distributions of shale-gas OGIP for 7 world regions

According to our study, global shale gas in place ranges from 33,000 (P10) to 72,000 (P90) Tcf (**Table 4.9**). Although the only significant production of shale gas is from North America currently, additional huge shale gas resources are expected in the Middle East and CIS.

Table 4.9—Assessment results of shale-gas OGIP worldwide, in Tcf

Region	P10	P50	P90
MET	10,803	15,416	22,285
CIS	9,852	15,880	21,972
NAM	3,950	5,905	8,878
AFR	2,730	3,882	5,586
LAM	2,659	3,742	5,372
AAO	1,405	2,690	4,447
EUP	1,607	2,194	3,125
World	33,005	49,709	71,667

4.5 Discussion

We used published assessments of North American conventional and unconventional resources to estimate most likely values of unconventional gas in place resources in 7 global regions. According to our study, large volume of shale gas resources is expected in the CIS and Middle East. Although the only significant production of shale gas is from North America currently, there is strong evidence that shale gas exists in every geologic basin that has significant deposits of shale and significant volumes of conventional oil and gas. The extent to which these shale deposits will affect the overall gas supply balance will largely depend on the speed at which exploration efforts advance. Shale gas will be developed only when the economics are

favorable and there is a market. However, we believe the gas is there to be developed when it becomes economic to do so and the proper drilling and completion technologies are available for use in the part of the world where the opportunity exists. It remains to be assessed how much of these in-place resources can be technically and economically recovered.

While a more robust evaluation that involves integrated basin-by-basin assessment of basin type, reservoirs, source rocks and resources may result in somewhat different results, that approach was impractical for this global study, This study considered only coal beds and shales as source rocks when calculating shale gas resources. Future work may include the contributions of carbonate source rocks and evaluate heavy oil and shale oil in-place resource.

We used our best judgment regarding the factors that affect how gas in place is distributed. While we attempted to quantify the uncertainty in our assessments, we suspect that there is likely more uncertainty than is represented in the distributions presented. However, we hope as more data (such as gas content of coal seams from other regions) are collected and published globally, we and others can continue to improve these estimates.

4.6 Summary

Our assessment of regional unconventional gas and conventional hydrocarbons (oil plus gas) in place (**Table 4.10)** indicate that 83,000 (P10)-184,000 (P90) Tcf of unconventional gas and 58,000 (P10)-182,000 (P90) Tcf of conventional hydrocarbons

exist worldwide. Several regions have more unconventional gas resources than conventional hydrocarbons, such as CIS, Middle East, AAO, and LAM. The reason is there is more tight sands gas in place than conventional hydrocarbon in these regions. However, more hydrocarbons were dispelled into conventional reservoir rocks rather than tight sands gas reservoirs in the rest of three regions.

Table 4.10—Summary of conventional hydrocarbons and unconventional gas by region

Region	Total unconventional OGIP, Tcf			Conventional hydrocarbons (oil plus gas) in-place, Tcfe		
	P10	P50	P90	P10	P50	P90
CIS	29,623	45,343	65,197	4,111	5,997	12,154
MET	21,330	30,872	44,718	8,047	11,900	24,612
NAM	11,833	18,318	27,787	14,661	20,693	39,788
AAO	6,108	10,291	16,217	4,903	7,605	16,805
AFR	5,461	7,901	11,428	19,303	29,699	64,922
LAM	4,957	7,122	10,283	2,422	3,552	7,252
EUP	4,066	5,895	8,592	4,822	7,404	16,139
World	83,378	125,742	184,222	58,268	86,850	181,671

The P50 of our estimated global unconventional gas in place (~126,000Tcf) is 4 times greater than Rogner's estimate of 33,000 Tcf (**Table 4.11**). We expect that large volumes of unconventional gas resources are likely to exist in the CIS and Middle East because they have a large endowment of conventional oil and gas.

Table 4.11—Comparison of region-level unconventional OGIP assessments, in Tcf

Region	Rogner (1997)				This study			
	Coalbed methane	Tight sands gas	Shale gas	Total	Coalbed methane (P50)	Tight sands gas (P50)	Shale gas (P50)	Total (P50)
AAO	1,724	1,802	6,151	9,677	1,348	6,253	2,690	10,291
NAM	3,017	1,371	3,840	8,228	1,629	10,784	5,905	18,318
CIS	3,957	901	627	5,485	859	28,604	15,880	45,343
LAM	39	1,293	2,116	3,448	13	3,366	3,742	7,122
MET	0	823	2,547	3,369	9	15,447	15,416	30,872
EUP	274	431	549	1,254	176	3,525	2,194	5,895
AFR	39	784	274	1,097	18	4,000	3,882	7,901
World	9,051	7,405	16,103	32,559	4,052	71,981	49,709	125,742

5. RESOURCE EVALUATION FOR SHALE GAS RESERVOIRS IN UNITED STATES

Many gas shale plays are currently under development in the United States. The U.S. has already experienced the "shale revolution", which saw shale gas production increase from 1% of overall U.S. gas consumption to 30% in 2011, with expectations for it to grow to 48% by 2035 (Figure 1.2). We have previously analyzed 15 basins in North America where shale gas resources have been evaluated and the results have been published in the section 4. The total volume of original shale gas in place for North America was estimated at 3,950 (P10)-8,878 (P90) Tcf (Table 4.9). It is clear that there are abundant volumes of natural gas in North America. In the section, we investigated drilling, stimulation and completion methods for shale gas in five key shale plays of the United States. Then, we applied workflow of UGRAS to assess the distribution of OGIP and TRR for the five key shale gas plays, and derived the representative distribution of recovery factor from shale gas plays.

5.1 Unique Properties of Shale

It is revealed that thickness, permeability, porosity, temperature, adsorbed gas, and vitrinite reflectance have the highest correlation to gas in place and gas production (Transform Software & Services 2011). These characteristics seem to be the greatest contributors to what makes a good shale gas reservoir.

5.1.1 Total Organic Carbon (TOC)

TOC, by convention in weight %, is the total amount of organic carbon in the rock. TOC relates to how much material there was to generate oil or gas and the adsorptive capacity of a shale to hold gas in the matrix, independent of porosity. Most gas shale plays are associated with the black, high TOC shale facies. Few are in the interbedded low TOC or "gray" shales, although these facies can be charged with gas from the black shale. TOC roughly correlates with high Gamma Ray, low bulk density, and high sonic travel time. Linear regressions against core data can provide reasonable first order estimates. Separating TOC from porosity can be problematic. Usually, gas content increases as the TOC increases.

5.1.2 Kerogen Type

Most production is found in marine shales with mostly oil prone, Type II Kerogen. Kerogen is gradually transformed as liquid and gaseous hydrocarbon is generated. TOC decreases as hydrocarbons are expelled from source rock; Kerogen moves from high H content to low H, OI also decreases (down and slightly to the left on VK diagrams); residual or spent Kerogen resembles Type IV with low HI and low OI (ultimately, graphite/pure C). Vitrinite reflectance (R_o) is a measure of the percentage of incident light reflected from a polished surface of vitrinite. It is a measure of the thermal maturity of a sedimentary rock containing kerogen. R_o is an indicator of whether a source rock has been heated enough to produce oil, oil and gas, or gas only (Cluff 2009).

5.1.3 Porosity

Shale porosity is not well understood. Core measurements indicate shales have 1 to 12% effective helium porosity, usually called gas filled porosity. These values of porosity do not count the pore space filled with clay bound water. Scanning Electron Microscopy (SEC) studies suggest much of this is associated with organic matter, but there is not a very good correlation between TOC and porosity. For logs both kerogen and porosity look about the same, so separating the two volumes is difficult.

5.1.4 Gas In Place

Gas in place is a combination of free gas in the matrix and adsorbed gas on the surface of the organics. Free gas becomes the dominant in-place resource for deeper, higher-clastic-content shales. Adsorbed gas can be the dominant in-place resource for shallow, organic-rich shales. Adsorbed gas-in-place is a function of organic matter type, maturity, organic content, and gas composition.

5.1.5 Geomechanical Properties

Brittlenness is critical to produce gas from shale. A brittle rock in an isotropic stress field tends to shatter when it is fractured. As the brittleness of the rock increases, the chance of making a successful well completion also increases. The brittleness index is a composite of Poisson ratio and Young's modules. The in-situ stress field is also a key parameter to determine the energy required to fracture treat the rock.

5.2 Drilling, Stimulation and Completion Methods in Shale Gas Reservoirs

Long horizontal wells (3,000-10,000 ft) are designed to place the gas production well in contact with as much of the shale matrix as technically and economically feasible. Large volume hydraulic fracture treatments, conducted in multiple, closely spaced stages (up to 20 stages), are designed to "fracture" the shale matrix and create permeable flow paths from the reservoir to the wellbore. The production from the hydraulically fracture treated well depends upon the mineralogy of the shale, particularly its relative quartz, carbonate and clay contents.

- Shale with a high percentage of quartz and carbonate tend to be brittle and will "shatter", leading to a vast array of small-scale induced fractures providing numerous flow paths from the matrix to the wellbore.
- Shale with high clay content tend to be ductile and to deform instead of shattering, leading to relatively few induced fractures.

Initially, cemented liners and multi-stage fracturing techniques were used in the Barnett shale (**Figure 5.1a**). This type of completion involves cementing casing in the horizontal wellbore and using "plug and perforation" stimulation. The inherent costs of multiple interventions with coiled tubing (CT), perforating guns and deployment of fracturing equipment needed for each stage are extremely high, not to mention very inefficient consuming. Production using this method can also be limited, since cementing the wellbore closes many of the natural fractures and fissures that would otherwise contribute to overall production (Lohoefer et al. 2010).

Between 2004 and 2006, a new open-hole, multi-stage system (OHMS) completion technology (**Figure 5.1b**) was run in Denton County, Texas (Lohoefer et al. 2006). This type of completion, on average, performed better than the cemented completion method (Lohoefer et al. 2010). The major advantage of OHMS is that all the fracture treatments can be performed in a single, continuous pumping operation without the need for a drilling rig, saving costs.

a) Cemented-liner, multi-stage fracturing method (Initial Barnett shale horizontal well completion)

b) Open-hole, multi-stage system (OHMS) completion (Latest Barnett shale horizontal well completion)

Figure 5.1—Lower-damage, more intensively stimulated horizontal well completions (Kuuskraa 2009)

5.3 Reservoir Model for Shale Gas Reservoirs

5.3.1 Reservoir Model

Typical completions for shale gas reservoirs are horizontal multi-stage fractured wells. As more knowledge is gained through micro-seismic monitoring of these fracture treatments, it appears that they are more likely creating a network of fractures. Thus, two permeabilities in gas shales need to be considered: matrix and system. System permeability is equivalent to matrix permeability plus the contribution of fracture network. Transient dual-porosity system (slab matrix blocks) has been used to model naturally fractured reservoirs (Kazemi 1969; Swaan 1976). The model can also be used

for modeling shale gas reservoirs where multi-stage fracture completions have created the fracture network. In the transient dual-porosity model, there are two transients-one moving through the fracture system, the second moving through the matrix toward the interior of the matrix blocks.

The transient dual-porosity (slab matrix blocks) model is characterized by the storativity ratio and the interporosity flow coefficient. The storativity ratio, ω, is the fraction of pore volume in the fractures as compared to the total pore volume (**Eq. 5.1**). The interporosity flow coefficient, λ, is proportional to the ratio of permeabilities between the matrix and the fractures (**Eq. 5.2**), and it determines the time when contribution from the matrix to the fractures becomes significant. A large value indicates that fluids flow easily between the two porous media, while a small value indicates that flow between the media is restricted. We can't find any literature reporting the value of λ and ω for the Barnett and Eagle Ford shales. The storativity ratio is usually in the range of 0.01 to 0.1. The interporosity flow coefficient for gas shales is usually in the range of 10^{-4} to 10^{-8}. These ranges are assumed to be representative of shales due to small pore volume of the fractures, and due to the large contrast between the permeabilities of the fractures and the matrix. The outer boundary is defined as a closed rectangle and the well is centered in the drainage area.

$$\omega = \frac{(\phi c_t)_f}{(\phi c_t)_f + (\phi c_t)_m} \tag{5.1}$$

$$\lambda = 4n(n+2)\frac{r_w^2}{L^2}\frac{k_m}{k_f} \quad \text{(For slab blocks, n=1)} \tag{5.2}$$

Table 5.1 lists the reservoir model used for shale gas reservoirs. Fractured shale is modeled as a transient dual porosity system (slab matrix blocks), with adsorbed gas. The adsorbed gas is assumed to be in equilibrium with the gas in the conventional pore system. The model is often pictured in terms of a layered reservoir, where a thin, high-permeability layer represents the fracture system, and a thick, lower permeability layer represents the matrix. The type of outer boundary for the shale gas reservoir is defined as closed rectangle. The well is centered in the drainage area.

Table 5.1—Reservoir model for shale gas reservoirs

Porosity	Transient dual porosity
Fracture Conductivity	Infinite
Inner Boundary	Horizontal with Transverse Fractures
Outer Boundary	Rectangle
Lithology	Shale
Pressure Step	Constant
Permeability	Isotropic
Well Location	Centered

5.3.2 Well Spacing Determination

We assumed the width of shale gas reservoir is 1,000 ft. For both sides, the margin from the end of horizontal well to the reservoir boundary is 400 ft (**Figure 5.2**). Thus, the well spacing is determined by the lateral length. **Table 5.2** lists the well spacing for the target shale gas plays. For example, the reservoir size is 4,800 ft × 1,000 ft (111 acres/well) for the Barnett shale since the average lateral length is 4,000 ft.

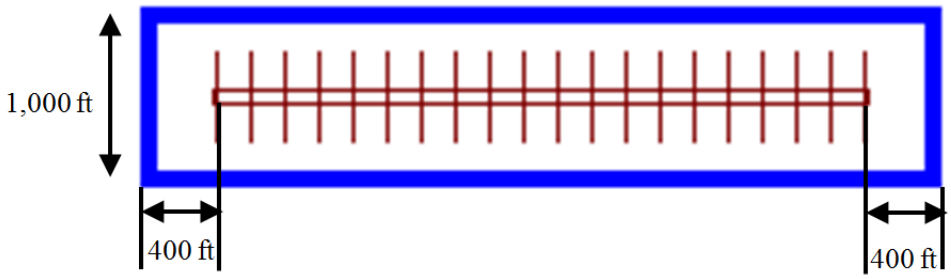

Figure 5.2—Well geometry for shale gas reservoirs

Table 5.2—Well spacing for the five target shale gas plays in the United States

Plays	Average Lateral Length, ft	Reservoir Size	Well Spacing, acres
Barnett	4,000	4,800 ft × 1,000 ft	111
Eagle Ford	5,600	6,400 ft × 1,000 ft	147
Marcellus	3,700	4,500 ft× 1,000 ft	104
Fayetteville	4,800	5,600 ft× 1,000 ft	129
Haynesville	4,700	5,500 ft× 1,000 ft	124

5.4 Reservoir Parameters Sensitivity Analysis

We investigated the essential reservoir properties that affect the prediction of OGIP or TRR from shale gas reservoirs. Fifteen different characteristics were analyzed. **Table 5.3** lists the primary properties. Beside area, net pay, porosity, and water saturation, shale-gas OGIP is affected by gas content. Gas production from shale gas reservoirs are affected most by completed gas-in-place resources, initial reservoir pressure, and gas desorption and diffusion characteristics, system permeability, and fracture half-length (**Figure 5.3**). Since Langmuir pressure controls the shape of the sorption curve, it impacts how fast gas content changes. Langmuir volume controls the endpoint of the Langmuir curve, but has almost no impact on the rate of change. Horizontal length and well spacing are controllable, we didn't consider them as

uncertain parameters. In this study, we only treat net pay, initial pressure, system permeability, porosity, water saturation and gas content as uncertain parameters.

Table 5.3—Data source for primary properties of shale gas reservoirs

Primary Property	Data Source	Controllable	Big Uncertainty
Thickness		No	Yes
Permeability	Core analysis, Well-test Analysis, Production analysis	No	Yes
Porosity	MICP, NMR, Log analysis	No	Yes
Water Saturation	PID, Openhole test	No	Yes
Gas Content	Desorption Canister Testing& Adsorption isotherms, Calibrated log analysis	No	Yes
Reservoir Pressure	PID, PITA, Openhole test	No	Yes
Fracture Half-length	Static: Post-fracture net-pressure analysis, post-fracture flow and buildup Flowing: Rate-transient analysis	No	No
Lateral Horizontal Length		Yes	No
Well Spacing		Yes	No

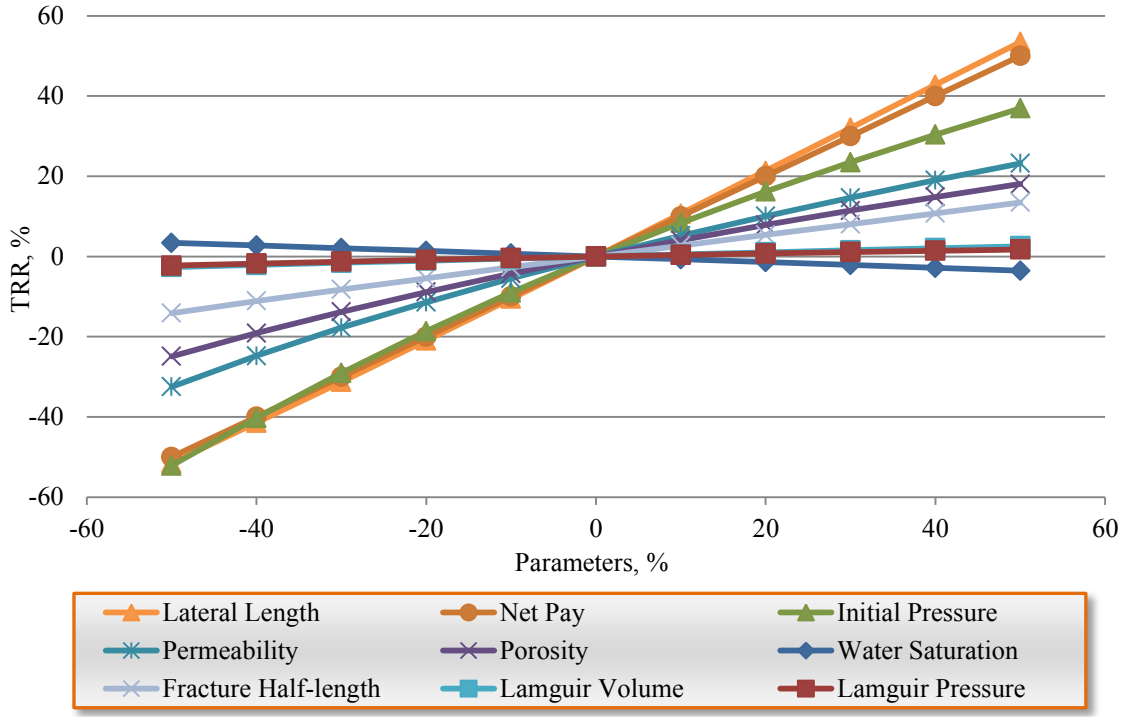

Figure 5.3—Sensitivity analysis result of shale gas TRR

5.5 Recent Production and Activity Trends

Between 2004 and 2011, shale gas production from the lower 48 states increased from 0.4 Tcf to 7.0 Tcf, and now accounts for 30 percent of total production (EIA 2012a). As of December 2011, the seven producing shale gas plays were Barnett, Haynesville, Marcellus, Fayetteville, Arkoma Woodford shale, Eagle Ford shale and Antrim shale (**Figure 5.4**).

The Barnett shale has been the country's leading shale gas producer during the past decade. Barnett shale production has grown from 0.06 Bcf in 2004 to 1,868 Bcf in 2011 (Figure 5.4). The Haynesville shale production in the East Texas-Louisiana-Mississippi Salt basin has skyrocketed from nothing in 2006 to produce 2,167 Bcf in

2011. Natural gas production from the Louisiana section of the Haynesville overtook the Barnett's volumes in early to mid-February of 2011 (**Figure 5.5**).

Unlike most other shale gas plays, the natural gas from the Antrim shale is biogenic gas generated by the action of bacteria on the organic-rich rock. The Antrim shale play is winding down as the economic limits have been reached.

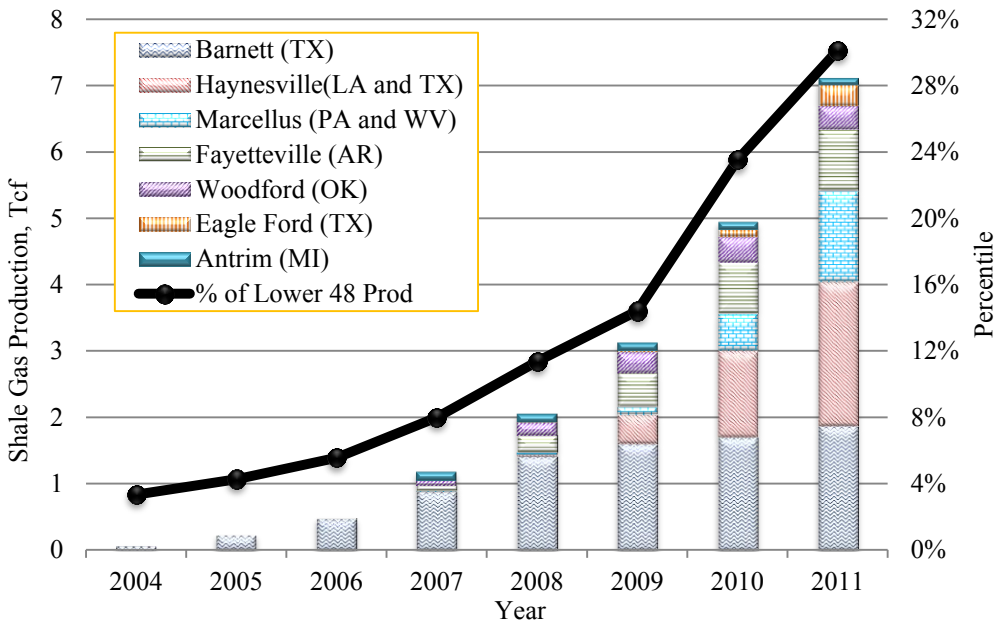

Figure 5.4—Shale gas annual production by plays (EIA 2012b)

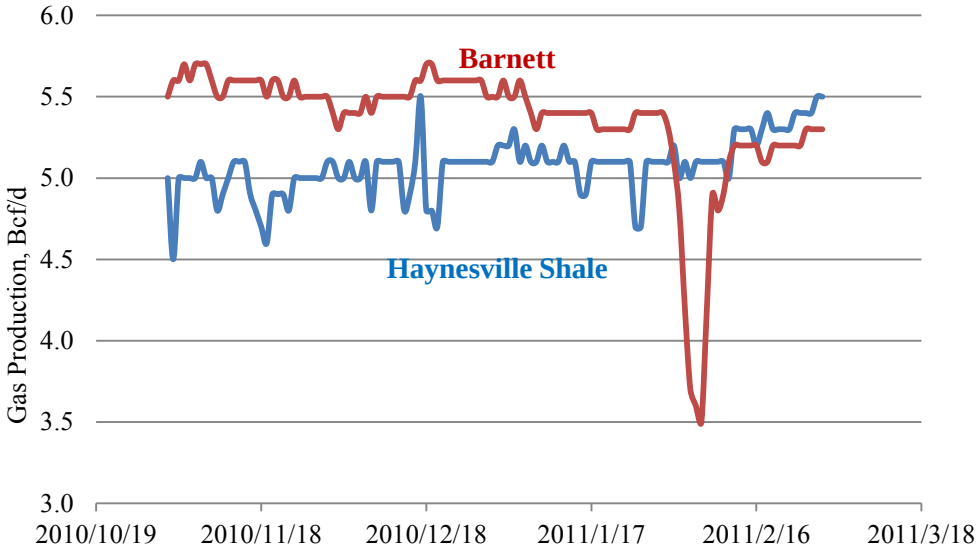

Figure 5.5—Haynesville shale gas production surpasses Barnett shale as the Nation's leading shale gas play (EIA 2011b)

5.6 Barnett Shale

The Barnett shale is an unconventional natural gas formation located in the Fort Worth basin of Texas. The Fort Worth basin is one of several that formed during the late Paleozoic Ouachita Orogeny, generated by convergence of Laurussia and Gondwana. It was part of the foreland basin situated on the southern leading edge of Laurussia (Bruner and Smosna 2010).

The Barnett shale consists of sedimentary rocks of Mississippian age (354-323 million years ago). The Mississippian stratigraphic section in the Fort Worth basin consists of limestone and organic-rich shale. The Barnett shale, in particular, consists of dense, organic-rich, soft, thin-beded, petroliferous, fossiliferous shale and hard, black, finely crystalline, petroliferous, fossiliferous limestone. The Barnett shale has acted as a source and sealing cap rock for more conventional oil and gas reservoirs in the area.

The formation underlies the city of Fort Worth and at least 17 counties. The size of the Barnett shale is approximately 3,200,000 acres (DOE 2009), and production occurs at depth from 6,500 to 8,500 feet (Hayden and Pursell 2005). The TOC by weight in the Barnett shale is reported to average 2.4-5.1%. The Barnett is a very good (TOC=2.4%) to excellent (TOC>4%) source rock in terms of its organic richness (Bruner and Smosna 2010). Thermal maturity increases toward the east-northeast. Vitrinite reflectance (R_o) ranges from 0.6 to 1.6% (Jarvie et al. 2004). The average bulk density of the Barnet shale is 2.5 g/cc (Kuuskraa et. al 1998). The Barnett shale is dominated by clay- and silt-size sediment with occasional beds of skeletal debris.

5.6.1 Production

The Barnett Shale produces primarily dry gas. In this work, we have only looked at the gas production and have not included any wells that may be in the oil window. Vertical wells were first drilled in the Barnett shale in the early 1980s, but development of the Barnett shale play was not seriously considered until almost two decades later with the advent of horizontal drilling in 2003 (**Figure 5.6**). As of December 2011, the Barnett shale play had over 12,561 wells, including 9,449 horizontal wells and 3,112 vertical wells. Over 8,270 Bcf of gas has been produced, of which 75% is from horizontal wells. Average daily gas production is 5.2 Bcf/d in 2011.

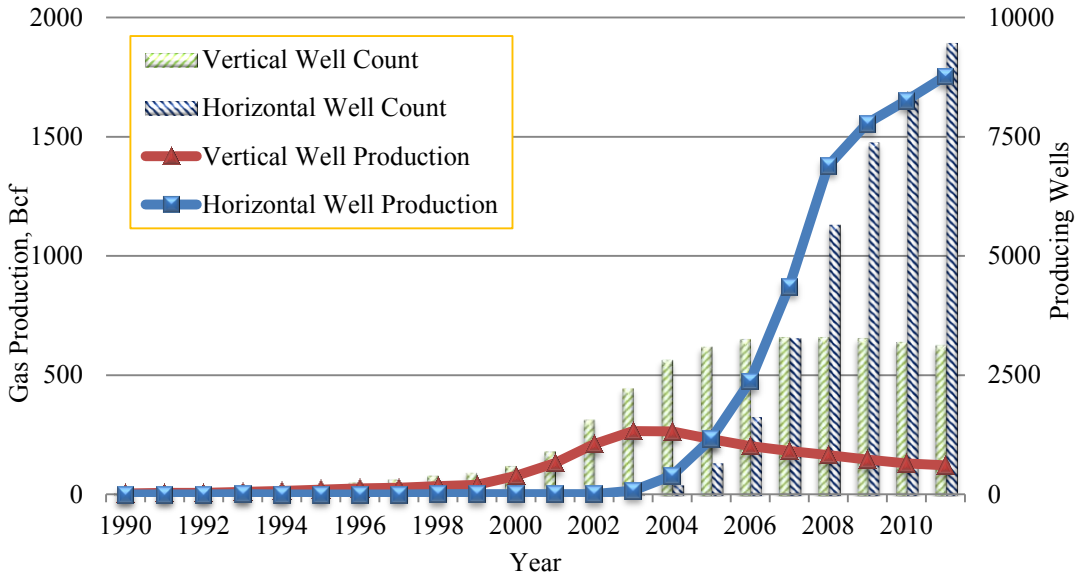

Figure 5.6—Gas production has rapidly increased in Barnett shale by horizontal wells (EIA based on HPDI 2011)

5.6.2 Well Drilling and Completion Processes

Horizontal wellbores are typically oriented northwest to southeast to take advantage of natural fracture orientation in the Barnett shale (Hale 2010). Across the Barnett shale, current best practice is to drill long horizontal wells with at least 60 to 160-acre spacing. Lateral lengths increased from about 3,000 ft in 2003 to as long as 8,965 ft in 2009 (Powell 2010). Typical fracture half-length of the Barnett shale is between 300 and 400 ft, with 7 to 9 fracture stages (Kennedy 2010).

5.6.3 Reservoir Parameters

Both thickness and reservoir pressure increase in the SE-NE direction, implying a significant increase in potential production rate from SW to NE. The thickness of the Barnett shale is from 100-600 feet (Grieser et al. 2008; Hayden and Pursell 2005).

Pressure gradient is in the overpressured category, typically 0.53 psi/ft (Lafollette et al. 2012). The most common reservoir pressure used for Barnett shale reservoir simulation is 3,000 to 5,000 psi (Chong et al. 2010). The average reservoir temperature is 200 ^{o}F (Transform Software & Services 2011). The average porosity in productive portions of the Barnett shale ranges from 4 to 5% (Hayden and Pursell 2005). Published values for permeability have variously been reported to be 0.00007 to 0.005 md (Grieser et al. 2008). Productive, organic-rich portions of the Barnett shale average 25-43% water saturation (Bruner and Smosna 2010). The organic matter in the shale was first reported to contain 60 scf/ton but could be as high as 125 scf/ton (Montgomery et al. 2005). It is reported that typical well spacing in the Barnett shale is 60-160 acres (Hayden and Pursell 2005). **Table 5.4** summarized the range of main reservoir parameters for the Barnett shale.

Table 5.4—Reservoir parameters of the Barnett shale

Parameter	Range	Parameter	Range
Net Pay, ft	100-600	Depth, ft	6,500-8,500
Porosity, %	4-5	Reservoir Pressure, psi	3,000-5,000
Permeability, md	0.00007-0.005	Well Spacing, acres	60-160
Water Saturation, %	25-43	R_o, %	0.6-1.6
Gas Content, scf/ton	60-125	TOC, %	2.4-5.1

The reservoir size is 4,800 ft × 1,000 ft (111 acres/well), with a fracture half-length of 400 ft and fracture spacing of 400 ft. **Table 5.5** shows the main fixed reservoir parameters used for the Barnett shale single-well reservoir simulations.

Table 5.5—Key fixed input parameters for the Barnett shale model

Parameters	Value	Parameters	Value
Reservoir Temperature, ^{o}F	200	Fracture Half-length, ft	400
Bottom Hole Pressure, psia	500	Lateral Length of Horizontal Well, ft	4,000
Reservoir Length, ft	4,800	Fracture Stage	10
Reservoir Width, ft	1,000	Langmuir Pressure, psia	1,241
λ (dimensionless)	7×10^{-7}	Langmuir Volume, scf/ton	150
ω (dimensionless)	0.01	Bulk Density, g/cc	2.5

5.6.4 Model Verification

Density functions were defined for net pay, initial reservoir pressure, permeability, porosity, water saturation, and gas content with honoring the range listed in Table 5.4, initially. These density functions were refined until a reasonable match between simulated and actual 5-year cumulative was obtained.

We used the HPDI database as our source for production data. Since 2004, 1,492 horizontal wells in the Barnett shale have been completed and produced more than 5 years. The red curve in **Figure 5.7** shows the distribution of 5-year cumulative gas production from the 1,492 horizontal wells. The blue curve in Figure 5.7 is the distribution of 5-year cumulative gas production simulated by UGRAS with the reservoir and well parameters in Table 5.5 and finalized density functions in **Table 5.6**. The consistent match between the two curves confirmed the reliability of the reservoir and well parameters listed in Tables 5.5 and 5.6. The distributions of the six uncertain parameters after calibration honored their range reported from literature (**Table 5.7**).

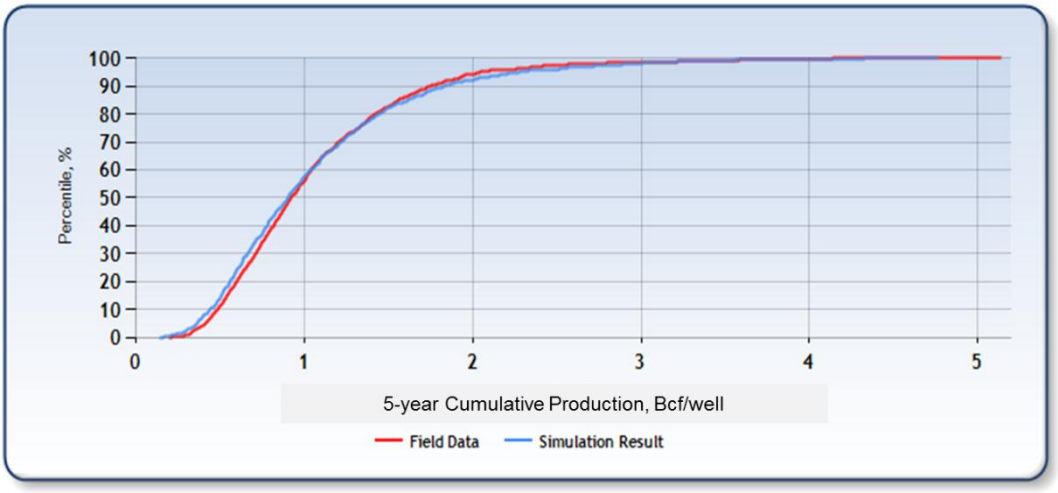

Figure 5.7—Probability distribution of cumulative gas production (5-year) match result for the Barnett shale

Table 5.6—Density functions of uncertain parameters after calibration for the Barnett shale

Parameters	Distribution Type	μ	σ	Min	Med	Max
Net Pay, ft	Lognormal	200	50			
Initial Pressure, psi	Uniform			3,000		5,000
System Permeability, md	Lognormal	0.0005	0.0005			
Porosity, f	Uniform			0.04		0.05
Water Saturation, f	Uniform			0.25		0.43
Gas Content, scf/ton	Triangular			60	100	125

Table 5.7—Comparison of the range of uncertain parameters

Parameter	Reported Range	Used by This Study(P1-P99)
Net Pay, ft	100-600	90-450
Initial Pressure, psi	3,000-5,000	3,000-5,000
System Permeability, 10^{-3}md	0.07-5	0.05-4
Porosity, f	0.04-0.05	0.04-0.05
Water Saturation, f	0.25-0.43	0.25-0.43
Gas Content, scf/ton	60-125	60-125

5.6.5 Resource Assessment

With a better understanding of the production mechanism of the Barnett shale and calibrated predictive models, OGIP calculation and a long-term gas production forecast can be made with more confidence. Detailed geologic and reservoir data were assembled to establish the free gas as well as adsorbed gas in place for the Barnett shale. The Barnett shale reservoir property distributions in Table 5.6 yield a log-logistic distribution of OGIP per well (**Figure 5.8**). The P10, P50 and P90 values are 8.4, 12.2 and 17.8 Bcf/111 acres, respectively.

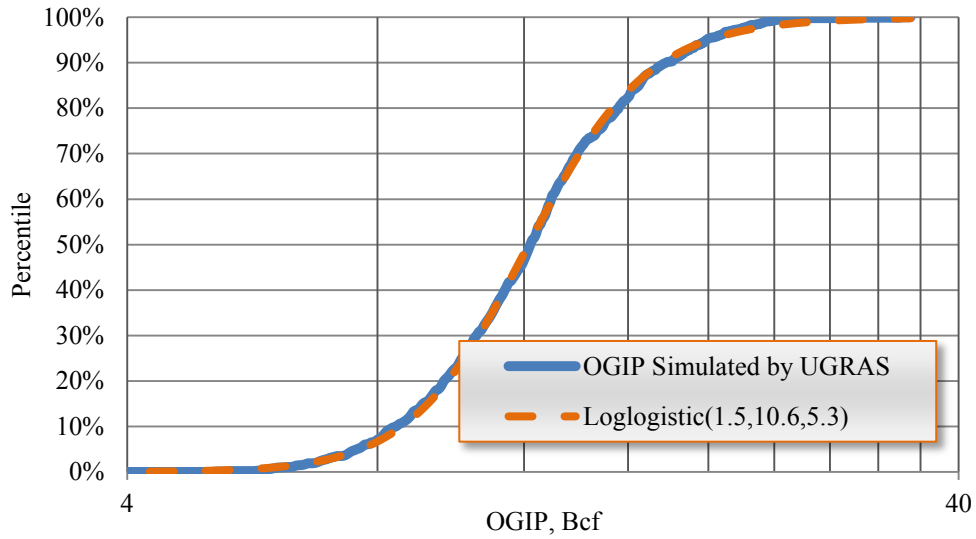

Figure 5.8—Probabilistic distribution of OGIP per 111 acres for the Barnett shale

To predict resource distribution, a thousand random single-well production forecasts using input parameters in Tables 5.5 and 5.6 and a 25-year recovery period were generated. We chose 25 years to determine TRR as a reasonable well life that is of interest to us now.

The simulation results yielded a TRR distribution with a P10 value of 1.1 Bcf/111 acres, a P50 of 2.2 Bcf/111 acres, and a P90 of 4.5 Bcf/111 acres (**Figure 5.9**). The distribution is quite wide, indicating significant uncertainty in forecasting Barnett shale gas production. The recovery factor in the Barnett shale also follows a lognormal distribution (**Figure 5.10)** with P10, P50 and P90 values of 10%, 18% and 35%, respectively.

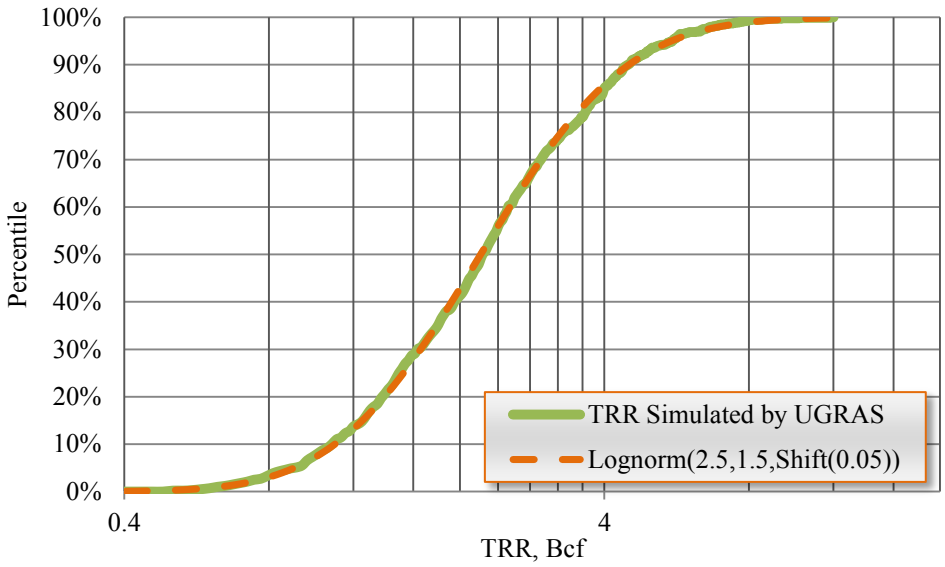

Figure 5.9—Probabilistic distribution of TRR per 111 acres with a 25-year life for the Barnett shale

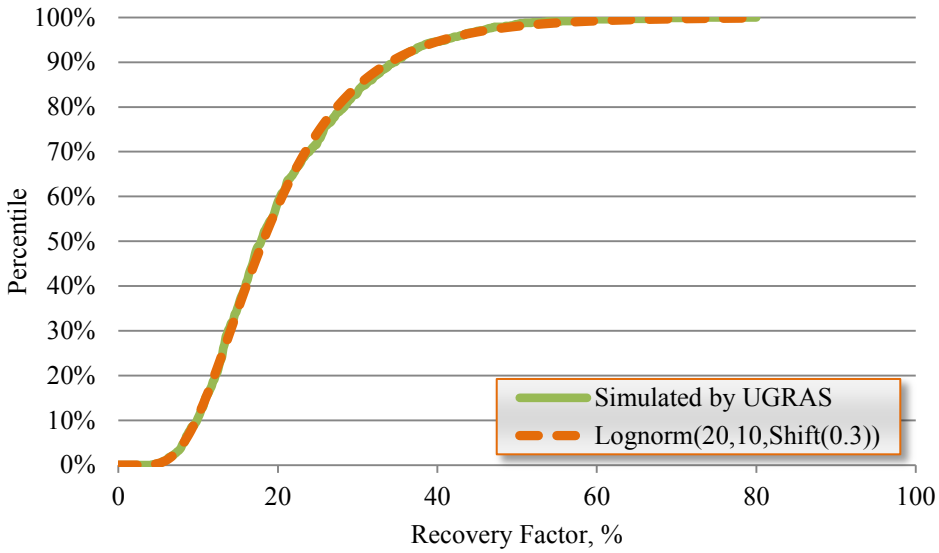

Figure 5.10—Probabilistic distribution of recovery factor with a 25-year life for the Barnett shale

With an estimated acreage of 3.2 million acres and assumed well spacing of 111 acres, 28,828 wells could be drilled in the Barnett shale. Thus, the resource potential for the entire Barnett shale is estimated at 352 Tcf of OGIP (P50) and 63 Tcf of TRR (P50) (**Table 5.8**). A mean value of OGIP in the Barnett shale was estimated at 327 Tcf, with TRR of 44 Tcf (DOE 2009).

Table 5.8—Resource potential for the Barnett shale

Category	P10	P50	P90
OGIP, Tcf	242	352	513
TRR, Tcf	32	63	130

5.7 Eagle Ford Shale

The Eagle Ford shale is a Cretaceous sediment that is located in South Texas (**Figure 5.11**). The Eagle Ford is the source rock for the Austin Chalk formation. The

Eagle Ford shale primarily covers an area of approximately 11 million acres and dips toward the Gulf of Mexico (Fan et al. 2011). The development of the Eagle Ford is in its infancy compared to other shale plays in the United States. In late 2008, the first few exploration wells in the Eagle Ford were drilled in LaSalle County in the gas window of the play.

The Eagle Ford is organic-rich shale, with 1% to 5% total organic content. Average thermal maturity (R_o) is 1.5% (Transform Software & Services 2011). The Eagle Ford shale producing interval extends from 5,500 to 14,000 ft deep. The production varies from oil at the shallowest portion of the play to wet gas in the middle and dry gas in the deepest portion of the play. In this dissertation, we evaluated only the dry gas portion of the Eagle Ford, which is also the deepest portion of the play where drilling costs are the highest. The estimated area in the dry gas window is 3 million acres.

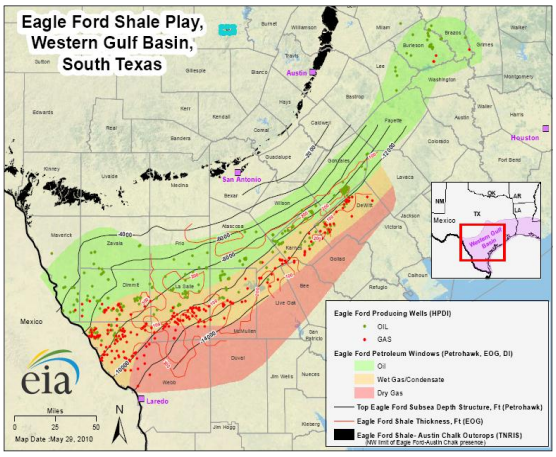

Figure 5.11—Eagle Ford shale extends across South Texas and has distinct up-dip oil, mid-dip gas condensate and down-dip gas windows

5.7.1 Production

In the Eagle Ford shale, there were 7 producing gas wells in 2008 and over 509 wells were producing in 2011 (**Figure 5.12)**. As of December 2011, more than 442 Bcf of dry gas has been produced. Dry gas production from the Eagle Ford shale is increasing annually (Figure 5.12). But due to the low gas price, the development has slowed and the average daily dry gas production only reached 854 MMcf/d in 2011.

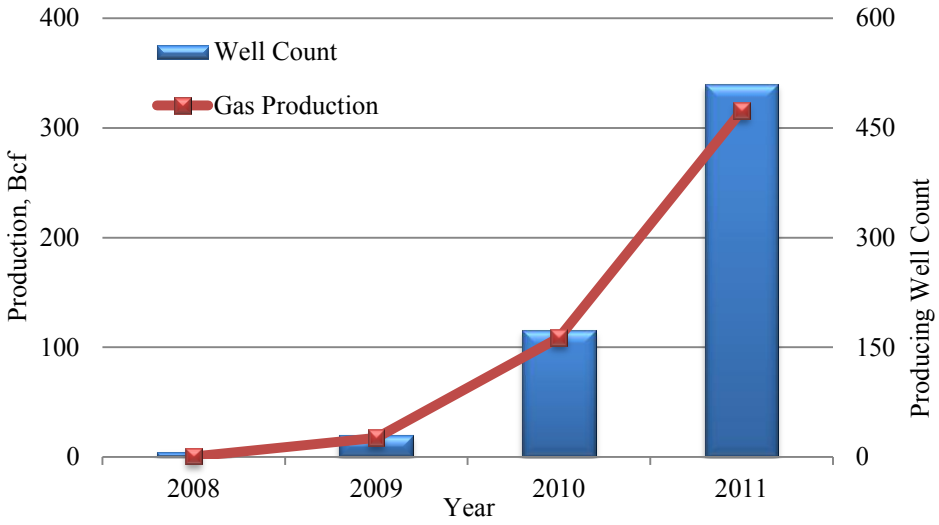

Figure 5.12—Annual dry gas production in the Eagle Ford shale (Data source: HPDI 2011)

5.7.2 Well Drilling and Completion Process

Across the dry gas window of the Eagle Ford shale, current best practice is for drilling long horizontal wells where well spacing varies from 40 to 640-acres. The average lateral length of the gas wells in the Eagle Ford shale is 5,600 ft (**Figure 5.13**). Unlike many other shale plays, the Eagle Ford shale does not exhibit very much natural fracturing within the formation. The carbonate content of the Eagle Ford can be as high

as 70%. The high carbonate content and consequently lower clay content make the Eagle Ford shale brittle and easier to stimulate through hydraulic fracturing than other shales with less carbonate. Typical fracture half-length of the Eagle Ford shale is 350 ft, with 8-18 fracture stages (Kennedy 2010, Rhine et al. 2011).

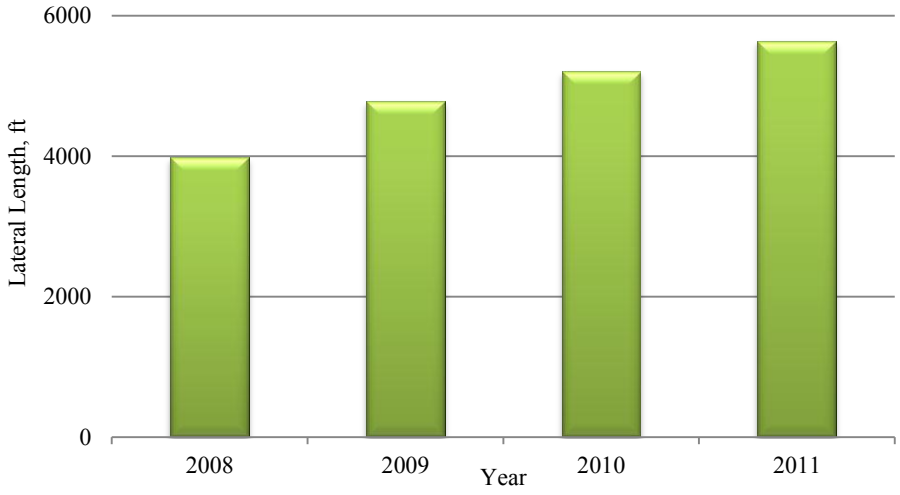

Figure 5.13—The trend of average lateral length of Eagle Ford horizontal wells over time (Data provided by Unconventional Resources, LLC)

5.7.3 Reservoir Parameters

We got the ranges of reservoir parameters from 121 horizontal gas wells in the Eagle Ford shale (**Table 5.9**). These well data were provided by W.D. Von Gonten & Company (personal communications). The Eagle Ford shale is overpressed, with pressure gradient of 0.75 psi/ft. The reservoir pressure ranges from 4,300 psi to 10,900 psi, with an average value of 9,600 psi. Reservoir temperature is in the range between 170 and 321 ^{o}F. The average bulk density for both upper and lower Eagle Ford is 2.51 g/cc.

Table 5.9—Reservoir parameters of the Eagle Ford shale

Parameter	Upper Eagle Ford		Lower Eagle Ford	
	Range	Mean	Range	Mean
Depth, ft	5,500-14,300	11,700	5,800-14,400	11,800
Net Pay, ft	3-236	100	8-326	163
System Permeability, md	0.0001-0.0005	0.0003	0.0001-0.0007	0.0004
Water Saturation, %	12-44	23	9-44	18
Porosity, %	3-9	6	3-12	8
Gas Content, scf/ton	7-96	41	18-118	82
Bulk Density, g/cc	2.44-2.65	2.55	2.36-2.63	2.46
TOC, %	0.3-4.0	1.9	0.7-5.4	3.6

Table 5.10 lists the key fixed reservoir and well parameters used for the Eagle Ford shale model. The case was based on a well with 11 multi-stage hydraulic transverse fractures, fracture half-length of 350 ft and a lateral length of about 5,600 ft, producing natural gas for a period of 25 years. The assumed well spacing is 147 acres/well.

Table 5.10—Key fixed input parameters for the Eagle Ford shale model

Parameters	Value	Parameters	Value
Reservoir Temperature, ^{o}F	247	Fracture Half-length, ft	350
Bottom Hole Pressure, psia	500	Lateral Length of Horizontal Well, ft	5,600
Reservoir Length, ft	6,400	Fracture Stage	18
Reservoir Width, ft	1,000	Langmuir Pressure, psia	1,000
λ (dimensionless)	1×10^{-6}	Langmuir Volume, scf/ton	60
ω (dimensionless)	0.01	Bulk Density, g/cc	2.51

5.7.4 Model Verification

We initially assigned density function for the six uncertain parameters with honoring their range listed in Table 5.9. These density functions were refined until a

reasonable match between simulated and actual 1-year cumulative gas production was obtained.

We used the HPDI database as our source for production data. Since 2010, 152 horizontal wells in the Eagle Ford shale have been completed and produced for more than 12 month. The red curve in **Figure 5.14** shows the cumulative probability distribution of 1-year cumulative gas production from the 152 horizontal wells. The red curve in Figure 5.14 is the cumulative probability distribution of 1-year cumulative gas production simulated by UGRAS with the reservoir and well parameters listed in Table 5.10 and density functions listed in **Table 5.11**. The consistent match between the two curves confirmed the reliability of the reservoir and well parameters listed in Tables 5.10 and 5.11. The distributions of the six uncertain parameters after calibration honored the range of these six uncertain parameters reported from literature (**Table 5.12**).

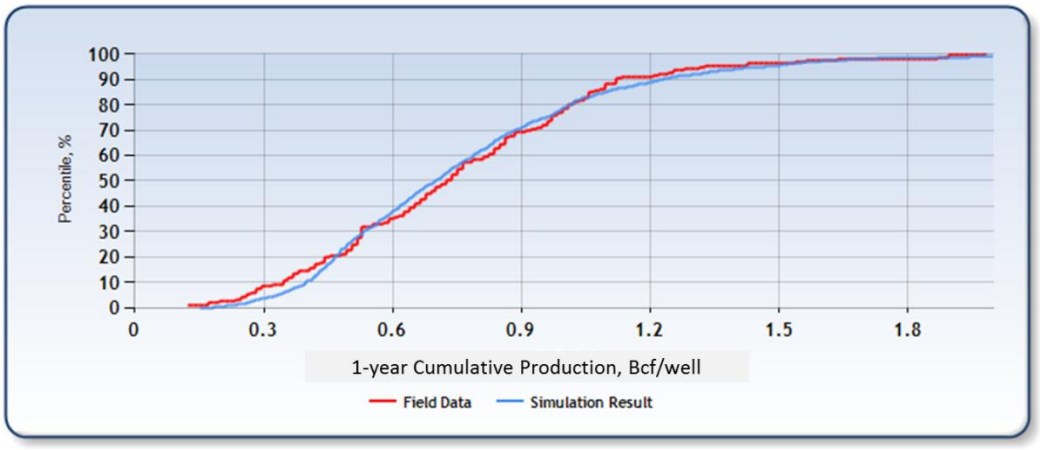

Figure 5.14—Probability distribution of cumulative gas production (1-year) match result for the Eagle Ford shale

Table 5.11—Density functions of uncertain parameters after calibration for the Eagle Ford shale

Parameters	Distribution Type	μ	σ	α	β	Shift
Net Pay, ft	Lognormal	130	50			
Initial Pressure, psi	Lognormal	7200	1100			
Water Saturation, f	Gamma	0.17	0.06	3.8	0.03	0.06
Porosity, f	InvGauss	0.1	6.8			-0.04
System Permeability, md	Lognormal	0.0004	0.0001			
Gas Content, scf/ton	Gamma	49	19	7	7	

Table 5.12—Comparison of the range of uncertain parameters

Parameter	Reported Range	Used by This Study(P1-P99)
Net Pay, ft	3-326	50-300
Initial Pressure, psi	4300-10900	4000-11000
System Permeability, 10^{-3}md	0.1-0.7	0.1-0.7
Water Saturation, f	0.09-0.44	0.07-0.43
Gas Content, scf/ton	7-120	4-120
Porosity, f	0.03-0.12	0.02-0.11

5.7.5 Resource Assessment

Figures 5.15 through **5.17** show the cumulative probability distributions for OGIP, TRR, and RF, respectively, for the dry gas wells in the Eagle Ford shale. The values of OGIP range from 7.5 (P10) to 25.3 (P90) Bcf/147 acres. TRR for a 25-year recovery period ranges from 2.3 (P10) to 8.5 (P90) Bcf/147 acres. Eagle Ford recovery factor ranges from 25% (P10) to 40% (P90).

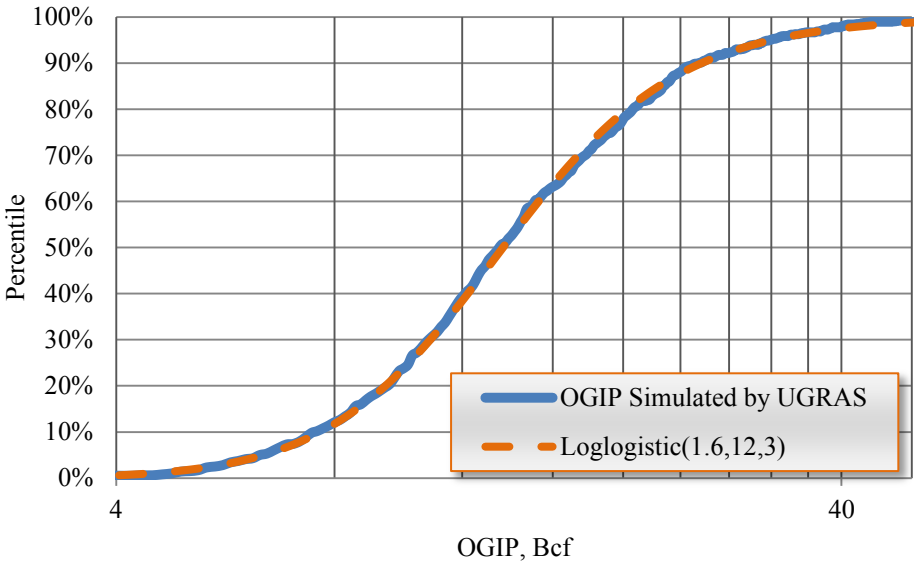

Figure 5.15—Probabilistic distribution of OGIP per 147 acres for the Eagle Ford shale gas window

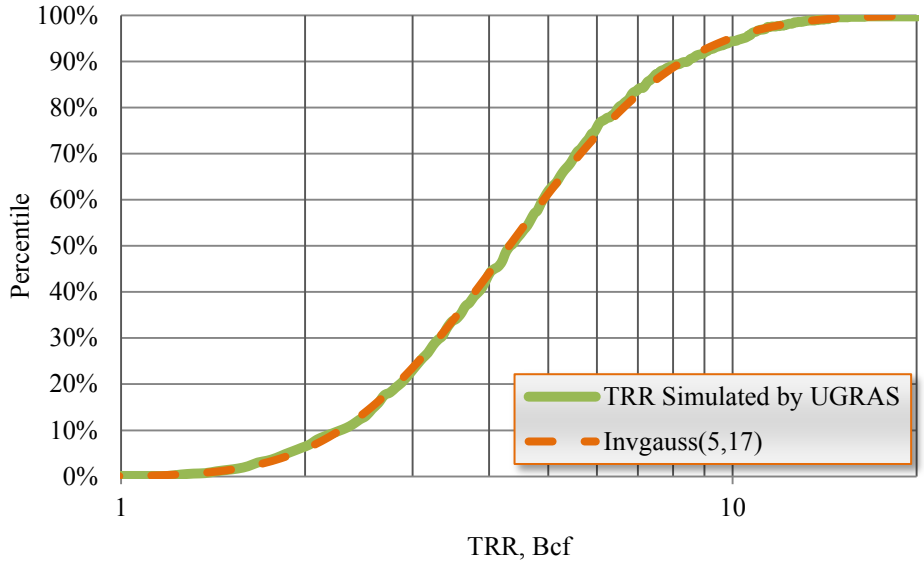

Figure 5.16—Probabilistic distribution of TRR per 147 acres with a 25-year life for the Eagle Ford shale gas window

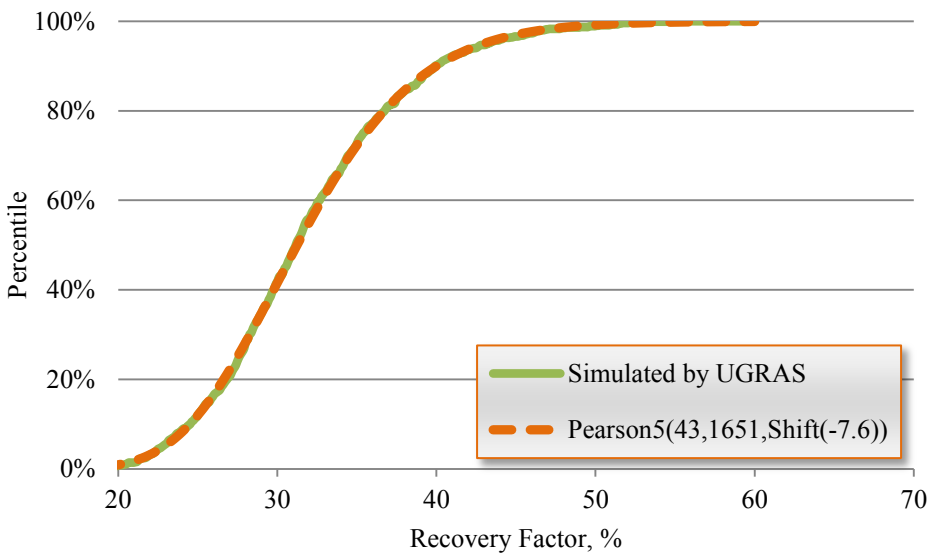

Figure 5.17—Probabilistic distribution of RF with a 25-year life for the Eagle Ford shale gas window

In the dry gas window, the estimated productive acreage is estimated to be 3 million acres. If we assume an average well spacing of 147 acres, 20,407 wells could be drilled in the dry gas portion of the Eagle Ford shale. Thus, the resource potential for the entire Eagle Ford dry gas window is 278 Tcf of OGIP (P50) and 90 Tcf of TRR (P50) (**Table 5.13**).

Table 5.13—Resource potential for dry gas in the Eagle Ford shale

Category	P10	P50	P90
OGIP, Tcf	153	278	516
TRR, Tcf	47	90	173

5.8 Marcellus Shale

The middle Devonian Marcellus shale underlies 34.6 million acres of the Appalachian basin (Lee et al. 2010). The Appalachian basin is an asymmetrical foreland

basin. **Figure 5.18** shows the distribution of the Marcellus shale, which spans regions of southern New York, northern and western Pennsylvania, eastern Ohio and West Virginia at an approximate average depth of 6,560 ft. The depth to the base of the shale increases to the southeast, varying from 2,000 ft along Lake Erie to 8,000 ft in northern West Virginia and Maryland to 8,000-10,000 ft in central Pennsylvania. In general, both the depth and thickness of the Marcellus increase toward the southeast. Thicker shale will likely contain more natural gas, but deeper formations will increase drilling costs.

The Marcellus shale and the overlying Mahantango formation constitute the Hamilton group, belonging to the Eifelian and Givetian stages of the Middle Devonian (DOE 2010). The Marcellus shale is a splintery, soft to moderately soft, gray to brownish black to black, carbonaceous, highly radioactive shale with beds of limestone and carbonate concretions.

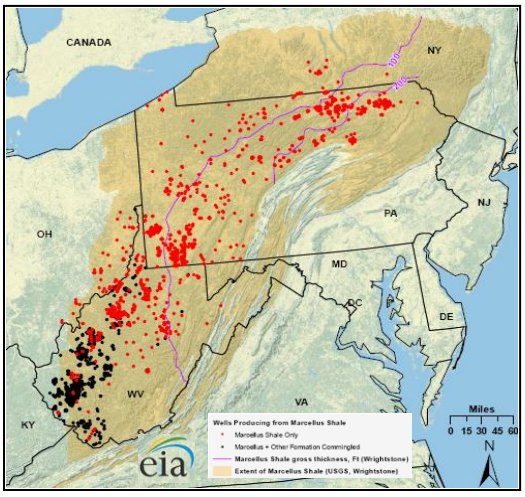

Figure 5.18—Marcellus shale, Appalachian basin

5.8.1 *Production*

Dry gas production from the Marcellus shale is increasing annually (**Figure 5.19**). Daily production increased from 42 MMcf/d in 2007 to 3,782 MMcf/d in 2011. 1,105 horizontal well produced 98 Bcf of dry gas in 2011. As of December 2011, more than 2.1 Tcf of dry gas has been produced from Marcellus.

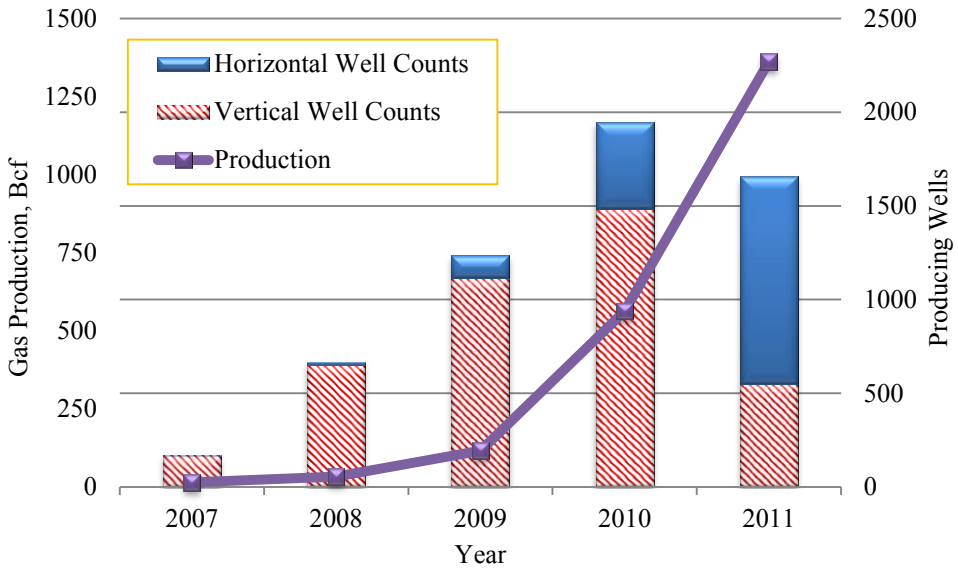

Figure 5.19—Annual gas production and producing wells in the Marcellus shale (Data source: HPDI 2011)

5.8.2 *Well Drilling and Completion Process*

Horizontal wells in the Marcellus shale cost approximately $3.5 million (USD) compared to $1 million for a vertical well (Lee et al. 2010). Across the Marcellus shale, current best practice calls for drilling long horizontal wells on 40 to 160-acre well spacing (DOE 2009). As the formation is developed, smaller well spacing is increasingly becoming the norm. Fracture gradients ranges from 0.75 to 1 psi/ft. Joint sets are

oriented east-northeast and indicate optimum azimuths of horizontal wells towards the north-northwest. Wells are being drilled and completed using the same basic process, which has evolved to drilling all wells first, before completion operations begin. Stages are isolated by using pump down fracture plugs (wireline) or packer/sleeve methods. Perforations use limited entry with clusters spaced throughout the lateral. There are 4-6 clusters/stage and 2 ft perforations/cluster, spaced 50-100 ft apart. Fracture treatments generally use slickwater or light gel with sand concentrations from 0.25 to 3 ppg. Treatment injection rates are 80-120 bb/min, with treating pressures of 5,000 to 11,500 psi. Laterals extend on average 3,700 ft and are fractured in 300-ft stages (Edwards et al. 2011). Typical fracture half-length of the Marcellus is 300 ft (Kennedy 2010).

5.8.3 Reservoir Parameters

We got the ranges of reservoir parameters from 332 horizontal wells in the Marcellus shale (**Table 5.14**). These data were provided by W.D. Von Gonten & Company (personal communications). The Marcellus shale can be slightly overpressed, especially in the northern section of the basin. In the core area of the Marcellus, the pressure gradient ranges from 0.46-0.51 psi/ft. But pressure gradients are 0.1 to 0.2 psi/ft in southwestern West Virginia and 0.2 to 0.35 psi/ft in central West Virginia (Bruner and Smosna 2010). Average thermal maturity (R_o) is 1.3% (Transform Software & Services 2011).

Table 5.14—Reservoir parameters of the Marcellus shale

Parameter	Range	Mean	Parameter	Range	Mean
Depth, ft	3,300-8,800	6,900	Reservoir Pressure, psi	2000-5100	4,021
Net Pay, ft	45-384	143	System Permeability, 10^{-3}md	0.2-0.9	0.0003
Gas Content, scf/ton	41-148	90	Bulk Density, g/cc	2.3-2.6	2.53
Porosity, %	3-13	5	Water Saturation, %	6.8-52.6	26
TOC, %	2-8	5	Reservoir Temperature, ^{o}F	110-160	144

Table 5.15 lists the reservoir and well parameters used for the Marcellus shale model. The case was based on a well with 12 multi-stage hydraulic transverse fractures, fracture half-length of 300 ft and a lateral length of 3,700 ft, producing natural gas for a period of 25 years. The assumed well spacing is 104 acres/well.

Table 5.15—Input parameters for the Marcellus shale model

Parameters	Value	Parameters	Value
Reservoir Temperature, ^{o}F	144	Fracture Half-length, ft	300
Bottom Hole Pressure, psia	500	Lateral Length of Horizontal Well, ft	3,700
Reservoir Length, ft	4,500	Fracture Stage	12
Reservoir Width, ft	1,000	Langmuir Pressure, psia	850
λ (dimensionless)	9×10^{-6}	Langmuir Volume, scf/ton	100
ω (dimensionless)	0.01	Bulk Density, g/cc	2.53

5.8.4 Model Verification

We initially assigned density function for each of six uncertain parameters with honoring their range listed in Table 5.14. These density functions were refined until a reasonable match between simulated and actual 2-year cumulative gas production was obtained.

We used the HPDI database as our source for gas production data. Since 2010, 372 horizontal wells in the Marcellus shale have been completed and produced for more than 1 year. The red curve in **Figure 5.20** shows the cumulative probability distribution of 1-year cumulative gas production from the 372 horizontal wells. The blue curve in Figure 5.20 is the cumulative probability distribution of 1-year cumulative gas production simulated by UGRAS with the reservoir and well parameters in Table 5.15 and density functions in **Table 5.16**. The consistent match between the two curves confirmed the reliability of the reservoir and well parameters listed in Tables 5.15 and 5.16. The distributions of the six uncertain parameters after calibration honored the range of these six uncertain parameters reported from literature (**Table 5.17**).

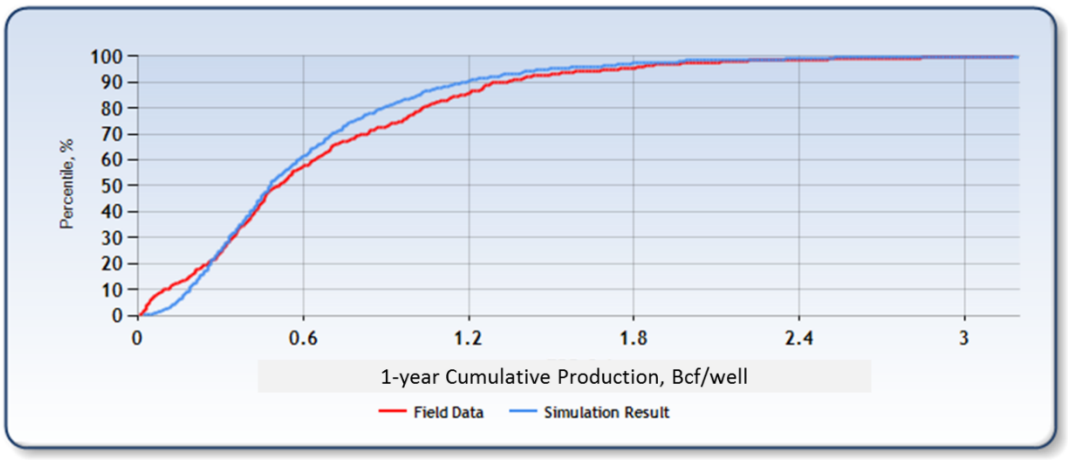

Figure 5.20—Probability distribution of cumulative gas production (1-year) match result for the Marcellus shale

Table 5.16—Density functions of uncertain parameters after calibration for the Marcellus shale

Parameters	Distribution Type	α	β	μ	σ	k	Min	Med	Max	Shift
Net Pay, ft	GEV			120	70	0.1				
Initial Pressure, psi	Triangular						2000	4100	5100	
Water Saturation, f	Normal			0.26	0.08					
Porosity, f	Gamma	4	0.007							0.03
System Permeability, md	Lognormal			0.0003	0.0002					0.0001
Gas Content, scf/ton	Lognormal			100	19					-41

Table 5.17—Comparison of the range of uncertain parameters

Parameter	Reported Range	Used by This Study(P1-P99)
Net Pay, ft	45-384	25-500
Initial Pressure, psi	2000-5100	2000-5100
System Permeability, 10^{-3}md	0.2-0.9	0.2-0.6
Water Saturation, f	0.07-0.53	0.02-0.51
Gas Content, scf/ton	41-148	10-150
Porosity, f	0.03-0.13	0.03-0.12

5.8.5 Resource Assessment

Figure 5.21 shows the probability distribution for OGIP simulated by this study. It follows a lognormal distribution. The values of OGIP range from 3.8 (P10) to 20.8 (P90) Bcf/104 acres.

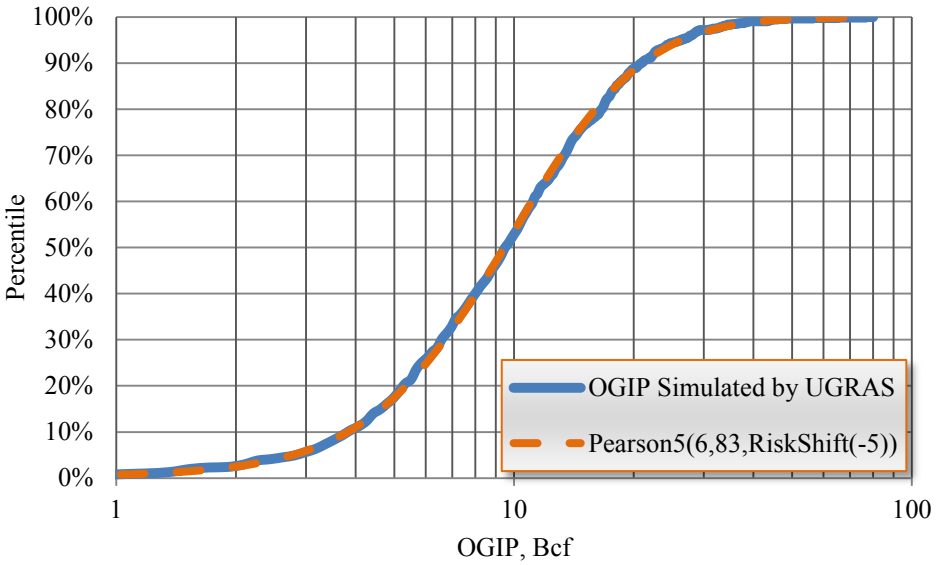

Figure 5.21—Probabilistic distribution of OGIP per 104 acres for the Marcellus shale

Figures 5.22 and **5.23** shows the cumulative probability plot of TRR and recovery factor simulated by this study for Marcellus shale, respectively. TRR of Marcellus shale for a 25-year recovery period ranges from 1.5 (P10) to 8.5 (P90) Bcf/104 acres. Recovery factor, which follows a Pearson type V distribution, ranges from 29% (P10) to 52% (P90).

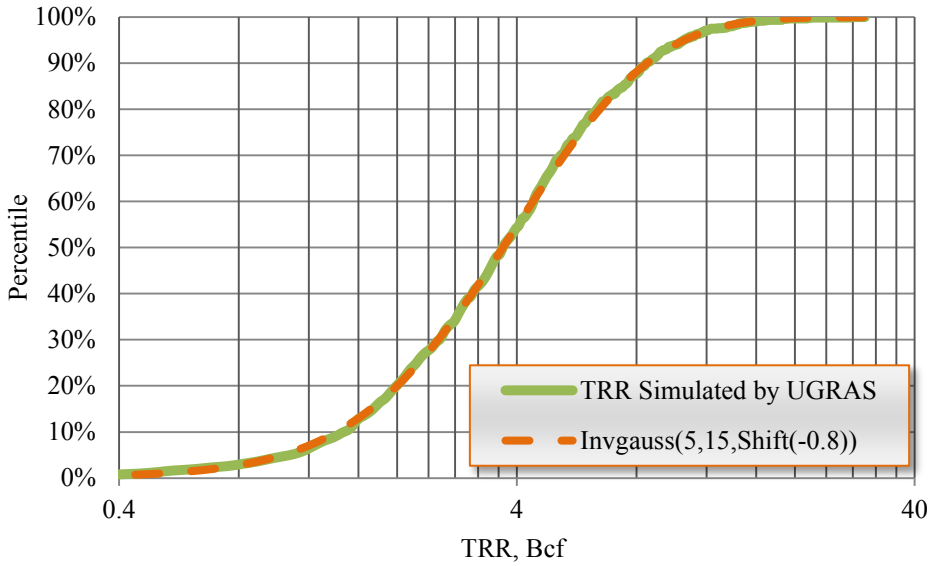

Figure 5.22—Probabilistic distribution of TRR per 104 acres with a 25-year life for the Marcellus shale

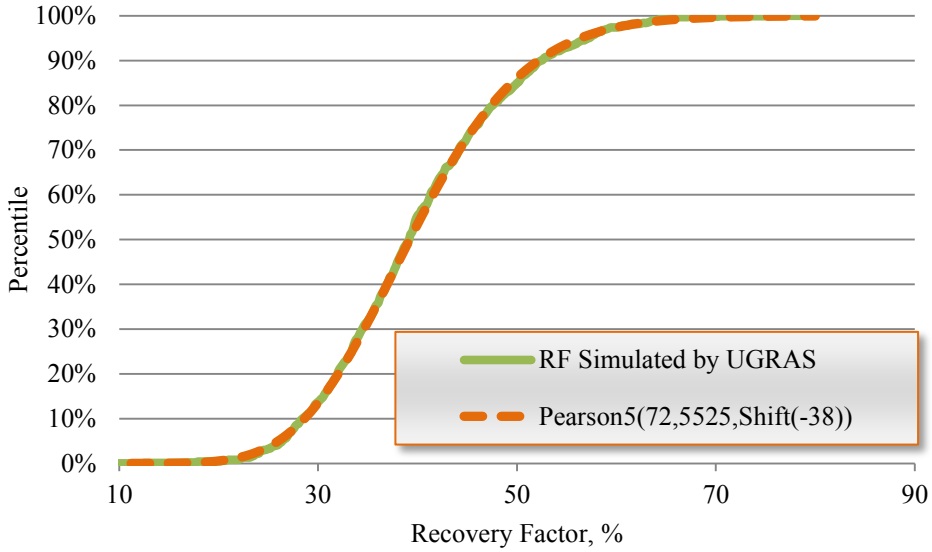

Figure 5.23—Probabilistic distribution of RF per 104 acres with a 25-year life for the Marcellus shale

In the Marcellus shale, the prospective area is estimated to be 15 million acres (Kulkarni 2010). If we assume an average well spacing of 104 acres, 144,231 wells could be drilled in the Marcellus shale. Thus, the resource potential for the entire Marcellus shale is 1,385 Tcf of OGIP (P50) and 534 Tcf of TRR (P50) (**Table 5.18**).

Several reputable reporters have confused various measures of gas in the Marcellus shale. For instance, it is reported that this supper giant gas filed contains an estimated 2,100 Tcf of natural gas in place (Kuuskraa 2009).

Table 5.18—Resource potential for dry gas in the Marcellus shale

Category	P10	P50	P90
OGIP, Tcf	548	1,385	3,000
TRR, Tcf	216	534	1,226

5.9 Fayetteville Shale

The Fayetteville shale play is present over much of the subsurface in north-central Arkansas. Fayetteville shale gas production has been established in 10 counties, covering an area of approximately 1.5 million acres (Janwadkar et al. 2010) (**Figure 5.24**). The Fayetteville shale is a Mississippian-age marine shelf deposit that includes transgressive and highstand system tracts of the Chesterian cycle separated by maximum flooding surfaces over a broad shelf area that comprises the northern Arkoma basin and the southern Ozark region (Ramakrishnan et al. 2011).

The Fayetteville shale compares favorably to other gas-producing shales: it is thermally mature, and its total organic carbon content ranges between 4%-9.5% (Hayden and Pursell 2005). Vitrinite Reflectance (R_o) is considered to be best between 1 and 5.

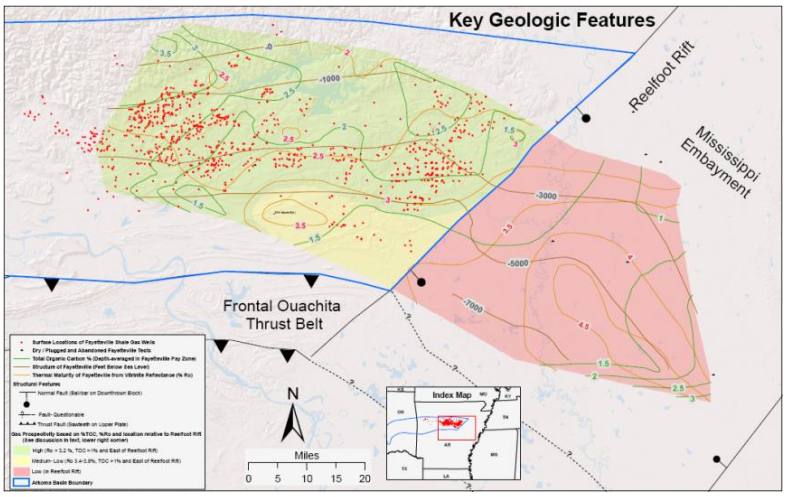

Figure 5.24—Fayetteville shale, Arkoma basin, Arkansas

5.9.1 Production

Approximately 3,200 wells are producing from the Fayetteville shale, the vast majority of which are horizontal wells as of December 2011 (**Figure 5.25**). Horizontal drilling started in late 2005, with approximately 849 Bcf of natural gas was produced in 2011 (Figure 5.25). Wells flow at an initial production averaging 1 to 3.4 Mcf/d and decline at a lesser rate than in other shale plays. Cumulative gas production in the play has reached 2.5 Tcf and average daily gas production is in excess of 2.6 Bcf/d in 2011.

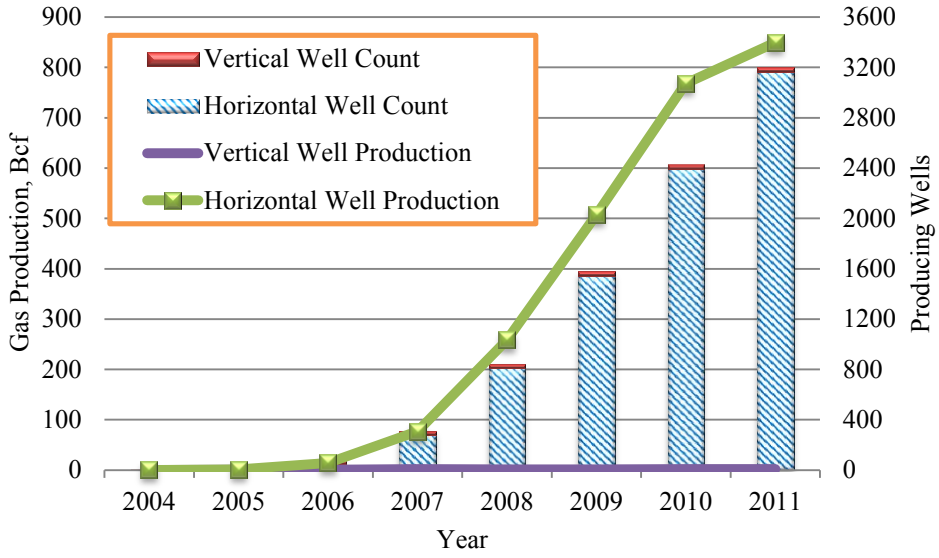

Figure 5.25—Annual gas production of the Fayetteville shale (Data Source: HPDI, 2011)

5.9.2 Well Drilling and Completion Process

Most of the wells are horizontals with an average of six to ten fracture stages. The maximum horizontal stress azimuth of the Fayetteville shale is NE-SW. The lateral interval is drilled through the lower Fayetteville shale and extends the borehole 2,500 ft to 4,500 ft. A few wells with lateral interval length of 5,500 ft to 6,100 ft have also been drilled (Janwadkar et al. 2010). Average drill time has decreased to 7.8 days in 2011 with average lateral length of 4,847 feet (Southwestern Energy 2011). Fracture treatments generally are slickwater using 300,000 to 400,000 lbm of proppant, with concentrations stepping from 0.1 up to 2.2 ppg. Typically, fracture half-length of the Fayetteville shale ranges from 250 to 300 ft, with 8-11 fracture stimulation stages (Kennedy 2010).

5.9.3 Reservoir Parameters

Production depths in the Fayetteville range from 1,200 ft true vertical depth (TVD) in the north to 8,000 ft TVD in the south (Janwadkar et al. 2010). The Fayetteville is shallower than the Barnett. The shale expands from a thickness of 50 feet in the Fairway to as much as 325 feet in the counties to the east, slightly over-pressured. Porosity ranges from 2 to 8% on average; water saturation is between 15% and 35% (Benedetto 2010); and its gas content is from 60 to 220 scf/ton (Hayden and Pursell 2005). There is so limited report on reservoir pressure and permeability in the Fayetteville shale. The Langmuir pressure is 500 psi and Langmuir volume is 90 scf/ton (Ramakrishnan et al. 2011). **Table 5.19** summarized the range of main uncertain parameters for the Fayetteville shale.

Table 5.19—Reservoir parameters of the Fayetteville shale

Parameter	Range
Net Pay, ft	50-325
Water Saturation, %	15-35
Gas Content, scf/ton	60-220
Porosity, %	2-8

Table 5.20 lists the key fixed reservoir and well parameters used for the Fayetteville shale model. Typical well spacing in the Fayetteville shale is 80-160 acres (DOE 2009). The case was based on a well with 12 multi-stage hydraulic transverse fractures, fracture half-length of 300 ft and a total wellbore length of about 4,800 ft,

producing natural gas for a period of 25 years. The assumed well spacing is 129 acres/well.

Table 5.20—Key fixed input parameters for the Fayetteville shale model

Parameters	Value	Parameters	Value
Reservoir Temperature, ^{o}F	120	Fracture Half-length, ft	300
Bottom Hole Pressure, psia	500	Lateral Length of Horizontal Well, ft	4,800
Reservoir Length, ft	5,600	Fracture Stage	12
Reservoir Width, ft	1,000	Langmuir Pressure, psia	500
λ (dimensionless)	1×10^{-7}	Langmuir Volume, scf/ton	90
ω (dimensionless)	0.01	Bulk Density, g/cc	2.58

5.9.4 Model Verification

Density functions were assigned for the six key uncertain parameters with honoring their range listed in Table 5.19, initially. These density functions were refined until a reasonable match between simulated and actual 4-year cumulative was obtained.

Since 2007, 524 horizontal wells in the Fayetteville shale have been completed and produced more than 4 years. The red curve in **Figure 5.26** shows the distribution of 4-year cumulative gas production from the 524 horizontal wells. The blue curve in Figure 5.26 is the distribution of 4-year cumulative gas production simulated by UGRAS with the reservoir and well parameters listed in Table 5.20 and density functions listed in **Table 5.21**. The consistent match between the two curves confirmed the reliability of the reservoir and well parameters listed in Tables 5.20 and 5.21. The distributions of net pay, water saturation, gas content, and porosity after calibration honored their range reported from literature (**Table 5.22**). The range of reservoir pressure is modeled to be 1,000-

4,000 psi, with an average value of 3,100 psi. The permeability is defined to follow lognormal distribution, with the mean value of 0.002 md.

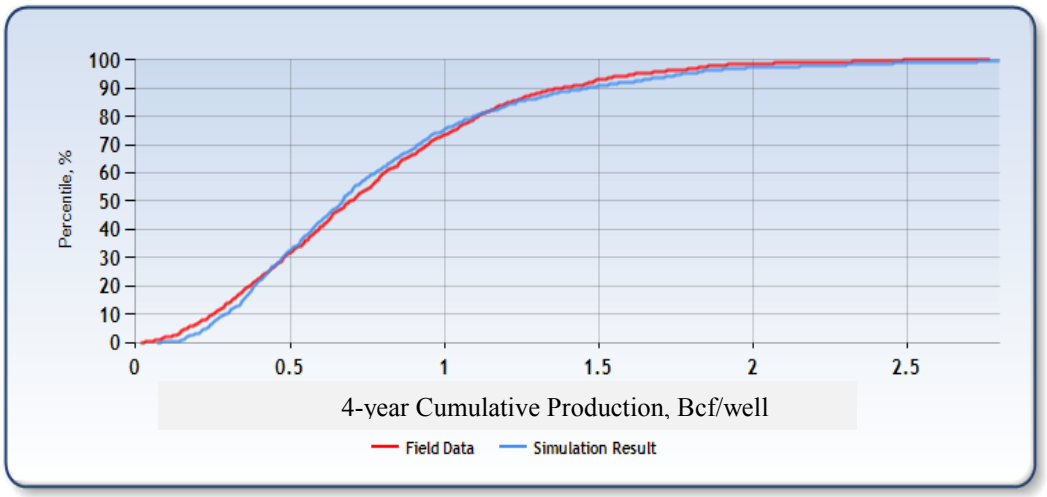

Figure 5.26—Probability distribution of cumulative gas production (4-year) match result for the Fayetteville shale

Table 5.21—Density functions of uncertain parameters after calibration for the Fayetteville shale

Parameters	Distribution Type	μ	σ	Min	Med	Max
Net Pay, ft	Lognormal	150	50			
Initial Pressure, psi	Triangular			800	3,100	4,000
System Permeability, md	Lognormal	0.002	0.0005			
Water Saturation, f	Uniform			0.15		0.35
Porosity, f	Lognormal	0.08	0.02			
Gas Content, scf/ton	Triangular			60	100	220

Table 5.22—Comparison of the range of uncertain parameters

Parameter	Reported Range	Used by This Study(P1-P99)
Net Pay, ft	50-325	50-400
Initial Pressure, psi	N/A	800-4,000
System Permeability, 10^{-3}md	N/A	1-2
Water Saturation, f	0.15-0.35	0.15-0.35
Gas Content, scf/ton	60-220	60-220
Porosity, f	2-8	3-15

N/A=Not Available

5.9.5 Resource Assessment

Figure 5.27 shows the cumulative probability distribution of OGIP simulated by this study. The values of OGIP range from 9.0 (P10) to 26.0 (P90) Bcf/129 acres.

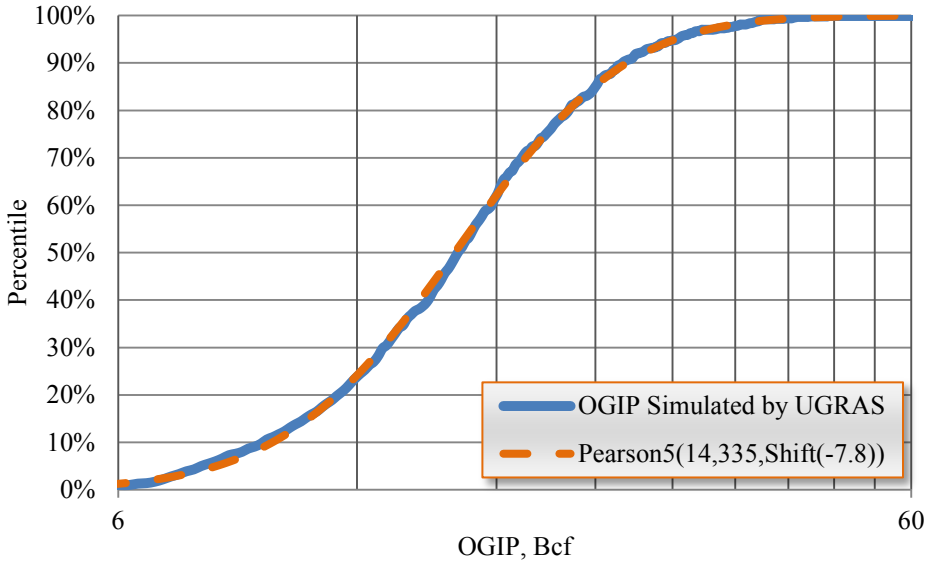

Figure 5.27—Probabilistic distribution of OGIP per 129 acres for the Fayetteville shale

Figures 5.28 and **5.29** show the cumulative probability plot of TRR and recovery factor simulated by this study for Fayetteville shale, respectively. TRR of Fayetteville shale for a 25-year recovery period ranges from 0.8 (P10) to 3.1 (P90) Bcf/129 acres. Recovery factor, which follows a general beta distribution, ranges from 7% (P10) to 15% (P90).

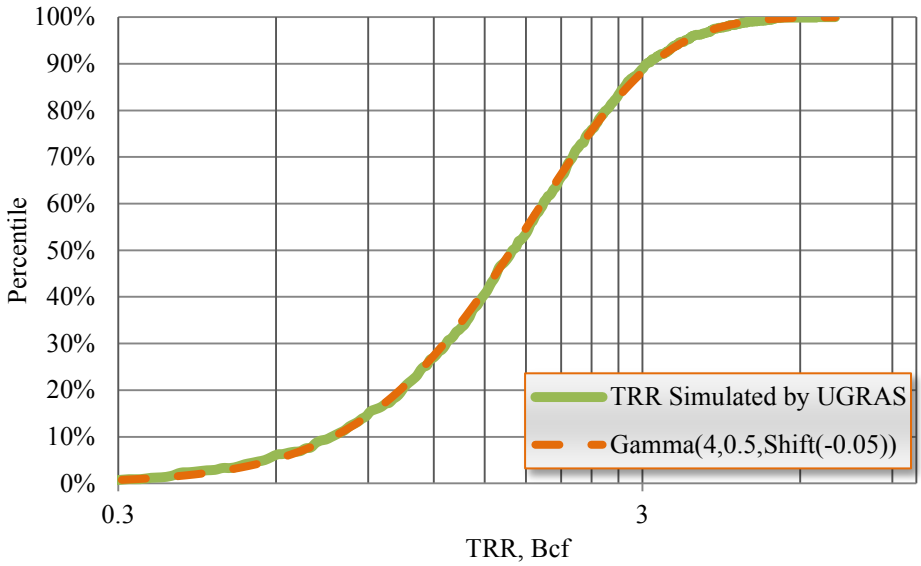

Figure 5.28—Probabilistic distribution of TRR per 129 acres with a 25-year life for the Fayetteville shale

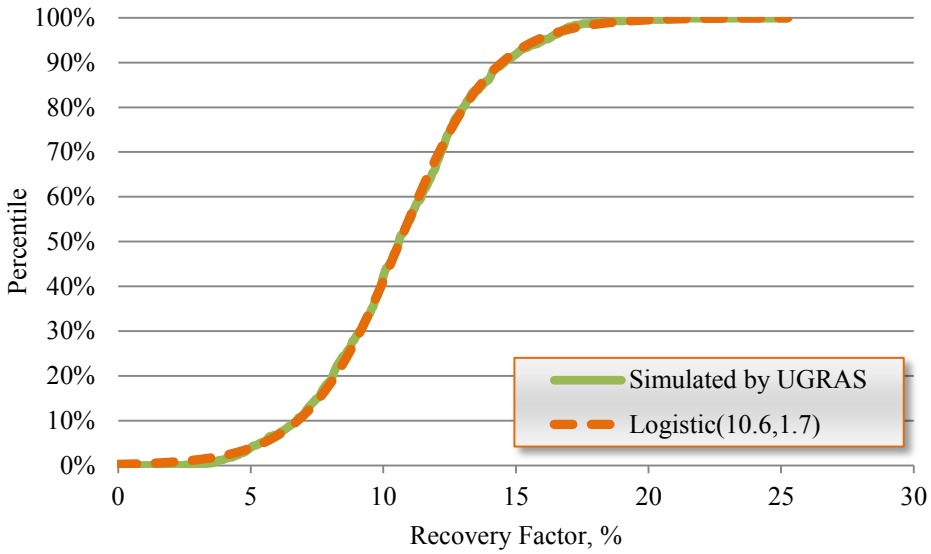

Figure 5.29—Probabilistic distribution of RF with a 25-year life for the Fayetteville shale

In the Fayetteville shale, the estimated productive acreage is estimated to be 2.56 million acres. With the assumed well spacing of 129 acres 19,844 wells could be drilled in the Fayetteville shale. Thus, the resource potential for the entire Fayetteville shale is 318 Tcf of OGIP (P50) and 34 Tcf of TRR (P50) (**Table 5.23**). The OGIP of Fayetteville

shale was estimated at 52 Tcf, with TRR of 42 Tcf (DOE 2009). But we believe the assessment made by DOE (2009) may underestimate the gas in-place resource in the Fayetteville shale. Gas-in-place in the Fayetteville shale is reported between 58 and 65 Bcf per section (Williams 2006b). It results in OGIP 232 to 260 Tcf in the Fayetteville shale.

Table 5.23—Resource potential for dry gas in the Fayetteville shale

Category	P10	P50	P90
OGIP, Tcf	179	318	516
TRR, Tcf	15	34	62

5.10 Haynesville Shale

The Haynesville shale extends over 5.76 million acres in the East Texas and North Louisiana Salt basin (DOE 2009). The Haynesville shale is overlain by the Bossier shale, followed by the Cotton Valley sandstone formation (**Figure 5.30**). The Haynesville shale was deposited with the opening of the Atlantic Ocean during the Kimmeridgian Stage of the Upper Jurassic.

The depositional setting was on the shelf of the Gulf of Mexico in a restricted marine basin. The structure of the basin was influenced by basement tectonics related to the opening of the Atlantic, along with movement of the deeper Louann Salt (Abou-sayed et al. 2011). Sedimentation from ancestral rives thickened the Haynesville along the Arkansas/Louisiana border to a maximum of 400 ft. To the south, the Haynesville interval thins to 180 ft thick through Bossier, Red River, and Desoto Parishes in Louisiana and Shelby County in Texas.

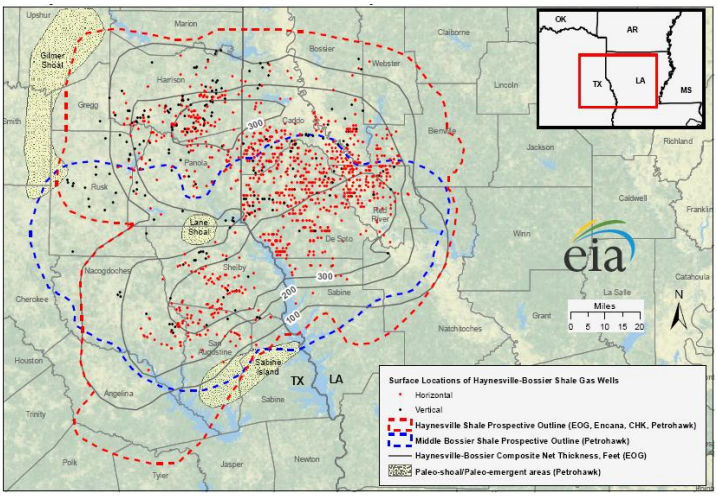

Figure 5.30—Haynesville shale, East Texas-Louisiana Mississippi salt basin

Gas-directed drilling continued to increase sharply in the newer Haynesville play during 2010-11, while flattening somewhat in the more mature Barnett play. As gas-directed drilling slows and natural gas prices remain relatively low, operators are turning their attention to the more liquids-rich areas of the play, thereby reducing the emphasis on gas.

Experience gained from early horizontal drilling programs in the Barnett has helped the operators in the Haynesville shale ramp up natural gas production far more rapidly. Based on reported pipeline flows, it took nearly a decade of shale-focused drilling to reach 5 billion cubic feet (Bcf) per day at the Barnett; that threshold was surpassed at the Haynesville in less than three years. Technology-driven efficiency gains and better reservoir characteristics have enabled the Haynesville producers to reach that level with far fewer wells.

Regional infrastructure is expanding to accommodate the Haynesville's rising natural gas production. For example, pipeline capacity expansions were recently

completed on the Regency, Midcon Express, and Gulf Crossing systems, each of which transports Haynesville gas.

5.10.1 Production

The Haynesville has seen outstanding initial gas productions rates in excess of 30 MMcf/d. Approximately 1,272 wells are producing from the Haynesville shale, the vast majority of which are horizontal wells as of December 2011(**Figure 5.31**). Cumulative gas production in the play has reached 3.9 Tcf and average daily gas production is in excess of 6.0 Bcf/d in 2011.

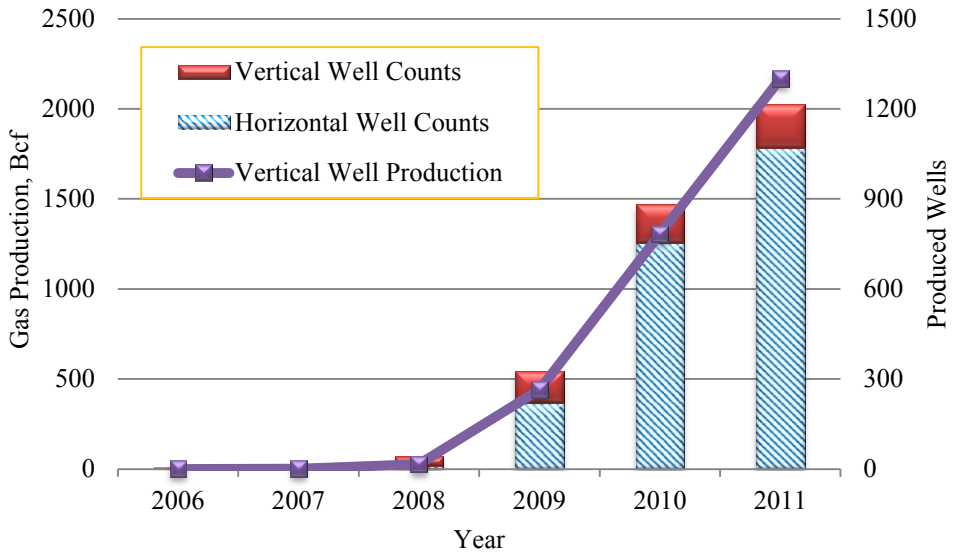

Figure 5.31—Annual gas production of the Haynesville shale (Data Source: HPDI, 2011).

5.10.2 Well Drilling and Completion Process

Horizontal drilling started in late 2007, with approximately 501 horizontal wells producing through the end of September 2011 (HPDI, 2011). The current development

concept includes horizontal wells with 4,600 ft laterals with 12-15 completion stages (Billa et al. 2011). Number of stages is determined by lateral length divided by approximately 350 ft. Each stage comprised of 4 perforation clusters, 2 feet in length, and spaced approximately 80-85 feet apart. The kick-off point for a typical well is between 10,500 and 13,500 ft, with a 4,600 ft horizontal leg (Billa et al. 2011). Typical fracture half-length of the Haynesville shale is 300 ft (Kennedy 2010). Total well depth is 16,500 to 18,500-ft MD (12,500 to 14,500-ft TVD). 2010 well costs expected to average $8.5-$9.5 million for 4,700-ft laterals.

5.10.3 Reservoir Parameters

Haynesville shale is a high-temperature, high-pressure (HTHP) formation in much of the better intervals (Abou-sayed et al. 2011). Pressure increases from 7,000 psi in Harrison County, Texas, to over 10,000 psi in San Augustine and Nacogdoches Counties, Texas, and Red River Parish, Louisiana. They are equivalent to pressure gradients from 0.6 psi to more than 0.95 psi/ft, with an average of 0.8 psi/ft (Wang and Hammes 2010). Aerially extensive basin gas with TVD ranging from 10,000-14,000 ft; productive interval of the Haynesville shale can have a gross thickness between 75 and 400 ft; net pay ranges from 200 ft (Boughal 2008) to 300 ft (Berman 2008); temperature from 300 to 350 ^{o}F; free gas volume greater than 80% of OGIP; most natural fractures healed (calcite cemented); dry gas with 0.58 gravity; high initial production performance in certain area (20 MMscf/d initial gas flow rate at 7,000 psi surface flowing pressure); TOC is in the range of 0.5-4.0% (Berman 2008); R_o is 2.2 (Transform Software &

Services 2011); produced gas is dry and typically contains 4-6% CO2 and 15-25 ppm H_2S; gas content estimates for the play are 100 to 330 scf/ton (DOE 2009). The average porosity is between 8% and 14%, with the average value of 12.6%; matrix permeability is 0.00007 to 0.001 md; connate water saturations from two cored Haynesville Shale wells vary from 15.6% to 40.8% with an average of 27.6% (Wang and Hammes 2010). Well spacing is typically between 40 and 560 acres (DOE 2009). Deeper wells and both high temperature (~340 ^{o}F) and high pressure environments result in horizontal wells costs in the range of $7 M, well over twice the cost of Barnett wells. **Table 5.24** summarized the range of reservoir parameters for the Haynesville shale.

Table 5.24—Reservoir parameters of the Haynesville shale

Parameter	Range	Parameter	Range
Depth, ft	10,000-14,400	Reservoir Pressure, psi	7,000-10,000
Net Pay, ft	200-300	Matrix Permeability, 10^{-3}md	0.072-1
Gas Content, scf/ton	100-330	Bulk Density, g/cc	<2.57
Porosity, %	8-14	Water Saturation, %	16-41
TOC, %	0.5-4.0	Reservoir Temperature, ^{o}F	300-350

Table 5.25 lists the other reservoir and well parameters used for the Haynesville shale model. The case was based on a well with 13 multi-stage hydraulic transverse fractures, fracture half-length of 300 ft and a total wellbore length of about 4,600 ft, producing natural gas for a period of 25 years. The assumed well spacing is 124 acres/well.

Table 5.25—Input parameters for the Haynesville shale model

Parameters	Value	Parameters	Value
Reservoir Temperature, ^{o}F	340	Fracture Half-length, ft	300
Bottom Hole Pressure, psia	500	Lateral Length of Horizontal Well, ft	4,600
Reservoir Length, ft	5,400	Fracture Stage	13
Reservoir Width, ft	1,000	Langmuir Pressure, psia	1,000
λ (dimensionless)	1×10^{-8}	Langmuir Volume, scf/ton	380
ω (dimensionless)	0.01	Bulk Density, g/cc	2.5

5.10.4 Model Verification

Density functions were assigned for the six key uncertain parameters with honoring their range listed in Table 5.24, initially. Before 2010, 476 horizontal wells in the Haynesville shale have been completed and produced more than 24 month. The density functions were refined until a reasonable match between simulated and actual 2-year cumulative was obtained.

We used the HPDI database as our source for gas production data of Haynesville shale. The red curve in **Figure 5.32** shows the distribution of 2-year cumulative gas production from the 476 horizontal wells. The blue curve in Figure 5.32 is the distribution of 2-year cumulative gas production simulated by UGRAS with the reservoir and well parameters listed in Table 5.25 and density functions listed in **Table 5.26**. The consistent match between the two curves confirmed the reliability of the reservoir and well parameters listed in Tables 5.25 and 5.26. The distributions of the six uncertain parameters after calibration honored their range reported from literature (**Table 5.27**).

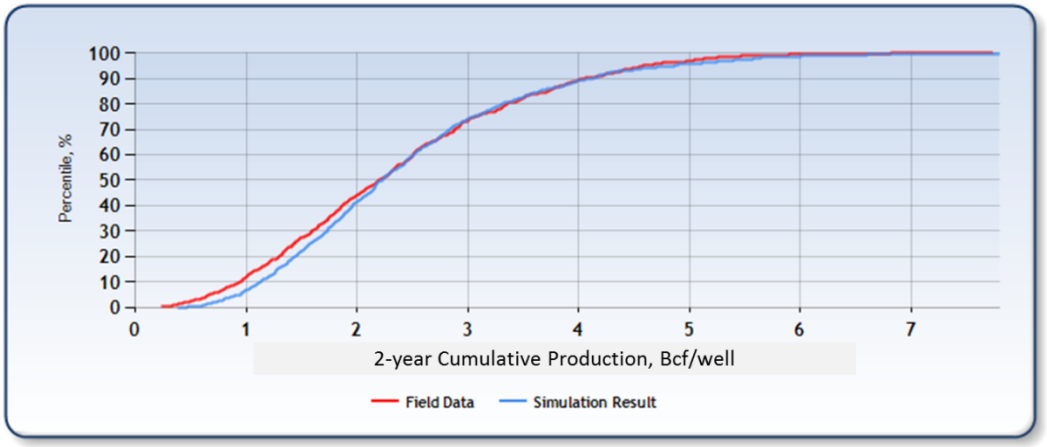

Figure 5.32—Probability distribution of cumulative gas production (2-year) match result for the Haynesville shale

Table 5.26—Density functions of uncertain parameters after calibration for the Haynesville shale

Parameters	Distribution Type	μ	σ	Min	Med	Max	Shift
Net Pay, ft	Lognormal	200	80				
System Permeability, md	Lognormal	0.034	0.032				-0.001
Water Saturation, f	Uniform	0.16	0.41				
Porosity, f	Lognormal	0.126	0.03				
Initial Pressure, psi	Uniform	7,000	10,000				
Gas Content, scf/ton	Triangular			100	200	330	

Table 5.27—Comparison of the range of uncertain parameters

Parameter	Reported Range	Used by This Study(P1-P99)
Net Pay, ft	200-300	70-400
Initial Pressure, psi	7000-10000	7000-10000
System Permeability, md	N/A	0.008-0.06
Water Saturation, f	0.16-0.41	0.16-0.41
Gas Content, scf/ton	100-300	100-320
Porosity, f	0.08-0.14	0.09-0.16

5.10.5 Resource Assessment

Figure 5.33 shows the cumulative probability distribution of OGIP simulated by this study. It follows a lognormal distribution. The values of OGIP range from 22.0 (P10) to 67.0 (P90) Bcf/124 acres.

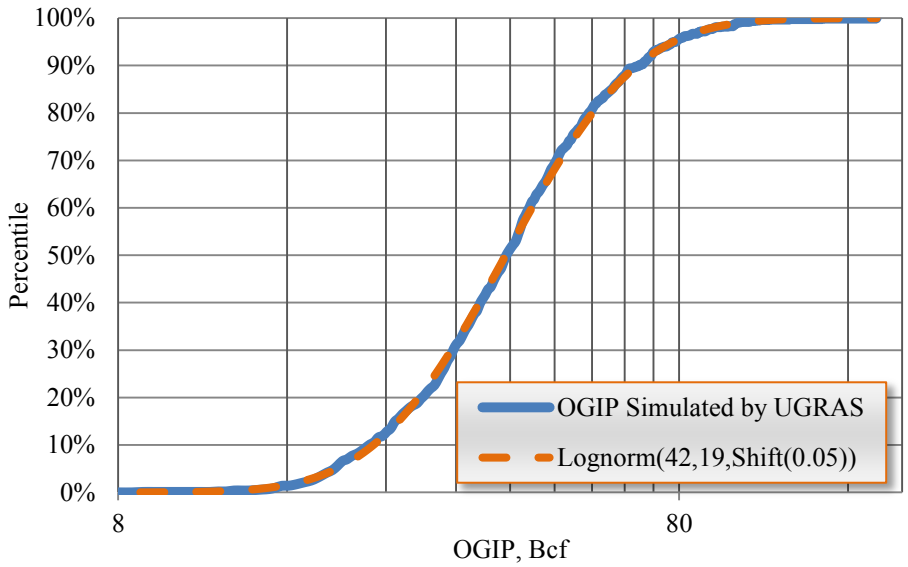

Figure 5.33—Probabilistic distribution of OGIP per 124 acres for the Haynesville shale

Figures 5.34 and **5.35** show the cumulative probability plot of TRR and recovery factor simulated by this study for Haynesville shale, respectively. TRR of Haynesville shale for a 25-year recovery period ranges from 3.2 (P10) to 15.2 (P90) Bcf/124 acres. Recovery factor, which follows a Person 5 distribution, ranges from 10% (P10) to 33% (P90).

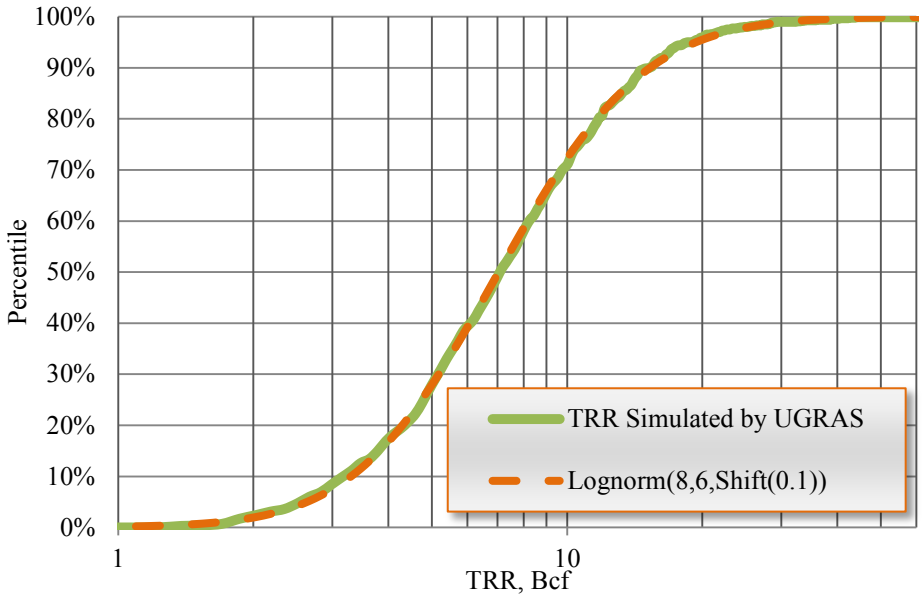

Figure 5.34—Probabilistic distribution of TRR per 124 acres a 25-year life for the Haynesville shale

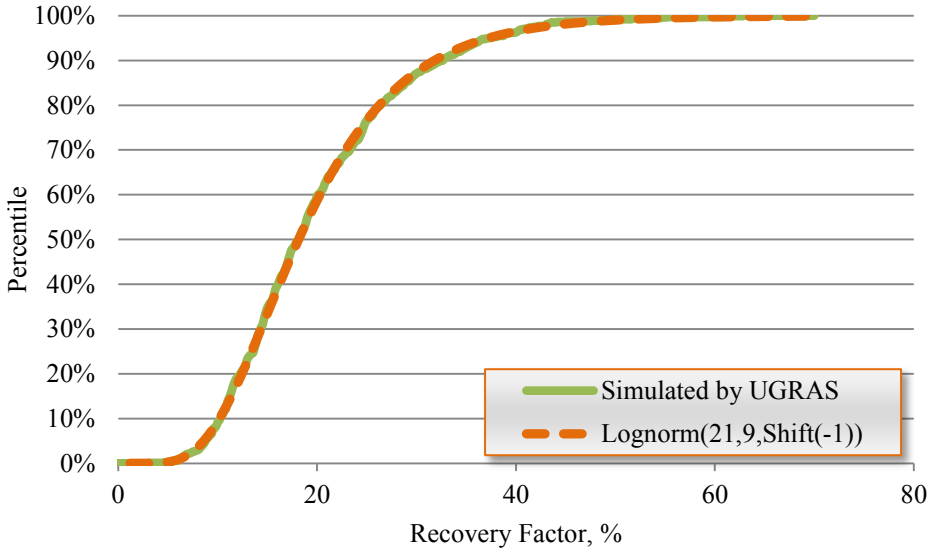

Figure 5.35—Probabilistic distribution of RF per 124 acres with a 25-year life for the Haynesville shale

In the Haynesville shale, the estimated productive acreage is estimated to be 5.76 million acres. With an average well spacing of 124 acres, 46,451 wells could be drilled in the Haynesville shale. Thus, the resource potential for the entire Haynesville shale is

1,858 Tcf of OGIP (P50) and 330 Tcf of TRR (P50) (**Table 5.28**). Shale-gas OGIP in the Haynesville shale was estimated at 217 to 245 Bcf per section (Cubic Energy, Inc 2008).

Table 5.28—Resource potential for dry gas in the Haynesville shale

Category	P10	P50	P90
OGIP, Tcf	1,022	1,858	3,159
TRR, Tcf	144	330	706

5.11 Discussion

Our resource assessments are high-level assessments. Although we estimate resources for entire plays, we do not model reservoir and well properties on a well-by-well basis. Instead, we model each play as a whole, using probability distributions that encompass the variability in reservoir properties across the field as well as the uncertainty in these properties. For example, the original gas in place varies from county to county because of differences in net thickness and other properties across the field. The distribution of net thickness we used in the Barnett study covered the greater net thickness in Tarrant County and the lower net thickness in the southwestern Barnett shale. Another limitation of our high-level assessments is related to vertical variability in properties. We did not consider vertical variations in properties, such as fracturability, throughout the zones evaluated. In some areas the net thickness of the shale gas plays are so thick that the entire pay zone cannot be completed and produced. However, we used the same distributions of net pay for the OGIP calculation and TRR prediction for the five shale gas plays in this section.

Little performance data exists for the Eagle Ford and Marcellus shale. Even though we calibrated the Eagle Ford and Marcellus dry gas forecasts against actual production data, there is uncertainty in these forecasts.

The typical shale-gas production profile shows a high initial production with a steep production decline (65-80%) in the first year, and decline rates begin to stabilize at a relatively low level over time (> 300 month). The five-year well production history from Barnett shale shows that well production decline rate begin to stabilize at a low level in the fourth year (**Figure 5.36**). The simulated production curves were run out by UGRAS to 25 years to observe the long-term production trends.

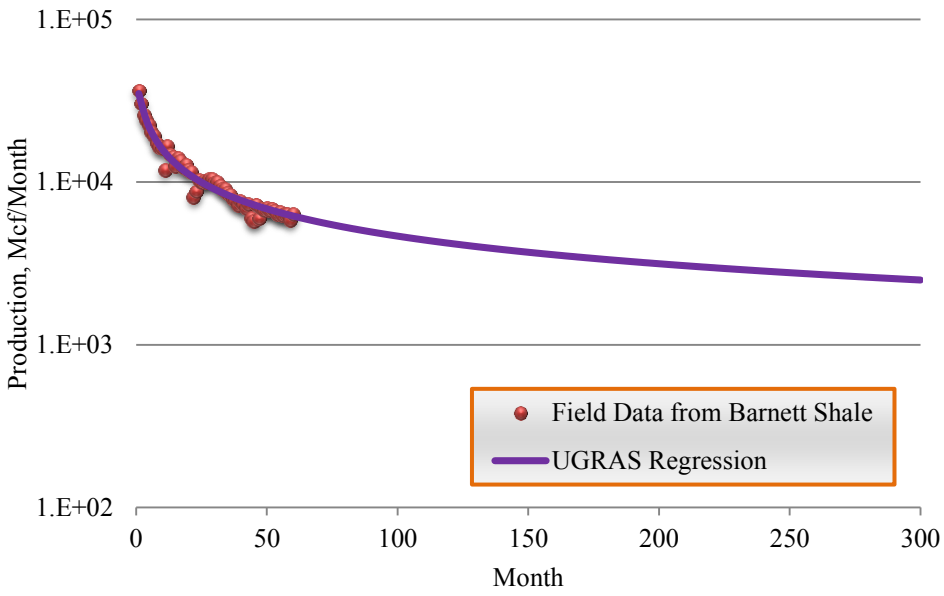

Figure 5.36—Five-year gas production for gas well in the Barnett shale

Well life affects TRR from shale gas plays (**Figure 5.37**). We chose a 25-year production history rather than 30 or 50 years. In the current economic environment, most

operators are looking at payout and return on investment. As such, production during the first 5-10 years is the most important.

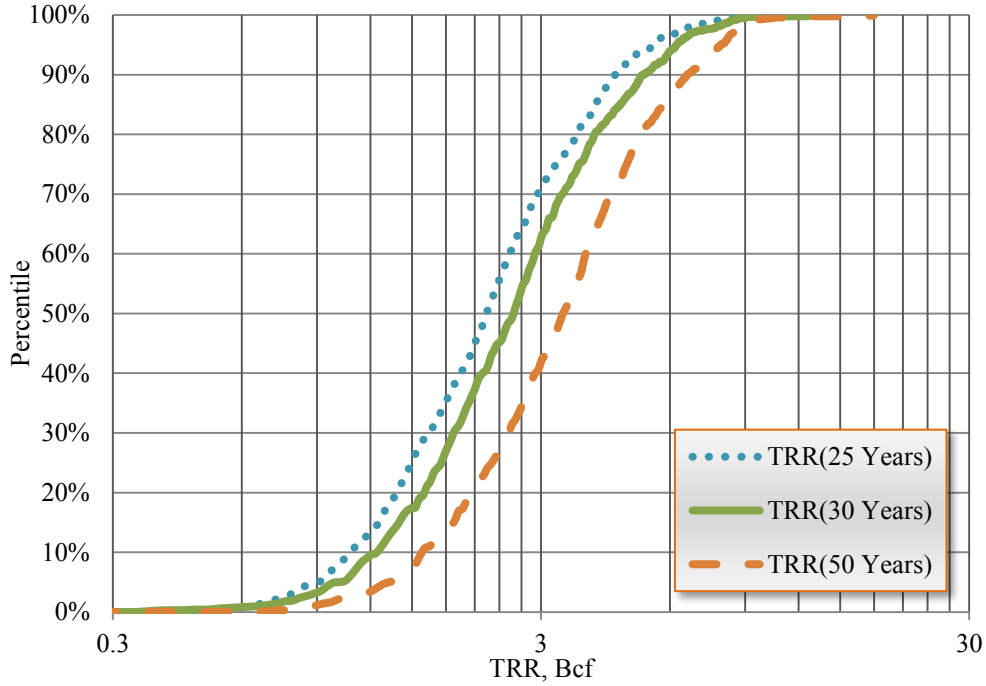

Figure 5.37—TRR in the Barnett shale increases with analysis life

5.12 Summary

We have evaluated the cumulative probabilistic distribution of OGIP, TRR and RF for the five key shale gas plays in the United States using a probabilistic and analytical reservoir model. Our assessment results of gas in place and technically recoverable gas for the five key shale gas plays in the United States have confirmed by comparing to previous work. **Table 5.29** summarized the key characteristics of the five key shale gas plays we assessed in the section.

Figure 5.38 shows the cumulative distribution of OGIP per section for the five shale gas plays. Haynesville have the most original shale gas in place per section due to its highest gas content (**Figure 5.39**).

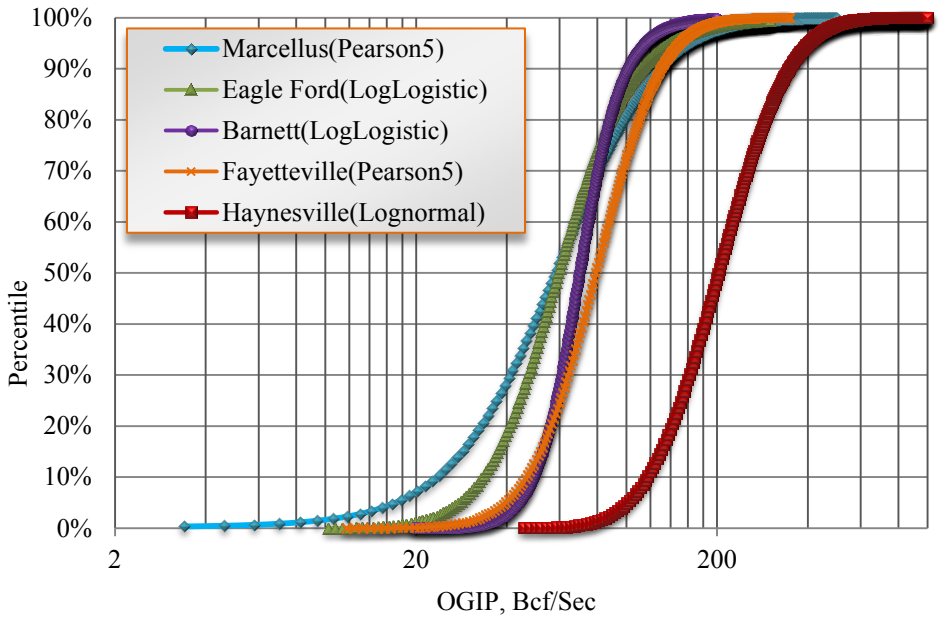

Figure 5.38—Comparison between probabilistic distributions of OGIP per section for five shale gas plays in the United States

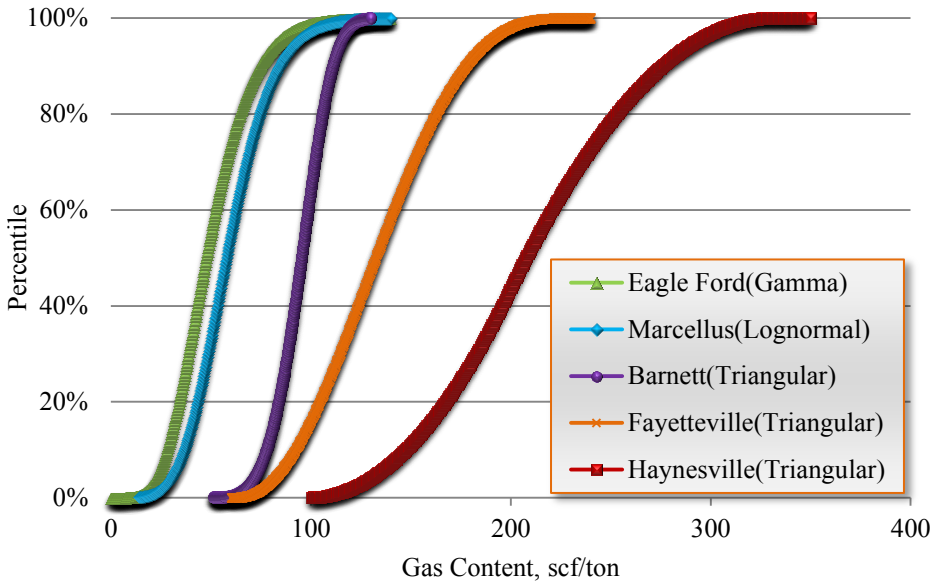

Figure 5.39—Haynesville has the highest value of gas content among the five shale gas plays

Figure 5.40 shows the cumulative distribution of TRR per section for the five shale gas plays. TRR is the most sensitive to the net pay besides lateral length (Figure 5.3). Haynesville has the most technically recoverable shale gas resource since it has the thickest net pay (**Figure 5.41**).

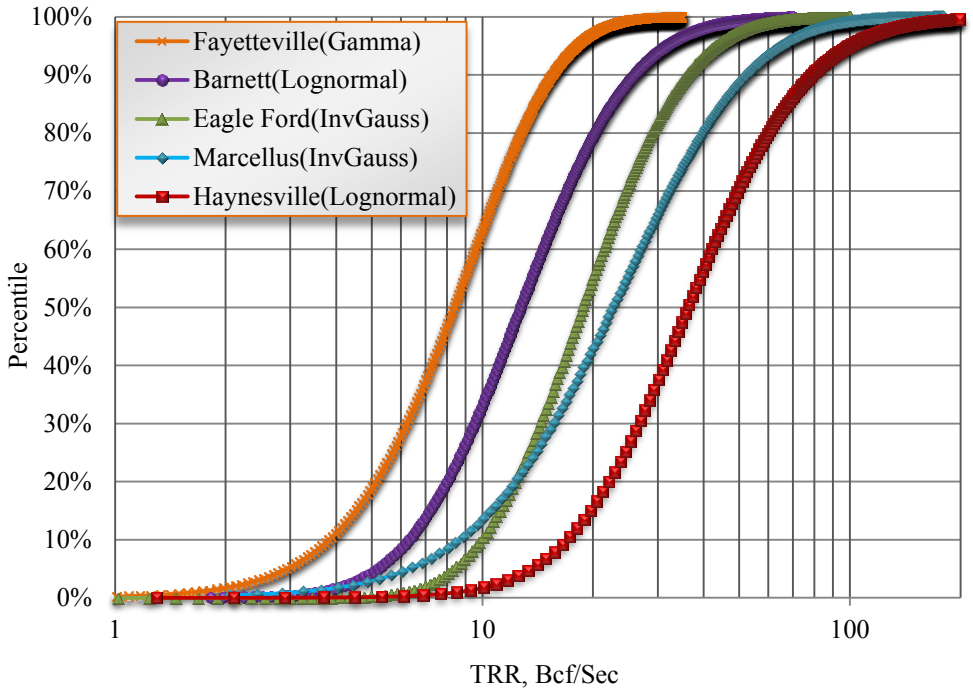

Figure 5.40—Comparison between probabilistic distributions of TRR per section for five shale gas plays in the United States

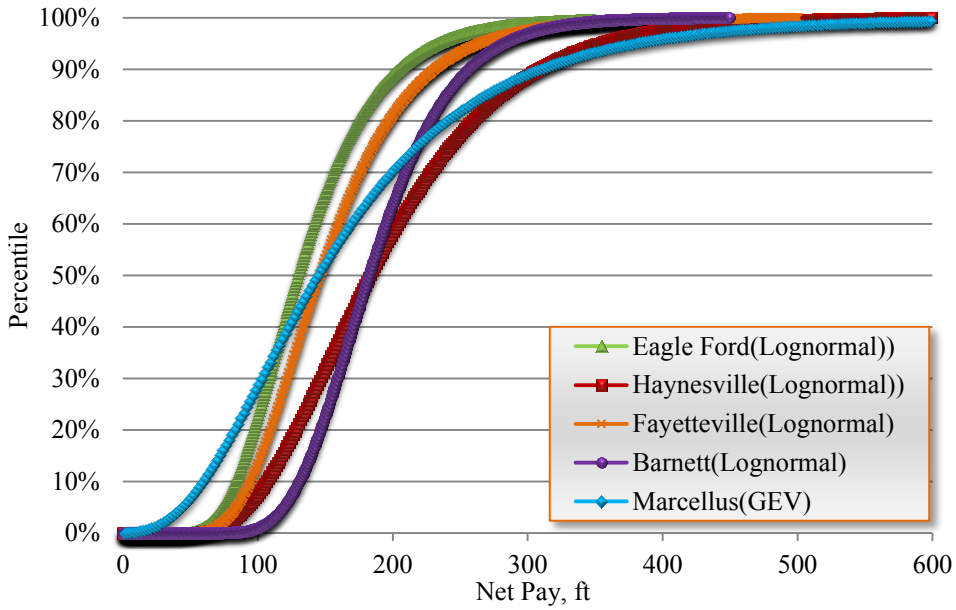

Figure 5.41—Haynesville has highest TRR due to its thickest net pay

Table 5.29—Summary of the key characteristics for five key shale gas plays in United States

Parameter	Eagle Ford	Fayetteville	Barnett	Marcellus	Haynesville
Area, Acres	3,000,000	2,560,000	3,200,000	15,000,000	5,760,000
Depth, ft	5,500-14,400	1,200-8,000	6,500-8,500	3,300-8,800	10,000-14,000
Net Pay, ft	3-326	50-325	100-600	45-384	200-300
Porosity, %	3-12	2-8	4-5	3-13	8-14
System Permeability, 10^{-3}md	0.1-0.7	1-4*	0.07-5	0.2-0.9	0.5-400*
λ (dimensionless)	1×10^{-6}	1×10^{-7}	7×10^{-7}	9×10^{-6}	1×10^{-8}
S_w,%	9-44	15-35	25-43	6-53	16-41
Average Pi, psia	4,300-10,900	800-4,000*	3,000-5,000	2,000-5,100	7,000-10,000
Gas Content, scf/ton	7-120	60-220	60-125	41-148	100-330
Temperature, ^oF	170-231	100-150	205	110-160	300-350
TOC,%	0.3-5.4	4.0-9.5	2.4-5.1	2.0-8.0	0.5-4.0
Ro, %	1.5	1.0-5.0	0.6-1.6	1.25	2.2
Bulk Density, g/cc	2.36-2.65	N/A	2.5	2.30-2.60	<2.57
Typical Well Spacing, acres/well	80-640	80-160	60-160	40-160	40-560
Well Spacing, acres	147	129	111	104	124
Horizontal Wells by 2011	177	3,170	9,449	837	1,156
Average Lateral Length, ft	5,600	4,800	4,000	3,700	4,600
Fracture Stage	12-18	8-11	7-9	6-8	12-15
Fracture Half-length, ft	350	250-300	300-400	300-400	300
Initial Production, MMcf/d	6	2.2	1.2-4.7	7.7	10
Production in 2011, Bcf/d	0.1	2.6	5.2	3.8	6
Cum. Prod by 2011, Bcf	442	2,593	8,270	2,090	3,940
OGIP by This Study (P50), Tcf	278	258	352	1,385	1,858
TRR by This Study (P50), Tcf	90	34	63	534	330

* Range is estimated by this study.

The Marcellus shale has high recovery factor due to high value of interporosity flow coefficient ($\lambda=9\times10^{-6}$) (**Figure 5.42**). High value of interporosity flow coefficient means that fluids flow easily between the fracture and matrix, while a small value indicates that flow between the media is restricted. Besides, high reservoir pressure is the other important reason that the Eagle Ford shale has high recovery factor.

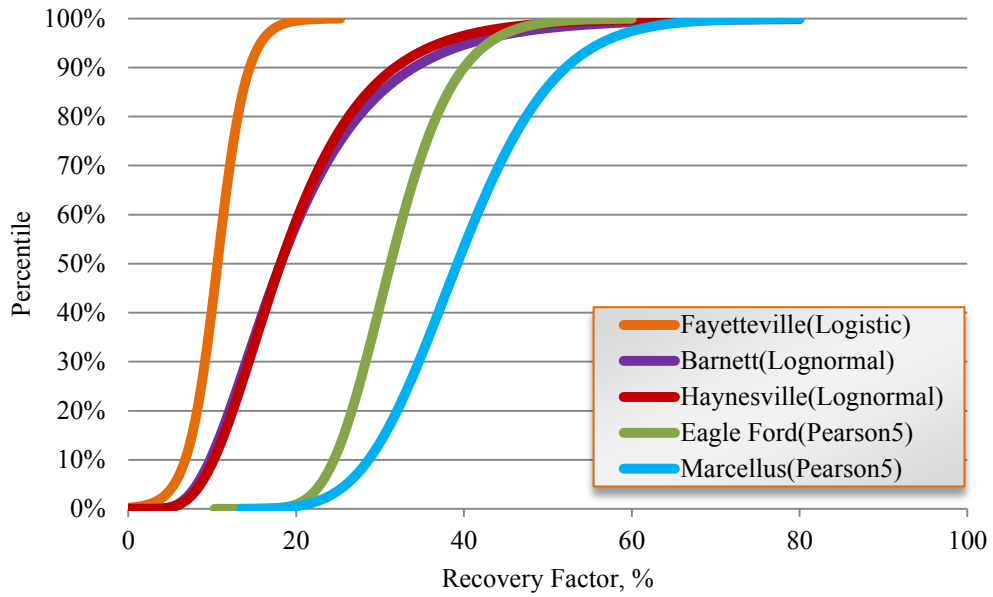

Figure 5.42—Comparison between probabilistic distributions of recovery factor for the five shale gas plays in the United States

Table 5.30, constructed for the five major shale gas plays, provided a concise summary of these resource assessments. Well life affects recovery factor from shale gas plays (**Figure 5.43**). We chose a 25-year production history rather than 30 or 50 years. In the current economic environment, most operators are looking at payout and return on investment. As such, production during the first 5-10 years is the most important. We gained a probabilistic distribution of technically recovery factors with 25-year recovery

period from the five key shale gas plays in the United States. It follows a general Beta distribution, with a mean value of 25% (**Figure 5.44**). We will apply this distribution to assess the TRR for the other six regions in Section 8. As a comparison, the mean value of recovery factor of shale gas in EIA (2011a) basin-level assessment which includes basins across 32 countries is 25% (Table 2.3).

Table 5.30—Summary of resource assessment for five key shale gas plays in United States

Parameter	Fayetteville	Barnett	Marcellus	Eagle Ford	Haynesville
Area, Acres	2,560,000	3,200,000	15,000,000	3,000,000	5,760,000
Well Spacing, acre	129	111	104	147	124
Well Number	19,844	28,828	144,230	20,407	46,451
Distribution of OGIP	Pearson type V	Log-logistic	Pearson type V	Log-logistic	Lognormal
OGIP (P10), Bcf/well	9.0	8.4	3.8	7.5	22.0
OGIP (P50), Bcf/well	16	12.2	9.6	13.6	40.0
OGIP (P90), Bcf/well	26.0	17.8	20.8	25.3	68.0
Distribution of TRR	Gamma	Lognormal	Inverse Gaussian	Inverse Gaussian	Lognormal
TRR (P10), Bcf/well	0.78	1.1	1.5	2.3	3.1
TRR (P50), Bcf/well	1.7	2.2	3.7	4.4	7.1
TRR (P90), Bcf/well	3.1	4.5	8.5	8.5	15.2
Distribution of RF	Logistic	Lognormal	Pearson type V	Pearson type V	Lognormal
RF (P10), %	7	10	29	25	10
RF (P50), %	11	18	39	31	18
RF (P90), %	15	35	52	40	33
OGIP (P10), Bcf/Section	45	48	23	33	114
OGIP (P50), Bcf/Section	79	70	59	59	206
OGIP (P90), Bcf/Section	129	103	128	110	351
TRR (P10), Bcf/Section	4	6	9	10	16
TRR (P50), Bcf/Section	8	13	23	19	37
TRR (P90), Bcf/Section	15	26	52	37	78

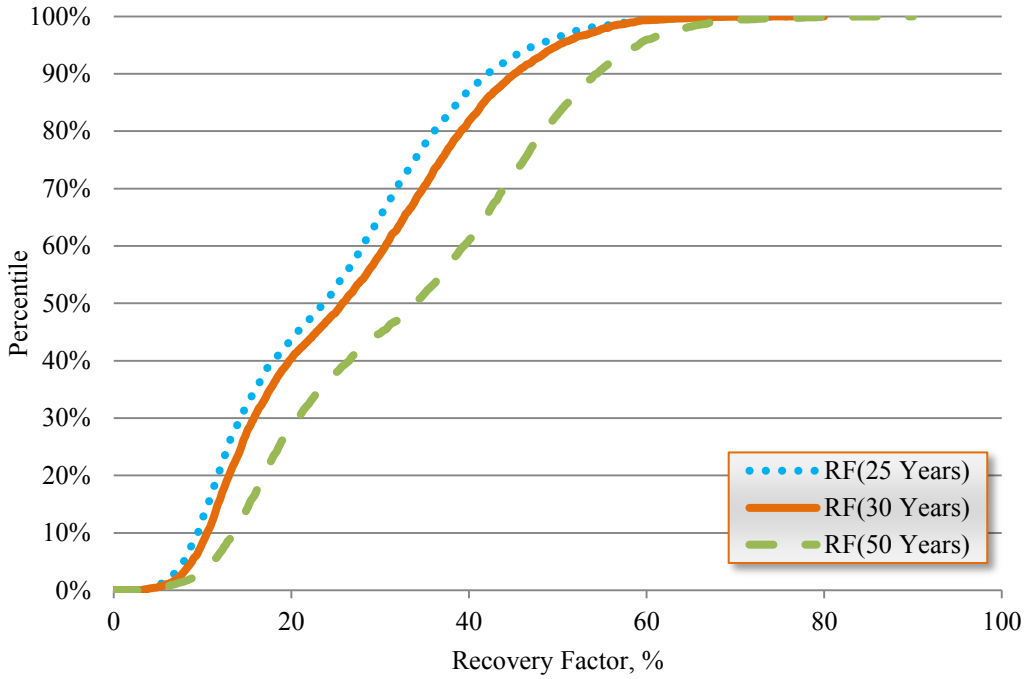

Figure 5.43—Recovery factor versus recovery period

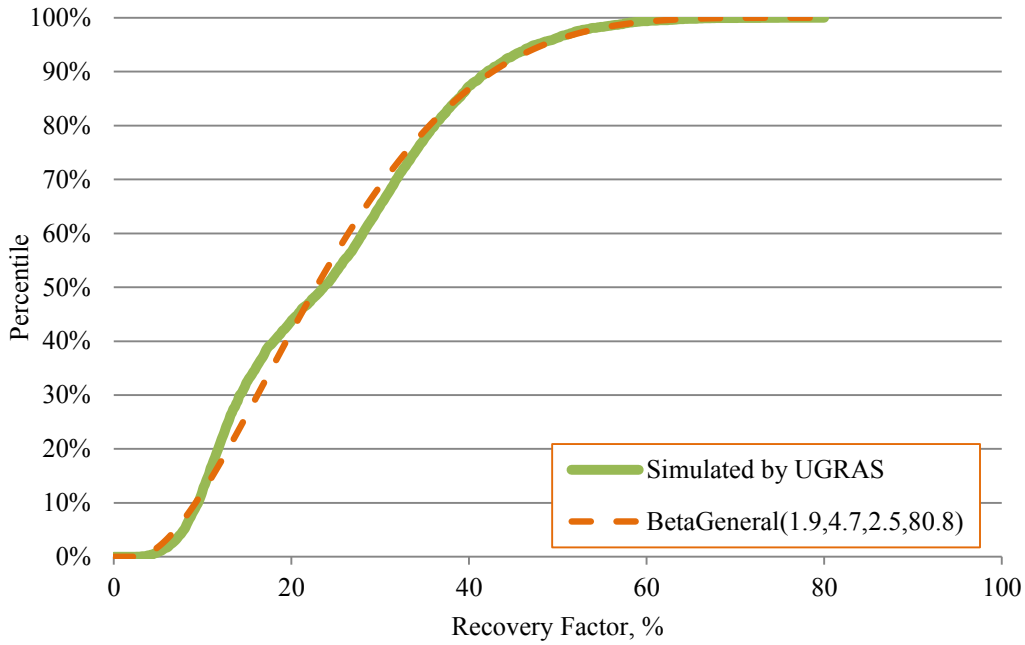

Figure 5.44—Recovery factor of shale gas for the United States

6. RESOURCE EVALUATION FOR TIGHT SANDS GAS RESERVOIRS IN UNITED STATES

Strong natural gas demand, sustained higher gas prices, and technological improvements have turned tight gas into a key element of the United States energy supply picture. The United States has been producing tight gas since 1970's, and it now accounts for approximately 23% of the country's natural gas consumption (Figure 1.2).

In the section, we investigated drilling, stimulation and completion method for tight sand gas in three key tight gas formations of United States. Then, we applied workflow of UGRAS to assess the distribution of OGIP, TRR and RF in the three key formations.

6.1 Drilling, Stimulation and Completion Methods in Tight Sands Gas Reservoirs

6.1.1 Drilling Methods

Horizontal wells have had great successes in high permeability oil sands, unconventional gas shales, and carbonates. With the advancement in drilling and completion technologies, there has been a recent trend to drill and complete horizontal wells in tight gas sandstones in North America. Baihly et al. (2009) researched the best sequential 12 months of production (where available) for all wells in the Bossier, Cotton Valley, Travis Peak, and Cleveland Sands. **Table 6.1** reveals that the average production for horizontal wells in the case of the Bossier Sand can be nearly five times that of offset

vertical wells, with PIF of 4.7. The Cleveland Sand has had an increasing PIF yearly since 2003 (**Table 6.2**). However, it is important to drill the well as quickly as possible to minimize rig costs.

Table 6.1—PIF and horizontal well percentage of East Texas sandstones

Formation	Bossier Sand		Cotton Valley Sand		Travis Peak Sand	
Year	PIF	% of Horizontal Wells	PIF	% of Horizontal Wells	PIF	% of Horizontal Wells
<2005	1.5	1.1	1.1	0.29	1.2	0.11
2005	3.8	2.7	2.6	0.44		
2006	4.7	8.3	1.9	1.25	1.9	0.6

Table 6.2—PIF and horizontal well percentage of the Cleveland Sand

Year	PIF	% of Horizontal Wells
<2003	1.1	4.08
2003	2.6	27.54
2004	2.6	62.50
2005	3.4	69.09
2006	3.5	71.72

6.1.2 Well Completion and Stimulation Considerations

If a single fracture treatment can be used to stimulate multiple layers, and no reservoir damage occurs by commingling the different zones, most tight gas wells should be completed and stimulated with a single-stage treatment. Normally, in dry-gas reservoirs, no reservoir damage occurs by commingling different layers. In fact, it is likely that more gas will be recovered by production all the layers in a commingled fashion because the abandonment pressure is lower at any given economic limit when the zones are commingled versus production the zones one at a time (Holditch 2006).

If two or more productive intervals are separated by a thick, clean shale (e.g. 50 ft or more) and this shale has enough in-situ stress contrast to be a barrier to vertical fracture growth, the design engineer might need to design the completion and stimulation treatments to consider that multiple hydraulic fractures will be created. In such cases, fracture treatment diverting techniques must be used to stimulate all producing interval properly.

Hydraulic fracturing is the key technology in tight-gas development. Most tight reservoirs have to be fractured before they will flow gas at commercial rates. In the 1980s, thick, cross-linked polymer fluids that carried tremendous volumes of sand were popular for tight-sand reservoirs, but the high cost of these treatments rendered some plays uneconomic. There were also problems with fracture fluid cleanup when the cross-linked fluids did not break as they were designed to do. In the 1990s, slick-water fracturing techniques were developed that used high volumes of water and low concentrations of proppant. These jobs were much less expensive and opened some new areas to commercial development. Slick water fracture treatments also used much less polymer, which improved clean up. Multi-stage fracturing was another advance, allowing several stages to be treated in quick succession. At present, operators use a variety of techniques, depending on the particular characteristics of a reservoir.

6.2 Reservoir Model for Tight Sands Gas Reservoirs

In this dissertation, tight sands gas reservoirs are modeled as a conventional single-porosity system. So there is only one type of pore space and one scale of pore size.

To develop tight sands gas reservoirs, we commonly use hydraulically fractured vertical well. The type of outer boundary for the tight sands gas reservoir is defined as a closed circle. The well is centered in the drainage area. **Table 6.3** summarizes the reservoir model used for tight sands gas reservoir in our research.

Table 6.3—Reservoir model for tight sands gas reservoirs

Porosity	Single porosity
Fracture Conductivity	Infinite
Inner Boundary	Vertical Fractured
Outer Boundary	Circular
Lithology	Sandstone
Pressure Step	Constant
Permeability	Isotropic
Well Location	Centered

6.3 Reservoir Parameters Sensitivity Analysis

We investigated the reservoir properties that affect the prediction of OGIP and TRR. Ten different characteristics were analyzed. **Table 6.4** lists the primary parameters. Uncertainty involves in the prediction of net pay, permeability, porosity, water saturation, initial pressure and fracture half-length. However, the well spacing is controllable.

OGIP of tight sands gas is calculated by using Eq. 3.4. Tight-sands OGIP is affected by area, net pay, porosity, and water saturation. Parameter sensitive analysis reveals that net pay, reservoir pressure, water saturation, porosity, permeability, and fracture half-length have highest correlation to production (**Figure 6.1**). These six parameters were treated as uncertain parameters in the section.

Table 6.4—Primary reservoir parameters that affect OGIP or TRR of tight sands gas reservoirs

Primary Property	Controllable	Uncertainty
Net Pay	No	Yes
Permeability	No	Yes
Porosity	No	Yes
Water Saturation	No	Yes
Reservoir Pressure	No	Yes
Fracture Half-length	No	Yes
Well Spacing	Yes	No

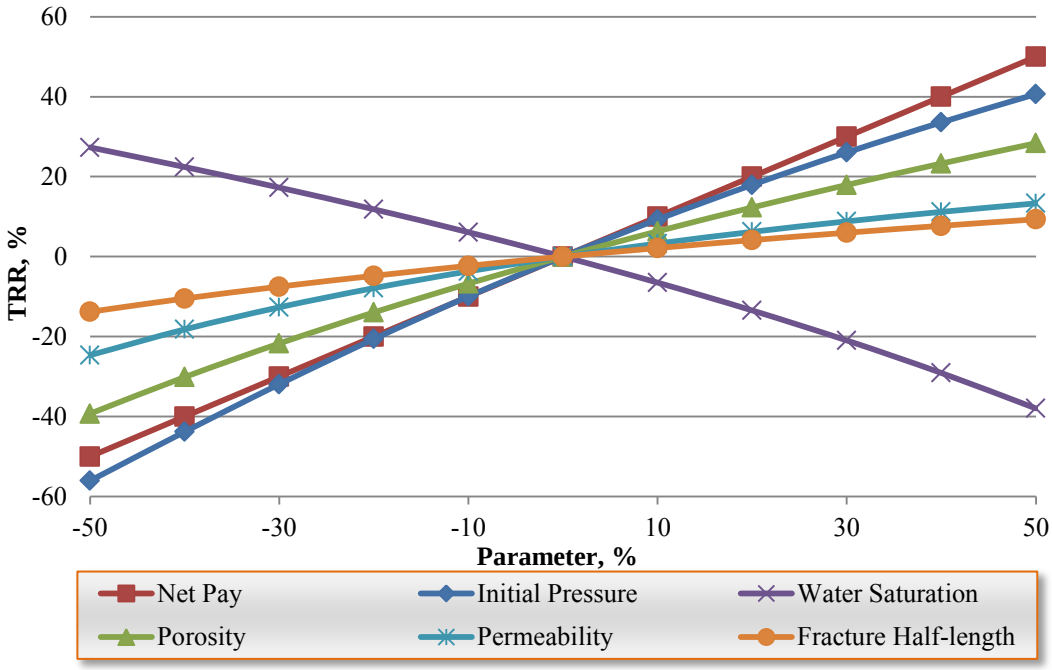

Figure 6.1—Sensitivity analysis result of tight sands gas TRR

6.4 Recent Production and Activity Trends

Between 2000 and 2011, tight gas production from the lower 48 states increased from 3.8 Tcf to 6.2 Tcf per year, and now accounts for 29% of total lower-48 gas production (EIA 2012a). **Figure 6.2** shows the production trend from all the tight sands gas formations listed in **Table 6.5**. As of 2011, the Greater Green River basin of

Wyoming and several formations in the East Texas basins dominates in terms of tight production gas activity (Figure 6.2). Resource estimates for these two basins are discussed in greater detail in the following section of this section. A detailed simulation study of the entire basins was not possible within any reasonable time or budget constraints. But one or more small scale simulations performed on the most productive formation of the basin could be representative of the basin as a whole. These assessments result in an optimal solution to the problem of characterizing well and reservoir performance and determining recovery factor.

Table 6.5—Tight sands gas formation in the United States

Basin	Formation
East Texas	Austin Chalk, Bossier, Cotton Valley, Travis Peak
Green River	Almond, Frontier, Fort Union, Fox Hills, Lance, Lewis, Mesaverde, Muddy-Dakota-Morrison
Wind River	Fort Union, Frontier, Lance, Lakota, Meeteetse, Mesaverde, Muddy
San Juan	Charca, Dakota, Mesaverde, Picture Cliff
Uinta	Mesaverde, Mancos, Wasatch
Williston	Bowdoin, Eagle, Greenhorn, Judith River, Niobrara, Phillips
Permian	Abo, Canyon, Morrow, Penn, Strawn
Piceance	Dakota, lles, Mancos, Rollins, Williams Fork, Williams Fork-Cameo
Appalachian	Berea, Bradford, Clinton, Devonian, Elk, Medina, Tuscarora
Anadarko	Atoka, Cherokee, Cleveland, Granite Wash, Red Fork
Arkoma	Atoka
Gulf Coast	Austin Chalk, Olmos, Vicksburg, Wilcox

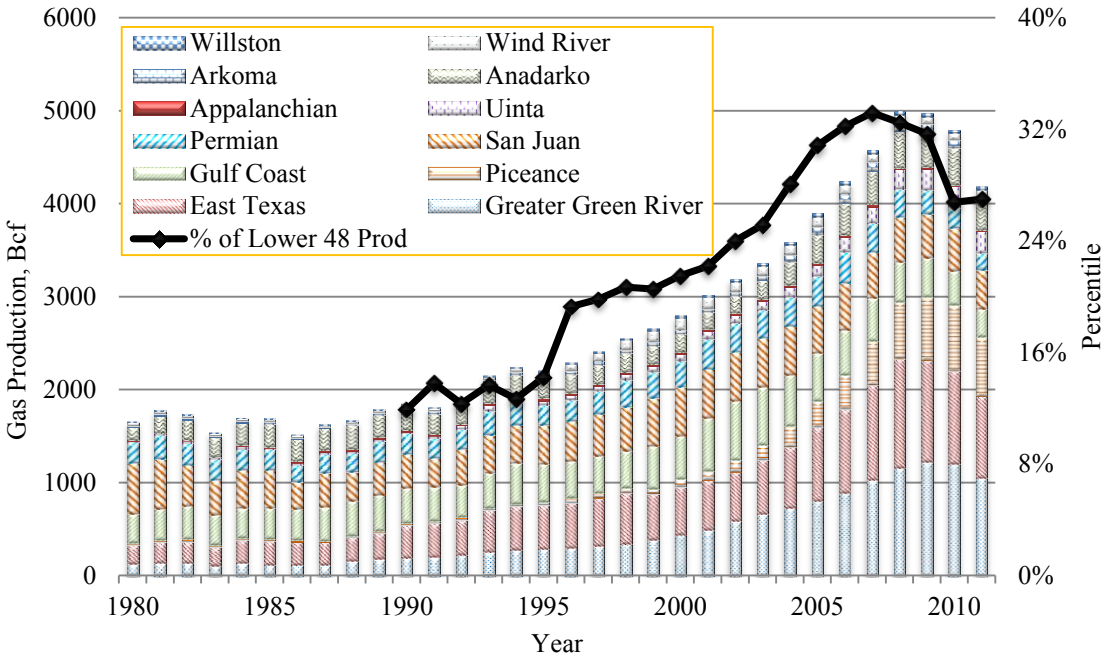

Figure 6.2—Annual tight gas production by basins (Data source: HPDI, 2011)

6.5 Greater Green River Basin

The Greater Green River basin (GGRB) is the dominant natural gas-producing basin in the Rocky Mountains. Major reserves of natural gas remain to be produced in the Greater Green River basin of southwestern Wyoming and northwestern Colorado. This basin, occupying approximately 13.44 million acres, includes four sub-basins. These are the Green River basin—west of the Rock Springs Uplift, Red Desert and Washakie in Wyoming, and the Sand Wash basin in Colorado—east side of the uplift (Newman III 1981). Thick sections of Tertiary and Upper Cretaceous rocks exist throughout most parts of the Greater Green River basin.

The volumetric analysis by NETL yielded an OGIP of 3,438 Tcf for Greater Green River basin (Boswell 2005) (**Figure 6.3**). The Mesaverde Group, Lewis, Lance and Lower Tertiary Fort Union and Wasatch formations have significant thick intervals of tight and near tight sandstones containing natural gas.

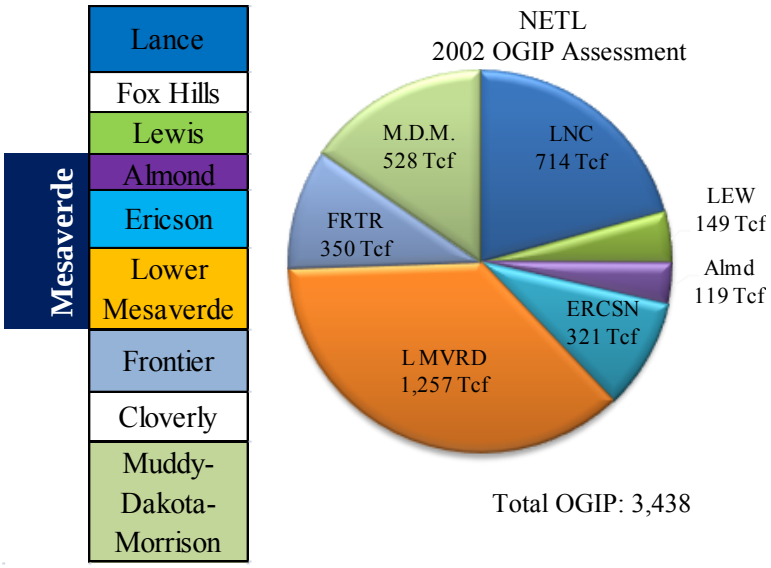

Figure 6.3—Tight sands formations in the Greater Green River basin (GGRB)

The Lance formation, the most prolific tight formation in the area, has been extensively developed, using vertical wells and hydraulic fracture treatments (**Figure 6.4**). We have focused on the Lance formation of the Great Green River basin in our research.

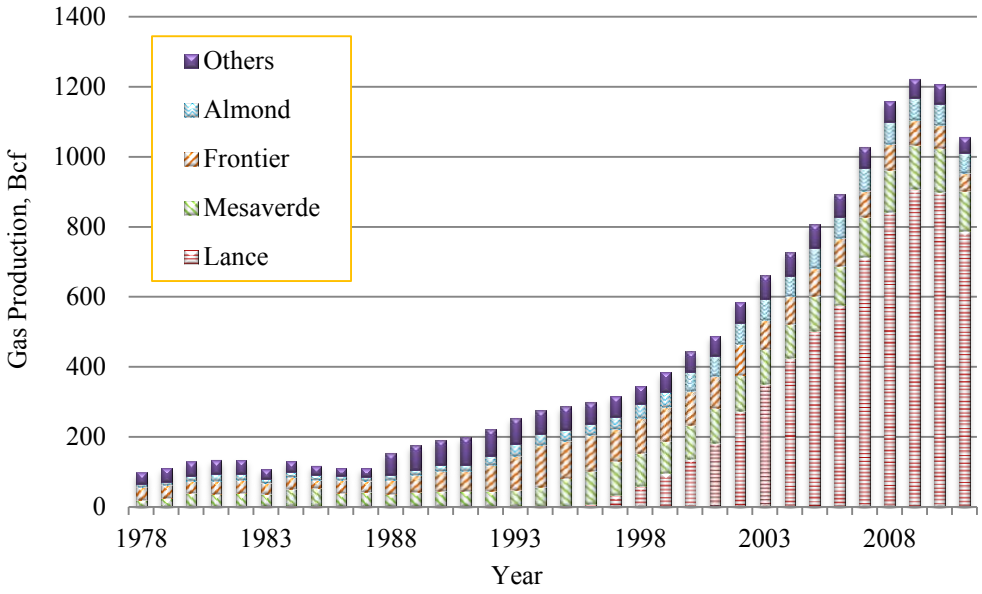

Figure 6.4—Lance formation is the most productive tight gas formation in Greater Green River basin (Data source: HPDI 2011)

6.5.1 Geological Overview of Lance Formation

The fluvial Cretaceous Lance formation is late Maastrichtian in age (dating to about 67.5-65.5 Ma), which lies below the fluvial Tertiary Fort Union and inter-fingers at its base with the Cretaceous Mesaverde formation. The Lance formation is from the Upper Cretaceous age and consists of 2,000 to 3,000 ft of interbedded fluvial sands, mudstones, and coals (Eberhard et al. 2000). The play area encompasses an area of about 2,600 thousand acres (Law et al. 1989).

6.5.2 Production

First production from the Lance formation of GGRB occurred in 1978. By the end of 2011, 6.85 Tcf of gas have been produced from the Lance formation. **Figure 6.5** shows annual production and producing wells in the Lance formation from 1990 to 2011.

Daily production reached 2.2 Bcf/d in 2011. Although direct wells are becoming more important to produce gas from this formation, vertical wells have been the main well type for the Lance formation until 2009.

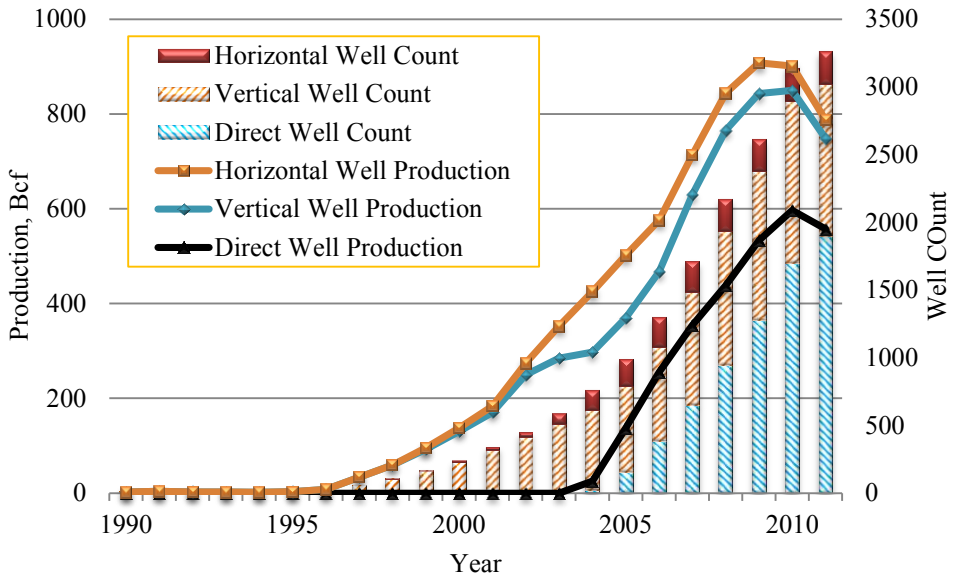

Figure 6.5—Annual production and producing wells in the Lance formation (Data source: HPDI 2011)

6.5.3 Reservoir Parameters

Drilling depths of the Lance formation range from 8,000 to 12,500 ft. Wells encounter overpressured gas at 8,100 to 9,300 ft (0.58 to 0.65 psi/ft gradient). Temperature gradient is 1.5 ^{o}F/ 100 ft. Gross interval thickness of the Lance formation ranges from 2,800 ft to more 3,600 ft. Within this interval the net-to-gross pay ratio varies from 25% to 40% (Wolhart et al. 2006). Individual sandstone bodies occur as 5-50 ft and net pay ranges from 300 to 600 ft (Eberhard et al. 2000; Wolhart et al. 2006). Productive sandstones in the Lance formation are extremely tight. Porosity in the economic intervals ranges from 5% to 14%. The relative gas permeability ranges from

0.001 to 0.02 md. Water saturation varies from 30% to 60% (Eberhard et al. 2000). Fracture half-length ranged from 350 ft to 500 ft and was fairly symmetric (Wolhart et al. 2006). **Table 6.6** summarized the range of main uncertain reservoir parameters for the Lance formation of Greater Green River basin.

Table 6.6—Reservoir parameters for the Lance formation

Parameter	Range
Net Pay, ft	300-600
Reservoir Pressure, psi	4,800-7,500
Water Saturation, %	30-60
Porosity, %	5-14
Permeability, md	0.001-0.02
Fracture Half-length, ft	350-500

Table 6.7 shows the key fixed reservoir parameters used for the Lance formation single-well reservoir simulations. Wells were put on a 1,000 psi bottomhole pressure control (Huffman et al. 2005). The well spacing, as a controllable parameter, is assumed 40 acres.

Table 6.7—Key fixed input parameters for the Lance formation model

Parameters	Value
Reservoir Temperature, ^{o}F	150
Bottom Hole Pressure, psia	1000
Wellbore Radius, ft	0.324
Gas Specific Gravity (air=1)	0.35
Bulk Density, g/cc	1.5
Well Spacing, acres	40

6.5.4 Model Verification

Figure 6.6 shows annual new producing vertical wells in the Lance formation. As of 2005, 681 vertical wells have been produced in the Lance formation for over 7 years. All the production histories for the 681 vertical wells were normalized for 7 years, which means we only used first 7-year production for all the wells.

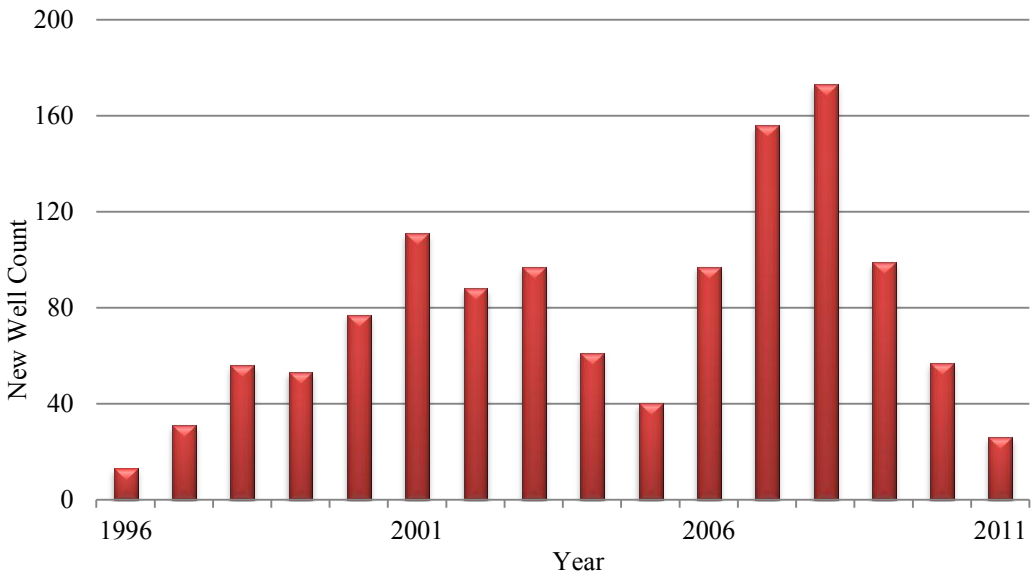

Figure 6.6—Annual new producing wells in the Lance formation

We initially defined the density functions for the six key parameters with honoring their range listed in Table 6.6. Then, the density functions for the key parameters were calibrated until a reasonable match between simulated and actual 7-year cumulative gas production from the wells in the Lance formation was reached.

The red curve in **Figure 6.7** shows the cumulative probability distribution of 7-year cumulative gas production for the 681 wells. The blue curve in Figure 6.7 is the cumulative distribution of 7-year cumulative gas production simulated by UGRAS with

the reservoir parameters in Table 6.7 and density functions in **Table 6.8**. The consistent match between the two curves finalized the density functions for the key parameters as in Table 6.8 and confirmed the well spacing of 40 acres. Note that the well spacing of 40 acres was by the end of 2005.

Compared to the reported range of net pay, we need to decrease the value of net pay to get this match (**Table 6.9**). The distributions of the other five uncertain parameters after calibration honored their range reported from literature.

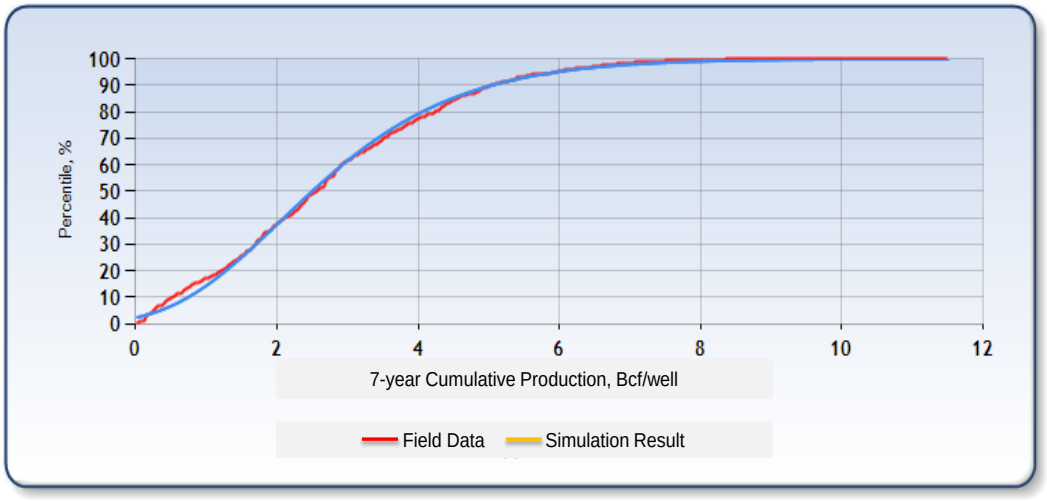

Figure 6.7—Probability distribution of cumulative gas production (7-year) match result for the Lance formation

Table 6.8—Density functions of uncertain parameters after calibration for the Lance formation

Parameters	Distribution Type	μ	σ	Min	Max	Shift
Net Pay, ft	Lognormal	180	100			-10
Initial Pressure, psi	Lognormal	6,100	800			
Water Saturation, f	Lognormal	0.45	0.06			
Permeability, md	Uniform			0.001	0.02	
Porosity, f	Uniform			0.05	0.14	
Fracture Half-length, ft	Uniform			350	500	

Table 6.9—Comparison of the range of uncertain parameters

Parameter	Reported Range	Used by This Study(P1-P99)
Net Pay, ft	300-600	30-600
Initial Pressure, psi	4,800-7,500	4,800-7,500
Permeability, md	0.001-0.02	0.001-0.02
Water Saturation, %	30-60	30-60
Porosity, %	5-14	5-14
Fracture Half-length, ft	350-500	350-500

6.5.5 Resource Evaluation for Current Well Spacing

The vertical well count in 2011 is about twice that the number as in 2005 (Figure 6.5). So it assumed that the well spacing is 20 acres currently. The resource assessment of the Lance formation was based on 20 acres in our work. To honor the reported range of net pay, we used a uniform distribution, ranging from 300 ft to 600 ft, as well as the density functions of other five parameters in Table 6.8 to general a distribution of OGIP per 20 acres (**Figure 6.8**)**.** The P10, P50 and P90 values are 3.6, 6.2, and 9.8 Bcf/20 acres, respectively.

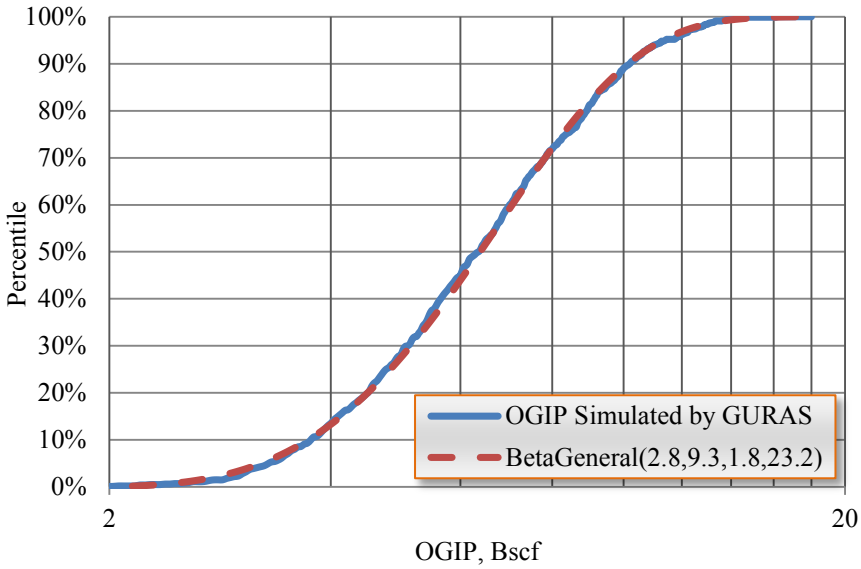

Figure 6.8—Probabilistic distribution of OGIP per 20 acres for the Lance formation

The simulation resulted in an inverse Gaussian distribution for TRR with a P10 value of 0.7 Bcf/20 acres, a P50 of 1.6 Bcf/20 acres, and a P90 of 3.7 Bcf/20 acres (**Figure 6.9**). The P10, P50 and P90 values of recovery factor for current well spacing of 20 acres are 74%, 78% and 81%, respectively (**Figure 6.10**).

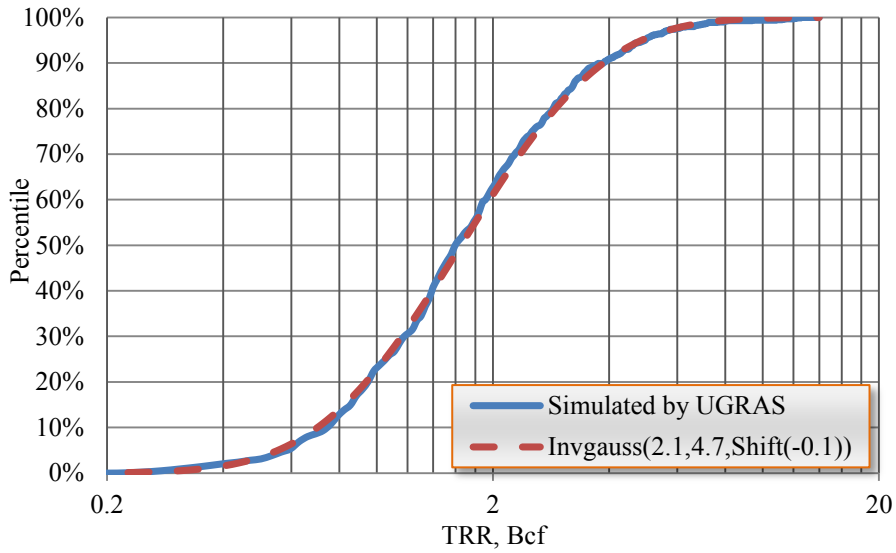

Figure 6.9—Probabilistic distribution of TRR per 20 acres with a 25-year life for the Lance formation

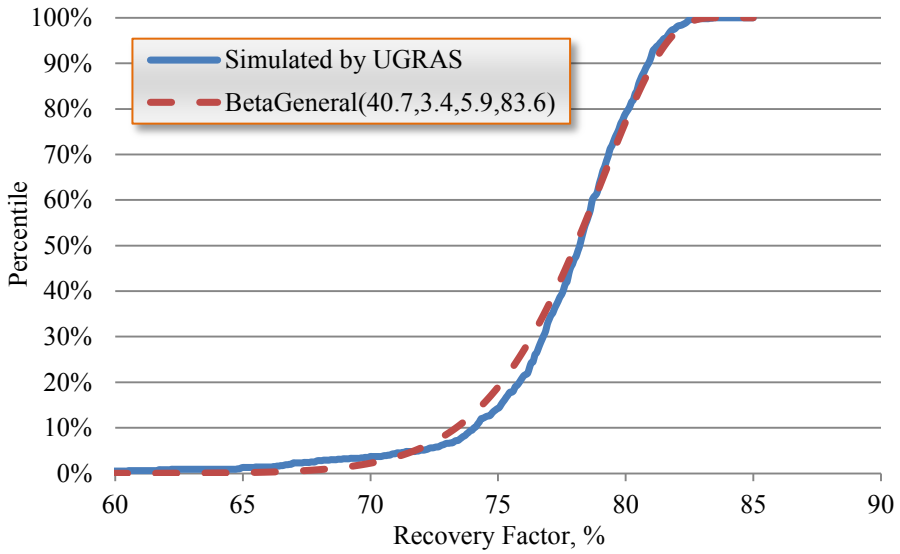

Figure 6.10—Probabilistic distribution of recovery factor per 20 acres with a 25-year life for the Lance formation

6.5.6 Resource Evaluation for Various Well Spacing

Tight sands gas OGIP is proportional to well spacing. We re-simulated the distribution of TRR from the Lance formation with varying well spacing to 40 acres and

20 acres. The TRR for single well is decreased with decreasing drainage area (**Figure 6.11**). However, the recovery factor can be enhanced with tighter well spacing (**Figure 6.12**). GTI's tight gas sand research indicates that the effective drainage radius is often approximately equal to the fracture half-length (Holditch 1992).The well spacing is not recommended to be lower than 20 acres (with reservoir radius of 530 ft) in the Lance formation, since the fracture half-length is predicted to be from 300 to 550 ft.

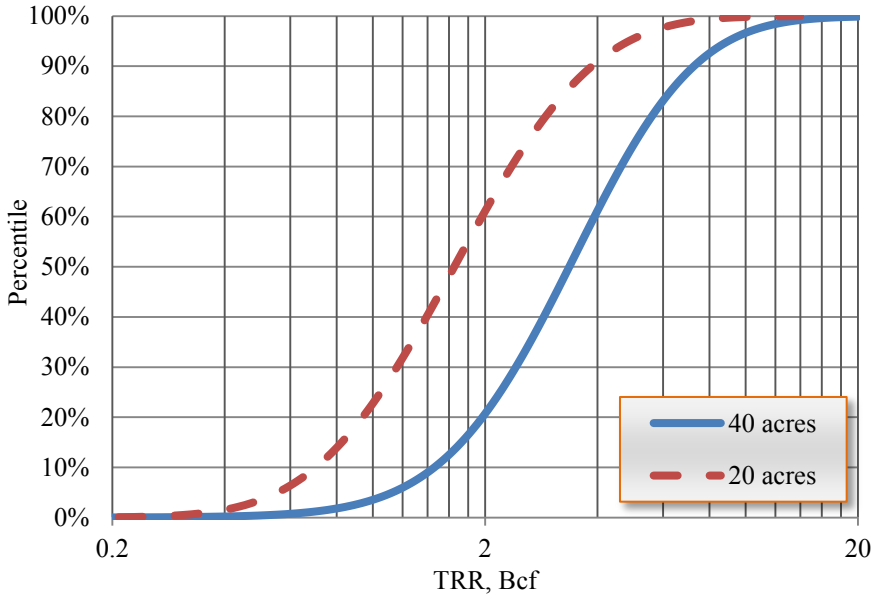

Figure 6.11—TRR versus well spacing in the Lance formation

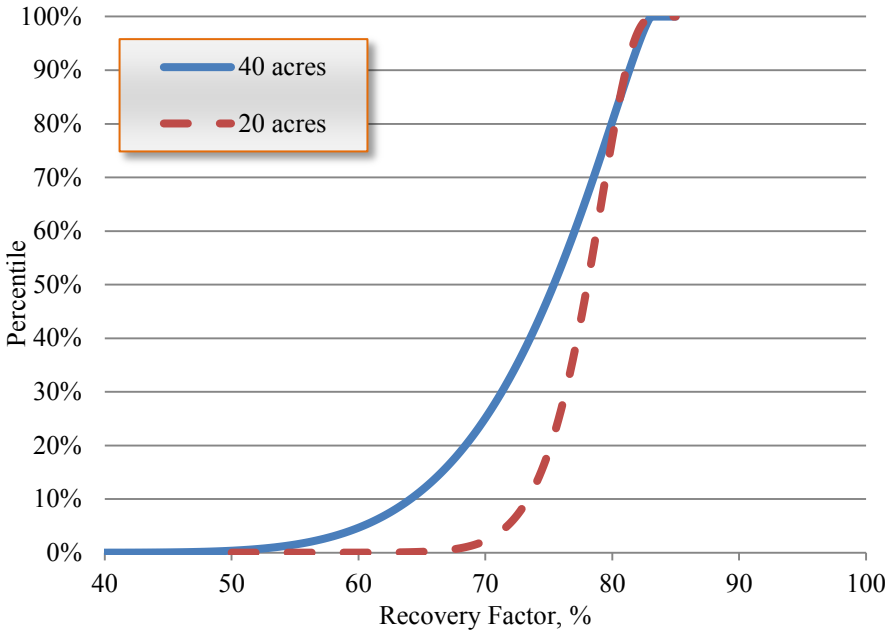

Figure 6.12—RF versus well spacing in the Lance formation

6.6 East Texas Basin

East Texas basin covers 32 million acres. In East Texas, tight-gas sands include four individual tight gas sands plays: Travis Peak, Cotton Valley, Bossier (found between 12,000 and 14,000 feet), and Deep Bossier (at 15,000 feet and deeper). So far, the Travis Peak and Deep Bossier development has been limited to East Texas. The Travis Peak in Louisiana is called the Hosston formation. The various Travis Peak and Cotton Valley formations are the most prolific unconventional sands in the East Texas basin. In 2011, wells in the Cotton Valley formation accounted for 52% of total unconventional production. The Travis Peak formation accounted for 18%, meaning the two formations accounted for more than 70% of the total unconventional production in the basin (**Figure 6.13**).

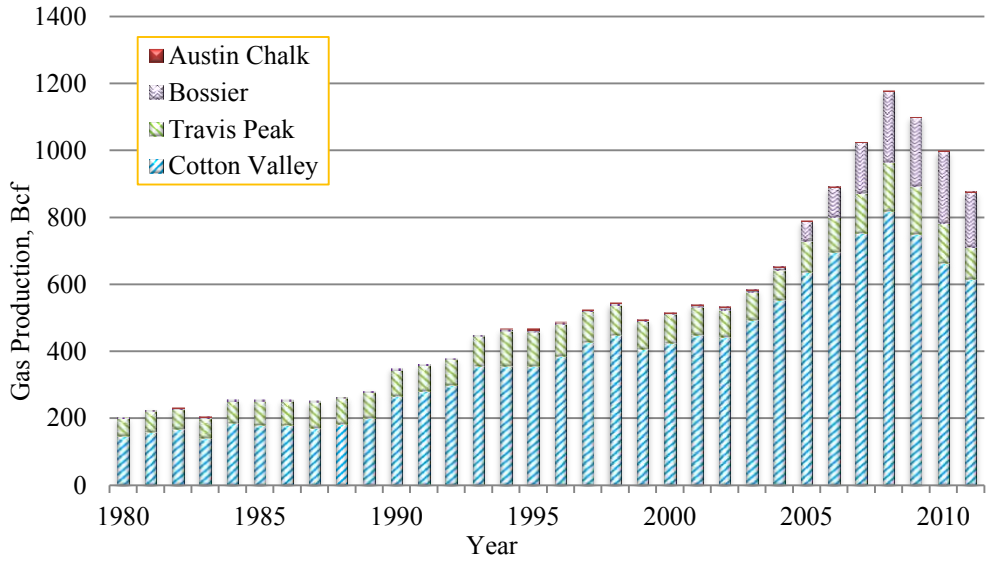

Figure 6.13—Cotton Valley formation is the most productive tight gas formation in the East Texas basin

6.6.1 Cotton Valley

The Cotton Valley sandstone is an Upper Jurassic age sandstone and is bounded by the Bossier shale below and by the Travis Peak formation above. The Cotton Valley formation is found throughout East Texas, covering 41,000 net acres. The Cotton Valley is basically a transgressive-regressive marine sequence. It was deposited along the northern margin of the Gulf Coast coastal plain and thickens basinward. This gas-bearing sandstone is found in the Overton Field in Gregg, Rusk and Smith counties, and in the Carthage Field of Panola County (Dyman and Condon 2006).

Production. By the end of 2011, 13.0 Tcf of gas have been produced and a cumulative total of 11,525 wells have been drilled and producing in Cotton Valley, including 249 horizontal wells and 9,747 vertical wells (**Figure 6.14**). Daily production decreased to 1.2 Bcf/d in 2011. All of these wells require multistage hydraulic fracture

treatments to economically produce. Over 180 operators have an active producing Cotton Valley sand well. With so many operators, there are many different completion approaches used to optimize Cotton Valley sand production, and these strategies are ever evolving over time.

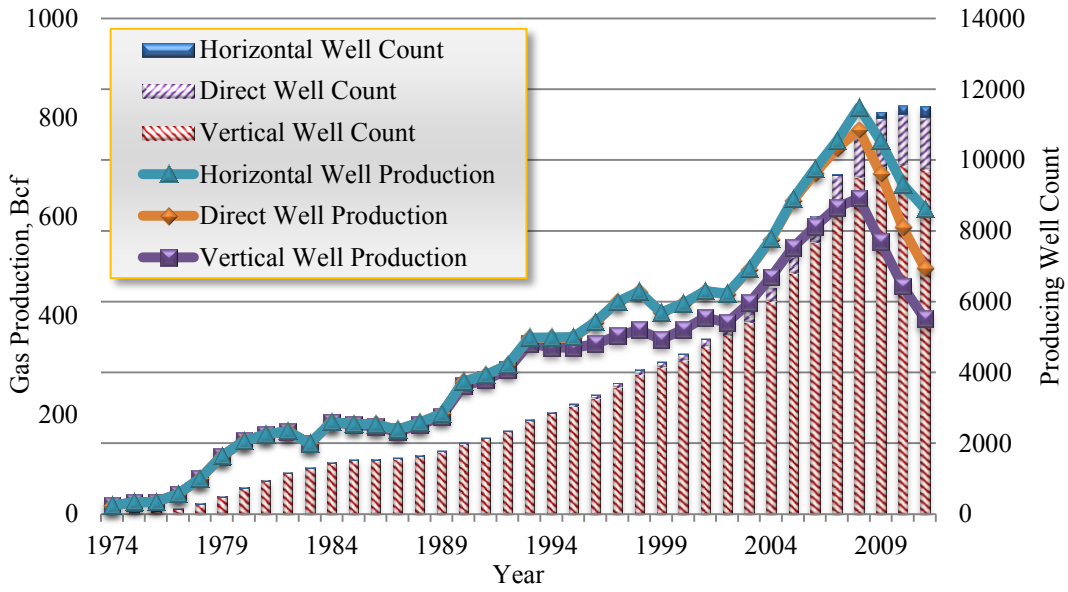

Figure 6.14—Annual production and producing wells in the Cotton Valley formation (Data source: HPDI 2011)

Reservoir Parameters. The Cotton Valley formation is typically found at depths ranging from 8,500 to 11,000 feet. The average pressure gradient equaled 0.55 psi/ft. the range of reservoir pressure can be calculated to be 4,600-6,000 psi. The gross interval in many of the Cotton Valley wells may be as much as 600 to 800 ft with 100 to 200 ft of net pay divided up into the smaller sand bodies (Jennings and Sprawls 1977). The average reservoir temperature and pressure in the Cotton Valley is 265 ^{o}F and 5,300 psi, respectively in the Rusk, Panola, and Harrison County area (Schlottman et al. 1981). The

water saturation ranges from 27 to 49%, with an average value of 30% (Jr. et al. 1988). The formation has grain densities ranging from 2.65 to 2.71 g/cm3. The porosity ranges from 1% to 12%, with a median value of 4% (Ganer 1985). The permeability of the Cotton Valley is typically between 0.0001 md and 0.3 md with a median of 0.012 md (Holditch 2006). **Table 6.10** summarized the range of main uncertain reservoir parameters for the Cotton Valley formation in the East Texas basin. **Table 6.11** shows the key fixed reservoir parameters used for the Cotton Valley formation single-well reservoir simulations. The well spacing is assumed 40 acres.

Table 6.10—Reservoir parameters for the Cotton Valley formation

Parameter	Range
Net Pay, ft	100-200
Reservoir Pressure, psi	4,600-6,000
Water Saturation, %	27-49
Porosity, %	1-12
Permeability, md	0.0001-0.3
Fracture Half-length, ft	N/A

Table 6.11—Key fixed input parameters for the Cotton Valley formation model

Parameters	Value
Reservoir Temperature, ^{o}F	265
Bottom Hole Pressure, psia	1000
Wellbore Radius, ft	0.324
Gas Specific Gravity (air=1)	0.65
Bulk Density, g/cc	2.7
Well Spacing, acres	40

Model Verification. As of 2005, 6,684 vertical wells have been produced for more than 7 years in the Cotton Valley formation of East Texas basin. **Figure 6.15** shows annual new producing vertical wells in the Cotton Valley formation. The production histories from these vertical wells were normalized for 7 years.

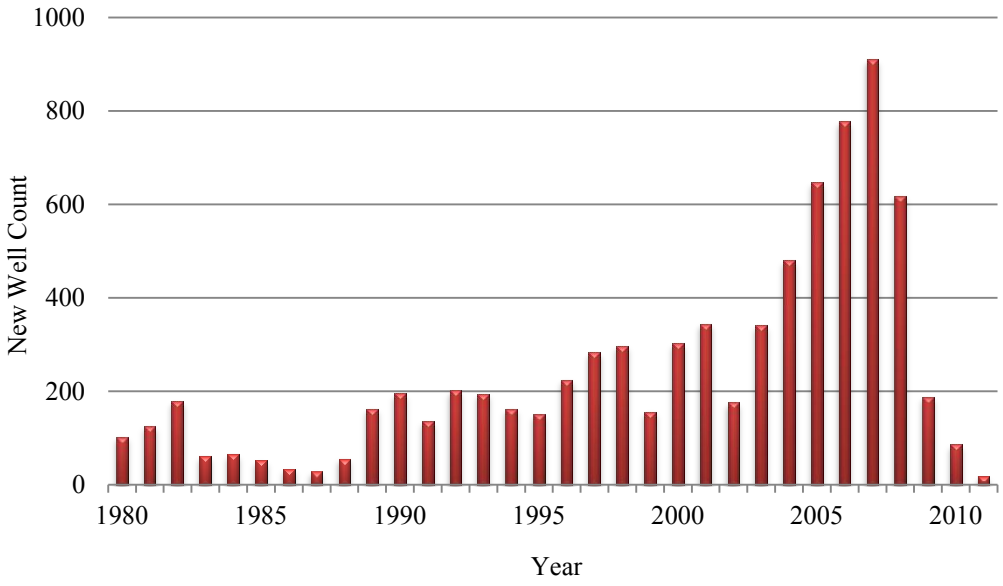

Figure 6.15—Annual new producing wells in the Cotton Valley formation

The density functions for net pay, initial pressure, porosity, water saturation, permeability, and fracture hale-length were defined with honoring the range in Table 6.10. The density functions for the key parameters were calibrated until a reasonable match between simulated and actual 7-year cumulative gas production from the wells in the Cotton Valley formation was reached.

The red curve in **Figure 6.16** shows the distribution of 7-year cumulative gas production from the 6,684 wells. The blue curve in Figure 6.16 is the distribution of 7-

year cumulative gas production simulated by UGRAS with the reservoir parameters in Table 6.11 density functions listed in **Table 6.12**. The consistent match between the two curves finalized the density functions for the key parameters as listed in Table 6.12 and confirmed the well spacing of 40 acres. The distributions of the six uncertain parameters after calibration honored their range reported from literature (**Table 6.13**).

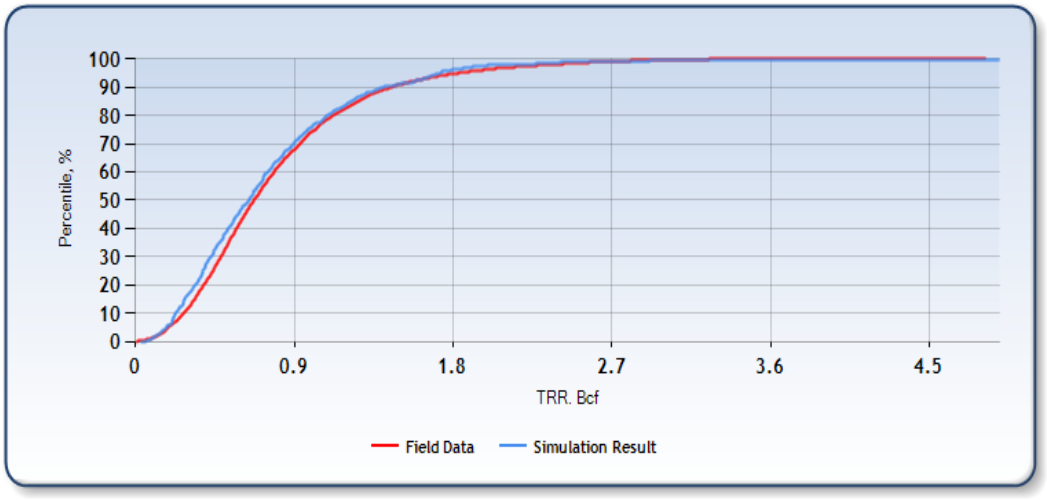

Figure 6.16—Probability distribution of cumulative gas production (7-year) match result for the Cotton Valley formation

Table 6.12—Density functions of uncertain parameters after calibration for the Cotton Valley formation

Parameters	Distribution Type	μ	σ	α	β	Min	Max
Porosity, f	Lognormal	0.04	0.015				
Net Pay, ft	Gamma			20	7.5		
Initial Pressure, psi	Gamma			50	100		
Permeability, md	Lognormal	0.012	0.021				
Water Saturation, f	Lognormal	0.35	0.04				
Fracture Half-length, ft	Uniform					100	200

Table 6.13—Comparison of the range of uncertain parameters

Parameter	Reported Range	Used by This Study(P1-P99)
Net Pay, ft	100-200	80-220
Initial Pressure, psi	4,600-6,000	3,600-7,000
Permeability, md	0.0001-0.3	0.0001-0.3
Water Saturation, %	27-49	24-52
Porosity, %	1-12	1-11
Fracture Half-length, ft	N/A	100-200

Resource Evaluation for Current Well Spacing. The vertical well count is 1.4 times greater than that as of 2005 (Figure 6.14). So it assumed that the well spacing is 30 acres currently. The reservoir property distributions of tight sands gas reservoirs in the Cotton Valley formation in Table 6.12 yield an inverse Gaussian distribution of OGIP per 30 acres (**Figure 6.17**). The P10, P50 and P90 values are 0.6, 1.1, and 2.0 Bcf/30 acres, respectively.

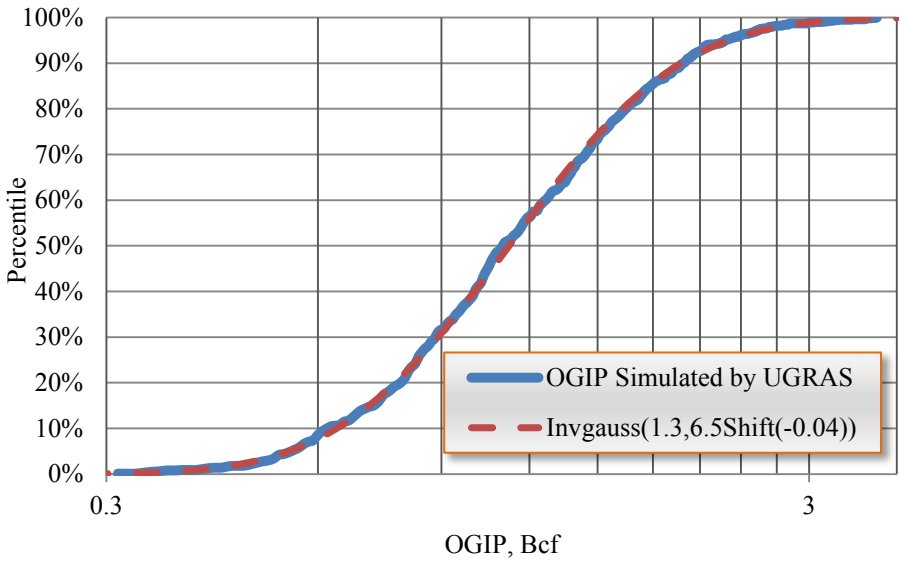

Figure 6.17—Probabilistic distribution of OGIP per 30 acres for the Cotton Valley formation

The simulation yielded a lognormal distribution for TRR with a P10 value of 0.5 Bcf/30 acres, a P50 of 0.8 Bcf/30 acres, and a P90 of 1.5 Bcf/30 acres (**Figure 6.18**). The P10, P50 and P90 values of recovery factor for current well spacing (30 acres) is 53%, 82% and 87%, respectively (**Figure 6.19**). Large range of permeability (0.0001-0.3 md) leads to the wide range of TRR and recovery factor.

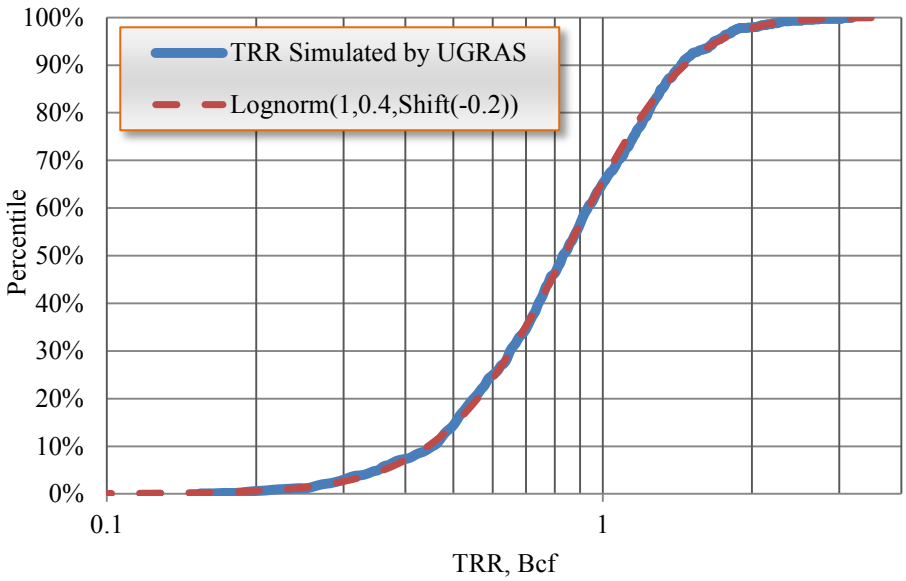

Figure 6.18—Probabilistic distribution of TRR per 30 acres with a 25-year life for the Cotton Valley formation

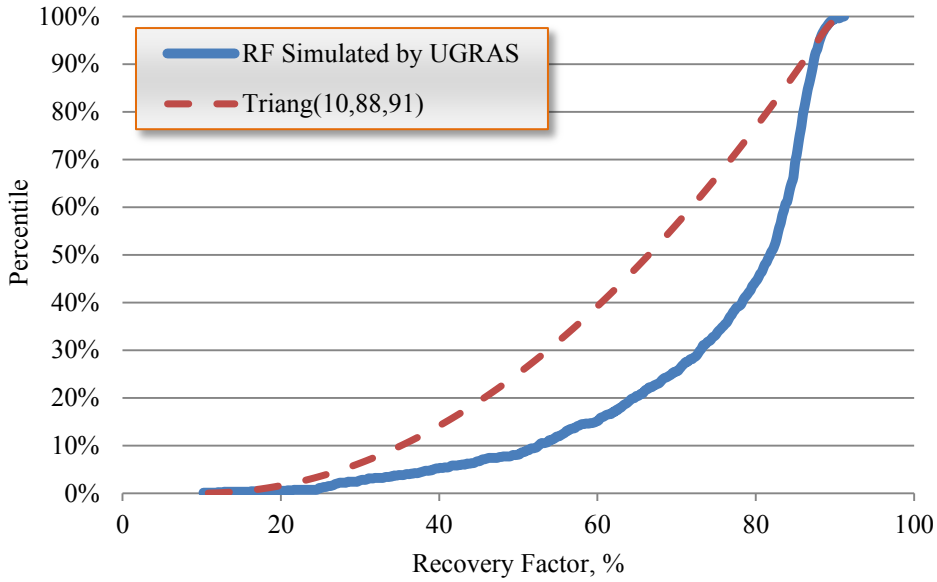

Figure 6.19—Probabilistic distribution of RF per 30 acres with a 25-year life for the Cotton Valley formation

Resource Evaluation for Various Well Spacing. We reran our simulator to generate other distributions TRR from the Cotton Valley formation with varying well spacing to 40, 30 and 10 acres. The TRR for single well doesn't decrease when well spacing is less than 40 acres (**Figure 6.20**). Consequently, there is no big difference in the distribution of recovery factor between various well spacing.

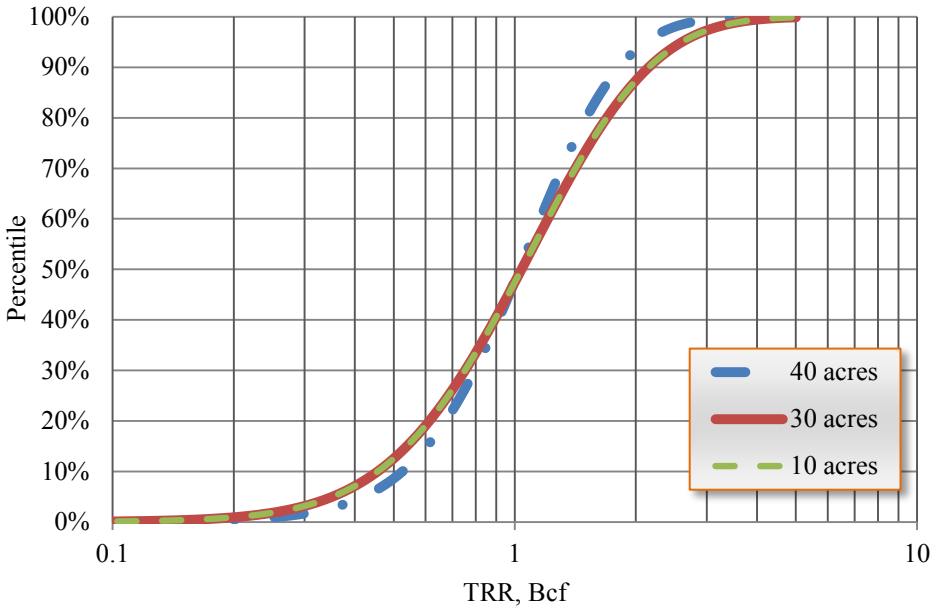

Figure 6.20—TRR versus well spacing in the Cotton Valley formation

6.6.2 Travis Peak

The Travis Peak formation is a basinward-thickening wedge of terrigenous clastics that extends in an arc from eastern Texas across southern Arkansas and northern Louisiana into southern Mississippi. This formation represents a sandstone-rich fluvial-deltaic depositional system (Saucier et al. 1985).

Production. First production from the Travis Peak formation of East Texas occurred in 1942. By the end of 2011, 4.0 Tcf of gas have been produced from the Travis Peak formation. **Figure 6.21** shows annual production and producing wells in the Travis Peak formation from 1980 to 2011. Daily production from Travis Peak formation decreased to 0.3 Bcf/d in 2011.Vertical wells have been the main well type for the Travis Peak formation.

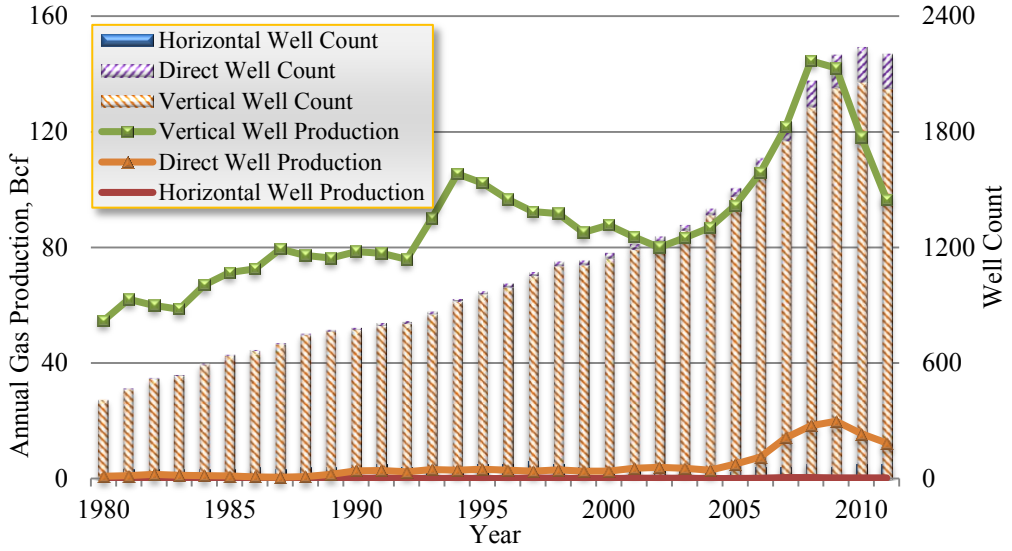

Figure 6.21—Annual gas production and producing wells in the Travis Peak formation of East Texas basin (Data source: HPDI 2011)

Reservoir Parameters. Fields for engineering studies have been completed include Whelan, Willow Springs, Percy-Wheeler, Pinehill Southeast, and Appleby North fields in the Travis Peak/Hosston formation. The perforated interval can be from 6,800 to 9,900 ft over most of its productive trend in Texas and Louisiana. According to Lin et.al (1985), average gas gravity is 0.63; average porosity ranges from 8.3% to 10.8%, average water saturation is 28%-42%; average net pay ranges from 23-238 ft; initial reservoir pressure ranges from 2,042 to 4,880 psi. Permeability range is 0.007 md to 0.66 md (**Table 6.14**). Average reservoir temperature and reservoir temperature gradient are 229 ^{o}F and 19.3 ^{o}F/1,000 ft, respectively. **Table 6.15** summarized the range of the six uncertain parameters for the Travis Peak formation.

Table 6.14—Summary of average reservoir properties in the Travis Peak formation (Lin and Finley 1985)

	Pinehill Southeast	Willow Springs	Whelan	Percy-Wheeler	Appleby North
Field Size, acres	8,521	17,884	8,100	9,384	8,355
Depth, ft	6,830-7,408	7,332-8,983	7,370-9,053	8,863-9,607	7,690-9,862
Net Pay, ft	25	46	238	23	62
Porosity	8.3	9.5	9	10.3	10.8
Water Saturation	42.4	35	40	32.7	28.2
Permeability, md	0.66	0.25	0.047	0.046	0.007
Temperature Gradient, ^{o}F/1,000 ft	18	20.4	18.6	19	20.7
Reservoir Temperature, ^{o}F	199	229	220	245	254
Pressure Gradient, psi/ft	0.429	0.437	0.383	0.494	0.438
Range of Pressure, psi	2,135-3,495	2,042-4,100	2,193-3,635	2,631-5,135	2,887-4,880
Initial Pressure, psi	3,071	3,421	3,076	4,543	2,890
SG	0.65	0.64	0.63	0.62	0.61
Gas-in-place, Bcf/sec	3	15	53	10	26

Table 6.15—Reservoir parameters for the Travis Peak formation

Parameter	Range
Net Pay, ft	20-240
Reservoir Pressure, psi	2,042-4,880
Water Saturation, %	28-42
Permeability, md	0.007-0.66
Porosity, %	8.3-10.8
Fracture Half-length, ft	300-400

Table 6.16 shows the key fixed reservoir parameters used for the Travis Peak formation single-well reservoir simulations. The well spacing is assumed 40 acres.

Table 6.16—Key fixed input parameters for the Travis Peak formation model

Parameters	Value
Reservoir Temperature, ^{o}F	229
Bottom Hole Pressure, psia	1000
Wellbore Radius, ft	0.324
Gas Specific Gravity (air=1)	0.63
Bulk Density, g/cc	1.6
Well Spacing, acres	40

Model Verification. By end of 2005, 2,219 vertical wells have been produced for more than 7 years in the Travis Peak formation of East Texas basin. **Figure 6.22** shows annual new drilled vertical wells in the Travis Peak formation. The production histories from these vertical wells were normalized for 7 years.

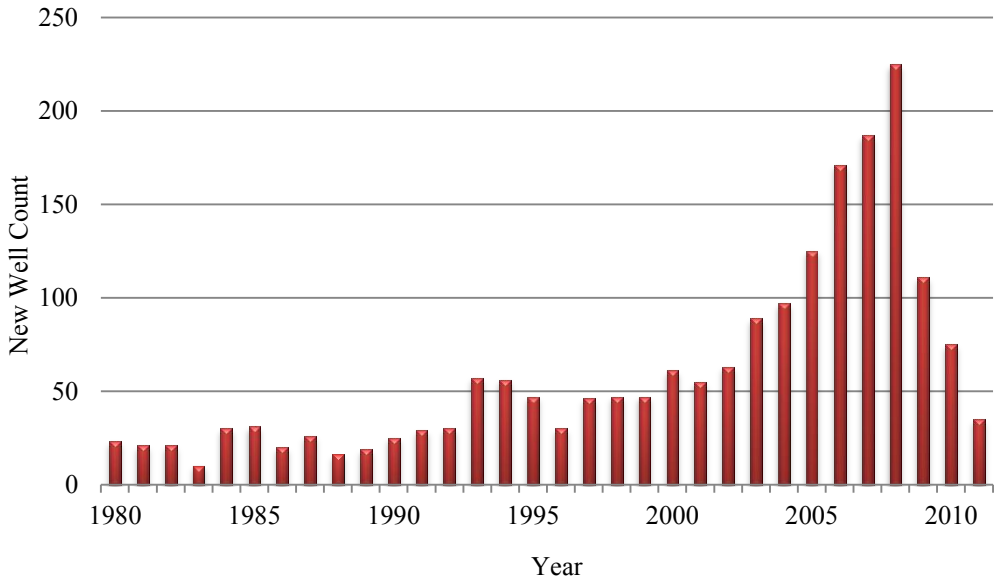

Figure 6.22—Annual new drilled vertical wells in the Travis Peak formation

The density functions for net pay, initial pressure, porosity, water saturation, permeability and fracture half-length were defined with honoring their range listed in

Table 6.15. The density functions for these key parameters were calibrated until a reasonable match between simulated and actual 7-year cumulative gas production from the wells in the Travis Peak formation was reached.

The red curve in **Figure 6.23** shows the distribution of 7-year cumulative gas production from the 2,219 wells. The blue curve in Figure 6.23 is the distribution of 7-year cumulative gas production simulated by UGRAS with the reservoir parameters in Table 6.16 and density functions in **Table 6.17**. The consistent match between the two curves finalized the density functions for the key parameters as listed in Table 6.17 and confirmed the well spacing of 40 acres. The distributions of the six uncertain parameters after calibration honored their range reported from literature (**Table 6.18**).

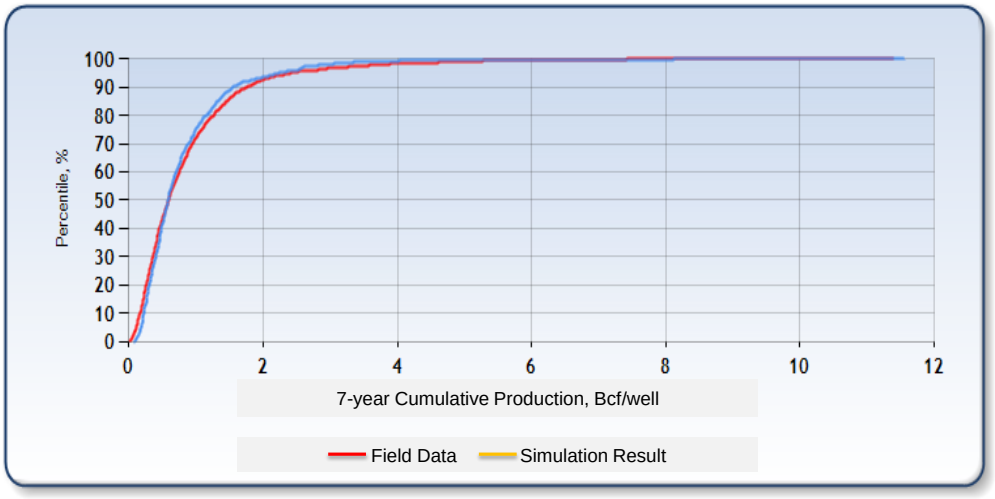

Figure 6.23—Probability distribution of cumulative gas production (7-year) match result for the Travis Peak formation

Table 6.17—Density functions of uncertain parameters after calibration for the Travis Peak formation

Parameters	Distribution Type	k	μ	σ	Min	Max
Net Pay, ft	GEV	0.3	39	25		
Initial Pressure, psi	Lognormal		3100	400		
Water Saturation, f	Lognormal		0.35	0.04		
Permeability, md	Lognormal		0.07	0.06		
Porosity, f	Lognormal		0.09	0.01		
Fracture Half-length, ft	Uniform				300	400

Table 6.18—Comparison of the range of uncertain parameters

Parameter	Reported Range	Used by This Study(P1-P99)
Net Pay, ft	20-240	10-480
Initial Pressure, psi	2,042-4,880	2000-4800
Permeability, md	0.007-0.66	0.005-0.7
Water Saturation, %	28-42	23-46
Porosity, %	8.3-10.8	6-13
Fracture Half-length, ft	300-400	300-400

Resource Evaluation for Current Well Spacing. The vertical well count as of 2011 is 1.3 times greater than that in 2005 (Figure 6.21). So it assumed that the well spacing is 30 acres currently. The resource assessment of the Travis Peak formation will base on 30 acres. The reservoir property distributions of tight sands gas reservoirs in Table 6.17 yield a log-logistic distribution of OGIP per 30 acres (**Figure 6.24).** The P10, P50 and P90 values are 0.35, 0. 9, and 2.2 Bcf/30 acres, respectively.

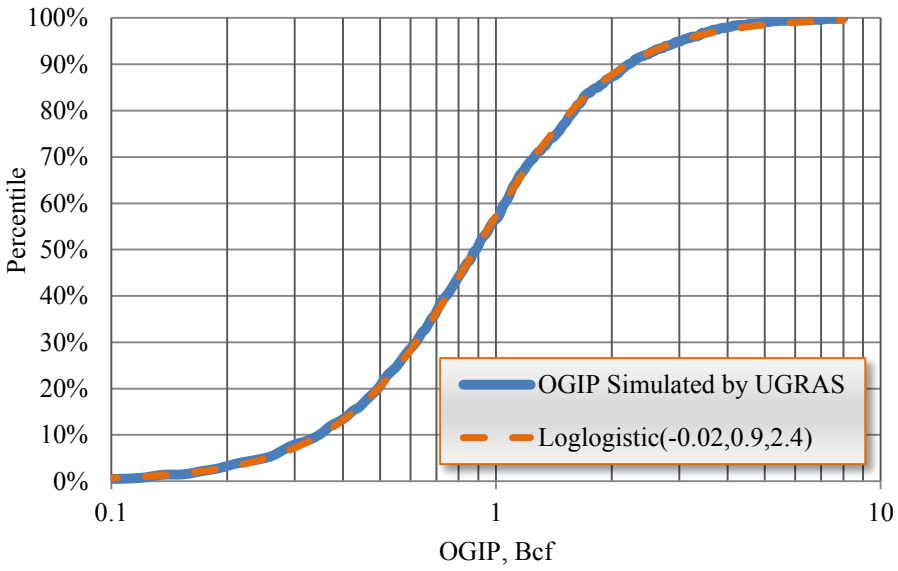

Figure 6.24—Probabilistic distribution of OGIP per 30 acres for the Travis Peak formation

The simulation results yielded an lognormal distribution for TRR with a P10 value of 0.3 Bcf/30 acres, a P50 of 0.7 Bcf/30 acres, and a P90 of 1.8 Bcf/30 acres (**Figure 6.25)**. The P10, P50 and P90 values of recovery factor for current well spacing (30 acres) is 79%, 81% and 83%, respectively (**Figure 6.26)**.

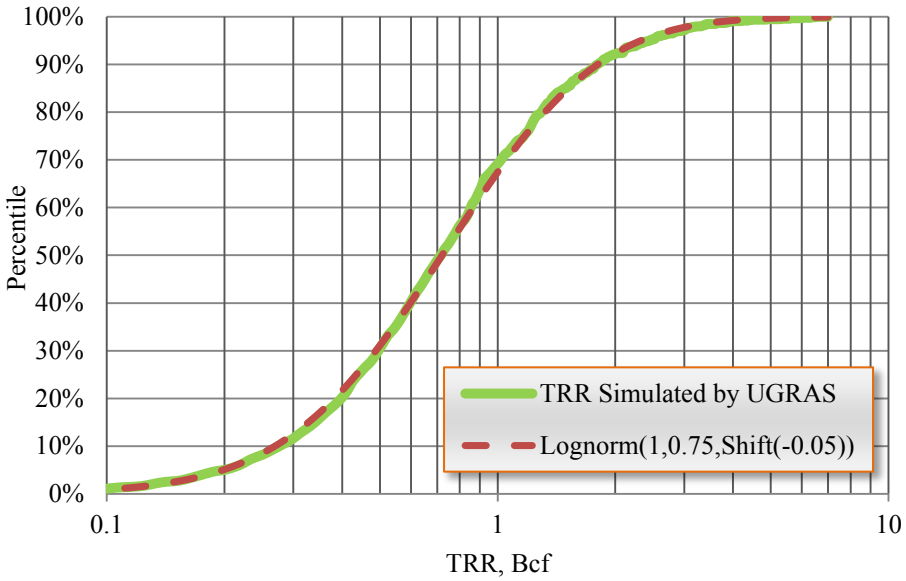

Figure 6.25—Probabilistic distribution of TRR per 30 acres with a 25-year life for the Travis Peak formation

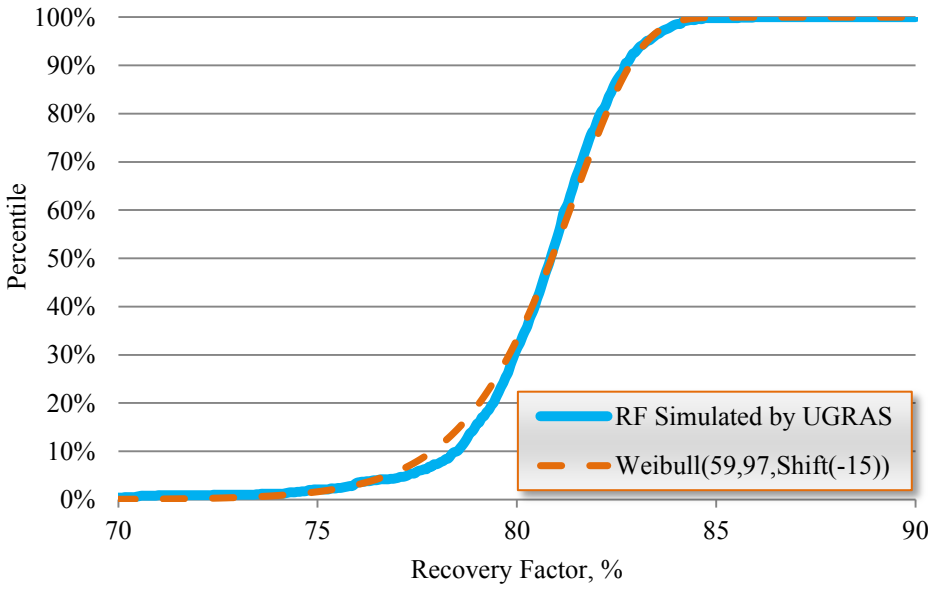

Figure 6.26—Probabilistic distribution of RF per 30 acres with a 25-year life for the Travis Peak formation

Resource Evaluation for Various Well Spacing. We reran our simulator to generate other distributions TRR from the Travis Peak formation with varying well

spacing to 40 acres and 30 acres. The TRR for single well doesn't decrease when well spacing is less than 40 acres (**Figure 6.27**). Consequently, there is no big difference in the distribution of recovery factor between various well spacing (**Figure 6.28**).

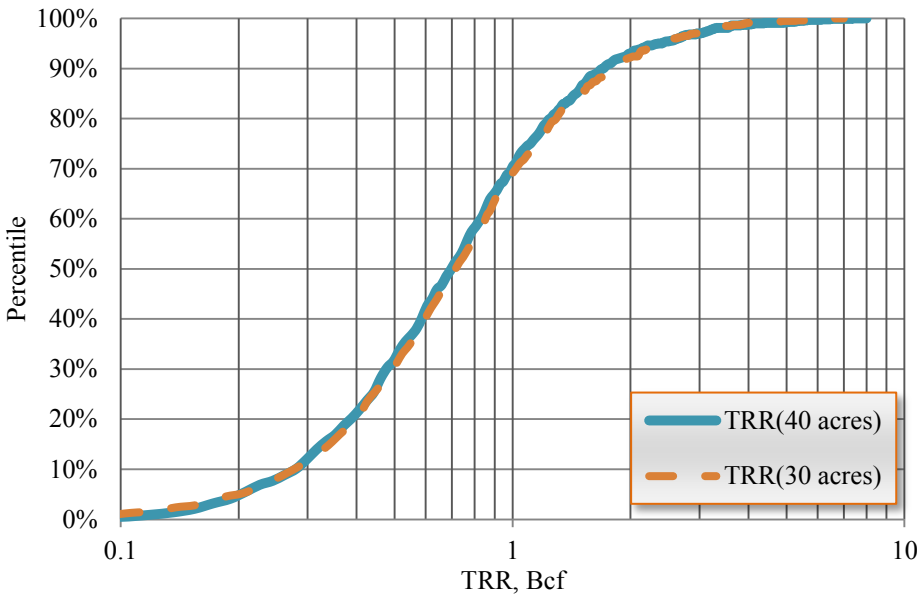

Figure 6.27—TRR versus well spacing in the Travis Peak formation

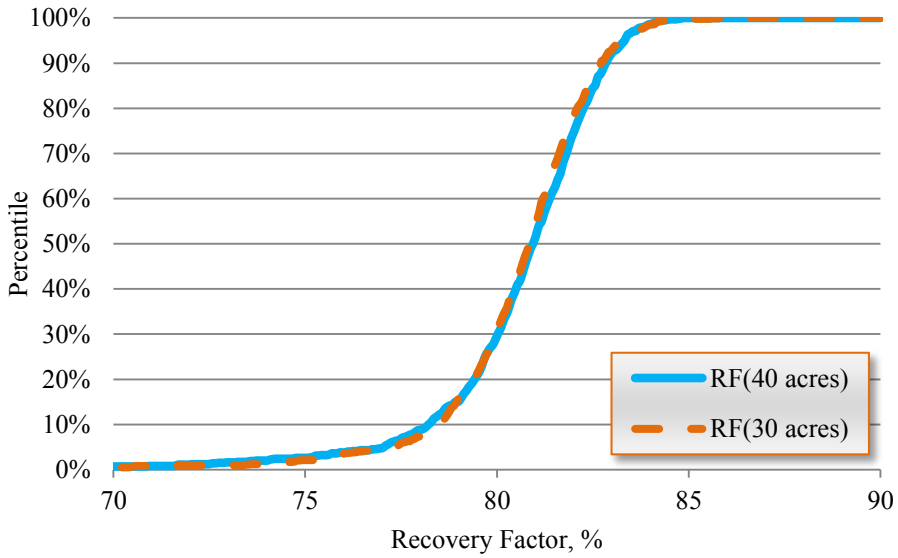

Figure 6.28—Recovery factor versus well spacing in the Travis Peak formation

6.7 Discussion

Well life doesn't affect TRR and recovery factor from tight sands gas formation when analysis year greater than 25 years (**Figure 6.29**). As such, we chose a 25-year production history to estimate TRR from tight sands gas formation.

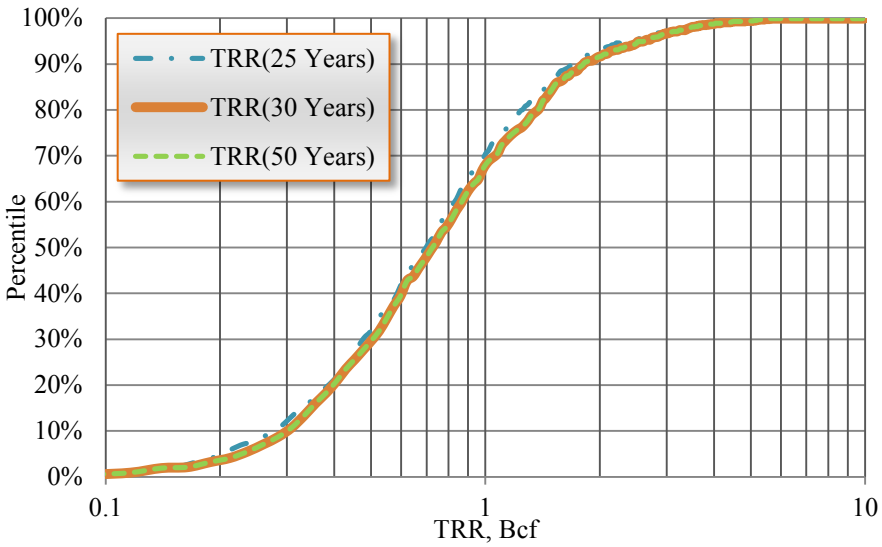

Figure 6.29—TRR from the Travis Peak versus various analysis years

6.8 Summary

Table 6.19 summarized the key characteristics of the three key tight sands formations we estimated. We have evaluated the cumulative probabilistic distribution of OGIP, TRR and RF for three most productive tight sand gas formations in the United States using a probabilistic, analytical reservoir model. **Figures 6.30** to **6.32** show the cumulative distribution of OGIP per section, TRR per section, and recovery factor for the three tight sands gas formations. The Lance formation has the most original tight sands gas in place and technically recoverable resource due to its thick net pay, high

reservoir pressure, and successful fracture treatment. High permeability (0.007-0.7 md) in the Travis Peak formation and high pressure (4,600-6,000 psi) in the Cotton Valley make these two formations are good tight sands gas reservoir. Compared to the other two tight sands gas formation, the range of recovery factor in the Cotton Valley is quite wide (Figure 6.32), ranging from 20%-90%, mainly due to its big range of permeability (0.0001-0.3 md). **Table 6.20**, constructed for the three tight gas formations, provided a concise summary of these resource assessments.

Table 6.19—Summary of the key characteristics for three dominate tight gas formations in United States

Parameter	Lance	Cotton Valley	Travis Peak
Basin	GGRB	East Texas	East Texas
Depth Range, ft	8,000-12,500	8,500-11,000	6,800-9,900
Net Pay, ft	300-600	100-200	20-240
Porosity, %	5-14	1-12	8-11
Permeability, md	0.001-0.02	0.0001-0.3	0.007-0.7
Water Saturation,%	30-60	27-49	28-42
Bulk Density, g/cc	2.6	2.65-2.71	2.8
Average Pi, psia	4,800-7,500	4,600-6,000	2,042-4,880
Temperature, ^{o}F	150	265	229
Fracture Half-length, ft	350-500	100-200*	300-400
Daily Gas Production in 2011, Bcf/d	2.2	1.2	0.3
Cumulative gas production by 2011, Tcf	6.85	10.3	4

*Range is estimated by this study

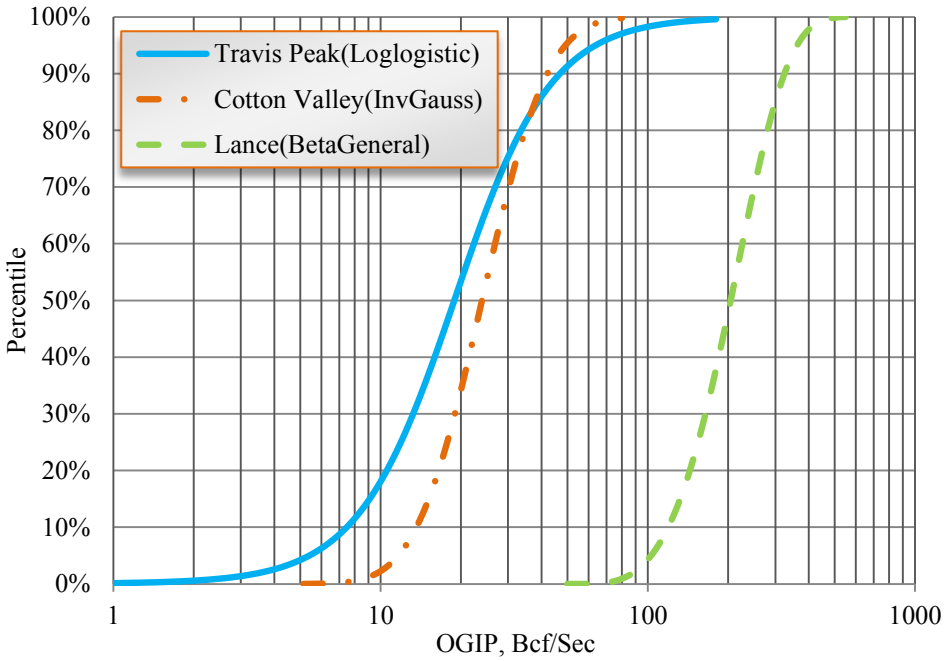

Figure 6.30—Comparison between the probabilistic distributions of OGIP per section for three tight sands gas formations in the United States

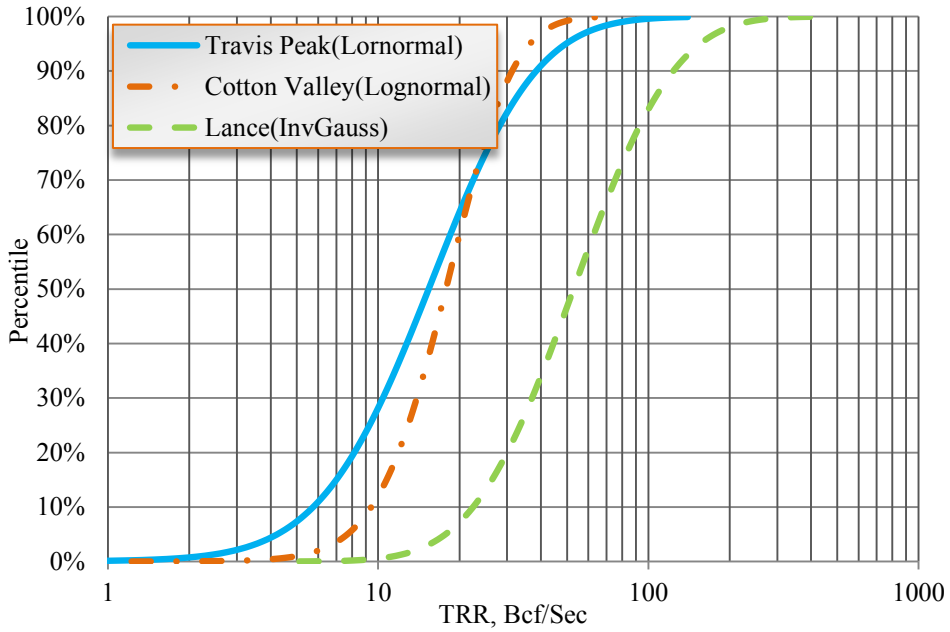

Figure 6.31—Comparison between probabilistic distributions of TRR per section for three tight sands gas formations in the United States

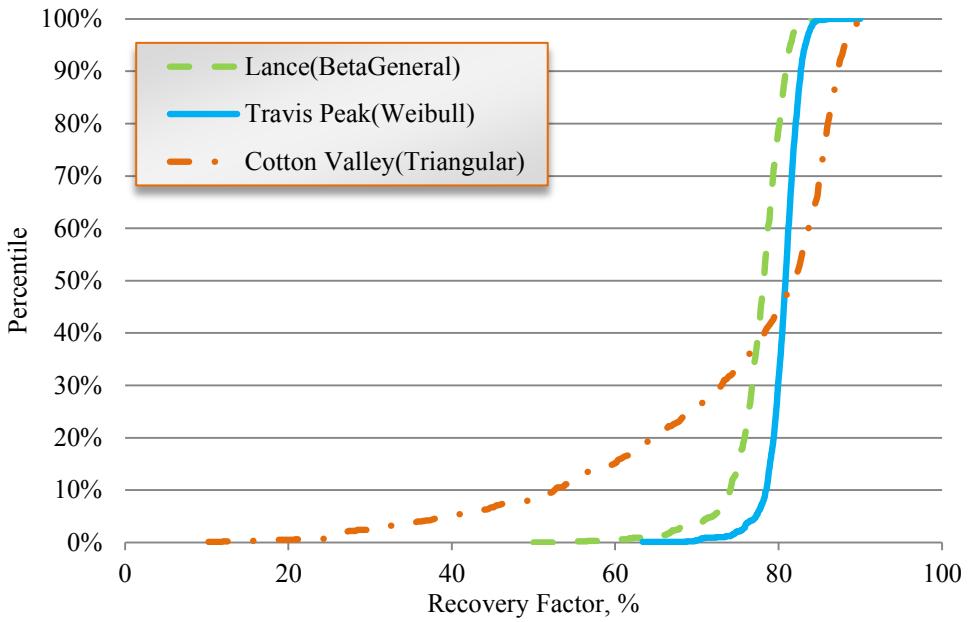

Figure 6.32—Comparison between probabilistic distributions of recovery factor from three tight gas formations in the United States

Once we know the reservoir properties with confidence, the OGIP can be calculated accurately and should not vary much as more data are collected. The estimates of TRR will be increased with time as advanced and new technology is available and wells are drilled to a denser spacing. Our resource assessment for the three formations was confirmed by previous study (**Table 6.21**). For instance, it is reported the mean value of OGIP in the Lance formation 688 Tcf for 2,600 million acres (Law et al. 1989). It results an OGIP of 172 Bcf/sec in the Lance formation. We computed a value for OGIP of 198 Bcf/sec in the Lance formation in this study.

Table 6.20—Summary of estimated resources from three key tight gas formations in the United States

Parameter	Lance	Cotton Valley	Travis Peak
Well Spacing, acres	20	60	30
Distribution type of OGIP	General Beta	Inverse Gaussian	Log-logistic
OGIP (P10), Bcf/well	3.6	0.62	0.35
OGIP (P50), Bcf/well	6.2	1.1	0.89
OGIP (P90), Bcf/well	9.8	2	2.2
Distribution type of TRR	Inverse Gaussian	Lognormal	Lognormal
TRR (P10), Bcf/well	0.7	0.5	0.3
TRR (P50), Bcf/well	1.6	0.8	0.7
TRR (P90), Bcf/well	3.7	1.5	1.8
Distribution type of RF	General Beta	Triangular	Weibull
RF (P10), %	74.0	53.0	79.0
RF (P50), %	78.0	82.0	81.0
RF (P90), %	81.0	87.0	83.0
OGIP (P10), Bcf/sec	115	7	7
OGIP (P50), Bcf/sec	198	12	19
OGIP (P90), Bcf/sec	314	21	47
TRR (P10), Bcf/sec	22	5	6
TRR (P50), Bcf/sec	51	9	15
TRR (P90), Bcf/sec	118	16	38

Table 6.21—Comparison of resource estimates between this study and previous study

		Lance	Cotton Valley	Travis Peak
This Study	OGIP(P50), Bcf/Sec	198.0	12.1	19.0
	TRR(P50), Bcf/Sec	51	9.1	15.0
Previous Study	OGIP(P50), Bcf/Sec	172.0 (Law et al. 1989)	11.5 (Kuuskraa et al. 1978)	18.5 (Haas et al. 1986)
	TRR(P50), Bcf/Sec	55.4 (Law et al. 1989)	N/A	10.4 (Haas et al. 1986)

We gained a probabilistic distribution of technically recovery factors from the three most productive tight sands gas formation in the United States. There is considerable uncertainty in the recovery factor, ranging from 20% to 90% (**Figure 6.33**).

It follows a logistic distribution, with a P50 value of 79%. The recovery factor from tight sands gas reservoir is so high, with a range from 70% (P10) to 85% (P90), because the induced hydraulic fractures almost go through the whole reservoir. We will apply the fitting distribution to assess the TRR from tight sands gas reservoirs for the other six regions in the Section 8.

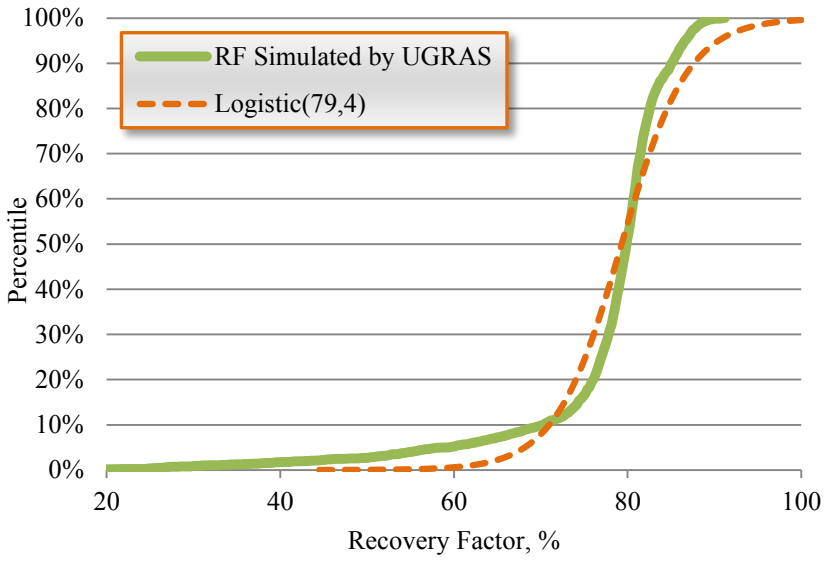

Figure 6.33—Recovery factor of tight sands gas reservoirs derived from the United States

7. RESOURCE EVALUATION FOR COALBED METHANE RESERVOIRS IN UNITED STATES

Coalbed methane is a large resource known to occur within or near virtually all coal formations, the extent and volume of this natural gas has been well defined or established in the United States. The total volume of original coalbed methane in place for 16 basins (including Alaska) in the United States and Western Canada Sedimentary basin was estimated at 1,763-2,343 Tcf in our study (Table 4.3). The EIA estimated coalbed methane to be the source of 10% of the United States' 2008 total gas consumption as of 2010 (Figure 1.2).

In the section, we investigated drilling, stimulation and completion methods for coalbed methane wells in coalbed formations of the United States. Then, we applied workflow of UGRAS to assess the distribution of OGIP and TRR in the two most productive coalbed formations in the United States.

7.1 Unique Properties of Coal

One of the most important properties of the coal is dual porosity. With natural fractures or cleats making up much of the porosity, the gas is held in the reservoir in three possible ways: (1) as adsorbed methane molecules on the surface of micropores; (2) as free gas within the fracture of the pores; and (3) as dissolved gas in the formation water. The adsorbed methane is primary source of the gas volume. It has been shown that coal can adsorb as much as 2,000 scf of methane per ton of coal, although the actual

volumes are usually much less. The free gas that is contained in the natural fractures is a very small portion of the gas volume.

Formation permeability is the critical parameter that controls production. If the permeability is not greater than a certain critical values, then the coalbed may not be an economical reservoir. Thus, in many cases, hydraulic fracture treatments serve to create a pathway that will connect the coal cleat system to the wellbore. However, in certain basins, several thin coalbeds that spread over several hundred feet may be encountered. For such coalbeds, it may be difficult to create long, propped fractures. If the formation permeability is too large and the coal is contacting an aquifer, it might be difficult to dewater the coal. Thus, any given coal seam might have permeability too low to produce gas at economic flow rates or too high, such that the coal is difficult to dewater.

Perhaps the biggest difference between coalbed methane reservoirs and sandstone reservoirs is the mechanism by which gas is stored and produced. In a conventional sandstone reservoir, gas is stored in the pore space and flows though the pores and pore throats to the hydraulic fracture and/or the wellbore. In a coalbed methane reservoir, most of the gas is adsorbed on the surface of the coal. To produce this gas, the reservoir pressure must be reduced so that the gas will desorb, diffuse through the coal matrix, and migrate into the coal cleat system. From there, the gas can flow through the coal cleat system to the hydraulic fracture and/or the wellbore. **Table 7.1** lists the difference between coalbed and conventional reservoirs.

Table 7.1—Comparison between coalbed and conventional reservoirs (Rogers et al. 2008)

Conventional Gas	Coalbed
Darcy flow of gas to wellbore	Diffusion through micropores by Fick's Law Darcy flow through fractures
Gas storage in macropores Real gas law	Gas storage by adsorption on micropore surfaces
Production schedule according to set decline curves	Initial negative decline
Gas content from logs	Gas content from cores Cannot get gas content from logs
Gas to water ratio decreases with time	Gas to water ratio increases with time in latter stages
Inorganic reservoir rock	Organic reservoir rock
Hydraulic fracturing may be needed to enhance flow	Hydraulic fracturing required in most of basins except the eastern part of the Powder River basin where the permeability is very high Permeability depends on fractures
Macropore size: 1μm to 1mm	Micropore size: $<5A^{o}$ to $50A^{o}$
Reservoir and source rock independent	Reservoir and source rock are the same
Permeability not stress dependent	Permeability highly stress dependent
Well interference detrimental to production	Well interference helps production Must drill multiple wells to develop

7.2 Drilling, Stimulation and Completion Methods in Coalbed Methane Reservoirs

On the basis of the unique properties of coal, the engineer must develop a completion strategy. The strategy should include specific details concerning the site of the perforations and the stimulation treatment needed to maximize gas recovery. **Table 7.2** concluded the drilling, completion and stimulation methods for the main coalbed methane basins in the United States and Canada.

Table 7.2—North American basins and engineering practices (Ramaswamy 2007)

Basin	Key Reservoir Properties	Value or Range	Drilling Method	Completion Methods	Stimulation Methods
Black Warrior	No. of Seams	3	Vertical	Cased Hole Completion Single Seam Single Stage Cased Hole, Completion Multi Seam Multi Stage	Cross Linked Gels Fracturing with Proppant Water Fracturing with Proppant, Linear Gels with Proppant
	Net Seam Thickness (ft)	1-10			
	Depth of Occurrence (ft)	800-3,500			
	Gas Content (scf/ft)	125-680			
	Water Saturation (%)	80-100			
	Coal Rank	HV-LV			
	Permeability (md)	0.01-10			
	Reservoir Pressure (psi)	70-420			
Central Appalachian	No. of Seams	9	Vertical, Horizontal	Cased Hole Completion Single Seam Single Stage, Single Lateral with Liner, Single Lateral without liner, Multi-lateral, Pinnate Pattern	Cross Linked Gels Fracturing Foam Fracturing with Proppant
	Net Seam Thickness (ft)	2-12			
	Depth of Occurrence (ft)	100-3,500			
	Gas Content (scf/ft)	285-573			
	Water Saturation (%)	80-100			
	Coal Rank	MV-LV			
	Permeability (md)	0.01-40			
	Reservoir Pressure (psi/ft)	0.35-0.43			
Northern Appalachian	No. of Seams	6	Vertical, Horizontal	Cased Hole Completion Single Seam Single Stage, Single Lateral with Liner, Single Lateral without liner, Multi-lateral	Water Fracturing with Proppant, Foam Fracturing with Prpppant
	Net Seam Thickness (ft)	2-20			
	Depth of Occurrence (ft)	1,030-6,570			
	Gas Content (scf/ft)	26-445			
	Water Saturation (%)	50-100			
	Coal Rank	HV-LV			
	Permeability (md)	0.01-40			
	Reservoir Pressure (psi/ft)	0.3-0.45			
Arkoma	No. of Seams	7	Vertical, Horizontal	Cased Hole Completion Single Seam Single Stage, Single Lateral with Liner, Single Lateral without liner, Multi-lateral, Pinnate Pattern	Cross Linked Gel Fracturing, Foam Fracturing with Proppant
	Net Seam Thickness (ft)	3-7			
	Depth of Occurrence (ft)	622-2,300			
	Gas Content (scf/ft)	73-570			
	Water Saturation (%)	50-100			
	Coal Rank	MV-LV			
	Permeability (md)	1-30			
	Reservoir Pressure (psi/ft)	<0.4			

Table 7.2—continued

Basin	Key Reservoir Properties	Value or Range	Drilling Method	Completion Methods	Stimulation Methods
Cherokee	No. of Seams	6	Vertical	Cased Hole Completion Single Seam Single Stage	Water Fracturing with Proppant, Foam Fracturing with Prpppant
	Net Seam Thickness (ft)	2-25			
	Depth of Occurrence (ft)	400-1,350			
	Gas Content (scf/ft)	28-444			
	Water Saturation (%)	50-100			
	Coal Rank	HV-LV			
	Permeability (md)	0.01-100			
	Reservoir Pressure (psi/ft)	<0.4			
Forest City	No. of Seams	13	Vertical	Cased Hole Completion Single Seam Single Stage	Water Fracturing with Proppant, Foam Fracturing with Prpppant
	Net Seam Thickness (ft)	2-22			
	Depth of Occurrence (ft)	720-2,096			
	Gas Content (scf/ft)	50-435			
	Water Saturation (%)	50-100			
	Coal Rank	HV-LV			
	Permeability (md)	0.01-100			
	Reservoir Pressure (psi/ft)	<0.4			
Powder River	No. of Seams	6	Vertical	Topset Under Ream	Water without Proppant
	Net Seam Thickness (ft)	70-150			
	Depth of Occurrence (ft)	400-1,800			
	Gas Content (scf/ft)	25-70			
	Water Saturation (%)	100			
	Coal Rank	Sub Bit-LV			
	Permeability (md)	N/A			
	Reservoir Pressure (psi/ft)	N/A			
San Juan	No. of Seams	2	Vertical, Horizontal	Cased Hole Completion Single Seam Single Stage, Cased Hole Completion Multi Seam Single Stage, Single Lateral	Cross Linked Gel with Proppant
	Net Seam Thickness (ft)	20-80			
	Depth of Occurrence (ft)	500-5,000			
	Gas Content (scf/ft)	100-600			
	Water Saturation (%)	80-100			
	Coal Rank	Sub Bit-LV			
	Permeability (md)	1-60			
	Reservoir Pressure (psi)	1,500-2,000			

Table 7.2—continued

Basin	Key Reservoir Properties	Value or Range	Drilling Method	Completion Methods	Stimulation Methods
Uinta and Piceance	No. of Seams	3	Vertical	Cased Hole Completion Single Seam Single Stage, Cased Hole Completion Multi Seam Single Stage, Cased Hole Completion Multi Seam Multi Stage	Cross Linked Gels Fracturing with Proppant, Water Fracturing with Proppant
	Net Seam Thickness (ft)	40-150			
	Depth of Occurrence (ft)	2,000-6,000			
	Gas Content (scf/ft)	25-750			
	Water Saturation (%)	50-100			
	Coal Rank	HV-Anthracite			
	Permeability (md)	0.01-100			
	Reservoir Pressure (psi/ft)	<0.45			
Raton	No. of Seams	3	Vertical	Cased Hole Completion Single Seam Single Stage, Cased Hole Completion Multi Seam Single Stage, Cased Hole Completion Multi Seam Multi Stage	Cross Linked Gels Fracturing with Proppant, Foam Fracturing with Proppant
	Net Seam Thickness (ft)	2-35			
	Depth of Occurrence (ft)	1,500-2,500			
	Gas Content (scf/ft)	4-810			
	Water Saturation (%)	50-100			
	Coal Rank	HV-LV			
	Permeability (md)	0.01-120			
	Reservoir Pressure (psi/ft)	<0.43			
Western Canadian Sedimentary	No. of Seams	10-30	Vertical	Cased Hole Completion Single Seam Single Stage, Cased Hole Completion Multi Seam Multi Stage	Gas (CO2 or N2) without Proppant, Gas (N2) with Proppant
	Net Seam Thickness (ft)	N/A			
	Depth of Occurrence (ft)	490-2,800			
	Gas Content (scf/ft)	64-448			
	Water Saturation (%)	0-5			
	Coal Rank	Sub Bit-HV			
	Permeability (md)	1-15			
	Reservoir Pressure (psi/ft)	0.18-0.5			

7.2.1 Drilling Methods

Coalbed methane reservoirs are often produced using vertical wells and much smaller fracture treatments than what are typically seen in shale gas production, although the dual porosity and anisotropic of coal beds makes them good candidates for horizontal wells. Horizontal wellbores were considered to be very effective in reservoirs which

were: (1) relatively thin; (2) naturally fractured; and (3) known to have anisotropic permeability. Advantage of horizontal wells over vertical fracture stimulated wells that are they:

- Can be drilled to a length of 8,000 ft, whereas the effective fracture lengths in the coalbed methane reservoirs are usually less than 200 ft, tip to tip;
- Can be oriented in the direction of maximum horizontal stress to intersect face cleats, to maximum horizontal permeability and wellbore stability;
- Are better in reservoirs having high permeability anisotropy;
- Can be better controlled to stay in seam (to avoid wet zones) than can induced fractures;
- May provide accelerated cash flow and small footprint; and
- Can be expanded to various combinations (multilateral or pinnate designs, and multiple fracturing options).

Some disadvantages of horizontal wells are that they are costly when there are many seams that require drilling multiple horizontals, and the chances of horizontals collapsing during drilling and production are high. A linear is highly recommended to prevent borehole collapse. In most cases, pre-perforated linear is used. Also, many coal seams are so thin and lenticular that it is impossible to drill horizontal holes more than a few hundred feet in length.

7.2.2 Completion Methods

Well completion design should be coordinated with the stimulation strategy. Three completion techniques commonly have been used to develop coalbed methane reservoirs, including openhole completion method, stable cavity completion method, and perforated casing (with a fracture treatment) completion method.

The methods for completion horizontal coalbed wells have evolved from completion experience with vertical coalbed wells and conventional oil and gas wells. In order to complete a horizontal wellbore in a coalbed reservoir there are a few properties of coal that much be understood. Some of the major properties are: (1) the coal cleat system must be effectively connected to the wellbore, (2) most coalbed must be dewatered before peak gas production can occur, and (3) the well should be produced at minimum bottomhole pressure to maximize gas desorption. The three completion techniques that used for vertical wells were applied to horizontal wells.

7.2.3 Stimulation Methods

The fracture half-length in vertical coalbed methane wells is normally less than 200 ft, on average. The reason for such short half lengths is the Young's modulus of coalbed is very small (between 1×10^5 and 1×10^6 psi) compared with normal fracturing candidates with Young's moduli between 3×10^6 and 1×10^7 psi. Hydraulic fracturing works well in some coal seams but has not been very successful in horizontal coalbed methane wells, because the costs are not been justified by the limited increase in

production. Hydraulic fracturing requires that the horizontal well be cased and cemented for best results.

7.3 Reservoir Model for Coalbed Methane Reservoirs

In our study, we modeled coalbed methane reservoir as a conventional single-porosity system with adsorbed gas (**Table 7.3**). As with shale gas, the adsorbed gas is assumed to be at equilibrium with the gas in the conventional porosity system, i.e. desorption is instantaneous. The hydraulically fractured well has been widely used in the coalbed methane reservoirs. The type of outer boundary for the coalbed methane reservoir is defined as closed circular. The well is centered in the drainage area.

Table 7.3—Reservoir model for coalbed methane reservoirs

Porosity	Single porosity
Fracture Conductivity	Infinite
Inner Boundary	Vertical Fractured
Outer Boundary	Circular
Lithology	Coal
Pressure Step	Constant
Permeability	Isotropic
Well Location	Centered

7.4 Reservoir Parameters Sensitivity Analysis

The essential reservoir properties required to predict production rates for coalbed methane reservoirs are shown in **Table 7.4** along with the data sources. There is uncertainty involving in the prediction of net pay, permeability, porosity, water

saturation, initial pressure and fracture half-length. However, the well spacing is controllable.

Thirteen characteristics were investigated by sensitive analysis. Beside acreage, net pay, porosity, and water saturation, OGIP of coalbed methane is affected by Langmuir isotherm. Gas production from coalbeds are affected most by values of gas-in-place, natural fracture permeability, initial reservoir pressure, and gas desorption and diffusion characteristics, relative permeability characteristics, and fracture half-length (**Figure 7.1**). In this section, we treat net pay, gas content, permeability, water saturation, initial pressure, fracture half-length and porosity as uncertain parameters.

Table 7.4—Data source for primary properties of coalbed methane reservoirs

Primary Property	Estimate Source	Big Uncertainty
Thickness	Openhole density logs	Yes
Permeability	Openhole well logging	Yes
Porosity	Openhole well logging	Yes
Water Saturation	Openhole well logging	Yes
Gas Content	On-site desorption tests	No
Sorptive Capacity	Sorption isotherm	No
Diffusion Coefficient	On-site desorption tests	No
Fracture Permeability	Openhole DST	Yes
Fracture Half-Length (static)	Post-fracture net-pressure analysis	Yes
Reservoir Pressure	Openhole DST	Yes

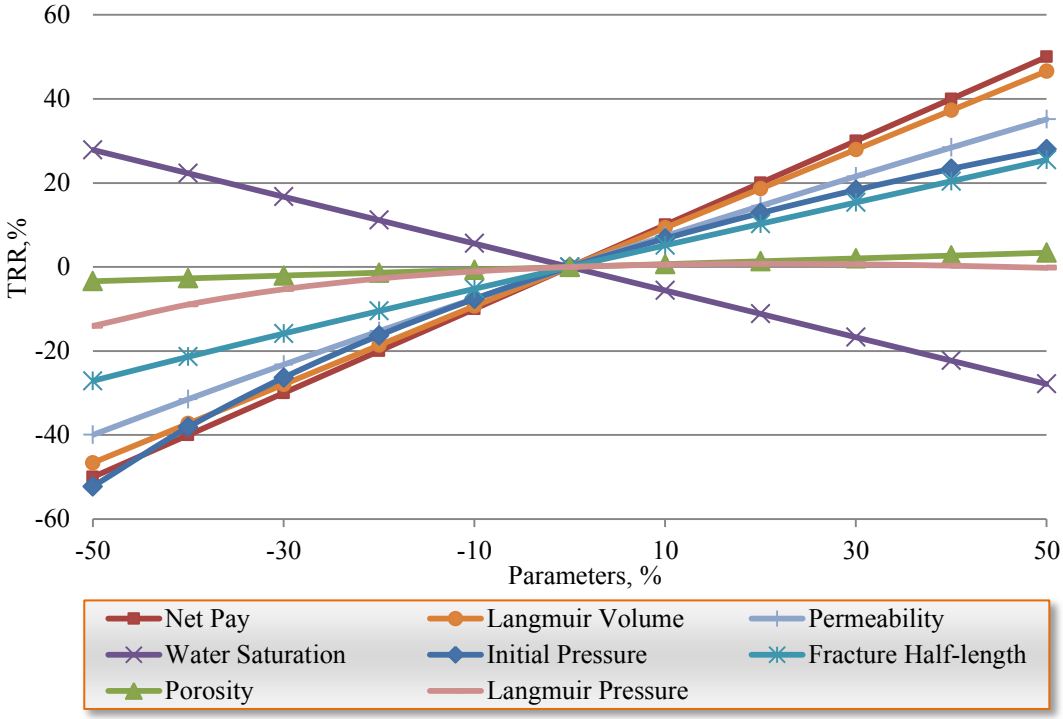

Figure 7.1—Sensitivity analysis of TRR from coalbed methane reservoirs

7.5 Recent Production and Activity Trends

Between 2000 and 2011, coalbed methane production from the lower 48 increased from 0.2 Tcf to 1.6 Tcf (**Figure 7.2**), and now accounts for 8% of total lower-48 gas production (EIA 2012a). The top two producing coalbed methane areas were San Juan and Powder River basin. Resource estimates for these two basins are discussed in greater detail in the section.

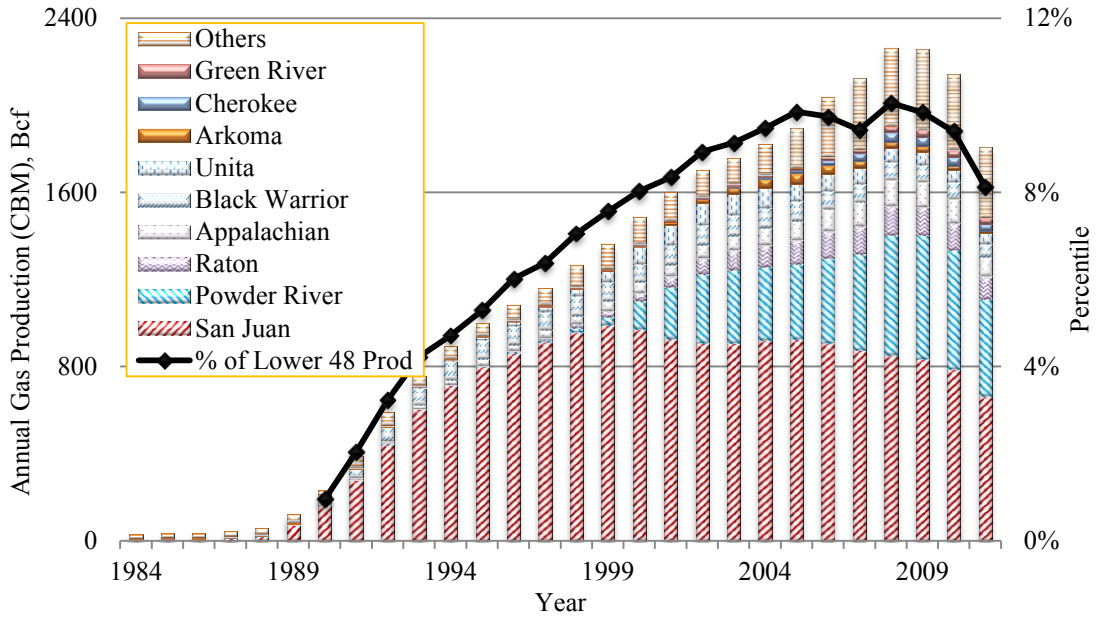

Figure 7.2—Annual coalbed methane gas production by basins

7.6 San Juan Basin

The San Juan basin covers an area of about 4.8 million acres straddling the Colorado-New Mexico state line in the Four Corners region. It measures roughly 100 mile long north to south and 90 miles wide. A review of activity in the San Juan basin suggests that the development activity is entirely in the Upper Cretaceous Fruitland coal, and in the area more weighted with high-rank coals. 99.2% of coalbed methane was produced from the Fruitland formation (**Figure 7.3**). The Fruitland coal contains in excess of 200 billion tons of coal throughout the basin and crops out around most of the margin of the basin. The Fruitland formation is composed of interbedded sandstone, siltstone, shale, and coal which conformably overlies the Pictured Cliffs formation. The multiple, bituminous-ranked coals in the Fruitland were deposited during the Late Cretaceous as peats, landward of the northeasterly prograding Pictured Cliffs shoreline.

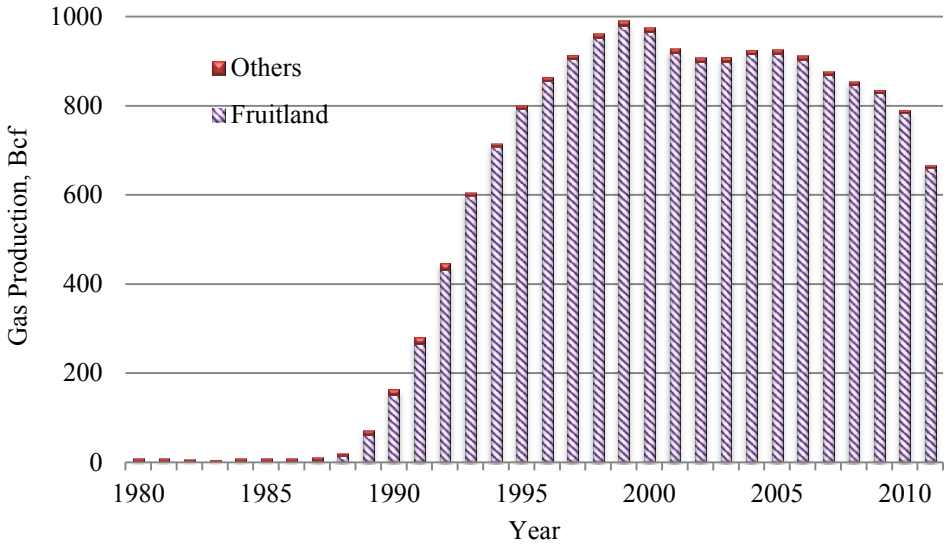

Figure 7.3—Annual coalbed methane production from San Juan basin (Data source: HPDI 2011)

7.6.1 Production

660 Bcf of coalbed methane was produced from about 6,407 wells in the Fruitland coal in 2011 (**Figure 7.4**). By then, Fruitland coal seams have a cumulative gas production of 17.1 Tcf. This gas production mainly come from San Juan county (NM), Rio Arriba county (NM) and La Plata county (CO).

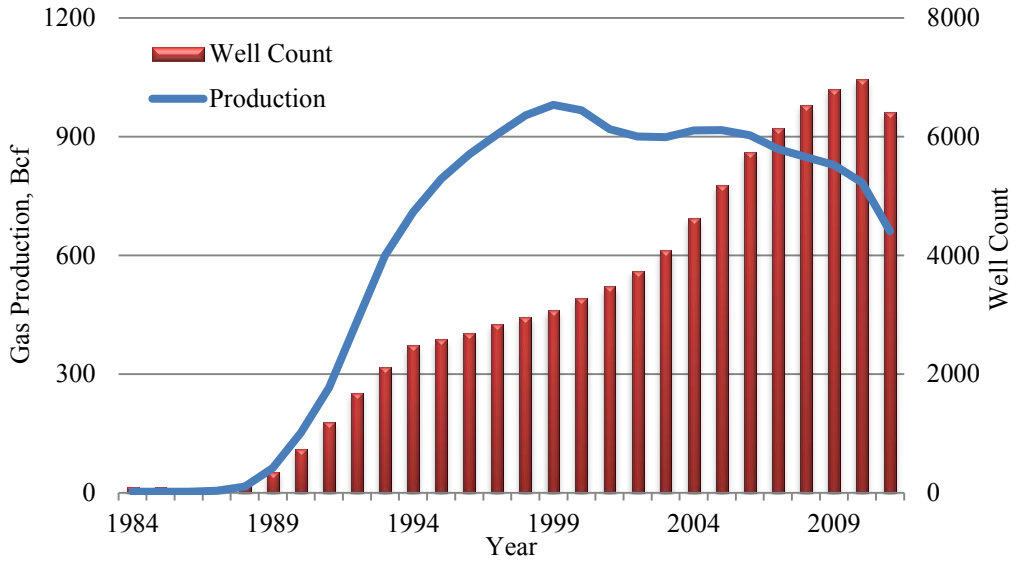

Figure 7.4—Annual producing CBM wells and gas production in the Fruitland coal (Data source: HPDI, 2011)

7.6.2 Reservoir Parameters

The Fruitland coals are thicker than coalbeds in eastern basins: the thickest coals range from 20 to over 40 feet. Total net thickness of all coalbeds ranges from 20 to over 80 feet throughout the San Juan basin, compared to 5 to 15 feet in eastern basin. Coalbed methane wells in the Fruitland coal range from 550 to 4,000 feet in depth (DOE 2004). Fruitland coal is abnormally pressured, with pressure gradient of 0.48 psi/ft (Palmer et al. 1993). Reservoir pressure is calculated to be from 260-1,900 psi in the Fruitland.

The reported permeability could be less than 5.0 md in outlying areas, and up to 15 to 60 md in the Fruitland coal 'fairway' (Ayers 2002). The ash content of Fruitland coal samples determined by proximate analyses of floated Fruitland coal samples collected as drill cuttings ranges from 10.5% to 35.7% and averages about 19%. Bulk-density logs can be used to accurately determine the density of coal beds in the ground.

The average coal density is 1.4 g/cm3. Fruitland is low porosity and high water saturated coal, with porosity of 0.25%-3% and water saturation of 80%-100% (Young et al. 1992). Fracture half-length of 100-300 ft was usually used to simulated production in the Fruitland coal (Young et al. 1992).

The isotherm determined from several measured isotherm curves for northern San Juan basin wells is characterized by a Langmuir volume of 427 scf/ton and a Langmuir pressure of 315 psia (Young et al. 1992). Gas content is generally 150 scf/t or less in the southern two-third of the San Juan basin, where thermal maturity is low (RO <0.65%). In the northern, thermally mature (R_O>0.78 %), over pressured area, ash-free gas content is generally greater than 300 scf/t, and in the fairway are, it commonly exceeds 500 scf/t (Dhir et al. 1991; Kelso et al. 1988; Meek and Bowser. 1993).**Table 7.5** summarized the range of main uncertain parameters for the Fruitland coal.

Table 7.5—Reservoir parameters for the Fruitland Coal

Parameter	Range
Net Pay, ft	20-80
Gas Content, scf/ton	150-500
Permeability, md	5-60
Water Saturation, %	80-100
Reservoir Pressure, psi	260-1,900
Fracture Half-length, ft	100-300
Porosity, %	0.25-3

Table 7.6 shows the key fixed reservoir parameters used for the Fruitland formation single-well reservoir simulations. Infill drilling—drilling wells on reduced

spacing requirements, at every 160 acres rather than 320 acres—has already begun (DOE 2004). The well spacing is assumed to be 160 acres.

Table 7.6—Key fixed input parameters for the Fruitland coal model

Parameters	Value
Reservoir Temperature, ^{o}F	110
Bottom Hole Pressure, psia	200
Wellbore Radius, ft	0.324
Gas Specific Gravity (air=1)	0.62
Bulk Density, g/cc	1.4
Ash Content, %	19
Langmuir Volume, scf/ton	427
Langmuir Pressure, psi	315
Well Spacing, acres	80

7.6.3 Model Verification

Detailed analysis of Fruitland coalbed methane production has demonstrated that even though Fruitland coals underlie the entire San Juan Basin, the Fruitland coalbed methane field comprises at least six reservoirs, each with distinct geologic and reservoir characteristics.

The northwest-trending Fruitland Fairway is the most productive of these reservoirs because coals there are highly fractured with high permeability; wells within this reservoir produce more than 1 MMCFGD and ultimate recoveries may reach or exceed 75% of the original gas in place (OGIP). The second reservoir is north of the Fairway, mostly in Colorado, and there coals are less permeable and wells there will probably produce less than 50% of OGIP. The other four reservoirs are south or

southeast of the Fairway and Fruitland coals in those areas are also far less permeable than those in the Fairway. These four areas are partially defined on the basis of the presence or absence of water, heavy hydrocarbons and waxes, and permeability differences. Ultimate coalbed methane recovery in these four areas will probably be less than 25% OGIP.

In this study, we estimate the whole Fruitland coal with similar reservoir characteristics. **Figure 7.5** shows the annual new producing vertical wells from 1990 to 2011 in the Fruitland coal. By the end of 2005, 5,383 vertical wells had been producing for more than 7 years.

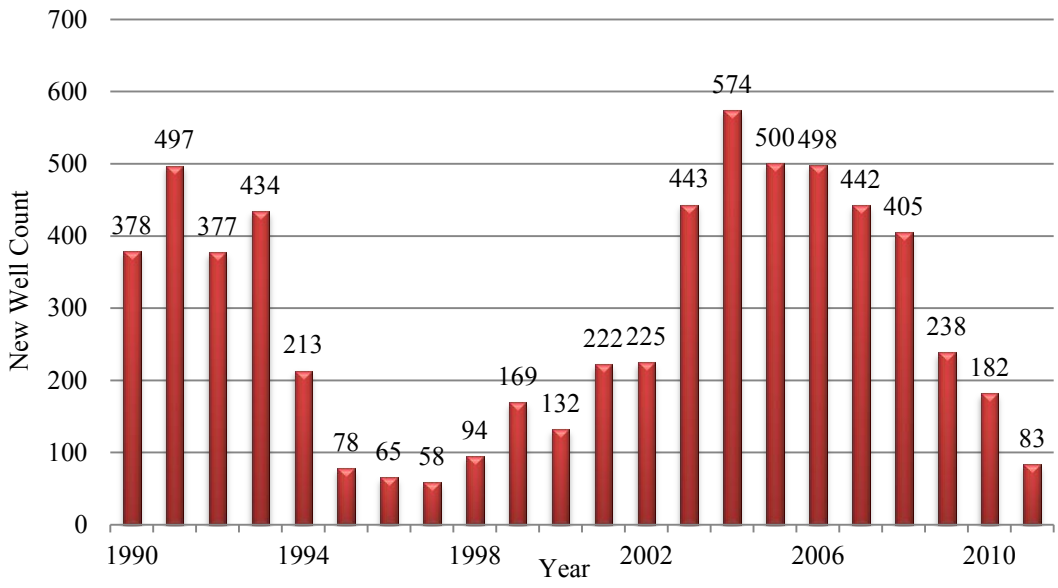

Figure 7.5—Annual new producing CBM wells in the Fruitland coal (Data source: HPDI, 2011)

Density functions for net pay, gas content, permeability, water saturation, initial pressure, fracture half-length and porosity were defined with honoring their range listed

in Table 7.5, initially. Then, these density functions were calibrated until a reasonable match between simulated and actual 7-year cumulative gas production from the wells in the Fruitland formation was reached.

The red curve in **Figure 7.6** shows the distribution of 7-year cumulative gas production from the 5,383 wells. The blue curve in Figure 7.6 is the distribution of 7-year cumulative gas production simulated by UGRAS with the reservoir parameters in Table 7.6 density functions in **Table 7.7**. The consistent match between the two curves finalized the density functions for the key parameters as listed in Table 7.7 and confirmed the well spacing of 160 acres. The distributions of the seven uncertain parameters after calibration honored their range reported from literature (**Table 7.8**).

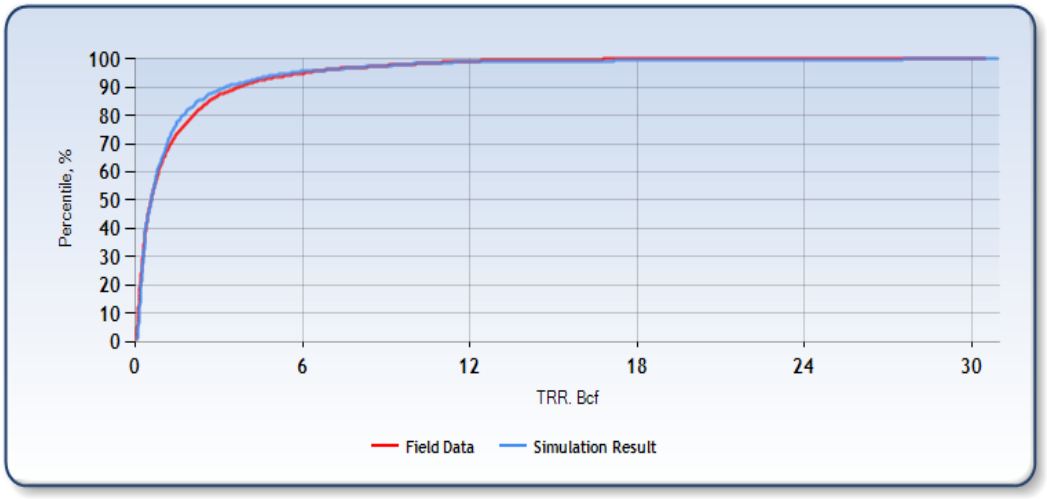

Figure 7.6—Probability distribution of cumulative production (7-year) match result for the Fruitland coal

Table 7.7—Density functions of uncertain parameters after calibration for the Fruitland coal

Parameters	Distribution Type	μ	σ	α	β	Min	Med	Max
Net Pay, ft	InvGauss	35	15					
Gas Content, scf/ton	Uniform					300		700
Permeability, md	Gamma			2	13			
Water Saturation, f	Uniform					0.8		1.0
Initial Pressure, psi	Triangular					260	1400	1900
Fracture Half-length, ft	Uniform					100		300
Porosity, f	Uniform					0.023		0.03

Table 7.8—Comparison of the range of uncertain parameters

Parameter	Reported Range	Used by This Study(P1-P99)
Net Pay, ft	20-80	5-200
Gas Content, scf/ton	150-500	150-500
Permeability, md	5-60	2-70
Water Saturation, %	80-100	80-100
Reservoir Pressure, psi	260-1,900	260-1,900
Fracture Half-length, ft	100-300	100-300
Porosity, %	0.25-3	0.25-3

7.6.4 Resource Evaluation for Current Well Spacing

The vertical well count is 1.4 times greater than that as of 2005 (Figure 7.4). So it assumed that the well spacing is 120 acres currently. The reservoir property distributions of Fruitland coal in Table 7.7 yield an lognormal distribution of OGIP per 120 acres for the Fruitland coal (**Figure 7.7**)**.** The P10, P50 and P90 values are 0.3, 1.3, and 6.1 Bcf/120 acres, respectively.

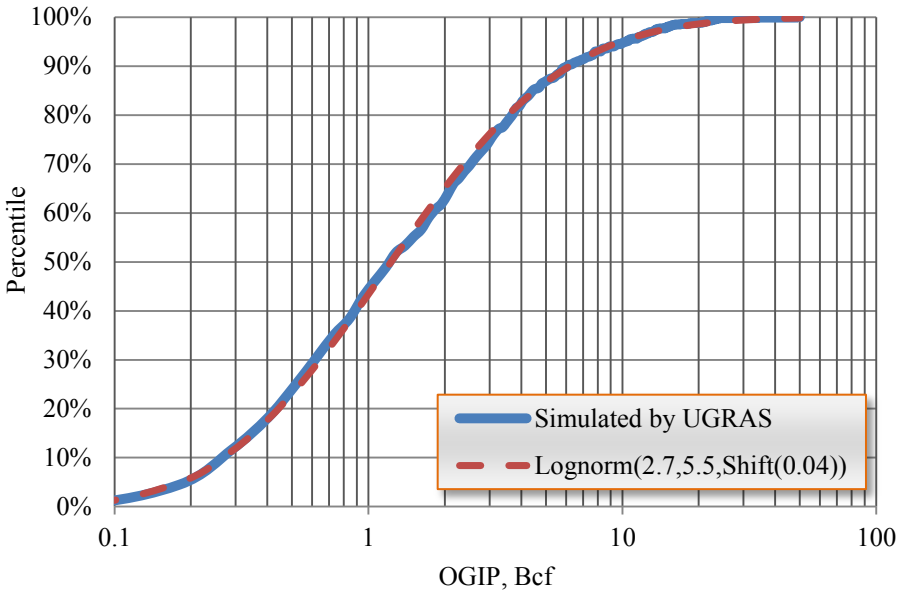

Figure 7.7—Probabilistic distribution of OGIP per 120 acres for Fruitland coal

The simulation yielded a lognormal distribution for TRR with a P10 value of 0.1 Bcf/120 acres, a P50 of 0.5 Bcf/120 acres, and a P90 of 2.6 Bcf/120 acres (**Figure 7.8**). Recovery factor of Fruitland coal follows a lognormal distribution (**Figure 7.9**) with P10, P50 and P90 values of 29%, 45% and 65%, respectively.

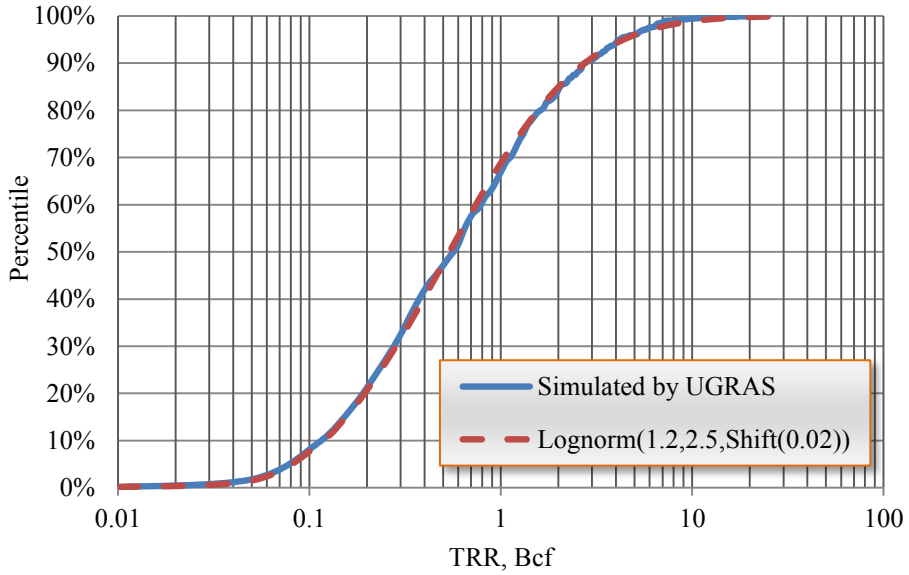

Figure 7.8—Probabilistic distribution of TRR per 120 acres with a 25-year well life for Fruitland coal

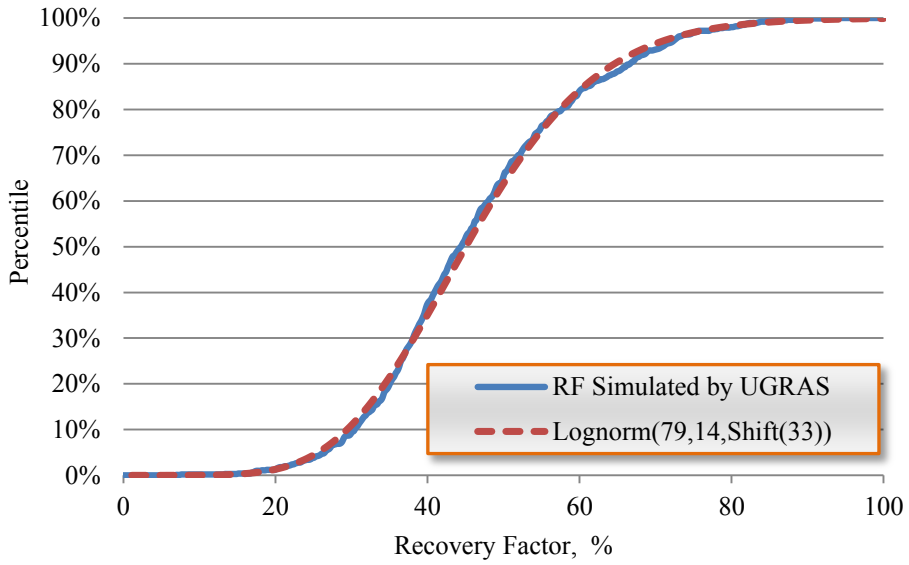

Figure 7.9—Probabilistic distribution of RF per 120 acres with a 25-year life for Fruitland coal

7.6.5 Resource Evaluation for Various Well Spacing

We re-simulated the distribution TRR from the Fruitland coal with varying well spacing to 160 acres, 120 acres and 40 acres. The TRR for single well decreases with

tighter well spacing (**Figure 7.10**). But there is no big difference in recovery factor (**Figure 7.11**).

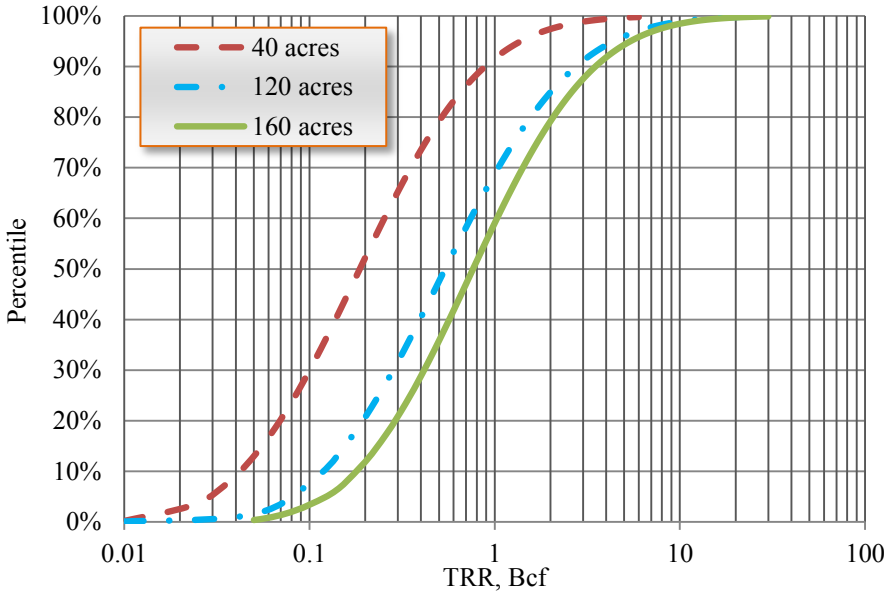

Figure 7.10—TRR versus well spacing in the Fruitland coal

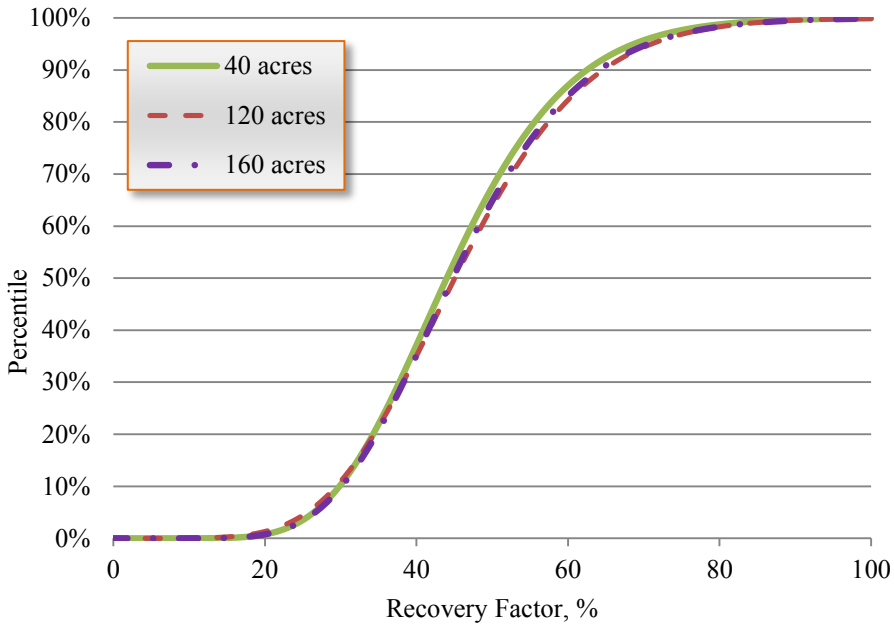

Figure 7.11—Recovery factor versus well spacing in the Fruitland coal

7.7 Powder River Basin

The Powder River basin is one of a series of coal-bearing basins along the Rocky Mountains, stretching from northern New Mexico to central Montana. The Powder River Basin has attracted the majority of the attention because of its high permeability and relatively shallow depth. The basin covers approximately 28,500 square miles, with about one-half of this area underlain by producible coals. The coals in the basin occur at depths less than 2,500 ft. The Powder River is filled mainly with thick Tertiary-age marine and fluvial deposits. The Tertiary unit contains the coal bearing Fort Union and Wasatch formation which are the major CBM producing formations in the Powder River basin. The Tongue River Member, consisting of sandstone, conglomerate, siltstone, limestone, and coal, is the principal coal-bearing unit of the Fort Union formation.

The Tongue River Member can be further divided into upper and lower units. The Upper Tongue River unit contains the Smith/Swartz, Anderson (Deitz), Canyon (Monarch), Wyodak (where the Anderson and Canyon have merged), the Big George and Cook (Carney) seams. The lower Tongue River contains the Wall Pawnee and Cache seams. The distribution of Powder River basin coal zones is shown in **Figure 7.12 (a)** and **(b)**, regarding the current active well count and cumulative gas production by the end of 2011, respectively.

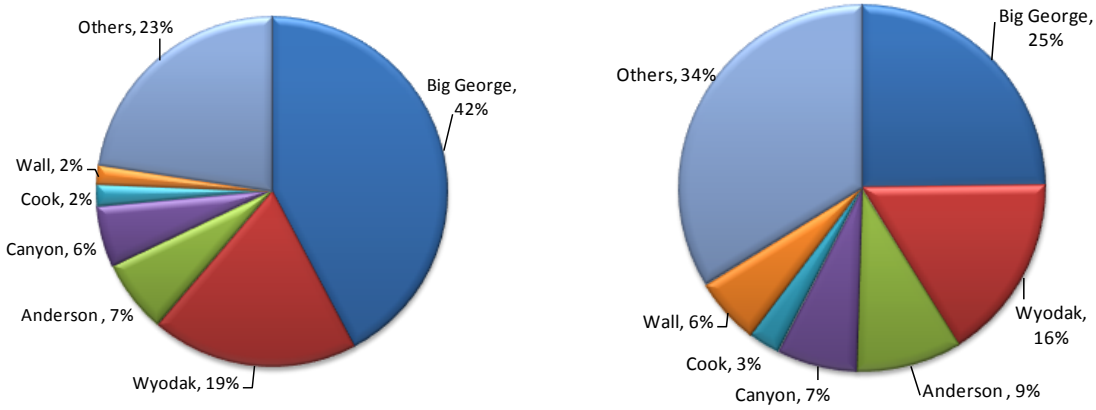

(a)Cumulative gas production from active wells of Powder River basin by coal zone-2011

(b)Active well count by coal zone-2011

Figure 7.12—Powder River basin

Our study focused on the sub-bituminous Big George coal of the Fort Union formation. Reflectance values obtained were between 0.3 and 0.4, indicating that Big George coal is subbituminous in rank (Chao et al. 1984). The beginning study group consisted of 7,385 Big George wells. Big George coal is now contributing 42% of total 4,640 Bcf cumulative coalbed methane production from the Powder River basin (**Figure 7.13**).

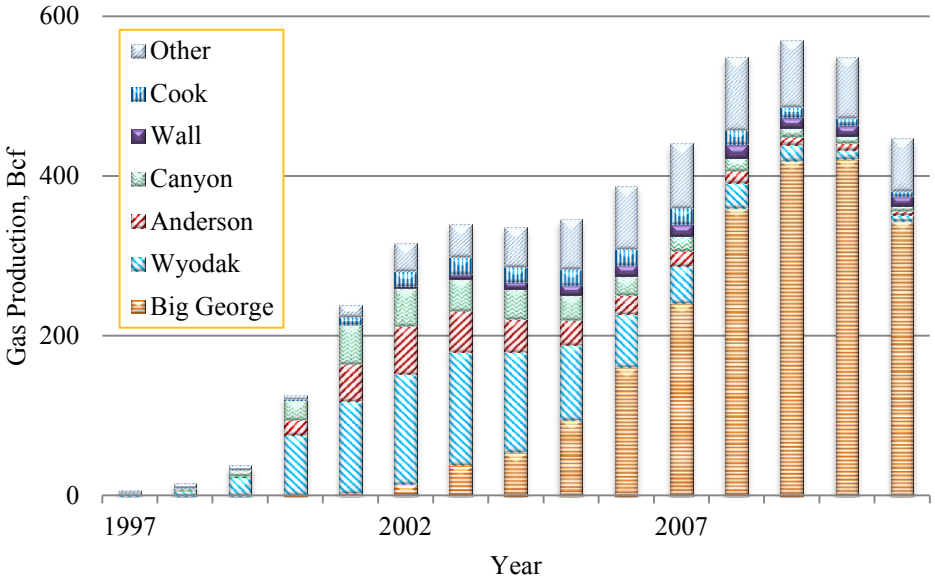

Figure 7.13—Annual gas production from CBM reservoirs of the Powder River basin (Data source: HPDI 2011)

7.7.1 Production

More than 5,800 wells in the Big George coal currently produce nearly 1.0 Bcf/d in 2011, and development of the Big George coal is driving rising volumes (**Figure 7.14**). 99.6% of the gas produced from vertical wells. As of Dec 2011, Big George coal seams have a cumulative gas production of 2.2 Tcf.

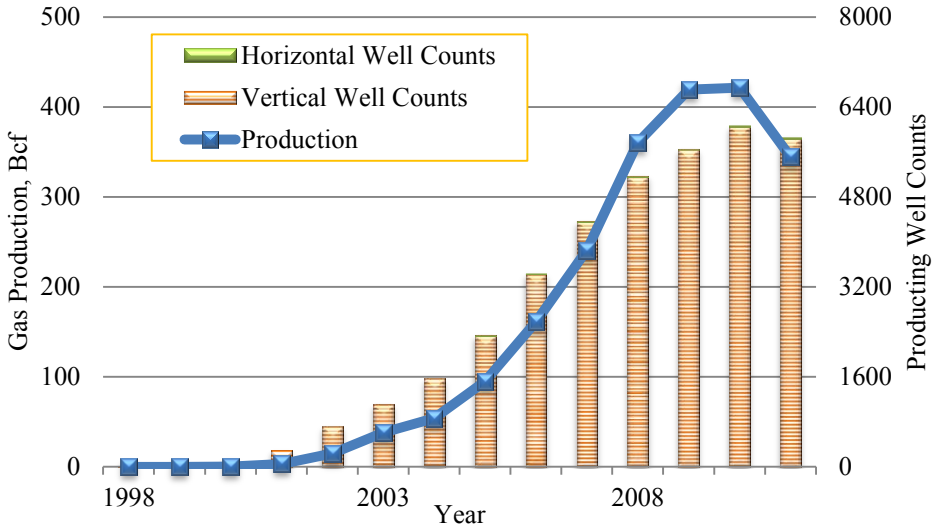

Figure 7.14—Annual gas production of Big George coal in Powder River basin (Data source: HPDI 2011)

7.7.2 Reservoir Parameters

The Big George seam extends about 100 km north-south, parallel to the basin axis, and about 25 km east-west. The average depth of the Big George coal is 1,100 ft (Flores and Bader 1999). Big George coal is usually water saturated and has a sub-normal hydrostatic pressure gradient of 0.315 psi/ft (ARI 2002). The average reservoir pressure is calculated to be 350 psi. To the north and northwest, the coals tend to become thinner and split into number of different seams, making correlations difficult. Net pay ranges from 50 to 300 feet (Ayers 2002; Swindell 2007). Average matrix porosity is 4%-10% (Bank and Kuuskraa. 2006). Permeability estimates are high, ranging from 10 md to 1000 md (Ayers 2002). Average bulk density of coal beds in the Fort Union formation of Powder River basin is 1.55 g/cc (Morin 2005).

Gas content and isotherm data, appropriate for the low rank coals of the PRB, were assembled using published desorption data and history matching of long-term

(4+year) gas and water production data in the PRB, shown in **Figure 7.15**. The Langmuir pressure is 350 psi and Langmuir volume is 140 scf/ton. Gas content is reported between 16 and 76 scf/ton (Ayers 2002).

To simulate the CBM wells, a small quantity of water is used without proppant in the Powder River basin. This method is usually used improve the connectivity of the reservoir to the wellbore in very high permeability (>100md) reservoir. But the created fracture half-length is usually short. Typical fracture half-length was found to be 34 ft in the Fort Union (Johnson 2002). **Table 7.9** lists the range of main uncertain parameters for the Big George coal (Fort Union formation).

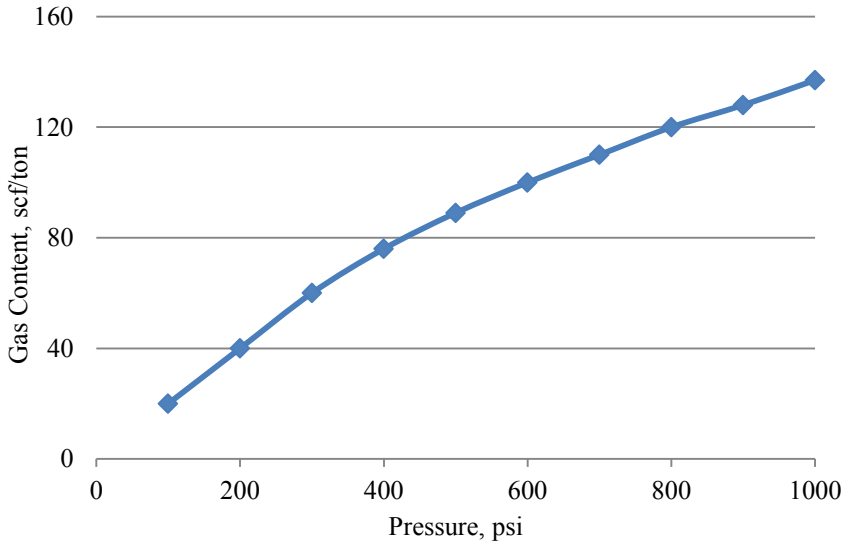

Figure 7.15—Typical coalbed methane isotherm of Powder River basin (Bank and Kuuskraa 2006)

Table 7.9—Reservoir parameters for the Big George coal

Parameter	Value/Range
Net Pay, ft	50-300
Gas Content, scf/ton	16-76
Permeability, md	10-1000
Average Reservoir Pressure, psi	350
Fracture Half-length, ft	34
Average Porosity, %	0.04-0.1

Table 7.10 shows the key fixed reservoir parameters used for the Big George formation single-well reservoir simulations. For the Big George coal, wells are typically drilled on 80 acres spacing with some test development on 40 acres (Swindell 2007). The well spacing is assumed 80 acres.

Table 7.10—Key fixed input parameters for the Big George coal model

Parameters	Value
Reservoir Temperature, ^{o}F	50
Bottom Hole Pressure, psia	200
Wellbore Radius, ft	0.324
Gas Specific Gravity (air=1)	0.62
Bulk Density, g/cc	1.55
Langmuir Volume, scf/ton	140
Langmuir Pressure, psi	350
Water Saturation, %	100
Well Spacing, acres	80

7.7.3 Model Verification

By the end of 2004, 1,414 new vertical wells were producing coalbed methane from Big George coal for more than 7 years. **Figure 7.16** shows annual new producing

vertical wells in the Big George coal. The production histories from these vertical wells were normalized for 7 years.

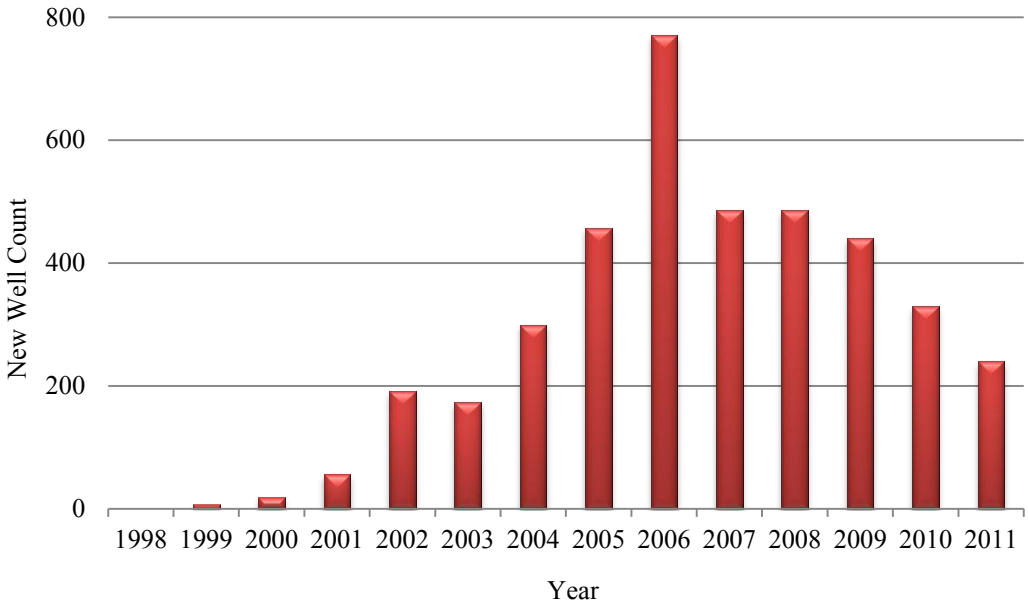

Figure 7.16—Annual new well counts for the Big George coal of Powder River basin

Density functions for the seven uncertain parameters were defined with honoring their range and value in Table 7.9. Then the density functions were calibrated until a reasonable match between simulated and actual 7-year cumulative gas production from the wells in the Lance formation was reached.

The red curve in **Figure 7.17** shows the distribution of 7-year cumulative gas production from the 1,414 wells. The blue curve in Figure 7.17 is the distribution of 7-year cumulative gas production simulated by UGRAS with the reservoir parameters in Table 7.10 and density functions in **Table 7.11**. The consistent match between the two curves finalized the density functions for the key parameters as listed in Table 7.11 and

confirmed the well spacing of 80 acres. The distributions of the seven uncertain parameters after calibration honored their range reported from literature (**Table 7.12**).

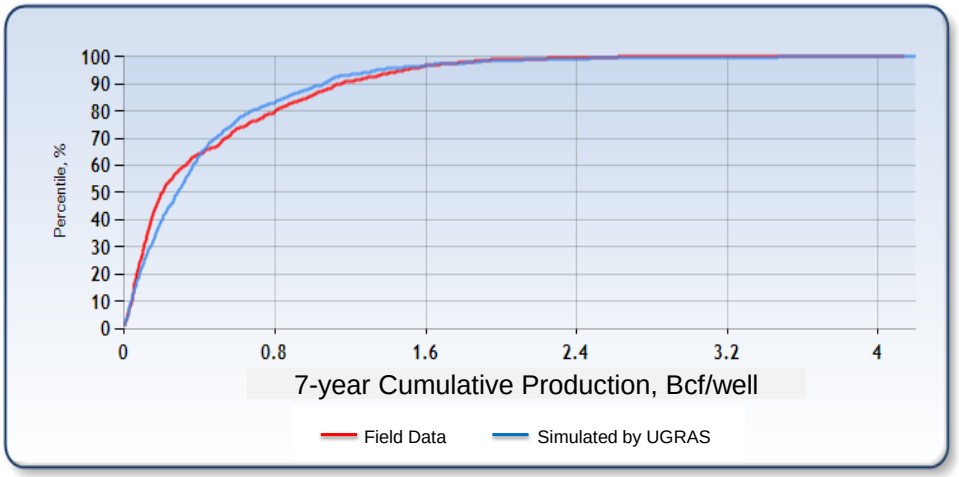

Figure 7.17—Probability distribution of cumulative gas production (7-year) match result for the Big George coal

Table 7.11—Density functions of uncertain parameters after calibration for the Big George coal

Parameters	Distribution Type	μ	σ	A	B	Min	Med	Max
Net Pay, ft	Weibull	100	1					
Porosity, f	Uniform			0.01	0.1			
Initial Pressure, psi	Lognormal	400	50					
Gas Content, scf/ton	Triangular					50	60	100
Permeability, md	Lognormal	1	1.3					
Fracture Half-length, ft	Triangular					50	80	100

Table 7.12—Comparison of the range of uncertain parameters

Parameter	Reported Range	Used by This Study(P1-P99)
Net Pay, ft	50-300	10-500
Gas Content, scf/ton	16-76	16-76
Permeability, md	10-1000	10-1000
Porosity, %	4-10	4-10

7.7.4 Resource Evaluation for Current Well Spacing

The vertical well count is 2.5 times greater than that as of 2005 (Figure 7.14). It assumed that the well spacing is 30 acres currently. The reservoir property distributions of Big George coal in Table 7.11 yield a lognormal distribution of OGIP per 30 acres (**Figure 7.18).** The P10, P50 and P90 values are 0.04, 0.17, and 0.66 Bcf/30 acres, respectively.

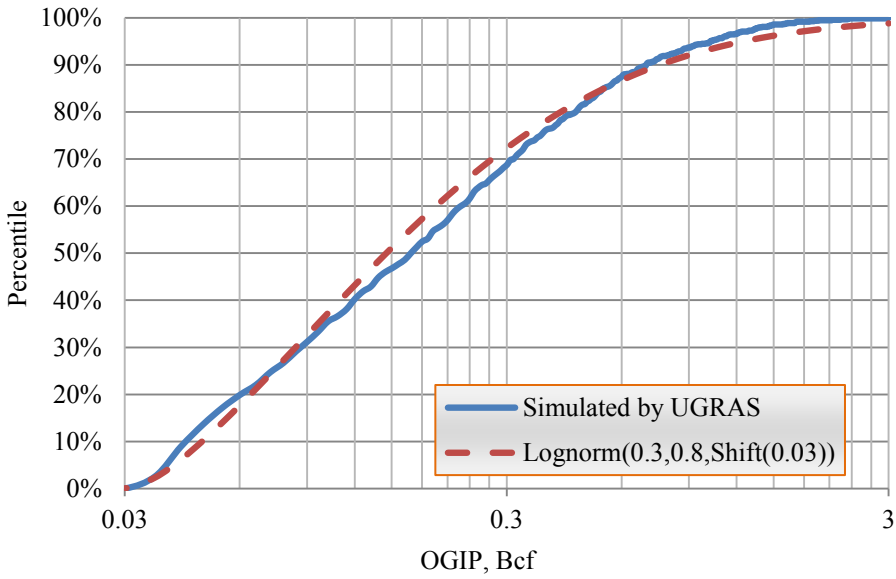

Figure 7.18—Probabilistic distribution of OGIP per 30 acres for Big George coal

The simulation results yielded an inverse Gaussian distribution for TRR with a P10 value of 0.01 Bcf/30 acres, a P50 of 0.06 Bcf/30 acres, and a P90 of 0.24 Bcf/30 acres (**Figure 7.19**). The P10, P50 and P90 values of recovery factor is 31%, 35% and 38%, respectively (**Figure 7.20)**.

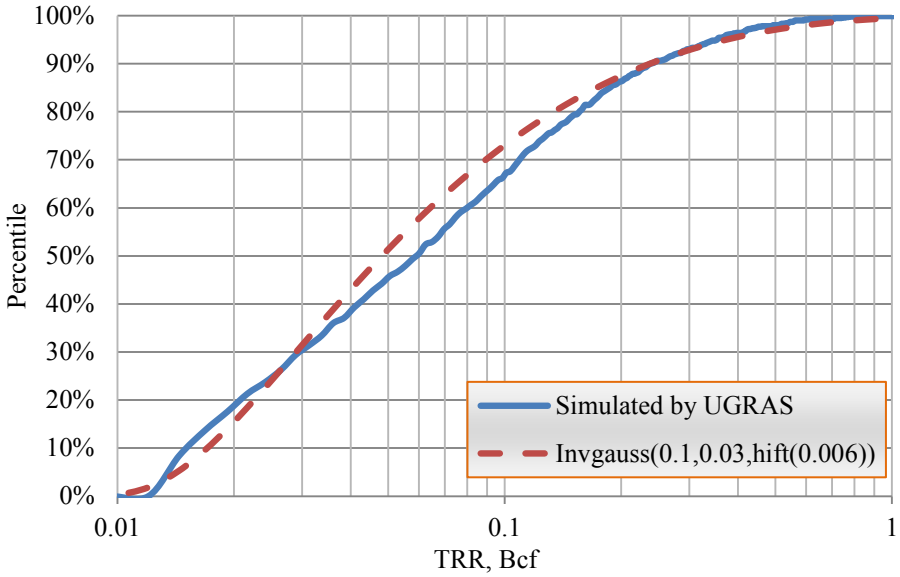

Figure 7.19—Probabilistic distribution of TRR per 30 acres with a 25-year life for Big George coal

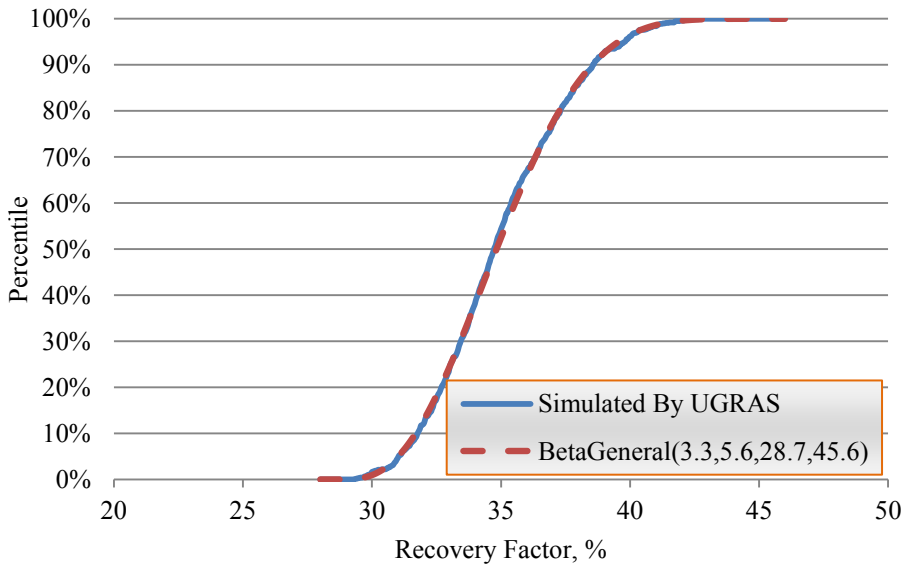

Figure 7.20—Probabilistic distribution of Recovery factor with 25-year life for Big George coal

7.7.5 Resource Evaluation for Various Well Spacing

We re-simulated the distribution TRR from the Big George coal with varying well spacing to 80, 40, and 30 acres. The TRR from single well decreases with a tighter

well spacing (**Figure 7.21**). However, there is no significant enhance in the recovery factor with the well spacing decreasing (**Figure 7.22**).

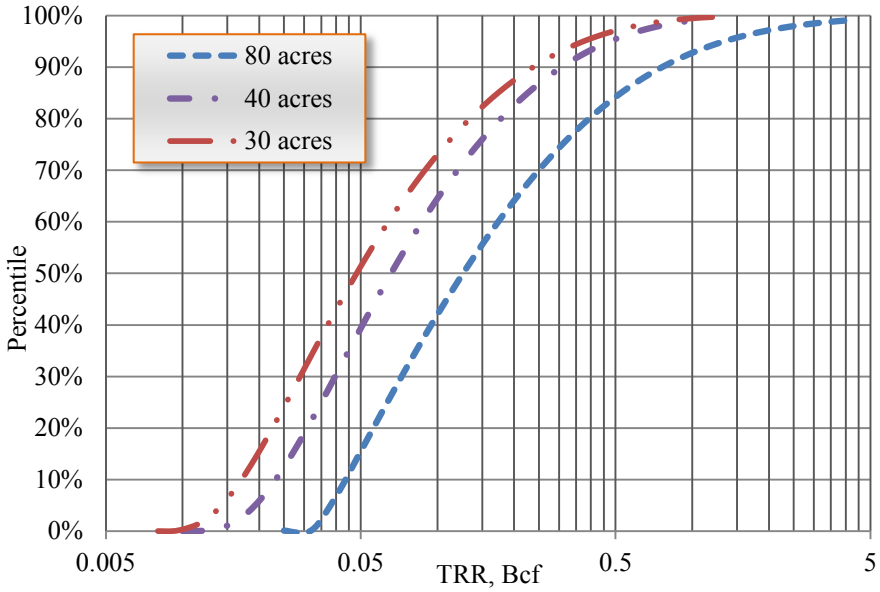

Figure 7.21—TRR versus well spacing in the Big George coal

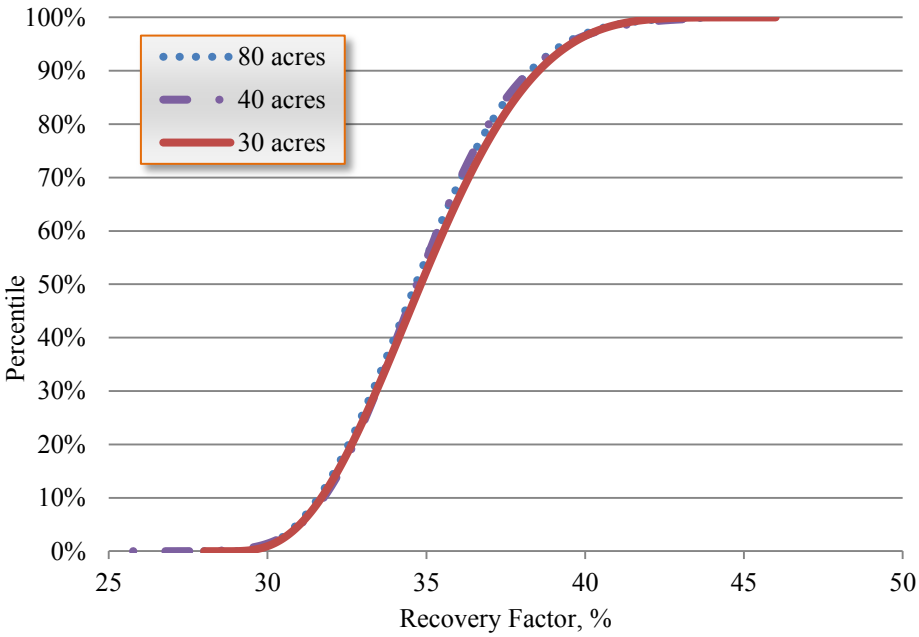

Figure 7.22—RF versus well spacing in the Big George coal

7.8 Discussion

Well life doesn't affect TRR and recovery factor from CBM formation when analysis year greater than 25 years (**Figure 7.23**). As such, we chose a 25-year production history to estimate TRR from CBM formation.

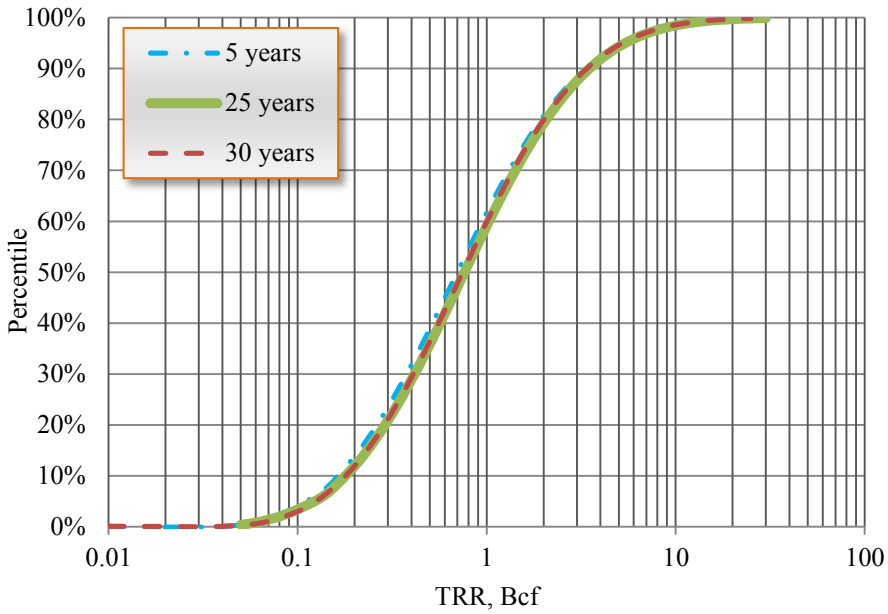

Figure 7.23—TRR from the Fruitland coal versus various analysis years

7.9 Summary

Table 7.13 summarized the key characteristics of the two key coal beds we estimated. We have evaluated the cumulative probabilistic distribution of OGIP, TRR and RF for the two most productive coal beds in the United States using a probabilistic, analytical reservoir model.

Table 7.13—Summary of the key characteristics for two dominate CBM formations in United States

Parameter	Fruitland	Big George
Basin	SJB	PPB
Depth Range, ft	550-4,400	<2,300
Net Pay, ft	20-80	50-300
Porosity, %	0.25-3	4-10
Permeability, md	5-60	10-1,000
Water Saturation,%	80-100	100
Bulk Density, g/cc	1.40	1.55
Gas Content, scf/ton	150-500	16-76
Average Pi, psia	260-1,900	350
Temperature, ^{o}F	110	50
Fracture Half-length, ft	100-300	34
Wells by 2011	6,407	5,865
Daily Gas Production in 2011, Bcf/d	2.0	1.0
Cumulative gas production by 2011, Tcf	17.1	2.2

Figures 7.24 through **7.26** show the cumulative distribution of OGIP per section, TRR per section, and recovery factor for the two coalbed methane formations. There is larger uncertainty in the resource assessment of Fruitland coal than in Big George coal. **Table 7.14**, constructed for the two coalbed methane formations, provided a concise summary of these resource assessments. Resources are greatest in the northern Fruitland coal of San Juan basin, coincident with high coalbed gas in place and with thick, northwest-trending, thermally mature, overpressured coal beds. In this area, CBM OGIP is 15-30 Bcf/sec. Fruitland CBM OGIP are less than 5 Bcf/sec in the southern San Juan basin (Ayers and Ambrose 1990). The OGIP is estimated at 1.6 (P10)-33.0 (P90) Bcf/sec. There is no resource assessment about Big George coal available. Volumetric OGIP calculations for CBM reservoirs are subject to significant error due to uncertainties in

assessing net pay, gas content and drainage area. Probabilistic method is available to reduce uncertainty, but data often is not.

Besides, more OGIP in the Fruitland coal, higher reservoir pressure and permeability, and longer fracture half-length result in more technically recoverable coalbed methane and higher recovery factor in this coal (Figures 7.25 and 7.26).

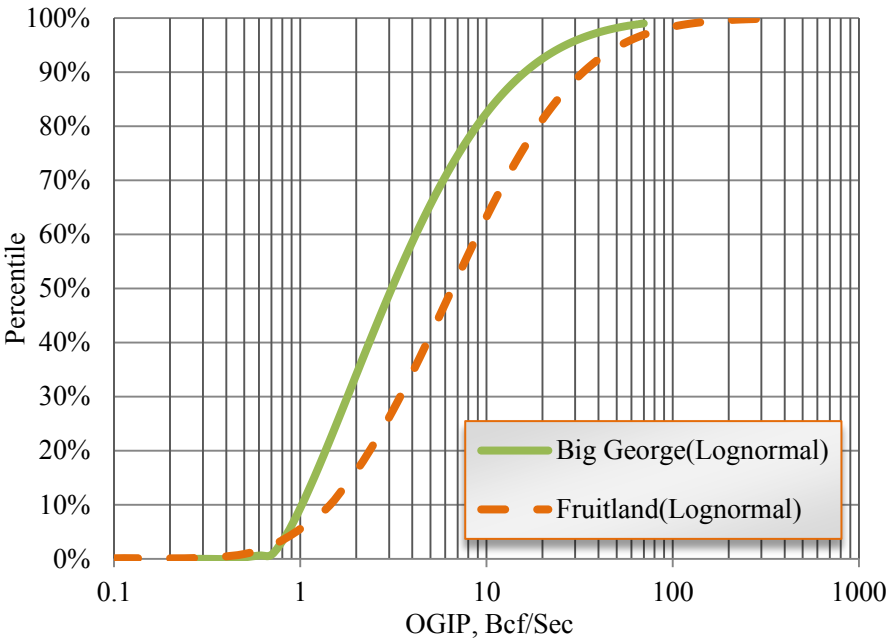

Figure 7.24—Comparison between probabilistic distributions of OGIP per section for two CBM formations in the United States

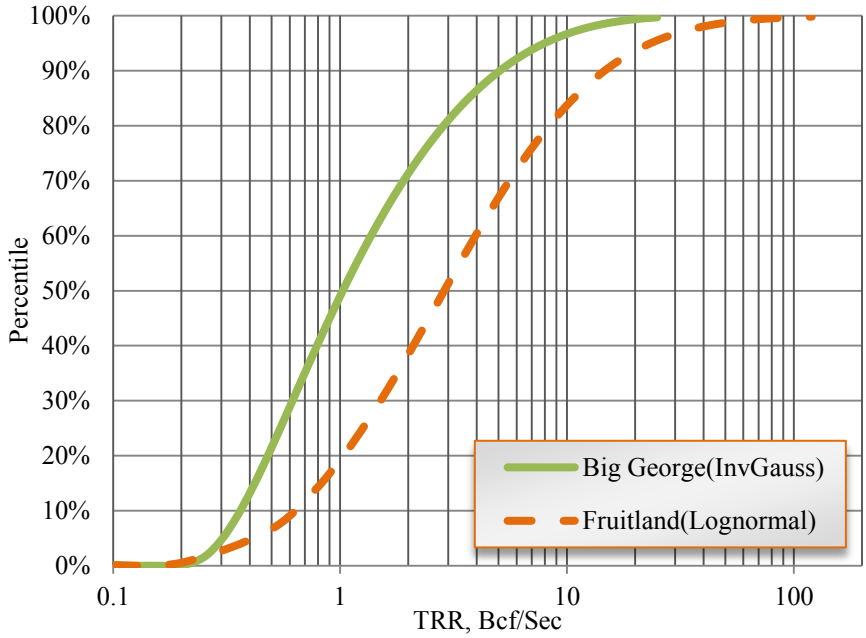

Figure 7.25—Comparison between distributions of TRR per section for two CBM formations in the United States

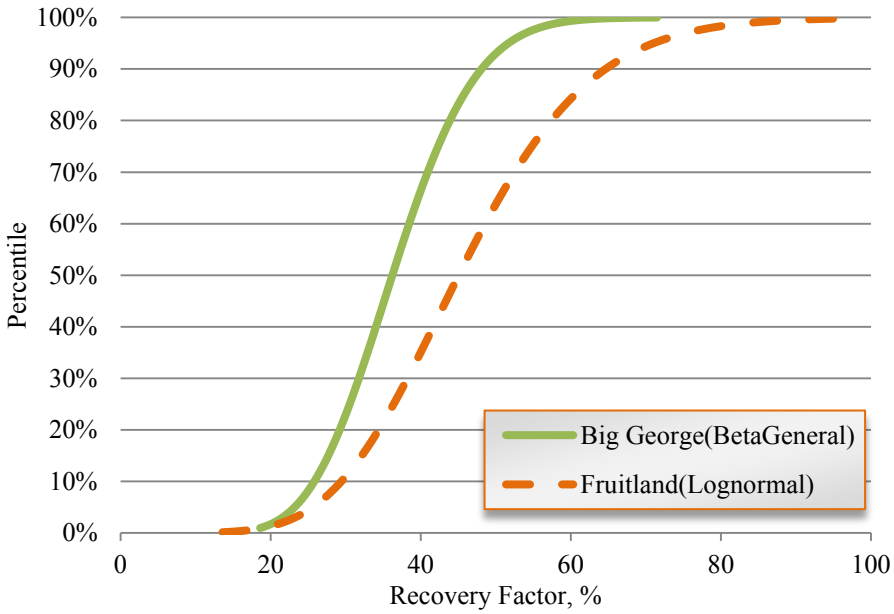

Figure 7.26—Comparison between distributions of recovery factor for two CBM formations in the United States

Table 7.14—Summary of estimated resources for the two key coal in the United States

Parameter	Fruitland	Big George
Current Well Spacing, acre	120	30
Probability Distribution of OGIP	Lognormal	Lognormal
OGIP (P10), Bcf/well	0.30	0.04
OGIP (P50), Bcf/well	1.30	0.17
OGIP (P90), Bcf/well	6.10	0.66
Probability Distribution of TRR	Lognormal	Inverse Gaussian
TRR (P10), Bcf/well	0.10	0.01
TRR (P50), Bcf/well	0.50	0.06
TRR (P90), Bcf/well	2.60	0.24
Probability Distribution of RF	Lognormal	General Beta
RF (P10), %	29	31
RF (P50), %	45	35
RF (P90), %	65	38
OGIP (P10), Bcf/sec	1.6	0.9
OGIP (P50), Bcf/sec	6.9	3.6
OGIP (P90), Bcf/sec	32.5	14.1
TRR (P10), Bcf/sec	0.5	0.2
TRR (P50), Bcf/sec	2.7	1.3
TRR (P90), Bcf/sec	13.9	5.1

We gained a probabilistic distribution of technically recovery factors from the two coalbed methane reservoirs in the United States. It follows a log-logistic distribution, with a mean value of 41% (**Figure 7.27**). We will apply the distribution to assess the TRR for the other six regions in the Section 8.

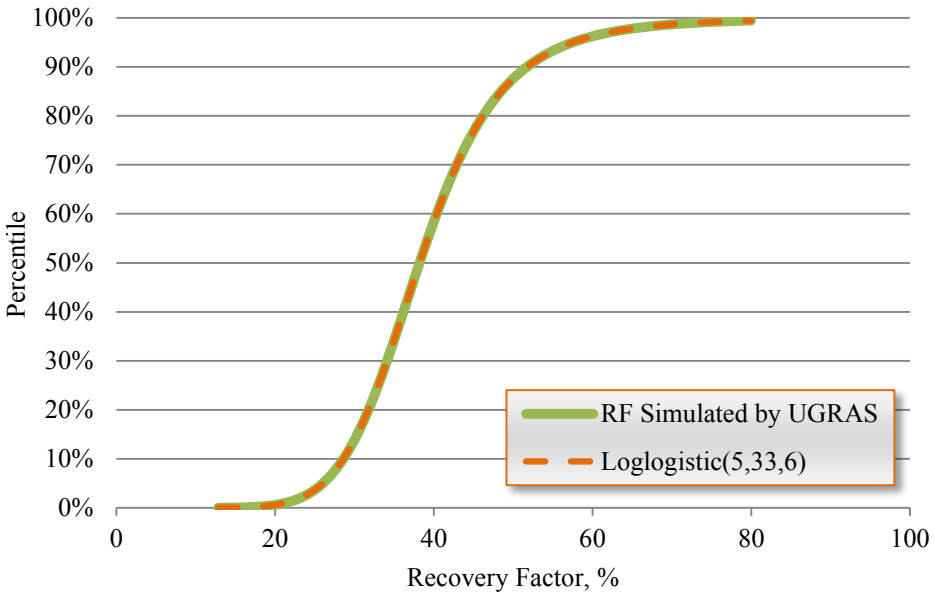

Figure 7.27—Recovery factor of coalbed methane derived from the United States

8. GLOBAL UNCONVENTIONAL GAS RESOURCE EVALUATION

In the section, we are now going to take what we have learned from the distributions of unconventional gas in place for the 7 world regions and the distributions of recovery factors from 10 unconventional gas plays/formations in the United States to estimate TRR from unconventional gas reservoirs in the rest of world.

8.1 Global Shale Gas TRR

The distributions of shale-gas OGIP for each of 7 world regions were determined (Figure 4.20). We have obtained the representative probabilistic distribution of technically recovery factor from shale gas plays in the United States. It follows general Beta distribution with a mean value of 25% (Figure 5.43). We multiplied the distributions of shale-gas OGIP by the distribution of recovery factor to assess the technically recoverable resource from shale gas reservoirs for the 7 world regions (**Figure 8.1**). According to our study, global shale gas TRR ranges from 4,000 (P10) to 25,000 (P90) Tcf (**Table 8.1**).

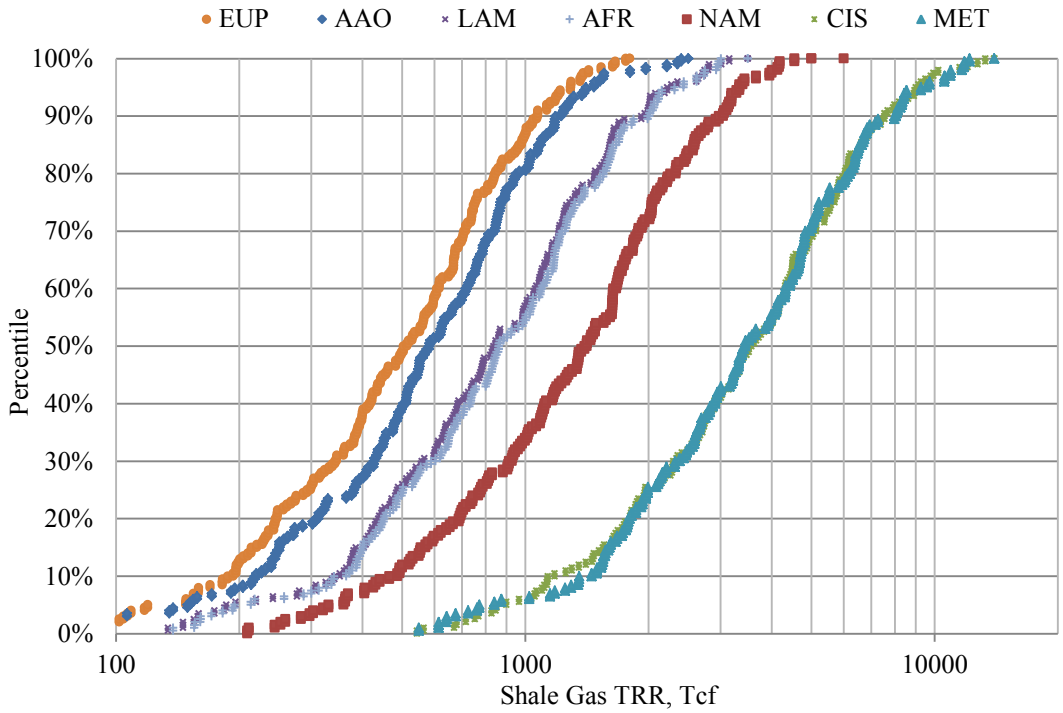

Figure 8.1—TRR from shale gas reservoirs for 7 world regions

Table 8.1—Assessment results of shale gas TRR worldwide, in Tcf

Region	TRR estimated by this study			EIA (2011a)
	P10	P50	P90	
MET	1,354	3,415	7,974	/
CIS	1,136	3,520	7,541	/
NAM	466	1,395	2,975	1,208
AFR	341	862	1,991	1,024
LAM	342	836	1,921	1,906
AAO	218	582	1,184	1,800
EUP	188	504	1,068	624
World	4,044	11,114	24,654	6,562

8.2 Global Tight Sands Gas TRR

The distributions of tight-sands OGIP for 7 world regions were determined (Figure 4.18). And we have derived the representative probabilistic distribution of

technically recovery factors from tight sands gas formations in the United States in Section 6. It follows logistic distribution with a mean value of 79% (Figure 6.33). We applied the distributions of tight-sands OGIP and the distribution of recovery factor to assess the technically recoverable resource from tight sands gas reservoirs for the 7 world regions (**Figure 8.2**). According to our study, global tight sands gas TRR ranges from 38,000 (P10) to 84,000 (P90) Tcf (**Table 8.2**).

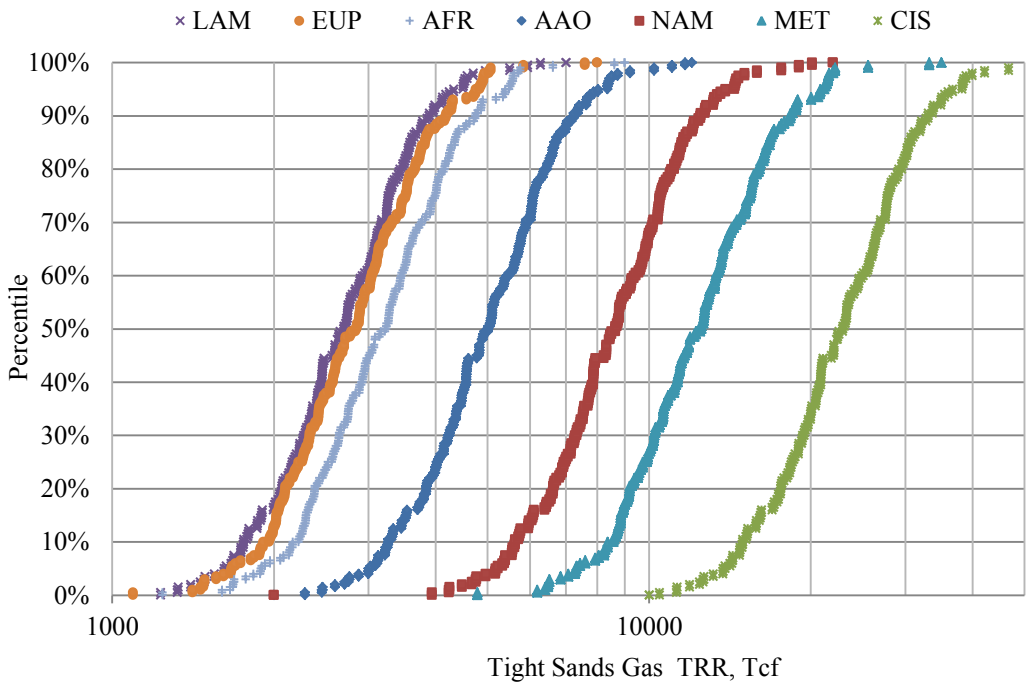

Figure 8.2—TRR from tight sands gas reservoirs for 7 world regions

Table 8.2—Assessment results of tight sands gas TRR worldwide, in Tcf

Region	P10	P50	P90
CIS	14,926	22,924	33,055
MET	8,371	12,434	18,309
NAM	5,627	8,642	12,462
AAO	3,263	5,011	7,226
AFR	2,168	3,220	4,742
EUP	1,911	2,838	4,179
LAM	1,756	2,698	3,890
World	38,022	57,767	83,863

8.3 Global CBM TRR

The distributions of CBM OGIP for the 7 global regions were established (Figure 4.16). And we have determined the probabilistic distribution of technically recovery factors from coalbed methane formations in the United States. It follows the Gamma distribution with the mean value of 41% (Figure 7.27). We applied the distributions of CBM OGIP and the distribution of recovery factor to estimate the technically recoverable resource from CBM reservoirs for the 7 world regions (**Figure 8.3**). According to our study, global CBM TRR ranges from 500 (P10) to 3,000 (P90) Tcf (**Table 8.3**).

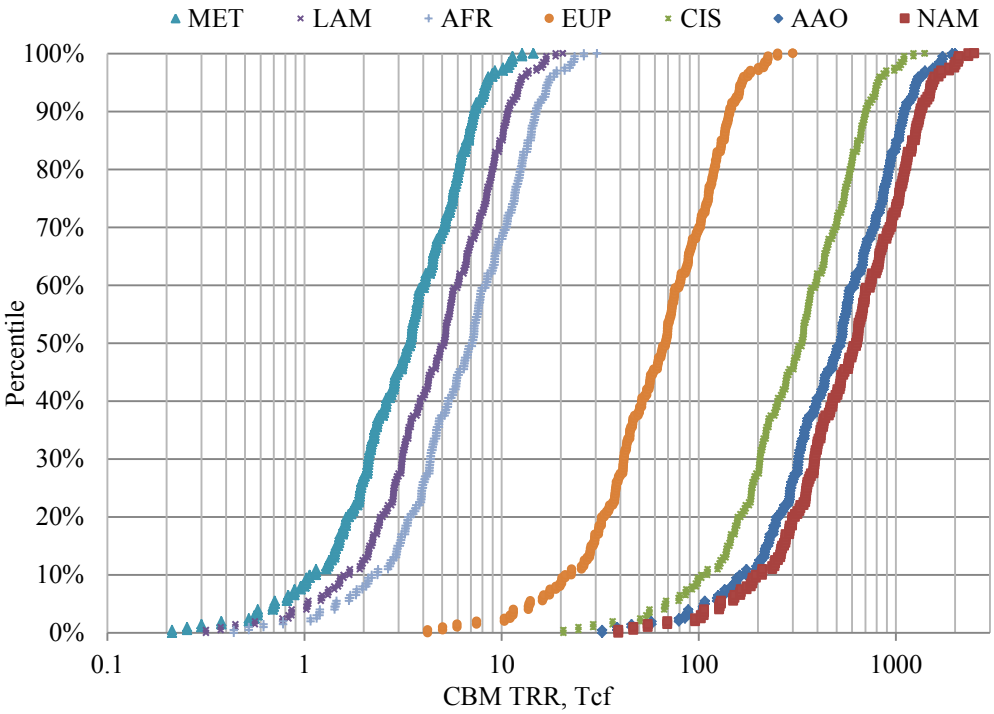

Figure 8.3—TRR from CBM reservoirs for 7 world regions

Table 8.3—Assessment results of CBM TRR worldwide, in Tcf

Region	P10	P50	P90
NAM	196	631	1,336
AAO	162	522	1,105
CIS	103	333	704
EUP	21	68	144
AFR	2	7	15
LAM	2	5	11
MET	1	3	7
World	487	1,569	3,322

The P50 of our total technically recoverable unconventional gas is estimated at 70,000 Tcf (**Table 8.4**), with a range of 43,000 (P10)-112,000 (P90) Tcf. We expect that large volumes of unconventional gas resources are likely to exist in the CIS and Middle East because they have a large endowment of unconventional gas in place.

Table 8.4—Summary of technically recoverable unconventional gas resources worldwide

Region	TRR (P50), Tcf			
	CBM	Tight gas	Shale gas	Total
CIS	333	22,924	3,520	26,776
MET	3	12,434	3,415	15,853
NAM	631	8,642	1,395	10,669
AAO	522	5,011	582	6,115
AFR	7	3,220	862	4,089
LAM	5	2,698	836	3,538
EUP	68	2,838	504	3,410
World	1,569	57,767	11,114	70,450

9. CONCLUSIONS

We conducted a global assessment of unconventional OGIP and TRR, quantified the uncertainty in these resources estimates, and reached the following conclusions.

1. Estimated global unconventional OGIP ranges from 83,000 (P10) to 184,000 (P90) Tcf, with a range between 43,000 (P10) and 112,000 (P90) Tcf technically recoverable.
2. The P50 of our total global unconventional OGIP assessment (126,000 Tcf) is 4 times greater than Rogner's 1997 estimate of 33,000 Tcf. About 70,000 Tcf (P50) of unconventional gas is recoverable globally. **Table 9.1** lists the P50 value of OGIP and TRR for the 7 world regions.
3. Global coalbed methane in place is estimated to be 1,000 (P10) to 8,000 (P90) Tcf, with TRR from 500 (P10) to 3,000 (P90) Tcf. North America holds the largest amount of CBM in place and technically recoverable CBM resources.
4. The volume of global tight-sands OGIP ranges from 49,000 (P10) to 105,000 (P90) Tcf, with TRR between 38,000 (P10) to 84,000 (P90) Tcf. CIS regions are expected to possess the largest tight sands gas in place and technically recoverable tight-gas resources.
5. The amount of shale-gas OGIP worldwide is 33,000 (P10) to 72,000 (P90) Tcf, with TRR of 4,000 (P10) to 25,000 (P90) Tcf. Significant shale-gas

resources exist in the CIS region and Middle East.

6. We developed a statistical method to determine the probabilistic distribution of OGIP and TRR from unconventional gas reservoirs.
7. We quantified the uncertainty in the resource size of the key unconventional gas plays/formations in the United States with a probabilistic method. **Table 9.2** summarized the P50 of OGIP, TRR and RF assessments in these formations/plays.
8. The probabilistic distribution of technical recovery factor from the five key shale gas plays in the United States follows a general Beta distribution, with a mean value of 25%.
9. The recovery factor of three key tight sands gas formations in the United States has considerable uncertainty. It ranges from 20% to 90%, with a P50 value of 79%.
10. The technical recovery factor of the two key coalbed methane formations in the United States follows a Gamma distribution, with a P50 value of 41%.

Table 9.1—Original gas in-place and technically recoverable unconventional gas worldwide

Region	OGIP (P50), Tcf				TRR (P50), Tcf			
	CBM	Tight gas	Shale gas	Total	CBM	Tight gas	Shale gas	Total
CIS	859	28,604	15,880	45,343	333	22,924	3,520	26,776
MET	9	15,447	15,416	30,872	3	12,434	3,415	15,853
NAM	1,629	10,784	5,905	18,318	631	8,642	1,395	10,669
AAO	1,348	6,253	2,690	10,291	522	5,011	582	6,115
AFR	18	4,000	3,882	7,901	7	3,220	862	4,089
LAM	13	3,366	3,742	7,122	5	2,698	836	3,538
EUP	176	3,525	2,194	5,895	68	2,838	504	3,410
World	4,052	71,981	49,709	125,742	1,569	57,767	11,114	70,450

Table 9.2—The P50 value of resource assessments for key unconventional gas formations in United States

Type	Basin	Formation	OGIP, Bcf/sec	TRR, Bcf/sec	OGIP, Tcf	TRR, Tcf	RF, %
Shale Gas	ARKB	Fayetteville	79	8	258	34	11
	FWB	Barnett	70	13	352	63	18
	APPB	Marcellus	59	23	1,385	534	39
	WGC	Eagle Ford	59	19	278	90	31
	ETB	Haynesville	206	37	1,858	330	18
Tight Gas	GGRB	Lance	198	51			78
	ETB	Cotton Valley	12	9			82
	ETB	Travis Peak	19	15			81
CBM	SJB	Fruitland	7	3			45
	PRB	Big George	4	1			35

REFERENCES

Abou-sayed, I.S., Sorrell, M.A., Foster, R.A. et al. 2011. Haynesville Shale Development Program-From Vertical to Horizontal. Paper SPE 144425-MS presented at North American Unconventional Gas Conference and Exhibition, Woodlands, Texas, 01/01/2011.

Allan, D.K. 2004. Coalbed Methane Development in the Western Canadian Sedimentary Basin: A Significant Emerging Resource for North America. Paper present at Rocky Mountain Natural Gas Conference, Denver, Colorado, 08/09/2004.

ARI. 2002. Powder River Basin Coalbed Methane Development and Produced Water Management, Advanced Resources International, Inc, Washington, D.C.

Ayers, W.B. 2002. Coalbed Gas Systems, Resources and Procution and a Review of Contrasting Cases from the San Juan and Powder River Basins. *AAPG Bulletin* **86**(11): 1853-1860.

Ayers, W.B., and Ambrose, W.A. 1990. Geologic Controls on the Occurrence of Coalbed Methane, Fruitland Formation, San Juan Basin, Gas Research Institute, Chicago, Illinois.

Baihly, J.D., Grant, D., Fan, L. et al. 2009. Horizontal Wells in Tight Gas Sands-A Method for Risk Management To Maximize Success. *SPE Production & Operations* **24**(2). SPE-110067-PA.

Bank, G.C., and Kuuskraa, V.A. 2006. The Economics of Powder River Basin Coalbed Methane Development, U.S. Department of Energy, Washington, D.C.

Barker, C.E. 2002. Coalbed Methane in Northern Alaska: Potential Resources for Rural Use and Added Supply for the Proposed Trans-Alaska Gas Pipeline. Paper present at AAPG Pacific Section/SPE Western Region Conference, Anchorage, Alaska, 05/18/2002.

Benedetto, L. 2010. An Update on Shale Activity in the US. Paper presented at PLANO Luncheon, New Orleans, Louisiana, 03/10/2010.

Berman, A. 2008. The Haynesville Shale Sizzles with the Barnett Cools. *World Oil Magazine* **229** (9): 18-22.

BGR. 2009. Reserves, Resources and Availability of Energy Resources, Federal Institute for Geosciences and Natural Resources, Hanover, Germany.

Billa, R.J., Mota, J F., Schneider, B. et al. 2011. Drilling Performance Improvement in the Haynesville Shale Play. Paper SPE 139842-MS presented at SPE/IADC Drilling Conference and Exhibition, Amsterdam, Netherlands, 03/01/2011.

Boswell, R. 2005. Assessments of Regional Gas Accumulations at the Department of Energy. Paper presented at AAPG Hedberg Conference—Understanding Tight Gas Sands, Morgantown, West Virginia, 04/28/2005.

Boughal, K. 2008. Unconventional Plays Grow in Number After Barnett Shale Blazed the Way. *World Oil Magazine* **29** (8): 20-24.

Bruner, K.R., and Smosna, R. 2010. A Comparative Study of the Mississippian Barnett Shale, Fort Worth Basin, and Devonian Marcellus Shale, Appalachian Basin, U.S. Department of Energy, Washington, D.C.

Byrer, C.W., Malone, R.D., and Hunt, A.E. 1982. Pre Preliminary Resource Assessment of Coalbed Methane in the U.S. Paper SPE 10799-MS presented at the SPE Unconventional Gas Recovery Symposium, Pittsburgh, Pennsylvania, 05/16/1982.

Chakhmakhchev, A. 2007. Worldwide Coalbed Methane Overview. Paper SPE 106850-MS presented at SPE Hydrocarbon Economics and Evaluation Symposium, Dallas, Texas, 04/01/2007.

Chao, E.C.T., Minkin, J.A., Back, J.M. et al. 1984. Petrographic Characteristics and Depostional Environment of the Paleocene 61-M-Thick Subbituminous Big George Coal Bed, Powder River Basin, Wyoming. Paper presented at Symposium on the Geology of Rocky Mountain Coal, Denver, Colarado, 10/02/1984.

Chong, K K., Grieser, W.V., Passman, A. et al. 2010. A Completions Guide Book to Shale-Play Development: A Review of Successful Approaches Towards Shale-Play Stimulation in the Last Two Decades. Paper SPE 133874-MS presented at Canadian Unconventional Resources and International Petroleum Conference, Calgary, Alberta, Canada, 10/19/2010.

Cluff, B. 2009. Shale Gas: Opportunities and Challenges for Independents. Paper presented at SIPES 2009 Annual Meeting, Denver, Colorado, 04/27/2009.

Crist, T.E., Kelso, B.S., and Boyer, C.M.1990. A Geologic Assessment of Natural Gas from Coal Seams in the Menefee Formation, San Juan Basin, Gas Research Institute, Chicago, Illinois.

Cubic Energy, Inc. 2008. A Penny for Your Thoughts. Zman's Energy Brain. http://zmansenergybrain.com/2008/06/03/cubic-energy-qbik-a-penny-for-your-thoughts/

Dhir, R., Mavor, M.J., and Close, J.C. 1991. Evaluation of Fruitland Coal Properties and Development Economics, San Juan Basin, Colorado and New Mexico. Paper present at Coalbed Methane of Western North America, Glenwood Springs, Colorado, 09/19/1990.

DOE. 2004. Coal Bed Methane Primer, U. S. Department of Energy, Washington, D.C.

DOE. 2009. Modern Shale Gas Development in the United States: A Primer, U. S. Department of Energy, Washington, D.C.

DOE. 2010. Impact of the Marcellus Shale Gas Play on Current and Future CCS Activities, U. S. Department of Energy, Washington, D.C.

Dyman, T.S., and Condon, S.M. 2006. Assessment of Undiscovered Conventional Oil and Gas Resources—Upper Jurassic–Lower Cretaceous Cotton Valley Group, Jurassic Smackover Interior Salt Basins Total Petroleum System, in the East Texas Basin and Louisiana-Mississippi Salt Basins Provinces, U.S. Geological Survey, Golden, Colorado.

Eberhard, M.J., Mullen, M.J., Seal, C.A. et al. 2000. Integrated Field Study for Production Optimization: Jonah Field - Sublette County, Wyoming. Paper SPE 59790-MS presented at SPE/CERI Gas Technology Symposium, Calgary, Alberta, Canada, 04/03/2000.

Edwards, K.L., Weissert, S., Jackson, J.B. et al. 2011. Marcellus Shale Hydraulic Fracturing and Optimal Well Spacing to Maximize Recovery and Control Costs. Paper SPE 140463-MS presented at SPE Hydraulic Fracturing Technology Conference, Woodlands, Texas, 01/01/2011.

EIA. 2011a. World Shale Gas Resources: An Initial Assessment of 14 Regions Outside the United States, Energy Infomration Administration, Washington, D.C.

EIA. 2011b. Haynesville Surpasses Barnett as the Nation's Leading Shale Play. Energy Infomration Administration, http://www.eia.gov/todayinenergy/detail.cfm?id=570

EIA. 2012a. Annual Energy Outlook 2012, Energy Infomration Administration, Washington, D.C.

EIA. 2012b. Monthly Dry Shale Gas Production. U. S. Energy Information Administration. http://www.eia.gov/naturalgas/weekly/

Fan, L., Martin, R.B., Thompson, J.W. et al. 2011. An Integrated Approach for Understanding Oil and Gas Reserves Potential in Eagle Ford Shale Formation. Paper SPE 148751-MS presented at Canadian Unconventional Resources Conference, Alberta, Canada, 11/15/2011.

Flores, R.M., and Bader, L.R. 1999. Fort Union Coal in the Powder River Basin, Wyoming and Montana: A Synthesis. *U.S. Geological Survey Professional Paper 1625-A*: PS1-PS71.

Ganer, B.L. 1985. Case History of Cotton Valley Sand Log Interpretation for a North Louisiana Field. *SPE Journal of Petroleum Technology* **37**(11):1995-2005. SPE-12182-PA.

GRI. 2001. North American Coalbed Methane Resource Map, Gas Research Institute, Chicago, Illinos.

Grieser, W.V., Shelley, R.F., Johnson, B.J. et al. 2008. Data Analysis of Barnett Shale Completions. *SPE Journal* **13** (3): 366-374. SPE-100674-PA.

Haas, M.R., and Stone, A. 1986. Productive and Economic Potential of Tight Gas From the Travis Peak Formation in East Texas. Paper SPE 14665-MS presented at SPE East Texas Regional Meeting, Tyler, Texas, 01/01/1986.

Hale, B.W. 2010. Barnett Shale: A Resource Play - Locally Random and Regionally Complex. Paper SPE 138987-MS presented at SPE Eastern Regional Meeting, Morgantown, West Virginia, 10/12/2010.

Hayden, J., and Pursell, D. 2005. The Barnett Shale: Visitor's Guide to the Hottest Gas Play in the US, Pickering Energy Partners, Inc, Houston, Texas.

Hill, D.G., and Nelson, C. R. 2000. Gas Productive Fractured Shales: An Overview and Update. *GasTIPS* **6** (2): 4-13.

Hinn, R. L., Glenn, J. M., and McNichol, K. C. 1988. Case History: Use of a Multiwell Model To Optimize Infill Development of a Tight-Gas-Sand Reservoir. *SPE Journal of Petroleum Technology* **40** (7): 881-886. SPE-14659-PA.

Holditch, S.A. 1992. Topical Report: Staged Field Experiment No. 3, Post-Fracture Pressure Buildup Analysis, April 10 - May 8, 1991. S.A. Holditch & Associates, Inc, College Station, Texas.

Holditch, S.A. 2006. Tight Gas Sands. *SPE Journal of Petroleum Technology* **58** (6): 86-93. SPE-103356-MS.

HPDI. 2011. HPDI Production Data Applications, Version 6.0.1.2. http://hpdi.com

Huffman, C., Apaydin, O.G., Ma, Y.Z. et al. 2005. Critical Parameters in Static and Dynamic Modeling of Tight Fluvial Sandstones. Paper SPE 95910-MS presented at SPE Annual Technical Conference and Exhibition, Dallas, Texas, 10/09/2005.

Janwadkar, S.S., Klotz, C., Welch, B. et al. 2010. Electromagnetic MWD Technology Improves Drilling Performance in Fayetteville Shale of North America. Paper SPE 128905-MS presented at IADC/SPE Drilling Conference and Exhibition, New Orleans, Louisiana, 01/01/2010.

Jarvie, D.M., Pollastro, R.M., Hill, R.J. et al. 2004. Geochemical Characterization of Thermogenic Gas and Oil in the Ft. Worth Basin, Texas. Paper presented at AAPG National Convention, Dallas, Texas, 04/18/2004.

Jennings, A.R., and Sprawls, B.T. 1977. Successful Stimulation in the Cotton Valley Sandstone—A Low-Permeability Reservoir. *SPE Journal of Petroleum Technology* **29** (10): 1267-1276. SPE-5627-PA.

Johnson, L.A. 2002. Fort Union Deep, Timberline Energy, Inc, Franktown, Colorado.

Johnson, R.C., Crovelli, R.A., Spencer, C.W. et al. 1987. An Assessment of Gas Resources in Low Permeablity Sandstones of the Upper Cretaceous Mesaverde Group, Piceance basin, U.S. Geological Survey, Denver, Colorado.

Johnson, R.C., Finn, T.M., Crovelli, R.A. et al. 1996. An Assessment of In-Place Gas Resource in Low Permeability Upper Cretaceous and Lower Tertiary Sandstone Reservoir, Wind River Basin,Wyoming, U.S. Geological Survey, Denver, Colorado.

Kazemi, H. 1969. Pressure Transient Analysis of Naturally Fractured Reservoirs with Uniform Fracture Distribution. *SPE Journal* **9**(4),451-462. SPE-2156-PA.

Kelafant, J.R. Wicks, D.E. and Kuuskraa, V.A. 1988. A Geologic Assessment of Natural Gas from Coal Seams in the Northern Appalachian Basin, Gas Research Institute, Chicago, Illinois.

Kelafant, J.R. and Boyer, C.M. 1988. A Geologic Assessment of Natural Gas from Coal Seams in the Central Appalachian Basin, Gas Research Institute, Chicago, Illinois.

Kelso, B.S., Wicks, D.E., and Kuuskraa, V.A. 1988. A Geologic Assessment of Natural Gas from Coal Seams in the Fruitland Formation, San Juan Basins, Gas Research Institute, Chicago, Illinois.

Kulkarni, P. 2010. Arrival of IOCs and Increasing Legislative Interest Signal Critical Mass for Marcellus. *World Oil* **231** (3): 77-85.

Kennedy, R.B. 2010. Shale Gas Challenges/Technologies Over the Asses Life Cycle. Paper present at U.S.-China Oil and Gas Industry Forum. Fort Worth, Texas 09/01/2010.

Kuuskraa, V.A., Brashear, J.P., Doscher, T.H. et al. 1978. Enhanced Recovery of Unconventional Gas, U.S. Department of Energy, Springfield, Virginia.

Kuuskraa, V.A., and Meyers, R.F. 1980. Review of World Resources of Unconventional Gas. Paper present at IIASA Conference on Conventional and Unconventional World Natural Gas Resources, Laxenburg, Austria, 06/30/1980.

Kuuskraa, V.A. 1992. Hunt for Quality Basins Goes Abroat. *Oil and Gas Journal* **90** (40): 49-54.

Kuuskraa, V.A., Koperna, G., Schmoker, J. et al. 1998. Barnett shale rising star in Fort Worth basin. *Oil & Gas Journal* **96** (21): 71-76.

Kuuskraa, V.A. 2009. Worldwide Gas Shales and Unconventional Gas: A Status Report. Paper present at United Nations Climate Change Conference, Copenhagen, Denmark, 12/09/2009.

Lafollette, R., Holcomb, W.D., and Aragon, J. 2012. Practical Data Mining: Analysis of Barnett Shale Production Results With Emphasis on Well Completion and Fracture Stimulation. Paper SPE 152531-MS presented at SPE Hydraulic Fracturing Technology Conference, Woodlands, Texas, 02/06/2012.

Laherrere, J. 2006. Oil and Gas, What Future? Paper presented at Groningen Annual Energy Convention, Groningen, Netherlands, 11/22/2006.

Law, B.E., Spencer, C.W., Charpentier, R.R. et al. 1989. Estimates of Gas Resources in Overpressured Low-Permeability Cretaceous and Tertiary Sandstone Reservoirs, Greater Green River Basin, Wyoming, Colorado, and Utah. In *Gas resources of Wyoming, 40th field Conference Guidbook*, ed. Eisert, J.L., Casper, Wyoming: Wyoming Geological Association.

Law, B.E. 1993. Tight Gas Reservoirs-An Emerging Major Source of Energy. In *The Future of Energy*, eds. Howeel, D.G., Wiese, K., Fanelli, M. et al., Denver, Colorado: U.S. Geological Survey.

Lee, D.S., Herman, J.D., Elsworth, D. et al. 2010. A Critical Evaluation of Unconventional Gas Recovery from the Marcellus Shale, Northeastern United States. *KSCE Journal of Civile Engineering* **15** (4): 679-687.

Lin, Z.S., and Finley, R.J. 1985. Reservoir Engineering Properties and Production Characteristics of Selected Tight Gas Fields, Travis Peak Formation, East Texas

Basin. Paper SPE 13901-MS presented at SPE/DOE Low Permeability Gas Reservoirs Symposium, Denver, Colorado, 01/01/1985.

Lohoefer, D.S., Seale, R.A., and Athans, J. 2006. New Barnett Shale Horizontal Completion Lowers Cost and Improves Efficiency. Paper SPE 103046-MS presented at SPE Annual Technical Conference and Exhibition, San Antonio, Texas, 09/24/2006.

Lohoefer, D.S., Snyder, D., Seale, R.A. et al. 2010. Comparative Study of Cemented Versus Uncemented Multi-Stage Fractured Wells in the Barnett Shale. Paper SPE 135386-MS presented at SPE Annual Technical Conference and Exhibition, Florence, Italy, 09/19/2010.

MacMillan, D.J., Pletcher, J.L., and Bourgeois, S.A. 1999. Practical Tools To Assist History Matching. Paper SPE 51888-MS presented at SPE Reservoir Simulation Symposium, Houston, Texas, 01/01/1999.

Mann, P., Gahagan, L., and Gordon, M.B. 2001. Tectonic Setting of the World's Giant Oil and Gas Fields. AAPG Memoir **78**:15-105.

Masters, J.A. 1979. Deep Basin Gas Trap, Western Canada. *AAPG Bulletin* **63** (2): 152-181.

McFall, K.S., Wicks, D.E., and Kuuskraa, V.A. 1986. A Geologic Assessment of Natural Gas from Coal Seams in the Warrior Basin, Alabama, Gas Research Institute, Chicago, Illinois.

Meek, R.H., and Bowser, P.D. 1993. The Transition Between the Low-rate and High-rate Producing Areas of the Fruitland Coal, San Juan Basin, New Mexico. *AAPG Bullentin* **65**(2): 1455-1470.

Montgomery, S.L., and Barker, C.E. 2003. Coalbed Methane, Cook Inlet, South-Central Alaska: A Potential Giant Gas Resource. AAPG Bulletin **87** (1): 1-13.

Montgomery, S.L., Jarvie, D.M., Bowker, K. A. et al. 2005. Mississippian Barnett Shale, Fort Worth Basin, North-Central Texas: Gas-shale Pay with Multindashtrillion Cubic Foot Potential. *AAPG Bulletin* **89** (2): 155-175.

Morin, R.H. 2005. Hydrologic Properties of Coal Beds in the Powder River Basin, Montana I. Geophysical Log Analysis. *Journal of Hydrology* **308**: 227-241.

Nakayama, K. 2000. Estimation of Reservoir Properties by Monte Carlo Simulation. Paper SPE 59408-MS presented at the SPE Asia Pacific Conference on Integrated Modelling for Asset Management, Yokohama, Japan, 04/25/2000.

Nelson, C.R. 2000. Coalbed Methane Potential of the U.S. Rocky Mountain Region. *GasTIPS* **6** (3): 4-12.

Newman III, H.E. 1981. Greater Green River Basin Stratigraphy as It Relates to Natural Gas Potential. Paper SPE 9845-MS presented at SPE/DOE Low Permeability Gas Reservoirs Symposium, Denver, Colorado, 05/27/1981.

Oudinot, A.Y., Koperna, G.J., and Reeves, S.R. 2005. Development of a Probabilistic Forecasting and History Matching Model for Coalbed Methane Reservoirs. Paper presented at 2005 International Coalbed Methane Symposium, Tuscaloosa, Alabama, 05/05/2005.

Petzet, A. 2007. More Operator Eye Maverick Shale Gas, Tar Sand Potential. *Oil & Gas Journal* **105** (30): 38-40.

Powell, G. 2010. Shale Energy: Developing the Barnett—Lateral Lengths Increasing in Barnett Shale. *World Oil* **231** (8).

PTAC. 2006. Filling the Gap: Unconventional Gas Technology Roadmap, Petroleum Technology Alliance Canada, Calgary, Alberta, Canada.

Ramakrishnan, H., Peza, E.A., Sinha, S. et al. 2011. Understanding and Predicting Fayetteville Shale Gas Production Through Integrated Seismic-to-Simulation Reservoir Characterization Workflow. Paper SPE 147226-MS presented at SPE Annual Technical Conference and Exhibition, Denver, Colorado, USA, 01/01/2011.

Ramaswamy, S. 2007. Selection of Best Drilling, Completion and Stimulation Methods for Coalbed Methane Reservoirs. MS Thesis, Texas A&M University, College Station, Texas.

Reeves, S.R. 2003. Assessment of CO2 Sequestation and ECBM Potential of US Coalbeds, Advanced Resources International, Inc, Washington, D.C.

Rhine, T., Loayza, M.P., Kirkham, B. et al. 2011. Channel Fracturing in Horizontal Wellbores: the New Edge of Stimulation Techniques in the Eagle Ford Formation. Paper SPE 145403-MS presented at SPE Annual Technical Conference and Exhibition, Denver, Colorado, 10/02/2011.

Rightmire, C.T., Eddy, G.E., and Kirr, J.N. 1984. Coalbed Methane Resources of the United States. *AAPG Studies in Geology* **17**: 1-13.

Rogers, R.E., Ramurthy, M., Rodvelt, G. et al. 2008. Coalbed Methane: Principles and Practices, Halliburton, Inc, Houston, Texas.

Rogner, H.H. 1997. An Assessment of World Hydrocarbon Resource. *Annual Review of Energy and the Environment* **22**: 217-262.

Saucier, A.E., Finley, R.J., and Dutton, S.P. 1985. The Travis Peak (Hosston) Formation of East Texas and North Louisiana. Paper SPE 13850-MS presented at SPE/DOE Low Permeability Gas Reservoirs Symposium, Denver, Colorado, 03/19/1985.

MacMillan, W.K., Zuber, M.D., and Williamson, J.R. 1999. A Simulation-Based Spreadsheet Program for History Matching and Forecasting Shale Gas Production. Paper SPE 57439-MS presented at SPE Eastern Regional Conference and Exhibition, Charleston, West Virginia, 10/21/1999.

Schepers, K.C., Gonzalez, R J., Koperna, G.J. et al. 2009. Reservoir Modeling in Support of Shale Gas Exploration. Paper SPE 123057-MS presented at Latin American and Caribbean Petroleum Engineering Nakayama Conference, Cartagena de Indias, Colombia, 05/31/2009.

Schlottman, B.W., Miller II,W.K., and Lueders, R.K. 1981. Massive Hydraulic Fracture Design for the East Texas Cotton Valley Sands. Paper SPE 10133-MS presented at SPE Annual Technical Conference and Exhibition, San Antonio, Texas, 01/01/1981.

Smead, R.G., and Pickering, G.B. 2008. North American Natural Gas Supply Assessment, Navigant Consulting, Inc, Chicago, Illinois.

Swaan, A.D. 1976. Analytic Solutions for Determining Naturally Fractured Reservoir Properties by Well Testing. *Society of Petroleum Engineers Journal* **16** (3): 117-122. SPE-5346-PA.

Swindell, G.S. 2007. Powder River Basin Coalbed Methane Wells-Reserves and Rates. Paper SPE 107308-MS presented at Rocky Mountain Oil & Gas Technology Symposium, Denver, Colorado, 01/01/2007.

Southwestern Energy, Inc. 2011. Fayetteville Shale-Third Quarter of 2011 Update. http://shale.typepad.com/fayettevilleshale/lateral-length/

Tabet, D.E., Hucka, B.P., and Sommer, S.N. 1995. Coalbed Methane Resource Potential of Ferron Sandstone Coals, Utah Geological Survey, Salt Lake City, Utah.

Thomas, J.D. 2003. Integrating Synsedimentary Tectonics With Sequence Stratigraphy to Understand the Development of the Fort Worth Basin. Paper present at AAPG Southwest Section Meeting, Fort Worth, Texas, 03/01/2003.

Transform Software & Services. A Comparative Study of North America's Largest Shale Gas Reservoirs. http://www.transformsw.com/papers-and-presentations/studies.html#Barnett.

Tyler, R.1994. Geologic and Hydrologic Assessment of Natural Gas from Coal Seams in the Mesaverde Group and Fort Union Formation, Greater Green River Basin, Wyoming and Colorado, Gas Research Institute, Chicago, Illinois.

Wang, F.P., and Hammes, U. 2010. Effects of Petrophysical Factors on Haynesville Fluid Flow and Production. *World Oil Magazine* **231** (6).

Williams, P. 2006a. The Grande Dame of Tight Gas. *A Supplement to Oil and Gas Investor*, March 2006: 5-7

Williams, P. 2006b. New Shale-Gas Play Unfolding. *A Supplement to Oil and Gas Investor*, January 2006:18-20.

Wolhart, S.L., Harting, T. A., Dahlem, J. E. et al. 2006. Hydraulic Fracture Diagnostics Used To Optimize Development in the Jonah Field. Paper SPE 102528-MS presented at SPE Annual Technical Conference and Exhibition, San Antonio, Texas, 09/24/ 2006.

Young, G.B.C., Paul, G.W., McElhiney, J.E. et al. 1992. A Parametric Analysis of Fruitland Coalbed Methane Reservoir Producibility. Paper SPE 24903-MS presented at SPE Annual Technical Conference and Exhibition, Washington, D.C., 10/04/1992.